Fundamental Studies on Vibration and Earthquake Response of Suspension Bridges(Dissertation_全文)

AUTHOR(S):

Yamada, Yoshikazu

FUNDAMENTAL STUDIES ON VIBRATION AND EARTHQUAKE RESPONSE OF SUSPENSION BRIDGES

BY

YOSHIKAZU YAMADA

JUNE 1961

FUNDAMENTAL STUDIES ON VIBRATION AND EARTHQUAKE RESPONSE OF SUSPENSION BRIDGES

BY

YOSHIKAZU YAMADA

JUNE 1961

TABLE OF CONTENTS

INTRODUCTION

1. Object and Scope

The collapse of the Tacoma Narrows Bridge on November 7, 1940 created a demand of investigations on aerodynamic stability of suspension bridges, and they have been done by many specialists during the past two decades. Because of the frightful typhoons in Japan, these studies are the most important ones in the design of long span suspension bridges. Earthquake proof designs or studies on earthquake response of the long span suspension bridges are also quite important since extremely great earthquake have been experienced in Japan.

The purpose of this investigation is to study by analytical and experimental means the behavior of suspension bridges, mostly long span suspension bdiges, under the action of earthquake ground motions, and to obtain rational methods of their earthquake resistant designs.

The analytical and experimental studies given in this paper are mostly applied to a particular bridge, Akashi Straits Bridge, which is now being planned by the Kobe City Authority. The methods and the results of the analysis derived from this investigation, however, are applicable to any other long span suspension bridges or sometimes to other types of structures.

The combination of deep piers, large anchor blocks, tall towers, long span cables and suspended structures, of various rigidities, results in unusual problems in the calculation of earthquake response of the long span suspension bridges. In the following (Arts. 2 and 3) therefore historical scope of designs and studies on earthquake resistance of long span suspension bridges will be briefly reviewed, and then, some of the fundamental concepts on dynamic effects of earthquakes to the structures with various rigidities will be given.

Due to the complication of earthquake ground motions, there arises another important but quite difficult problem, that is the estimation of future probable earthquakes. Art. 4 will be spent in describing the characteristics of earthquake ground motions.

The main part of this paper consists of three parts, PART I, PART II, and PART III.

In PART I, an analytical method of studies of a suspension bridge subjected to ground motion in the direction of the bridge axis is presented, and some of the fundamental characteristics of the suspension bridge due to earthquake are investigated. In this analysis the suspension bridge is approximated by the system with finite degrees of freedom and analysed by linear dynamics of the structures. High speed computers are used in evaluating the frequencies and modes of vibration and the dynamic response of the system.

In PART II, an approximate analysis of elastic-plastic behavior of the suspension bridge due to earthquake ground motions is presented. According to the results obtained in PART I, special attention was concentrated upon the suspension bridge towers in this analysis. The high speed digital computer, KDC-I, was employed in the numerical computation.

In PART III, some experimental studies on fundamental characteristics of suspension bridges are presented. The experimental investigations were done on a full scale model (1/1000 scale), a tower model (1/100 scale), and actual simple suspension bridges with comparatively small bridge spans about 100m. Since the vibration damping of structures plays a major role in structural dynamics, some of the fundamental behaviors of the structural damping will be also discussed in this part.

The subjects presented in this paper are limited to particular problems and they leave important subjects to be investigated in more detail. Such general problems will be given in the CONCLUDING REMARKS of this paper.

2. Brief Review of Aseismic Design of Long Span Suspension Bridges

In the design of the great suspension bridges in the State of California, earthquake stresses were treated with considerable detail. (1) (2) (3)

(a) San Francisco-Oakland Bay Bridge

The San Francisco-Oakland Bay Bridge was designed to resist a ground motion with horizontal acceleration of 0.1 g, with a period of 1.5 sec. and a corresponding amplitudes of 2.2 inch (5.6 cm). This is a longer period than is probable but was chosen because, with other assumptions used in the design, it generally produce higher stresses than the same acceleration with a shorter period. The horizontal acceleration of 10% of gravity was determined refering to a Japanese

specification on earthquake resistant design, and there were no other reasons.

In an earthquake of transverse direction, earthquake stresses in the tower are caused by inertia in the suspended structures as well as in the towers themselves. In the design, these inertia forces were replaced by the statical displacements and the statical horizontal forces specified by 10% of gravity.

The report [3] pointed out that the suspension bridge as a whole, has many characteristics of a steel springs, but no rational considerations on these were given.

It was concluded that the amplitudes of any earthquake motion and their accompanying stresses would be relatively small.

(b) Golden Gate Bridge

The Golden Gate Bridge was designed for an assumed horizontal acceleration of 7.5% of gravity, the resultant stresses on the substructres were relatively small. A period and corresponding amplitudes of the ground motion were assumed as 1.3 sec. and 1.24 inch (3.15 cm).

In the design of towers the effect of the earthquake was reduced to a static force of 3.75 % of the weight of the tower acting horizontally because of the flexibility of the towers. According to the analysis which will be discussed in this paper this is not true when the higher mode vibrations of the system are concerned to the dynamic response.

For the substructures in which there will be no elastic deformation, the horizontal force of 10 % of gravity was assumed. For the piers which are in deep water, the effect of water was also included in the calculations.

Three papers [4] [5] [6] on studies of earthquake proof design of suspension bridges were reported at the Second World Conference on Earthquake Engineering held in Japan in 1960. These were all written by Japanese authors, and each of them has its characteristics.

Prof. Kubo investigated on Aseismicity of Suspension Bridges Forced to Vibrate Longitudinally. [5] He pointed out that the damping constants of suspension bridges are much smaller than those of other types of bridges, and the dynamic considerations are necessary because of the possibility of resonance. In the analysis of dynamic response he employed simple harmonic ground motions and the conception of a growth coefficient, and then estimated the maximum dynamic response.

He also carried out some of the field experiments and obtained the damping constants of the suspension bridges. His method of analysis

treated only the fundamental mode of vibration of suspension bridge and is considered to be applicable, though there are some doubtful points on his method, to suspension bridges with comparatively small bridge spans.

Prof. Hirai and his stuffs investigated on Lateral Stability of a Suspension Bridge Subjected to Foundation Motion.[6] They studied the behavior of vibration with lateral direction of a suspension bridge theoretically and expdrimentally and obtained some fundamental characteristics of the lateral vibration and the lateral stability of suspension bridges.

The other paper [4] is given by the author of this paper and will be given in a more progressive form, in PART I of this paper.

3. Dynamic Effects of Earthquake and Fundamental Considerations on Earthquake Resistant Design of Structures

Suspension bridges are composed of structural system with various rigidities. Dynamic response of structures depend on the rigidities of structures and the nature of ground motions in great extent. Different methods of earthquake resistant design have to be applied to the structures with different rigidities.

The structures or the structural elements can be classified into some groups depending upon their rigidities which are relatively determined on the periods of ground motions. These will be explained in the following refering to a system with sigle degree of freedom.

Consider a simple structure shown in Fig. 1. Dynamic equilibrium condition is given in the following equation.

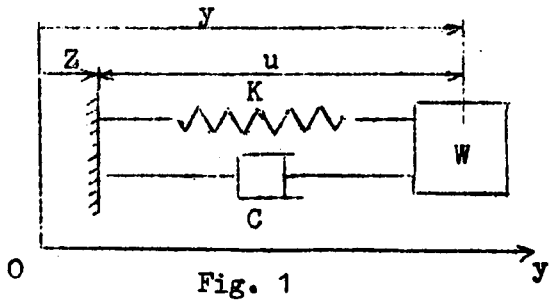

Fig. 1

$$\frac{W}{g}\ddot{y} + C\dot{u} + Ku = 0 \qquad (1)$$

where

W = weight of the structure,

g = acceleration of gravity,

y = total displacement of the structure,

u = relative displacement of the structure,

K = structural stiffness,

C = damping coefficient.

It is convenient to express the total acceleration as the sum of the ground acceleration and the relative acceleration of the structure with respect to the ground, thus,

$$\ddot{y} = \ddot{Z} + \ddot{u}$$

where

Z = ground motion (displacement)

Then, Eq. (1) may be rewritten as

$$\ddot{u} + 2\beta p\dot{u} + p^2 u = -\ddot{Z} \qquad (2)$$

where

$$p^2 = \frac{K g}{W}, \qquad 2\beta p = \frac{C g}{W}$$

and

p = circular frequency of the structure,

β = damping constant of the structure.

If the ground displacement is a simple harmonic motion with the circular frequency ω given as

$$Z = Z_0 \sin \omega t$$

where

Z_0 = maximum ground displacement,

Eq. (2) can be expressed as

$$\ddot{u} + 2\beta p\dot{u} + p^2 u = Z_0 \omega^2 \sin \omega t \qquad (3)$$

A particular solution to Eq. (3) is obtained in the form

$$u = u_0 \sin (\omega t - \alpha)$$

where

$$u_0 = \frac{Z_0}{\sqrt{\left(\frac{p^2}{\omega^2} - 1\right)^2 + 4\beta^2\frac{p^2}{\omega^2}}} \tag{4}$$

= maximum displacement of the structure

The maximum stress produced in the structure is

$$F = Ku_0 = \frac{KZ_0}{\sqrt{\left(\frac{p^2}{\omega^2} - 1\right)^2 + 4\beta^2\frac{p^2}{\omega^2}}} \tag{5}$$

From Eq. (5) it is clear that the response of the structure depends on the natural frequency of vibration of the structure, which depends on its stiffness and weight.

If the frequency of the structure is large in comparison with that of ground motion, the maximum stress is approximately given as

$$F \doteq \frac{\omega^2}{p^2} KZ_0$$
$$= kW \tag{6}$$

Under the condition of

$$\frac{\omega^2}{p^2} << 1 \text{ and } \beta^2 = 0$$

where

$$k = \frac{\omega^2 Z_0}{g} = \text{seismic coefficient.}$$

Eq. (6) indicates that the method of the seismic coefficient is applicable to comparatively rigid structures. This concept provided the basis for the lateral force provisions of some of the earthquake codes, which specified that a structure should be designed for a certain percentage of gravity fegardless of the characteristics of the structures.

If the frequency of the structure is very small in comparison with that of the ground motion, i.e. $\frac{\omega^2}{p^2} >> 1$, the maximum stress due to external ground motion is approximately

$$F \doteqdot K Z_0 \tag{7}$$

Eq. (7) shows that the maximum dynamic stress of very flexible structure depend chiefly upon the maximum ground displacement. The method of seismic coefficient is useless for the design of such structure.

If the frequency of the structure coincide with the frequency of the simple harmonic ground motion, the maximum stress is well known as resonant stress and given as

$$F = \frac{K Z_0}{2\beta} = \frac{k W}{2\beta} \tag{8}$$

The maximum stress depends chiefly upon the damping constant β.

The earthquake ground motions may not be represented by simple harmonic motion. The only reason for this explanation is to emphasize, with simple example, the important influence of the period of vibration of the structure on its response to a specific ground motion. As the suspension bridges are composed of the structural parts with various rigidities, the explanation given plays an important role in the investigation of this paper.

According to the explanation given, the author will define the following classifications of structures depending upon their rigidities.
(I) Rigid Type Structure : the structures in which the maximum dynamic response is given or approximately given by Eq. (6).
(II) Flexible Type Structures : the structures in which the maximum dynamic response is approximately given by Eq. (7).
(III) Resonant Type Structure : the structures occasionally resonant with the ground motions.

4. Earthquake Ground Motion

One of the most important and difficult problems in the analysis of earthquake response of structures is the estimation of the magnitude and the nature of probable future strong earthquakes. The past strong earthquake records are only direct information to predict the probable future strong earthquakes. Accurate records of ground motion due to strong earthquake are necessary. The strong motion program by the U. S.

Coast and Geodetic Survey was started in 1932 and obtained considerable number of strong earthquake records. In spite of the frequent strong earthquakes we have in our country, such program had been disregarded for about two decades, and the Strong Motion Acceleration Committee was established in 1951 in Japan. The strong motion accelerograph known as SMAC have been installed recently. The number of these recorders is limited, and almost no strong motion records are available up to the present in Japan.

For the reason which will be explained lately in the analysis of earthquake response of suspension bridges, ground displacement records are also necessary. These are obtainable by integrating the acceleration records with respect to time. This procedure, however, is quite complicated and it was pointed out [7] that any significant departures from true acceleration in the record will usually results in a larger departure from true displacement. Displacement meters, like Carder Displacement Meter at the USCGS is also necessary in Japan. It is especially important in the analysis of the suspension bridges.

The types of ground motions which will be adoptable in the analysis of earthquake response can be classified as follows.

(1) Simple functions like trigonometric functions are adoptable in the primary analysis, especially when no strong motion records available.

(2) Strong motion records, as mentioned above can be directly used as a ground motion in analytical studies. This method is mostly applied to the analyses of the recent studies in the U. S.

(3) Some artificial ground motions whether obtained theoretically or experimentally can be used as random external disturbances. These motions may sometimes be given refering to the strong motion records obtained and must have more universality than recorded strong motions. Studies on random process can develop this method. Application of white noise is one of the example of this method.[8] [9]

The ground motions applied in the studies of this paper are (a) some types of simple harmonic motion, and (b) the ground motion obtained by strong motion seismograph.

Since no strong motion records are available in Japan, some of the SMAC records have been obtained but their magnitude are not large enough to be used in the analysis, the strong motion records obtained by USCGS were applied to the numerical computations. Of course there might be some expectable differences of the nature of the earthquake

in the U. S. and in Japan, and this is only a tentative application.

1940 El Centro Earthquake has the maximum recorded acceleration in the U. S. and is considered as a standard earthquake in the U. S. In the analysis of earthquake response of the suspension bridges the records of displacement meter is necessary. The strong motion displacement record of 1957 South California Earthquake obtained by Carder Displacement Meter at Port Hueneme will be mostly used in the analyses of this paper.[10] The ground motion record are shown in Fig. 2. The maximum displacement of this earthquake is about 1.4 cm, and the maximum recorded acceleration is 167 cm/sec^2 -0.17 g-.

5. The Proposed Suspension Bridge over the Akashi Straits

The analytical methods derived in this paper will be mostly applied to the suspension bridge which is now being planned by the [illegible] Division of Public Works of the City of Kobe. This suspension bridge will connect the Honshu and the Awaji Island.

The proposed main dimensions of the bridge, Plan II*, are the following.

Total span length	2600 m
Center span length	1300 m
Side span length	650 m
Cable sag at the center	108 m
Width of the bridge	19.0 m
Center to center distance of the cables	24.0 m
Total height of the tower shaft from the center of the cable to H.W.L.	192.5 m
Height of the stiffening truss	14.0 m
Horizontal tension of the main cable due to dead load	H_g = 19560 ton
Horizontal tension of the main cable due to live load	H_p = 3960 ton

Other data necessary in the analysis will be given as occasion arises. These are the dimensions of the main bridge.

Fig. 3 shows the general view of the main bridge of the Akashi Straits Bridge.

---

* Two plans, Plan I and Plan II, had been designed. Plan I has ten traffic lanes and Plan II, four. Plan II will be used in the investigations of this paper except the full model test in PART III.

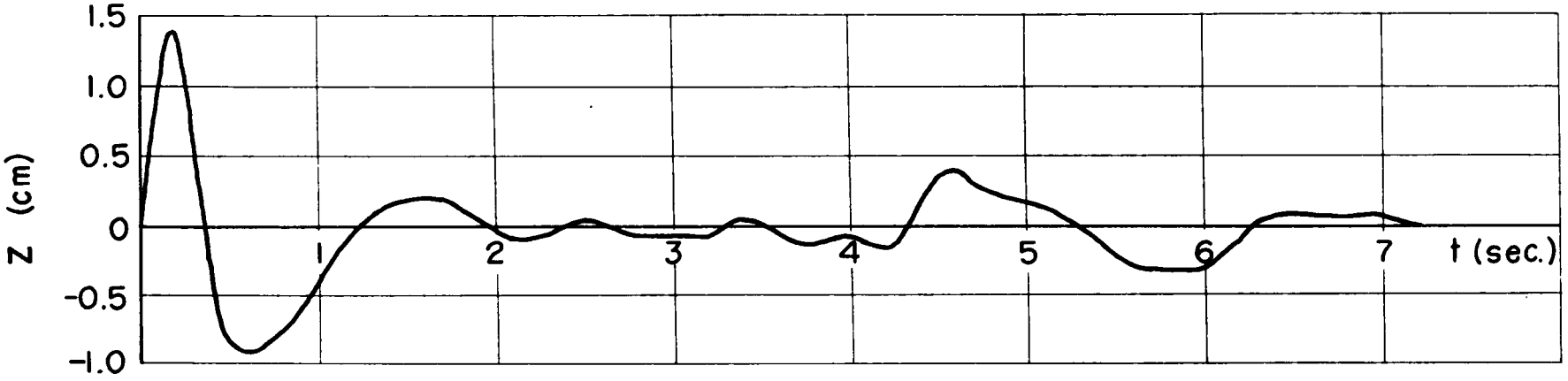

Fig. 2 1957 South California Earthquake

Recorded at Port Hueneme, California
Navy Research and Evaluation Laboratory
March 18, 1957

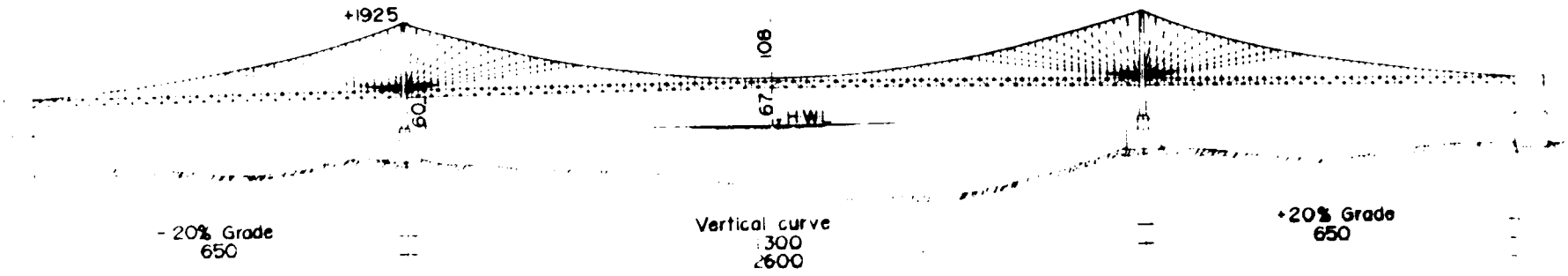

Fig. 3

PROPOSED AKASHI STRAITS BRIDGE (MAIN BRIDGE)

PART I. LINEAR ANALYSIS ON DYNAMIC RESPONSE OF A SUSPENSION BRIDGE SUBJECTED TO EARTHQUAKE GROUND MOTIONS

I. FUNDAMENTAL EQUATIONS OF MOTION OF SUSPENSION BRIDGE

101. Introduction

The combination of structural parts of the various rigidities in suspension bridges results in unusual problems in the analysis of earthquake response of the long span suspension bridges, as Golden Gate Bridge or San Francisco-Oakland Bay Bridge, therefore the suspension bridge was devided into some parts with specific rigidities, and approximate design methods were applied.

The analysis in this part, Part I, aims chiefly to investigate the fundamental properties of suspension bridge subjected to ground motions. In this investigation, the suspension bridge will be simplified into a physically analogous system to which the theory of finite degrees of freedom can be applied.

102. Physical System Considered

The system considered in this analysis is as shown in Fig. 101. Suspended structures of the suspension bridge are considered to consist of rigid bars connected with elastic hinges. Elastic constants of the hinges are so selected that the analogy of bending properties to the original suspended structures might be satisfied. Dead weight of the suspended structures and cables are assumed to be concentrated at the

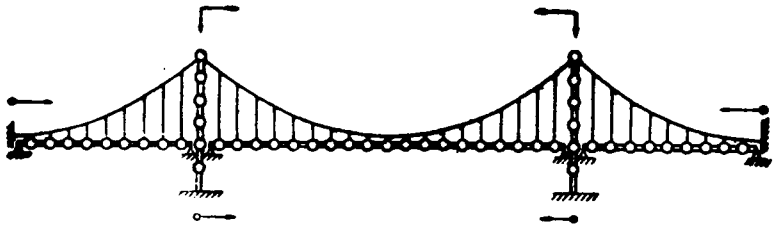

Fig. 101 Physical System Considered

hinged points considered. Each hinged point has a single degree of freedom of motion to the vertical direction specified by a deflection coordinate y_r.

Towers of the bridge are also replaced by the same physically analogous system. Only the horizontal motion is assumed to be allowable to the points in the towers. Axial forces and horizontal forces acting to the top of the towers are taken into consideration.

Ordinary assumption in the analysis of suspension bridges, such as suspenders being inextensible, are assumed in the analysis.

The piers and anchor blocks of the suspension bridges are assumed to be rigid structures and considered to be upward extensions of rocks.

Vibration damping of the structures will be considered under some assumptions but omitted in the first derivation of equations.

Using such simplified system, theory of systems with finite degrees of freedom can be applied to the problem. When the suspension bridge is devided into fairly large number of segments, a good approximation is obtained. Only high speed computers can execute numerical calculations for such systems.

103. Equation of Motion of Suspended Structures

A point considered here is the elastic hinged point of the system specified above, and the dead load is assumed to be concentrated on this point. In Fig. 102, three adjoining points in the suspended structure are shown, and the equilibrium of the point r will be discussed here. Solid lines in Fig. 102 show the condition of static equilibrium due to dead load. As the suspended structures of suspension bridges carry no dead weight, the following static equilibrium condition is derived regarding the point r.

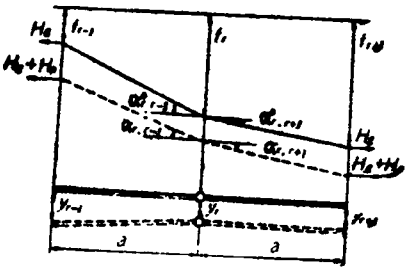

Fig. 102

$$\tan \alpha^{0}_{r,r+1} - \tan \alpha^{0}_{r,r-1} = \frac{W_r}{H_g} \qquad (101)$$

where,

H_g = horizontal component of dead load cable tension,

W_r = dead load concentrated at the point r.

Using cable sag of three points, Eq. (101) is

$$\frac{1}{a}(f_{r-1}-2f_r+f_{r+1}) = -\frac{W_r}{H_g} \tag{102}$$

Two kinds of internal reactions take place with the displacement of the point. One is due to bending of the suspended structure, and the other is due to increment of the cable tension.

Reaction due to the bending of the suspended structure is

$$R_r^M = -\frac{1}{a}(M_{r-1}-2M_r+M_{r+1}) \tag{103}$$

where,

M_r = bending moment at the point r in the suspended structure.

Bending moment M_r is assumed to be expressed by the deflections of three adjoining points in the suspended structure as

$$M = -\frac{B_r}{a}(y_{r-1}-2y_r+y_{r+1}) \tag{104}$$

where,

B_r = elastic constant selected to satisfy the bending properties of the suspended structure.

With the increment in cable stress due to vibration, horizontal component of cable stress increases from H_g to H_g+H_p. Reaction due to cable tension H_g+H_p is

$$R_r^{(H_g+H_p)} = (H_g+H_p)(\tan\alpha_{r,r+1} - \tan\alpha_{r,r-1}) \tag{105}$$

in which

$$\begin{aligned}\tan\alpha_{r,r-1} &= \frac{1}{a}\left[(f_r+y_r)-(f_{r-1}+y_{r-1})\right]\\ \tan\alpha_{r,r+1} &= \frac{1}{a}\left[(f_{r+1}+y_{r+1})-(f_r+y_r)\right]\end{aligned} \tag{106}$$

Substituting Eq. (106) into Eq. (105), and using the relation of Eq. (102), the reaction due to increment of cable tension is

$$R^{H_p}_r = \frac{H_p}{a}(f_{r-1}-2f_r+f_{r+1}) + \frac{H_g+H_p}{a}(y_{r-1}-2y_r+y_{r+1}) \qquad (107)$$

Total reaction at the point r due to deflections of the suspended structure is, therefore,

$$R_r = \frac{1}{a}(M_{r-1}-2M_r+M_{r+1}) + \frac{H_p}{a}(f_{r-1}-2f_r+f_{r+1}) + \frac{H_g+H_p}{a}(y_{r-1}-2y_r+y_{r+1}) \qquad (108)$$

No external force being applied to the point r, the equation of motion of the point r is given as

$$\frac{W_r}{g}\ddot{y}_r = \frac{1}{a}(M_{r-1}-2M_r+M_{r+1}) + \frac{H_p}{a}(f_{r-1}-2f_r+f_{r+1}) + \frac{H_g+H_p}{a}(y_{r-1}-2y_r+y_{r+1}) \qquad (109)$$

Bending moment M_r in Eq. (109) is given in Eq. (104).

104. Cable Equation

The increment of horizontal component of cable tension, H_p, in Eq. (109) is the function of deflection of the suspended structure, and it can be obtained from so-called cable equation.

Assuming that the cable element (r : r+1) moves to the position (r':r+1') as shown in Fig. 103, due to the increment of the cable tension, the following relation is given neglecting small quantities of higher order.

$$(u_{r+1}-u_r)\cos\alpha^0_{r,r+1} + (y_{r+1}-y_r)\sin\alpha^0_{r,r+1} = \frac{t_{r,r+1}L_{r,r+1}}{E_c A_c} \qquad (110)$$

where,

$t_{r,r+1}$ = the increment of cable tension of the cable element r : r+1,

$L_{r,r+1}$ = length of the cable element r : r+1,

E_c = Young's modulus of the material of the cable,

A_c = cross sectional area of the cable,

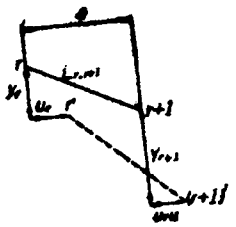

Fig. 103

u_r = horizontal component of the displacement of the point r,

y_r = vertical component of the displacement of the point r.

The horizontal component of the elongation of the cable element r : r+1 is

$$\Delta u_{r,r+1} = u_{r+1} - u_r$$

$$= \frac{t_{r,r+1} L_{r,r+1}}{E_c A_c} \cos \alpha^0_{r,r+1} - (y_{r+1}-y_r) \tan \alpha^0_{r,r+1} \qquad (111)$$

Using H_p, and a,

$$\Delta u_{r,r+1} = \frac{H_p a}{E_c A_c} \cos^3 \alpha^0_{r,r+1} - (y_{r+1}-y_r) \tan \alpha^0_{r,r+1} \qquad (112)$$

The total elongation of the cable is

$$u = \sum \Delta u$$

$$= \frac{H_p}{E_c A_c} \sum \frac{a}{\cos^3 \alpha^0_{r,r+1}} + \sum y_r (\tan \alpha^0_{r,r+1} - \tan \alpha^0_{r,r-1}) \qquad (113)$$

Using Eq. (101), Eq. (113) will be

$$u = \frac{H_p L_E}{E_c A_c} - \frac{W_r}{H_g} \sum y_r \qquad (114)$$

where

$$L_E = \sum \frac{a}{\cos^3 \alpha^0_{r,r+1}} \qquad (115)$$

Eq. (114) must be applied to each span of the suspension bridge, and the value of H_p is different for each span. Expressing the quantities of the left side span by suffix 1, of the center span by suffix c, and of the right side span by suffix 2, one obtains

$$\begin{aligned} u_1 &= \frac{H_{p1} L_{E1}}{E_c A_c} - \frac{W_r}{H_g} \sum_{(1)} y_r \\ u_c &= \frac{H_{pc} L_{Ec}}{E_c A_c} - \frac{W_r}{H_g} \sum_{(c)} y_r \\ u_2 &= \frac{H_{p2} L_{E2}}{E_c A_c} - \frac{W_r}{H_g} \sum_{(2)} y_r \end{aligned} \qquad (116)$$

The following conditions must be also satisfied, taking the positive direction of the horizontal displacement as in Fig. 101.

$$u_1 = y_{Tl} - Z_A$$
$$u_c = -y_{Tl} - y_{Tr} \qquad (117)$$
$$u_2 = y_{Tr} - Z_D$$

where,

y_{Tl} = displacement of the top of the left side tower,
y_{Tr} = displacement of the top of the right side tower,
Z_A = displacement of the ground motion at the left side anchorage,
Z_D = displacement of the ground motion of the right side anchorage.

105. Equations of Motion of Towers

Towers of the suspension bridge are also divided into small segments which consist of rigid bars and elastic hinges. Fig. 104 shows the tower subjected to ground motion at the base and the horizontal and vertical forces at the top.

The same method of derivation of equations of motion as before is used, then the equations of motion for inner points of the tower are obtained as follows.

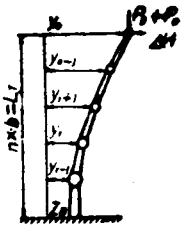

Fig. 104

$$\frac{W_r}{g}\ddot{y}_r = \frac{1}{b}(M_{r-1} - 2M_r + M_{r+1}) - \frac{P_g + P_p}{b}(y_{r-1} - 2y_r + y_{r+1}) \qquad (118)$$

At the top of the tower, the following equation is to be applied as the horizontal force ΔH is acting there.

$$\frac{W_n}{g}\ddot{y}_n = \frac{1}{b}M_{n-1} - \frac{P_g + P_p}{b}(-y_n + y_{n-1}) + \Delta H \qquad (119)$$

where,

P_g = axial force due to dead load acting at the top of the tower,
P_p = increment to the axial force due to inertia force,
ΔH = horizontal force acting at the top of the tower during vibration.

W_r = dead weight of the tower concentrated at the point r.

Bending moment M_r in Eqs. (118) and (119) are given by

$$M_r = -\frac{B_r}{b}(y_{r-1} - 2y_r + y_{r+1}) \tag{120}$$

If the tower is assumed to be fixed at the base, the bending moment at the base is

$$M_B = -\frac{B_B}{b}(2y_{r-1} - 2Z_B) \tag{121}$$

The horizontal force ΔH are given as

$$\begin{aligned} \Delta H_1 &= H_{pc} - H_{p1} \qquad \text{(for the left side tower)} \\ \Delta H_2 &= H_{pc} - H_{p2} \qquad \text{(for the right side tower)} \end{aligned} \tag{122}$$

106. Relations to Fundamental Partial Differential Equations of Motion of the Suspension Bridge

The equations of motion, Eqs. (109), (118), and (119) were derived from physical investigation on a model shown in Fig. 101. These equations are mathematically the finite difference expressions of the following fundamental equations of motion of the suspension bridges. (101) (102)

For the suspended structures, the equation is

$$EI\frac{\partial^4 y}{\partial x^4} - (H_g + H_p)\frac{\partial^2 y}{\partial x^2} - H_p\frac{\partial^2 f}{\partial x^2} = -\frac{w}{g}\frac{\partial^2 y}{\partial t^2} + p \tag{123}$$

For the towers,

$$EI_T\frac{\partial^4 y}{\partial x^4} + (P_g + P_p)\frac{\partial^2 y}{\partial x^2} = -\frac{w_T}{g}\frac{\partial^2 y}{\partial t^2} + p \tag{124}$$

Cable equation is

$$u = -\frac{H_p L_E}{A_c E_c} - \int_{(span)} \frac{w}{H_g} y\, dx \tag{125}$$

107. Linearization of the Equations

The equations of motion derived are originally depending upon the deflection theory of suspension bridges and have non-linear properties even the internal stresses are within the elastic limit of materials.

If the increment of the cable tension specified by H_p is small in comparison to H_g, Eq. (109) is simplified to the linear differential equation using so-called linearized deflection theory outlined by Fr. Bleich.(103)

The linearized equation is

$$\frac{W_r}{g}\ddot{y}_r = \frac{1}{a}(M_{r-1}-2M_r+M_{r+1}) + \frac{H_p}{a}(f_{r-1}-2f_r+f_{r+1}) + \frac{H_g}{a}(y_{r-1}-2y_r+y_{r+1}) \tag{126}$$

Employing the same method of linearization Eqs. (118) and (119) can be simplified as follows if the incremental axial force P_p is small compared to the axial force due to dead load.

$$\frac{W_r}{g}\ddot{y}_r = \frac{1}{b}(M_{r-1}-2M_r+M_{r+1}) - \frac{P_g}{b}(y_{r-1}-2y_r+y_{r+1}) \tag{127}$$

$$\frac{W_n}{g}\ddot{y}_n = \frac{1}{b}M_{n-1} - \frac{P_g}{b}(-y_n+y_{n-1}) + \Delta H \tag{128}$$

Investigations on the incremental axial force P_p will be discussed in Part II of this paper.

108. System of Equations of Motion

Substituting Eqs. (116) and (122) into the linearized differential equations, Eqs. (126), (127), and (128), a system of fundamental equations of motion can be derived in the following form.

$$[A](\ddot{y}_r) + [B](y_r) + (P_r(t)) = 0 \tag{129}$$

In Eq. (129), $[\ ]$, and $(\ )$ show a square symmetric and a vector matrix respectively, and

y_r = displacement of a point in the suspended structure, or the tower,

$P_r(t)$ = an element of vector matrix $(P_r(t))$ and is determined from the ground motions,

$[A]$ = diagonal matrix with the diagonal element $a_{rr} = \frac{W_r}{g}$,

$[B]$ = stiffness matrix.

Vector matrix $(P_r(t))$ is determined from the ground motions of the left side anchorage, of the left side tower base, of the right side tower base, and of the right side anchorage which are denoted by Z_A, Z_B, Z_C, and Z_D respectively.

Matrices $[A]$, $[B]$, and $(P_r(t))$ will be given in the following article for a practical example.

The problem given by Eq. (129) is physically the vibration problem with multi-degrees of freedom and can be effectively solved by applying modal analysis of vibration if the natural frequencies and modes of vibration are obtained.

109. Practical Examples of the Analysis and Physical Constants of the System

The numerical computation of the analysis derived will be done on the Akashi Straits Bridge which was mentioned already.
In the simplification of the bridge two models were employed, one is having 21 degrees of freedom, and the other is having 29 degrees. In the numerical analysis of Part I, they will be specified by Approximation I, and Approximation II.

Approximation I :

The model of Approximation I is shown in Fig. 105. The suspended structures are devided into the segments with an equal length, 162.5 m, and the tower was devided into four segments.

Then, the dimensions are,

$$a = L/8 = 1300/8 = 162.5 \text{ m}$$
$$b = L_T/4 = 200/4 = 50.0 \text{ m}$$

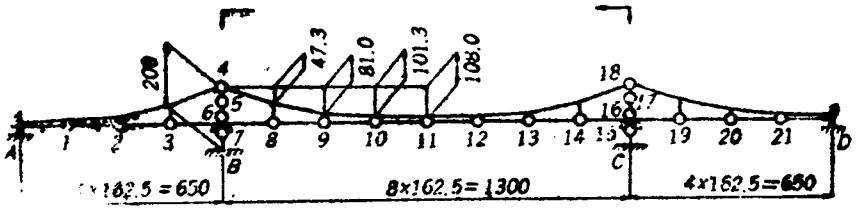

Fig. 105 Approximation I

The concentrated weight W_r, and the stiffness constants B_r are given in Table 101. The suspended structures are considered to have uniform cross section for each span, and the towers to have varying cross sections. Numbers of the elastic hinged points are given in Fig. 105.

Approximation II :

The model of Approximation II is given in Fig. 106. The number of the segments of the tower is doubled to obtain accurate results.

Then, the dimensions are,

$a = L/8 = 1300/8 = 162.5$ m

$b = L_T/8 = 200/8 = 25.0$ m

The concentrated weight W_r, and the stiffness constants B_r are given in Table 102.

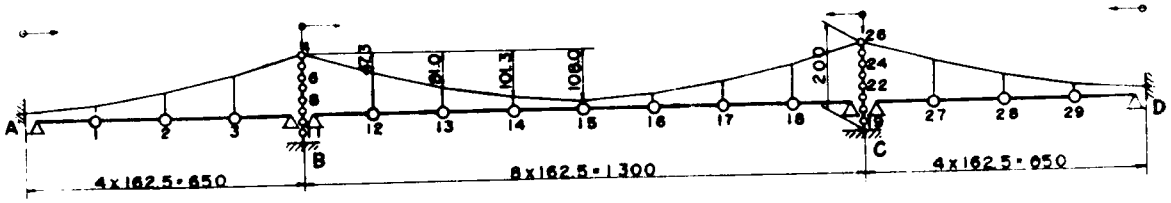

Fig. 106 Approximation II

110. Summary of Equations

General forms of matrices $[A]$, $[B]$, and $(P_r(t))$ of the Approximation II are given in Table 103 in the form of the Equations of motion.

By using physical constants given, the equations of motion can be given in numerical form as shown in Table 104.

The system of the equations of motion for the Approximation I is omitted here as it has almost the same form as in the Approximation II.

Table 101 Approximation I

Point r	W_r (ton)	B_r (ton-m)
1, 21	1625	6.462×10^5
2, 20	1625	6.462×10^5
3, 19	1625	6.462×10^5
4, 18	340	0
5, 17	1165	46.158×10^5
6, 16	1778	107.52×10^5
7, 15	2521	216.05×10^5
8, 14	1625	5.169×10^5
9, 13	1625	5.169×10^5
10, 12	1625	5.169×10^5
11,	1625	5.169×10^5
B, C		391.3×10^5

Table 102 Approximation II

Point r	W_r (ton)	B_r (ton-m)
1, 29	1625	6.462×10^5
2, 28	1625	6.462×10^5
3, 27	1625	6.462×10^5
4, 26	171	..9
5, 25	455	55.86×10^5
6, 24	585	92.316×10^5
7, 23	731	144.060×10^5
8, 22	893	215.040×10^5
9, 21	1071	309.540×10^5
10, 20	1266	432.096×10^5
11, 19	1476	588.000×10^5
12, 18	1625	5.169×10^5
13, 17	1625	5.169×10^5
14, 16	1625	5.169×10^5
15	1625	5.169×10^5
B, C		782.628×10^5

Table 103 System of Equations of Motion

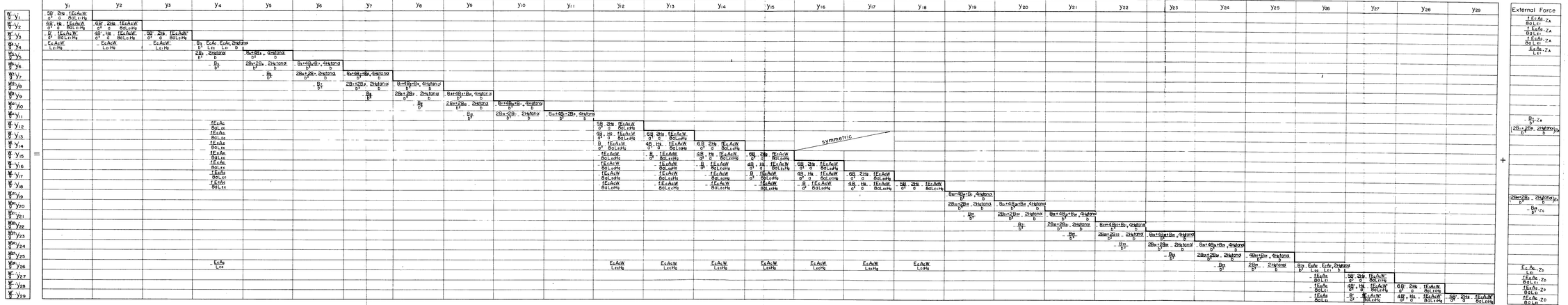

Note. $W_i = W'$ and $B_i = B'$ for $i = 1,2,3,27,28,29$. $W_j = W$ and $B_j = B$ for $j = 12,13,14,15,16,17,18$.

Table 10⁴ System of Equations

r	$(Wr/g)\ddot{y}_r$	y_1	y_2	y_3	y_4	y_5	y_6	y_7
1	165.816	-450.2259	131.1093	-111.6086	-1048.8932			
2	165.816	131.1093	-474.6956	131.1093	-1048.8392			
3	165.816	-111.6086	131.1093	-450.2259	-1048.8392			
4	17.449	-1048.8932	-1048.8932	-1048.8932	-27420.951	17420.20	-8937.60	
5	46.429				17420.200	-49610.96	46961.32	-14770.56
6	59.694				-8937.600	46961.32	-90159.44	75185.32
7	74.592					-14770.56	75185.32	-140465.36
8	91.122						23049.60	114457.00
9	109.286							-34406.40
10	129.184							
11	150.612							
12	165.816				524.4466			
13	165.816				524.4466			
14	165.816				524.4466			
15	165.816				524.4466			
16	165.816				524.4466			
17	165.816				524.4466			
18	165.816				524.4466			
19	150.612							
20	129.184							
21	109.286							
22	91.122							
23	74.592							
24	59.694							
25	46.429							
26	17.449				-6312.784			
27	165.816							
28	165.816							
29	165.816							

Table 104 System of Equations
(continued)

r	y_8	y_9	y_{10}	y_{11}	y_{12}	y_{13}	y_{14}	y_{15}
1								
2								
3								
4					524.4466	524.4466	524.4466	524.4466
5								
6	-23049.400							
7	114457.00	-34406.40						
8	-209291.60	167410.60	-49526.40					
9	167410.60	-300737.36	236868.52	-69135.36				
10	-49526.40	236868.52	-419237.84	325975.72				
11		-69135.36	325975.72	-694986.32				
12					-382.1868	155.1029	-63.1452	-43.5694
13					155.1029	-401.7625	155.1029	-63.1452
14					-63.1452	155.1029	-401.7625	155.1029
15					-43.5694	-63.1452	155.1029	-401.7625
16					-43.5694	-43.5694	-63.1452	155.1029
17					-43.5694	-43.5694	-43.5694	-63.1452
18					-43.5694	-43.5694	-43.5694	-43.5694
19								
20								
21								
22								
23								
24								
25								
26								
27								
28								
29								

Table 10⁴ System of Equations
(continued)

r	y_{16}	y_{17}	y_{18}	y_{19}	y_{20}	y_{21}	y_{22}	y_{23}
1								
2								
3								
4	524.4466	524.4466	524.4466					
5								
6								
7								
8								
9								
10								
11								
12	-43.5694	-43.5694	-43.5694					
13	-43.5694	-43.5694	-43.5694					
14	-63.1452	-43.5694	-43.5694					
15	155.1029	-63.1452	-43.5694					
16	-401.7625	155.1029	-63.1492					
17	155.1029	-401.7625	155.1029					
18	-63.1452	155.1029	-382.1868					
19				-694086.32	325975.72	-69135.36		
20				325975.72	-419237.84	236868.52	-49526.40	
21				-69135.36	236868.52	-300737.36	167410.60	-34406.40
22					-49526.40	167410.60	-209291.60	114457.00
23						-34406.40	114457.00	-140465.36
24							-23049.60	75185.32
25								-14770.56
26								
27								
28								
29								

Table 104 System of Equations
(continued)

r	y_{24}	y_{25}	y_{26}	y_{27}	y_{28}	y_{29}	External Forces
1							1048.893 Z_A
2							1048.893 Z_A
3							1043.893 Z_A
4			-8912.784				12625.567 Z_A
5							
6							
7							
8							
9							
10							-94080.00 Z_B
11							438145.96 Z_B
12			524.4466				
13			524.4466				
14			524.4466				
15			524.4466				
16			524.4466				
17			524.4466				
18			524.4466				
19							438145.96 Z_C
20							-94080.00 Z_C
21							
22	-23049.60						
23	75185.32	-14770.56					
24	-90159.44	46961.32	-8937.60				
25	46961.32	-49610.96	17420.20				
26	-8937.60	17420.20	-27420.95	-1048.8932	-1048.8932	-1048.8932	12625.567 Z_D
27			-1048.8932	-450.2259	131.1093	-111.6085	1048.893 Z_D
28			-1048.8932	131.1093	-474.6956	131.1093	1048.893 Z_D
29			-1048.8932	-111.6085	131.1093	1450.2259	1048.893 Z_D

II. NATURAL FREQUENCIES AND MODES OF THE SUSPENSION BRIDGE

111. Natural Frequencies and Modes

To investigate the fundamental dynamic properties and to apply the modal analysis to the problems of dynamic response, natural modes and their frequencies must be firstly investigated. Method of analysis of estimating the natural modes and frequencies of the structures had been limited to the analysis of the fundamental mode or first few modes because of the complexity of the numerical analysis. However, this complexity has been removed by the application of high speed digital computers.

Frequency equation of the system is

$$| [B] - \lambda [A] | = 0 \qquad (130)$$

where,

$\lambda = \omega^2$ = characteristic values,

ω = circular frequencies of the system.

The characteristic roots and vectors of this determinantal equation represent the natural frequencies and modes of the system.

Because the systems of Figs. 105 and 106 are symmetric with respect to the center of the center span of the systems, the natural modes of vibration are either symmetric or asymmetric, and it becomes convenient to evalute the natural frequencies and modes in two separate groups.

Computations of the natural frequencies and modes were done on the ILLIAC, the University of Illinois high speed digital computer. (103)

Values λ and characteristic vectors for the symmetric and asymmetric modes are given in Table 105 (a), (b) for the system of Approximation I, and in Table 106 (a), (b) for the system of Approximation II.

Configurations of these modes are shown in Figs. 107 and 108 for the systems of Approximation I and Approximation II respectively.

For convenience of the following analysis the natural modes of the systems shown in Tables 105 and 106 are normalized so as to satisfy the following condition.

$$\sum_{r=1}^{n} \frac{W_r}{g} (Y_r^{(i)})^2 = 1 \qquad (131)$$

(n = 21 for Approximation I)
(n = 29 for Approximation II)

where, i indicates a specific mode of vibration.

112. Comparison of the Results on Approximation I and II

In first seven symmetric and six asymmetric modes, displacements of the suspended structures are predominent, and there are almost no differences in these corresponding modes and frequencies of the systems, Approximation I and Approximation II.

Natural periods of the modes in which the displacements of the towers are predominent are tabulated in Table 107 and are being compared.

Table 109 Natural Periods (sec)

Modes	Approximation I	Approximation II	(II-I)/II %
Symmetric			
8	1.3477	1.2765	5.6
9	0.5514	0.4634	19.0
10	0.3319	0.2522	31.6
11	0.2247	0.1701	32.1
Asymmetric			
7	1.3657	1.2994	5.1
8	0.5611	0.4858	15.5
9	0.3354	0.2748	22.1
10	0.3028	0.1900	59.4

The errors included are not small especially for higher mode vibrations. For the purpose of practical disign, it is preferable to use the model with higher accuracy, but the effects of natural frequencies of the models are not conclusively important because there is much uncertainty in the estimation of earthquake motions.

In the investigation of the fundamental nature of the vibration of suspension bridges, Approximation I is applicable although its accuracy is less than that of Approximation II.

113. Natural Frequencies and Modes Obtained by the Bleich Method

To compare the results obtained to the results obtained by other m methods the Bleich Method was applied to the same structure, and its natural periods and modes were obtained.

Fr. Bleich applied the Ritz Method to the problems of natural vibration of suspension bridges. (104) He assumed the Fourier sine series on the configurations of natural modes and applied the condition T - V = minimum, where,

T = maximum value of the kinetic energy of the structure,

V = total potential energy of the structure in extreme position.

Applying the Bleich Method and assuming the vibration modes,

$$y = a_1 \sin\frac{\pi x}{l} + a_2 \sin\frac{2\pi x}{l} + a_3 \sin\frac{3\pi x}{l} + a_4 \sin\frac{4\pi x}{l} + a_5 \sin\frac{5\pi x}{l} + a_6 \sin\frac{6\pi x}{l} \quad \text{(for center span)}$$

$$\bar{y} = \bar{a}_1 \sin\frac{\pi x}{l_1} + \bar{a}_2 \sin\frac{2\pi x}{l_1} + \bar{a}_3 \sin\frac{3\pi x}{l_1} \quad \text{(for side span)} \qquad (132)$$

the natural periods and modes were obtained as shown in Table 108. Configurations of these modes are shown in Fig. 109. These were obtained on the high speed digital computer, FACOM 128B.

Comparing Table 108 and Fig. 109 with Tables 105, 106 and Figs. 107, 108, it is concluded that the natural modes and periods obtained by the equations derived in this paper fairly well coincide with the results obtained by the Bleich Method especially in the first few modes of vibration.

114. Summary on the Natural Periods and Modes

Studies in this chapter have been concerned with the computation of the natural periods and modes of free vibration of the suspension bridge.

Vibration modes of the system can be separated into two groups with different characteristics. In one group, the displacement of the suspended structures are predominent, such as the 1st through the 7th symmetric and the 1st through 6th asymmetric modes in Figs. 107 and 108, and in the other group, displacements of the towers are predominent. The vibration

modes in which displacement of the towers are predominent are only obtainable by taking the effects of the stiffness and the masses of the towers.

From the results obtained in this chapter, it might be concluded that the vibration modes with the predominent displacements of the towers contribute much to the earthquake response of the suspension bridge because their natural periods are in the range of periods of earthquake ground motions. Effects of these vibration modes will be discussed in more detail in the next chapter.

Two vibration modes of the towers, such as the 8th symmetric and the 7th asymmetric modes, are almost the same as shown in Figs. 107 and 108 excepting that they are symmetric and asymmetric. This means that the coupling action between the suspended structures and the towers are not significant in the system considered.

The natural periods and modes obtained in this chapter will be used for modal analysis on forced vibration and static deflections effectively. One of the objects of obtaing the natural periods and modes is their application to the modal analysis.

Table 105 (a) Symmetric Modes (Approx. I)

Modes	1	2	3	4	5	6	7	8	9	10	11
	Characteristic Values										
λ_i	.2930	1.0208	1.9928	2.0421	2.9491	4.2385	4.5435	21.734	129.83	358.37	781.86
T_i	11.608	6.2191	4.4511	4.3969	3.6588	3.0519	2.9478	1.3477	.5514	.3319	.2247
	Natural Modes, Normalized (10^{-1}m)										
$Y_1=Y_{21}$	-.1734	-.0834	-.1697	.3883	-.0203	.2901	.0122	-.0105	.0044	-.0013	-.0097
$Y_2=Y_{20}$	-.2413	-.1251	-.3042	0	-.0583	-.3626	-.0058	-.0099	.0044	-.0013	-.0097
$Y_3=Y_{19}$	-.1734	-.0834	-.1697	-.3883	-.0203	.2901	.0122	-.0106	.0044	-.0013	-.0097
$Y_4=Y_{18}$	.0547	.0156	-.0006	0	-.0059	-.0063	.0015	-.0321	.0881	-.0720	-1.193
$Y_5=Y_{17}$	.0274	.0080	-.0003	0	-.0033	-.0037	.0009	-.4501	.4377	-.1504	.0549
$Y_6=Y_{16}$	.0105	.0031	-.0001	0	-.0014	-.0016	.0004	-.3529	-.2623	.2854	-.0266
$Y_7=Y_{15}$	.0022	.0006	0	0	-.0003	-.0004	.0001	-.1110	-.2371	-.3546	.0070
$Y_8=Y_{14}$	.0934	.3100	-.1564	0	-.3845	.0208	.1543	.0107	-.0044	.0013	.0097
$Y_9=Y_{13}$	.2005	.1991	-.3092	0	.2284	.0243	-.2705	.0101	-.0044	.0013	.0097
$Y_{10}=Y_{12}$	.2864	-.2078	-.1755	0	.1195	.0027	.3620	.0102	-.0044	.0013	.0097
Y_{11}	.3192	-.4313	-.0335	0	-.4076	.0355	-.3827	.0102	-.0044	.0013	.0097

Table 105 (b) Asymmetric Modes (Approx. I)

Modes	1	2	3	4	5	6	7	8	9	10
	Characteristic Values									
λ_i	.4658	.5011	1.9241	2.0421	3.8546	4.1984	21.167	125.39	350.79	430.40
T_i	9.2067	8.8771	4.5297	4.3969	3.2003	3.0666	1.3657	.5611	.3354	.3028
	Natural Modes, Normalized (10^{-1}m)									
$Y_1 = -Y_{21}$	0	-.2731	0	.3883	0	.2744	-.0219	.0101	-.0072	-.0164
$Y_2 = -Y_{20}$	0	-.3871	0	0	0	-.3884	-.0202	.0100	-.0072	-.0164
$Y_3 = -Y_{19}$	0	-.2731	0	-.3883	0	.2744	-.0219	.0101	-.0072	-.0164
$Y_4 = -Y_{18}$	0	.0763	0	0	0	-.0134	-.0640	.1960	-.3978	-1.111
$Y_5 = -Y_{17}$	0	.0385	0	0	0	-.0078	-.4544	.4255	-.1064	.1421
$Y_6 = -Y_{16}$	0	.0149	0	0	0	-.0034	-.3486	-.2689	.2595	-.1192
$Y_7 = -Y_{15}$	0	.0031	0	0	0	-.0008	-.1087	-.2330	-.3467	.0895
$Y_8 = -Y_{14}$	-.2746	0	.3883	0	.2746	0	0	0	0	0
$Y_9 = -Y_{13}$	-.3883	0	0	0	-.3883	0	0	0	0	0
$Y_{10} = -Y_{12}$	-.2746	0	-.3883	0	.2746	0	0	0	0	0
Y_{11}	0	0	0	0	0	0	0	0	0	0

Table 106 (a) Symmetric Modes (10^{-3} m)

Modes	1	2	3	4	5	6	7	8
λ_i	0.29289	1.02074	1.99274	2.04212	2.94913	4.23837	4.54347	24.2289
T_i (sec)	11.6099	6.2190	4.4510	4.3968	3.6588	3.0520	2.9477	1.2765
$Y_{1}=Y_{29}$	-17.3369	-8.3377	-16.9752	38.8261	-2.0305	29.0137	1.2199	-1.1630
$Y_{2}=Y_{28}$	-24.1286	-12.5068	-30.4211	0	-5.8263	-36.2623	-0.5841	-1.0886
$Y_{3}=Y_{27}$	-17.3369	-8.3375	-16.9620	-38.8320	-2.0308	29.0135	1.2200	-1.1630
$Y_{4}=Y_{26}$	5.4676	1.5572	-0.0589	0	-0.5873	-0.6337	0.1497	-3.9678
$Y_{5}=Y_{25}$	4.0243	1.1596	-0.0446	0	-0.4523	-0.5003	0.1189	-30.6719
$Y_{6}=Y_{24}$	2.7952	0.8153	-0.0319	0	-0.3289	-0.3727	0.0891	-44.1279
$Y_{7}=Y_{23}$	1.8222	0.5376	-0.0213	0	-0.2235	-0.2586	0.0621	-44.2953
$Y_{8}=Y_{22}$	1.0192	0.3253	-0.0131	0	-0.1389	-0.1634	0.0394	-35.5998
$Y_{9}=Y_{21}$	0.5739	0.1725	-0.0070	0	-0.0753	-0.0899	0.0218	-23.1780
$Y_{10}=Y_{20}$	0.2376	0.0720	-0.0030	0	-0.0320	-0.0387	0.0094	-11.3238
$Y_{11}=Y_{19}$	0.0543	0.0166	-0.0007	0	-0.0075	-0.0092	0.0022	-3.0215
$Y_{12}=Y_{18}$	9.3435	30.9957	-15.6410	0	-38.4454	2.0821	15.4286	1.1711
$Y_{13}=Y_{17}$	20.0526	19.9085	-30.9159	0	22.8378	2.4342	-23.8837	1.1132
$Y_{14}=Y_{16}$	28.6422	-20.7786	-17.5510	0	11.9482	0.2702	36.1968	1.1227
Y_{15}	31.9179	-43.1283	-3.3493	0	-40.7592	3.5530	-38.2706	1.1218

Table 106 (a) Symmetric Modes (10^{-3} m)
(continued)

Modes	9	10	11	12	13	14	15
λ_i	183.9116	620.5125	1364.1351	2186.5340	3055.6526	4607.7709	7263.6993
T_i (sec)	0.4633	0.2522	0.1701	0.1344	0.1137	0.0926	0.0737
$Y_1=Y_{29}$	0.6341	-0.4632	0.4098	-0.3547	0.1203	-0.0120	-0.0004
$Y_2=Y_{28}$	0.6294	-0.4623	0.4094	-0.3545	0.1202	-0.0120	-0.0004
$Y_3=Y_{27}$	0.6341	-0.4632	0.4098	-0.3547	0.1203	-0.0120	-0.0004
$Y_4=Y_{26}$	18.1741	-45.2513	88.2091	-122.4710	58.0688	-8.7166	-0.4688
$Y_5=Y_{25}$	53.3473	-58.1771	28.8967	31.4858	-40.3609	11.1214	0.9382
$Y_6=Y_{24}$	41.4264	2.9362	-42.0030	1.0848	48.5059	-23.8276	-3.0493
$Y_7=Y_{23}$	4.8028	37.8977	-2.6621	-30.3438	-29.4200	37.6871	8.0227
$Y_8=Y_{22}$	-25.0006	15.8678	31.8939	14.5594	-6.5672	-42.1675	-17.1725
$Y_9=Y_{21}$	-33.2365	-19.5593	4.9033	17.3276	26.6776	25.4974	29.3909
$Y_{10}=Y_{20}$	-23.3324	-28.8501	-24.8140	-15.0526	-9.5354	5.3224	-37.4683
$Y_{11}=Y_{19}$	-7.9546	-13.3862	-17.2160	-16.6948	-21.0987	-27.8081	35.6705
$Y_{12}=Y_{18}$	-0.6348	0.4634	-0.4099	0.3548	-0.1203	0.0120	0.0004
$Y_{13}=Y_{17}$	-0.6310	0.4626	-0.4096	0.3546	-0.1203	0.0120	0.0004
$Y_{14}=Y_{16}$	-0.6314	0.4627	-0.4096	0.3546	-0.1203	0.0120	0.0004
Y_{15}	-0.6314	0.4627	-0.4096	0.3546	-0.1203	0.0120	0.0004

Table 106 (b) Asymmetric Modes (10^{-3} m)

mModes	1	2	3	4	5	6	7
λ_i	0.46575	0.50079	1.92507	2.04212	3.85462	4.19823	23.37987
T_i (sec)	9.2067	8.8787	4.5297	4.3968	3.2003	3.0665	1.2994
$Y_1=-Y_{29}$	0	-27.3079	0	38.8291	0	27.4399	-2.3827
$Y_2=-Y_{28}$	0	-38.7116	0	0	0	-38.8400	-2.2238
$Y_3=-Y_{27}$	0	-27.3081	0	-38.8290	0	27.4398	-2.3828
$Y_4=-Y_{26}$	0	7.6266	0	0	0	-1.3415	-7.8084
$Y_5=-Y_{25}$	0	5.6320	0	0	0	-1.0582	-32.5701
$Y_6=-Y_{24}$	0	3.9254	0	0	0	-0.7876	-44.5771
$Y_7=-Y_{23}$	0	2.5673	0	0	0	-0.5462	-43.9347
$Y_8=-Y_{22}$	0	1.5425	0	0	0	-0.3449	-34.9752
$Y_9=-Y_{21}$	0	0.8130	0	0	0	-0.1896	-22.6391
$Y_{10}=-Y_{20}$	0	0.3373	0	0	0	-0.0816	-11.0170
$Y_{11}=-Y_{19}$	0	0.0773	0	0	0	-0.0194	-2.9302
$Y_{12}=-Y_{18}$	-27.4564	0	38.8290	0	27.4563	0	0
$Y_{13}=-Y_{17}$	-38.8290	0	0	0	-38.8291	0	0
$Y_{14}=-Y_{16}$	-27.4562	0	-38.8291	0	27.4562	0	0
Y_{15}	0	0	0	0	0	0	0

Table 106 (b) Asymmetric Modes (10^{-3} m)
(continued)

Modes	8	9	10	11	12	13	14
λ_i	167.2663	522.6413	1093.9553	1902.8347	3002.8718	4606.2799	7263.6945
T_i (sec)	0.4858	0.2748	0.1900	0.1440	0.1147	0.0935	0.0737
$Y_{1}=-Y_{29}$	1.3673	-0.9934	0.6366	-0.2827	0.0753	-0.0093	-0.0004
$Y_{2}=-Y_{28}$	1.3563	-0.9908	0.6359	-0.2825	0.0753	-0.0093	-0.0004
$Y_{3}=-Y_{27}$	1.3673	-0.9936	0.6366	-0.2827	0.0753	-0.0093	-0.0004
$Y_{4}=-Y_{26}$	35.5916	-81.6658	109.8379	-84.9183	35.7281	-6.7708	-0.4119
$Y_{5}=-Y_{25}$	56.7457	-48.6481	-5.7756	49.5532	-38.4806	10.8799	0.9344
$Y_{6}=-Y_{24}$	37.6375	15.0736	-36.3005	-18.2287	50.0487	-23.6895	-3.0472
$Y_{7}=-Y_{23}$	1.0389	35.0868	13.6664	-28.1570	-32.7091	37.6832	8.0221
$Y_{8}=-Y_{22}$	-25.8889	8.4415	29.3668	23.5142	-5.4944	-42.2275	-17.1723
$Y_{9}=-Y_{21}$	-31.9925	-21.5822	-2.5342	15.9129	28.2049	25.5584	29.3909
$Y_{10}=-Y_{20}$	-21.8399	-26.4421	-25.1196	-19.8990	-10.6626	5.3160	-37.4684
$Y_{11}=-Y_{19}$	-7.3268	-11.5654	-15.1129	-18.5769	-22.3541	-27.8549	35.7023
$Y_{12}=-Y_{18}$	0	0	0	0	0	0	0
$Y_{13}=-Y_{17}$	0	0	0	0	0	0	0
$Y_{14}=-Y_{16}$	0	0	0	0	0	0	0
Y_{15}	0	0	0	0	0	0	0

Table 108 Natural Periods and Modes obtained by the Bleich Method

(a) Symmetric Modes

Modes	1	2	3	4	5	6
Periods (sec)	11.7843	5.8806	4.4742	3.8312	2.9297	2.0686
a_1	1	-0.2726	1.1907	0	0.05148	0.03340
a_3	-0.05945	1	1	0	0.02287	0.01294
a_5	-0.00794	0.01641	-0.17136	0	1	0.01302
$\bar{a}_1$	-0.7488	-0.4440	1.5132	0	0.05646	0.03497
$\bar{a}_2$	0	0	0	1	0	0
$\bar{a}_3$	-0.00639	0.0116	-0.10310	0	-0.016996	1

$a_2 = a_4 = a_6 = 0$

(b) Asymmetric Modes

Modes	1	2	3	4	5	6
Periods (sec)	8.9516	8.8508	3.9662	3.8312	2.2690	2.1452
a_2	1	0	0	0	0	0
a_4	0	0	1	0	0	0
a_6	0	0	0	0	1	0
$\bar{a}_1$	0	1	0	0	0	0
$\bar{a}_2$	0	0	0	1	0	0
$\bar{a}_3$	0	0	0	0	0	1

$a_1 = a_3 = a_5 = 0$

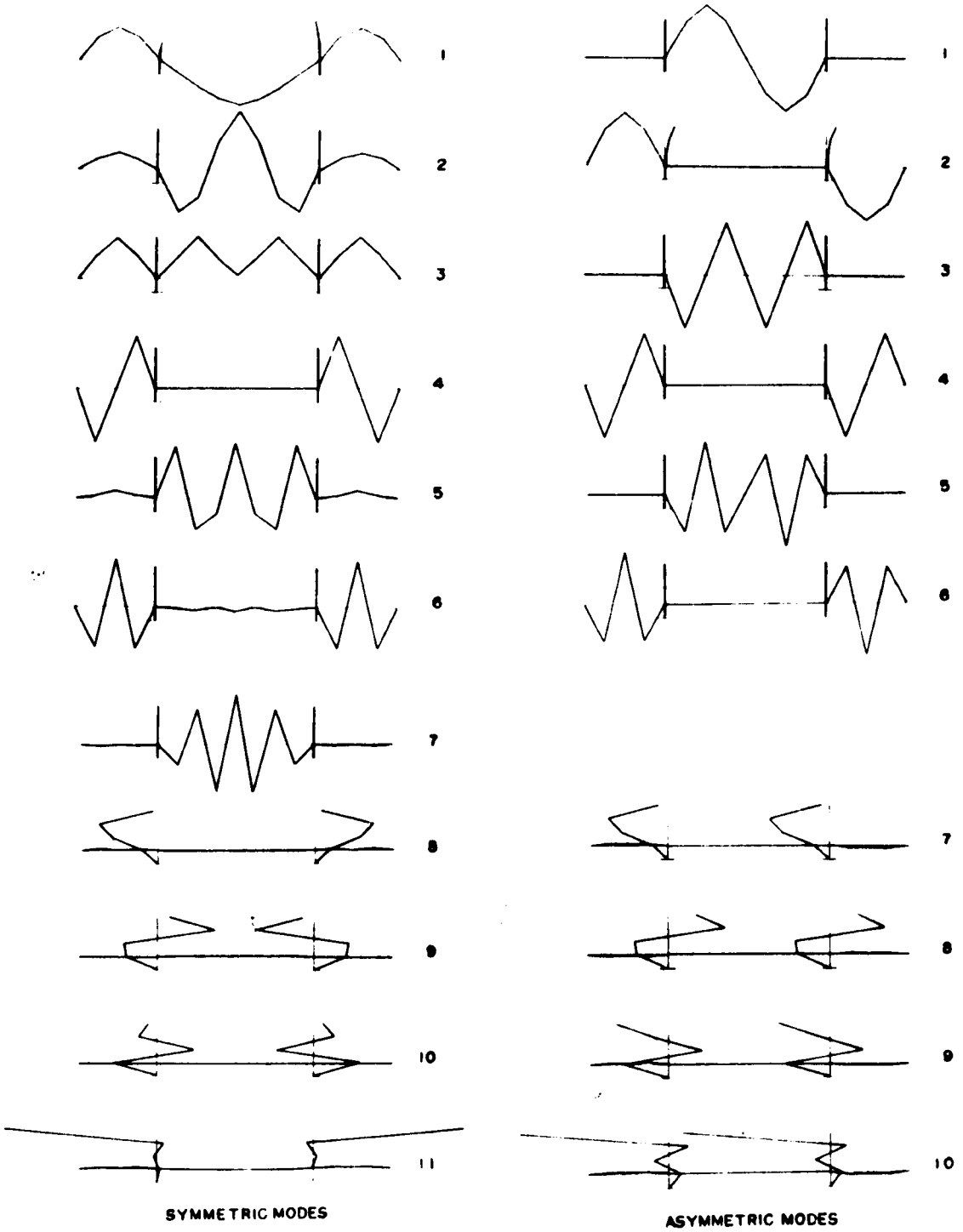

Fig. 107 Vibration Modes
(Approximation I)

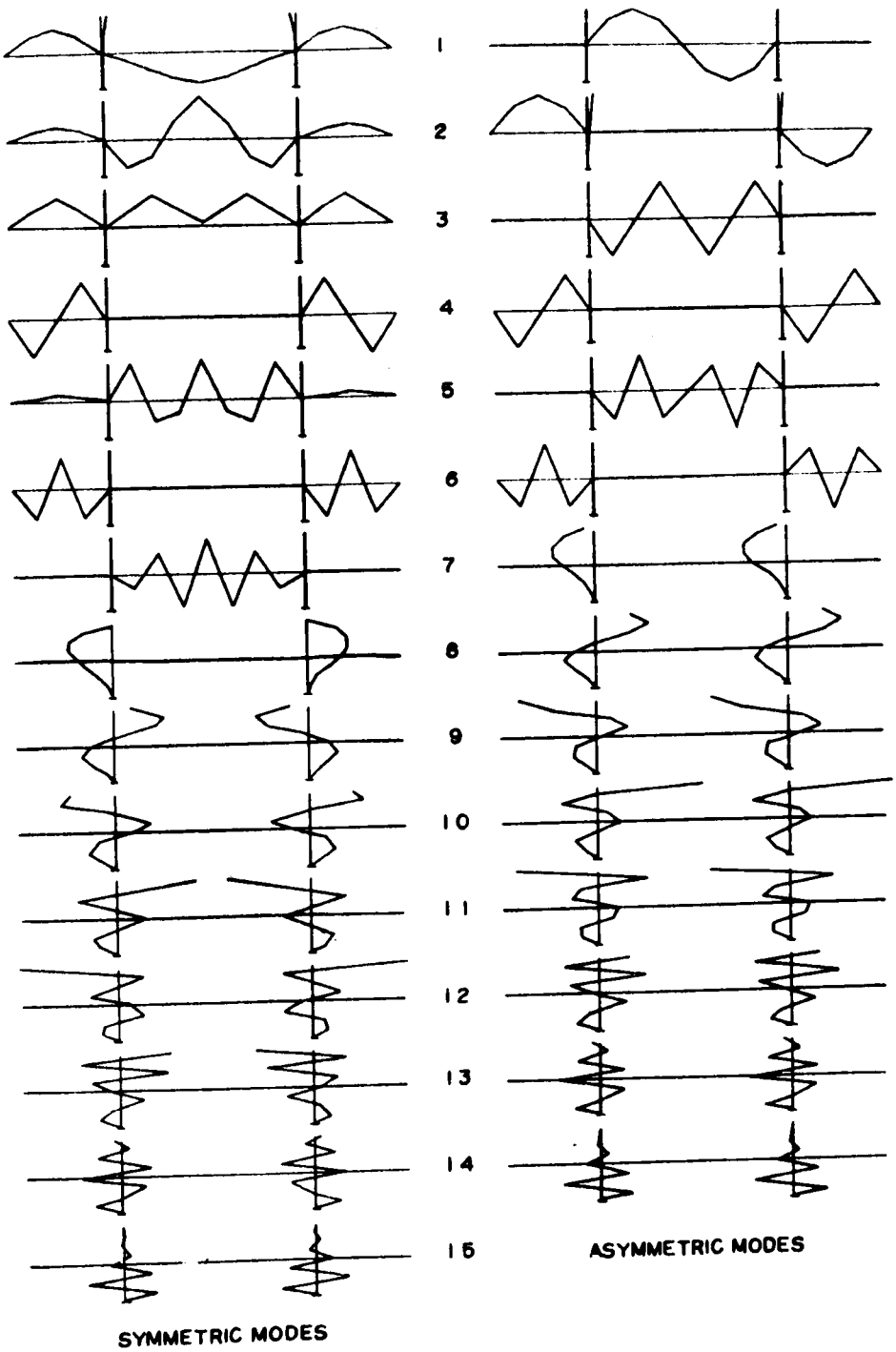

Fig. 108 Vibration Modes
(Approximation II)

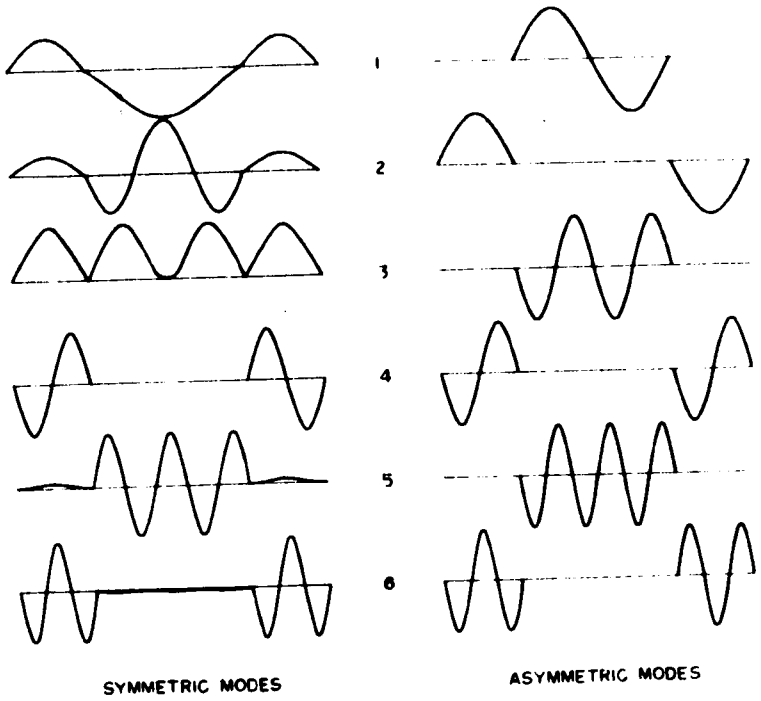

Fig. 109 Vibration Modes
(Bleich Method)

III. FORCED VIBRATION DUE TO GROUND MOTIONS

115. Modal Analysis

The problems of multi-degrees of freedom systems can be solved by applying the modal analysis.

The equation of motion given by

$$[A]\ (\ddot{y}_r) + [B]\ (y_r) + (P_r(t)) = 0 \tag{133}$$

has dependent variable y_r which specifies the deflection of the system.

The displacement y_r of the system can be transformed to the other time function q_i which specifies time dependency of the ith mode of vibration as the following employing the normal modes obtained in the previous chapter.

$$(y_r) = [Y]\ (q_i) \tag{134}$$

In Eq. (134) (y_r) and (q_i) are the column vector with elements y_r and q_i, and $[Y]$ is the matrix of the normal modes of the system and contains element $Y_r^{(i)}$ in its ith column and rth row. In these notations, r specifies a number of the point of the system, and i specifies a number of the normal modes.

Substituting Eq. (134) into Eq. (133), one obtains

$$[A]\ [Y]\ (\ddot{q}_i) + [B]\ [Y]\ (q_i) + (P_r(t)) = 0 \tag{135}$$

Multiplying the transposed matrix $[Y']$ of the matrix $[Y]$, and using the conditions of orthogonality of the normal modes of vibration and the relation

$$\lambda_i = (Y_r^{(i)\prime})\ [B]\ (Y_r^{(i)})$$

the following matrix equation can be obtained provided that all the modes of vibration are normalized.

$$(\ddot{q}_i) + [\lambda_i]\ (q_i) + [Y']\ (P_r(t)) = 0 \tag{136}$$

where,

$[\lambda_i]$ = diagonal matrix with the diagonal element λ_i.

Eq. (136) can be written in the form

$$(\ddot{q}_i) + (\lambda_i q_i) + [Y'] \ (P_r(t)) = 0 \tag{137}$$

Matrix equation Eq. (137) consists of the system of differential equations having a separated single dependent variable q_i and can be solved by ordinary method of solution of one mass system.

If all q_i's are obtained for the specific external force $(P_r(t))$ the displacements can be computed by Eq. (134).

Eq. (137) is given in the following in practical form.

$$\ddot{q}_i + \lambda_i q_i + \sum_{r=1}^{n} Y_r^{(i)} P_r(t) = 0 \tag{138}$$

$$(i = 1, 2, 3, \ldots\ldots, n)$$

116. Application of the Modal Analysis to Static Displacements

The modal analysis is applicable to the problems of statics letting the acceleration of the time function q equal to zero, and $P_r(t) = P_r(st)$. Then

$$q_{i,st} = - \frac{\sum_{r=1}^{n} Y_r^{(i)} P_r(st)}{\lambda_i} \tag{139}$$

where;

$q_{i,st}$ = static response of time function q_i due to the static external force $P_r(st)$,

$P_r(st)$ = static external force determined from the static ground displacement $Z_A(st)$ etc.

Substituting Eq. (139) into Eq. (134), one obtains static displacements $y_{r,st}$ of the system.

The static displacements of the system of Approximation II due to the ground motions (static displacements) $Z_A(st) = 1$ or $Z_B(st) = 1$ were computed.

Table 109 shows the values of $q_{i,st}$ due to the ground displacements $Z_A(st) = 1$, $Z_B(st) = 1$, $Z_C(st) = 1$, and $Z_D(st) = 1$. Table 110 shows static displacements due to the ground displacements $Z_A(st) = 1$, and $Z_B = 1$.

Figs. 110 (a) and (b) show their configurations.

The static displacements are also obtainable directly from the system of the equations, Eq. (133), setting $\ddot{y}_r = 0$.

The effects of the displacement of the anchorage to the suspended structures are much more greater than those of the tower as shown in Fig. 110.

117. Steady Forced Vibration and Resonance Curves

To obtain the fundamental characteristics of the dynamic response of the structures, it is preferable to examine the steady forced vibration before studying the more general case of transient vibration.

Assuming that a ground motion

$$Z = 1 \times \sin \frac{2\pi t}{T_\omega}$$

is applied at the base of the tower or the anchorage, Eq. (138) is given by

$$\ddot{q}_i + \lambda_i q_i + \sum_{r=1}^{n} Y_r^{(i)} P_r(st) \sin \frac{2\pi t}{T_\omega} = 0 \qquad (140)$$

When the free vibration died away, the solution may be written in the form of

$$q_i = \frac{q_{i,st}}{1 - (\frac{T_i}{T_\omega})^2} \sin \frac{2\pi t}{T_\omega} \qquad (141)$$

where,

T_i = natural period of the ith mode vibration.

The value of $q_{i,st}$ are given in Table 109. Substituting Eq. (141) into Eq. (134), one obtains the dynamic displacement as

$$y_r = \sum_{i=1}^{n} q_i Y_r^{(i)} = \sum_{i=1}^{n} \frac{q_{i,st} Y_r^{(i)}}{1 - (\frac{T_i}{T_\omega})^2} \sin \frac{2\pi t}{T_\omega} \qquad (142)$$

The maximum amplitude is

$$y_{r,max} = \sum_{i=1}^{n} \frac{q_{i,st} Y_r^{(i)}}{1 - (\frac{T_i}{T_\omega})^2} \qquad (143)$$

If the period of the ground motion is infinitively large, the maximum amplitude coincide with the static displacement $y_{r,st}$.

Dynamic response of the bending moments can be obtained by substituting Eq. (143) into Eqs. (104), (120), or (121).

Figs. 111 (a) through (g) show steady forced responses of the bending momsnts due to the ground motion

$$Z_B = 1 \times \sin \frac{2\pi t}{T_\omega}$$

in the form of amplification factors which are defined by

$$AF = M_{r,max} / M_{r,st} \qquad (144)$$

where,

$M_{r,max}$ = maximum dynamic response of the bending moment M_r due to the ground motion $Z_B = 1 \times \sin (2\pi t/T_\omega)$,

$M_{r,st}$ = bending moment due to the statical displacement $Z_B = 1$.

118. Transient Response to a Simple Ground Motion

As the first illustration of the problems of transient vibration of the system, response to a simple ground motion will be discussed. Because no strong motion records of earthquakes are available in Japan, such a simple method of application is only a method adoptable in the primary analysis.

In this example the ground motion is assumed to be a displacement with a simple harmonic shape given as

$$Z = A (1 - \cos \frac{2\pi t}{T_\omega}) \qquad 0 \leq t \leq T_\omega$$
$$= 0 \qquad t > T_\omega \qquad (145)$$

and shown in Fig.112.

In numerical analysis the amplitude is assumed to be A = 1m, then the maximum displacement of the ground motion is 2 m. Because of the linearity of the system considered, response to any amplitude can be obtained by linear reduction.

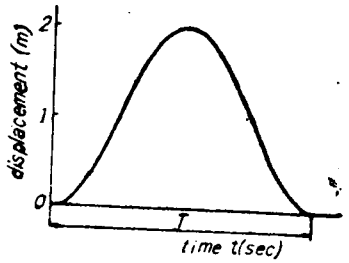

Fig. 112 Ground Motion

Substituting Eq. (145) into Eq. (138) one obtains

$$\ddot{q}_i + \lambda_i q_i + \left(\sum_{i=1}^{n} Y_r^{(i)} P_r(st) \right) \left(1 - \cos \frac{2\pi t}{T_\omega}\right) = 0 \qquad (146)$$

Assuming the initial conditions

$$q_i = \dot{q}_i = 0 \text{ at the time } t = 0,$$

complete solution of the problem is given as follows.

In the range of $0 \leq t \leq T_\omega$ (forced vibration era)

$$q_i = q_{i,st} \left(1 - \frac{1}{1 - (\frac{T_i}{T_\omega})^2} \cos \frac{2\pi t}{T_\omega} - \frac{1}{1 - (\frac{T_i}{T_\omega})^2} \cos \frac{2\pi t}{T_i}\right) \qquad (T_i \neq T_\omega)$$

$$q_i = q_{i,st} \left(1 - \cos \frac{2\pi t}{T_\omega} - \frac{1}{2} \frac{2\pi t}{T_\omega} \sin \frac{2\pi t}{T_\omega}\right) \qquad (T_i = T_\omega)$$

In the range of $t > T_\omega$ (free vibration era)

$$q_i = 2\, q_{i,st} \frac{1}{1 - (\frac{T_\omega}{T_i})^2} \sin \left(\frac{2\pi t}{T_i} + \frac{\pi T_i}{T_\omega}\right) \qquad (T_i \neq T_\omega)$$

$$q_i = -\pi\, q_{i,st} \sin \frac{2\pi t}{T_i} \qquad (T_i = T_\omega)$$

..... (147)

In the design purpose, responses of the bending moments in the system are much more important than those of the displacements. The responses of the bending moments on the following cross sections were computed :

(1) the tower base, (2) the center of the tower, and (3) the center of the center span suspended structure.

The ground motion of Eq. (145) is possible to act to any points connecting the structure to the ground, those are left and right side cable anchorages and two tower bases, and each ground motion has an individual effect on the structure as shown in Fig. 113. Fig. 113 shows an example for the ground motion with period T_ω = 0.75 sec. Because the structure has long span lwngths, any phase differences between each disturbance is possible. The responses which are given in the following are obtained by adding the effect of each disturbance graphically so as to make the resultant bending moment maximum.

Fig. 114 (a) and (b) show the bending moment-time curves to the point of the center of the tower due to the disturbances with different durations of ground motions, T = 0.125, 0.250, 0.375, (Fig. 114 (a)), 0.50, 0.75, 1.00, 1.50 (Fig. 114 (b)) in sec. Fig. 115 shows the bending moment-time curves for the center of the center span due to the same disturbances. In Fig. 115, are given fairly different response properties from Fig. 114, and the maximum moment is much less than that of the tower.

Fig. 116 shows the spectra for the maximum bending moment at the center of the tower resulting from the disturbance of Eq. (145). Fig. 117 shows the spectra for the maximum bending moment at the tower base, and Fig. 118 shows the spectra at the center of the center span suspended structure. The spectra of Figs. 116 and 117 have their maximum values at about the period T_ω = 0.25 sec. and Fig. 118 at about T_ω = 4 sec.

119. Response for Arbitrary Ground Motion and Computer Program

The problem in the preceding section was solved analytically and its solution was given in Eq. (147). For an arbitrary ground motion such as the earthquake, Eq. (138) has to be solved by methods of numerical integration.

Many methods have been introduced for numerical integration but these are just too time consuming if these calculations are carried out by desk calculators.

The numerical integration procedure which may be adopted to the high speed digital computers are the Runge-Kutta Method and the Newmark β Method. (105) (106)

Newmark β Method will be explained in detail in PART II of this paper. The general program of "Solution of n-Simultanious Second Order Differential Equations by Newmark β Method" was provided by the author and listed as one of the KDC-I Subroutines. This program will be applied to the problem considered.

To apply the subroutine mentioned (NEWM) two auxiliary routines are necessary. One is the routine of computing the accelerations by the fundamental equations of motion, Eq. (138) in this case, and the other is the routine of printing the results in the given format. The first auxiliary routine, specified by (AUX), for the computation of Eq. (138) is given in Prog. 101, and its flow diagram is in Fig. 119. The second auxiliary routine, specified by (PRINT) is given in Prog. 102 and in Fig. 120. By using the routine (PRINT) the complete time history is printed out at every three time interval given by h.

Lincages of these auxiliary routines and the other forms of the program are almost the same as in the problem given in PART II.

120. Response to 1957 South California Earthquake

Response to the 1957 So. California Earthquake was computed on the KDC-I, Kyoto University High Speed Digital Computer, using the programs given.

To save the computing time, a number of responses obtained on the computer was limited to the bending moments at the section 2, 6, 8, 10, and 15 and the displacements at the sections 2, 4, 6, 8, 10, 11, and 15. A time interval in the numerical integration is selected as h = 0.018939 sec and the dynamic responses were printed out at every three time intervals, 0.056867 sec.

Time history curves were obtained for two kinds of different external disturbances, which are

(Type A) : ground motion applied to the left side anchorage.

(Type B) : ground motion applied to the base of the left side tower.

The computing time required for three steps of time interval is, including 20 sec printing time, about 110 sec, and it required about 3.5 hours for complete computing run for each type of ground motions.

Figs. 121 (a) through (d) show response time history curves to the Type A ground motions, and Figs. 122 (a) through (d) are to the Type B ground motions.

The maximum responses in these computing runs are tabulted in Table 111. The maximum values of time function $q_i(t)$ of each mode, the modal maxima, are given in Table 112.

According to the theory of random vibration the maximum dynamic response can be approximately computed by the following relation.

Approximate Maximum Response

$$= \sqrt{\sum (\text{Modal Maximum Responses})^2} \qquad (148)$$

The approximate maximum response computed from Eq. (148) by using the modal maximum response given in Table 112 are also shown in Table 111. Comparing the values in Table 111, Eq. (148) can be roughly applied to the problem of earthquake response of the suspension bridges.

121. Equation of Motion of the System with Damping

Damping forces were disregarded in the analysis discussed so far. For a damped system, with certain exceptions, the damped modes will be coupled, and free vibration can not take place in any mode shape. If the damping coefficients of the system satisfy certain conditions described hereafter, the modal analysis is applicable to the system with damping.

If the damping force acting to a point r is assumed to be proportional to the velocity of the point and to be expressed as

$$\text{Damping Force} = \alpha \dot{y}_r = \sum_{i=1}^{n} \delta_{r.i} \dot{q}_i \nu_r^{(i)} \qquad (149)$$

and assuming the condition

$$\delta_{r,i} = 2 \beta_i \omega_i \left(\frac{W_r}{g}\right) \qquad (150)$$

where $\omega_i = \sqrt{\lambda_i}$,

the system of equation of motion Eq. (138) to the system without damping can be rewritten as follows.

$$\ddot{q}_i + 2 \beta_i \omega_i \dot{q}_i + \lambda_i q_i + \sum_{r=1}^{n} \nu_r^{(i)} p_r(t) = 0 \qquad (151)$$

$$(i = 1, 2, 3, 4, \ldots\ldots, n)$$

In Eq. (151), the damping constant β_i is a magnitude fixed to a vibration mode under the assumptions of Eqs. (149) and (150). Actually, β_i is the function of the vibration modes but for the ordinary steel structures it has not much relation to the vibration velocity. β_i is also the function of vibration amplitude as shown in PART III.

The effects of damping force is illustrated in Fig. 123 in which the response history curves of the systems with and without damping. Damping constant β is chosen as $\beta = 0.02$ for the system with damping. This is somewhat overestimated, and real damping constant may probably be less than this value.

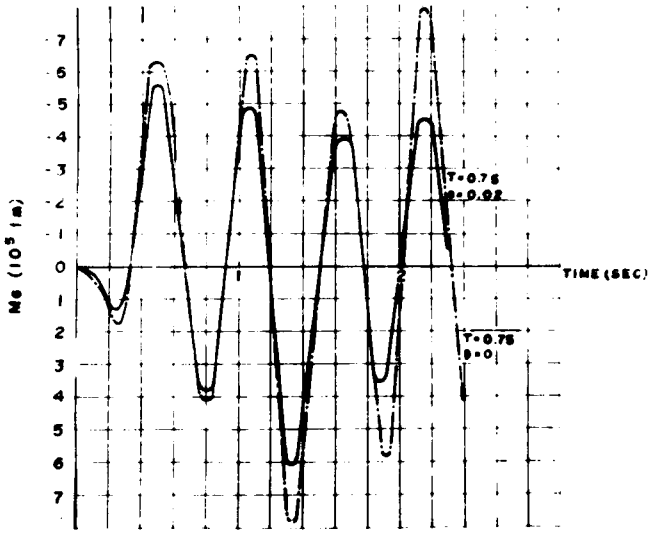

Fig. 123

Table 109 $q_{i,st}$ (Approximation II)

Mode i	for $Z_A = 1$	for $Z_B = 1$	for $Z_C = 1$	for $Z_D = 1$
SYMMETRIC				
1	25.109891	4.981658	4.981658	25.109891
2	-10.725641	0.492322	0.492322	-10.725641
3	-34.248832	-0.011761	-0.011761	-34.248832
4	0	0	0	0
5	-6.031013	-0.098022	-0.098022	-6.031013
6	3.498690	-0.093800	-0.093800	3.498690
7	0.844487	0.021825	0.021825	0.844487
8	-2.215390	-10.669723	-10.669723	-2.215390
9	1.258476	-7.015065	-7.015065	1.258476
10	-0.923075	-5.077886	-5.077886	-0.923075
11	0.817352	-3.818245	-3.818245	0.817352
12	-0.707687	-2.697694	-2.697694	-0.707687
13	0.240041	-2.731554	-0.731554	0.240041
14	-0.023892	-2.752897	-2.752897	-0.023892
15	-0.000815	2.636935	2.636935	-0.000815
ASYMMETRIC				
1	0	0	0	0
2	-3.435452	4.300319	-4.300319	3.435452
3	0	0	0	0
4	0	0	0	0
5	0	0	0	0
6	-0.026885	-0.198900	0.198900	0.026885
7	-4.530240	-10.580115	10.580115	4.530240
8	2.712169	-6.908281	6.908281	-2.712169
9	-1.978794	-4.935787	4.935787	1.978794
10	1.269481	-3.892629	3.892629	-1.269481
11	-0.563911	-3.293670	3.293670	0.563911
12	0.150297	-2.927597	2.927597	-0.150297
13	-0.018565	-2.758112	2.758112	0.018565
14	-0.000716	2.638857	-2.638857	0.000716

Table 110 Static Displacements $y_{r,st}$
(Approximation II)

Point r	due to $Z_A = 1$	due to $Z_B = 1$
1	0.46501	-0.18724
2	0.63291	-0.25480
3	0.46499	-0.18724
4	0.82819	0.06846
5	0.60854	0.31745
6	0.42063	0.52822
7	0.27296	0.69382
8	0.16104	0.81699
9	0.08534	0.90426
10	0.03520	0.96061
11	0.00807	0.99083
12	0.68558	0.05642
13	1.19512	0.09817
14	1.49828	0.12326
15	1.60034	0.13165
16	1.49828	0.12326
17	1.19512	0.09817
18	0.68558	0.05642
19	-0.00081	-0.00023
20	-0.00380	-0.00025
21	-0.00922	-0.00084
22	-0.01940	-0.00179
23	-0.02950	-0.00250
24	-0.04530	-0.00384
25	-0.06576	-0.00557
26	-0.09216	-0.00752
27	0.24393	0.02054
28	0.33147	0.02806
29	0.24395	0.02054

Static Displacements due to $Z_A = 1$

Static Displacements due to $Z_B = 1$

Fig. 110

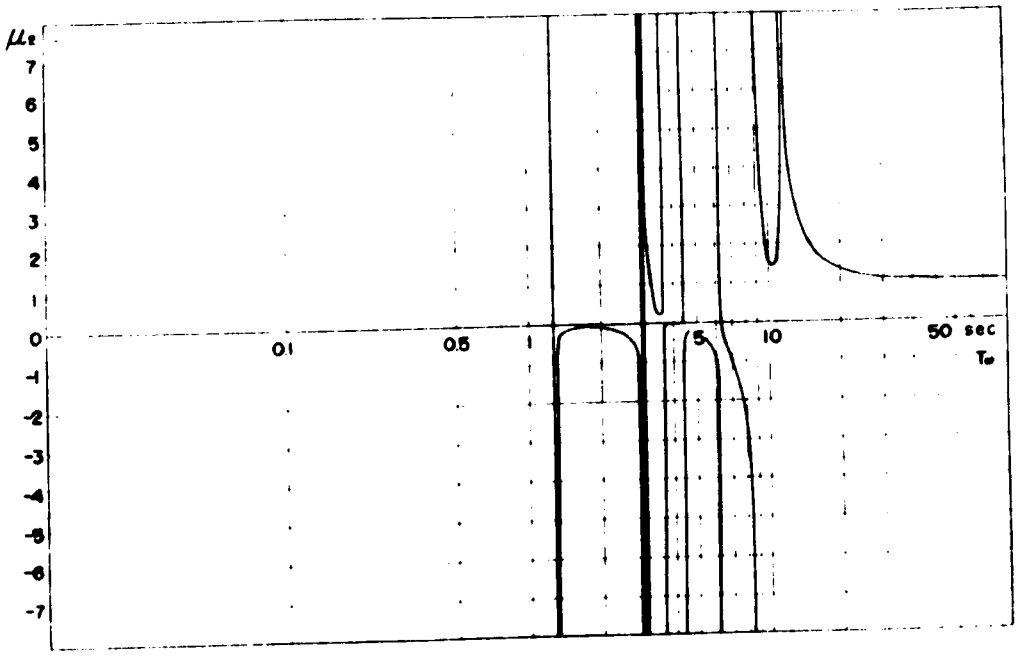

Fig. 111 (a) Resonance Curve
(section 2)

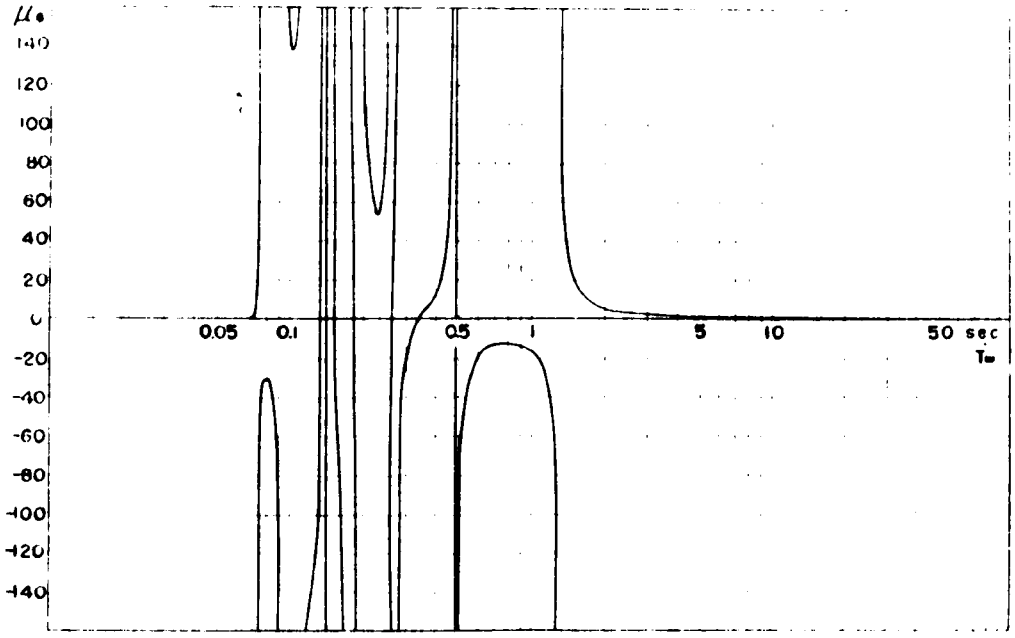

Fig. 111 (b) Resonance Curve
(section 6)

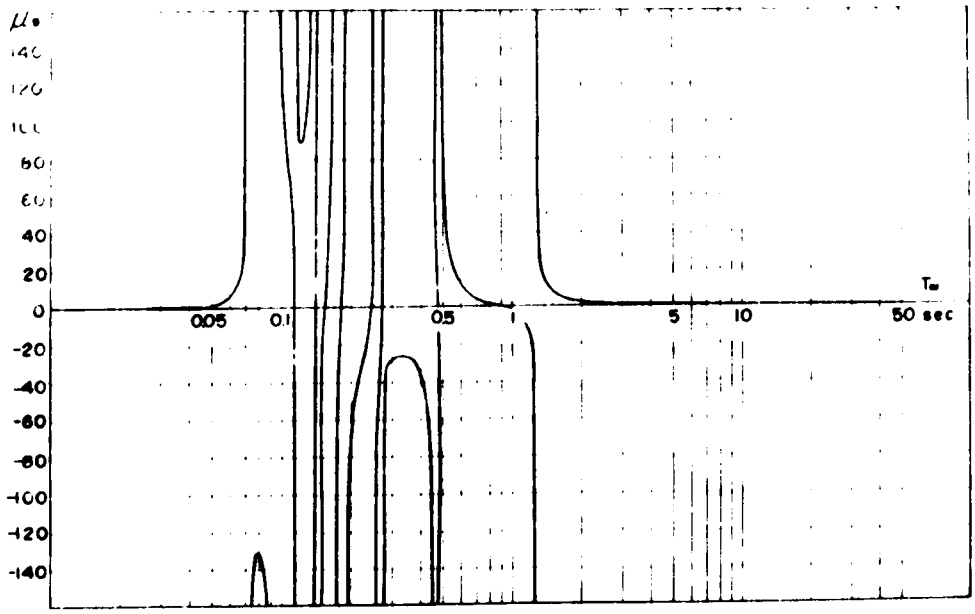

Fig. 111 (c) Resonance Curve
(section 8)

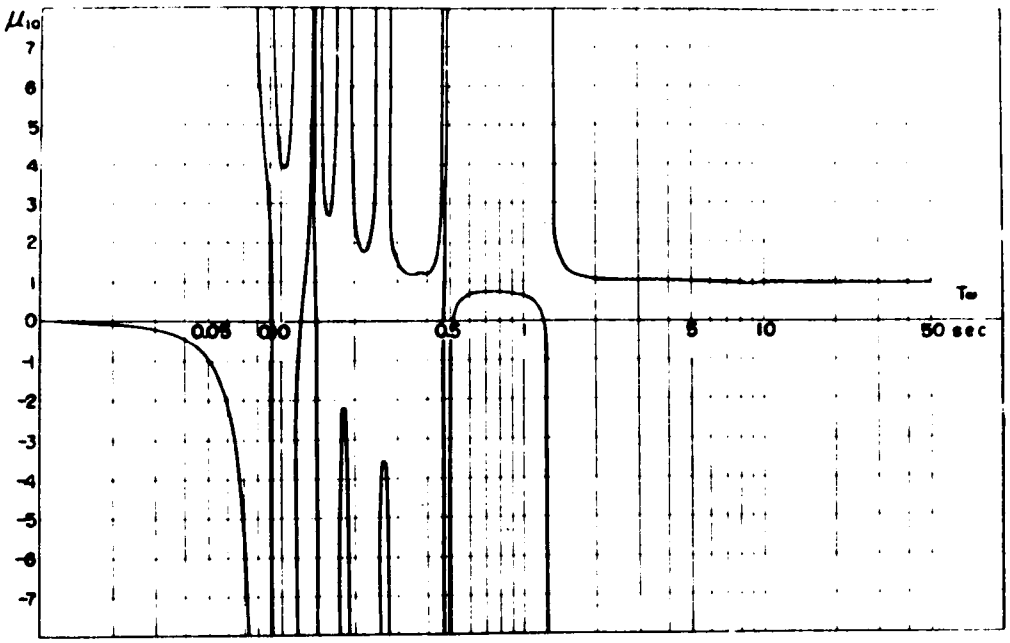

Fig. 111 (d) Resonance Curve
(section 10)

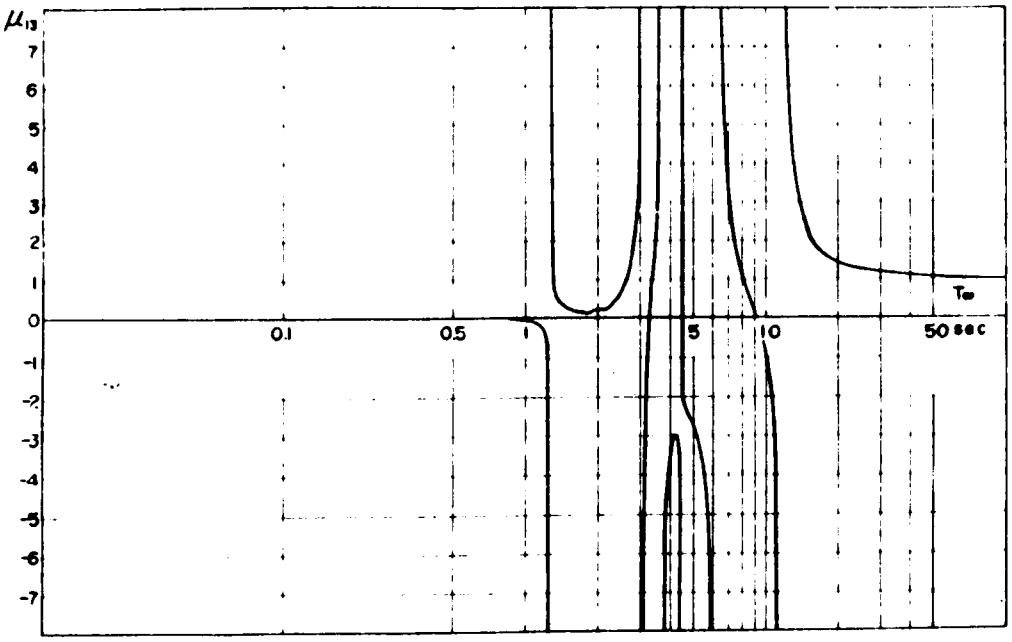

Fig. 111 (e) Resonance Curve
(section 13)

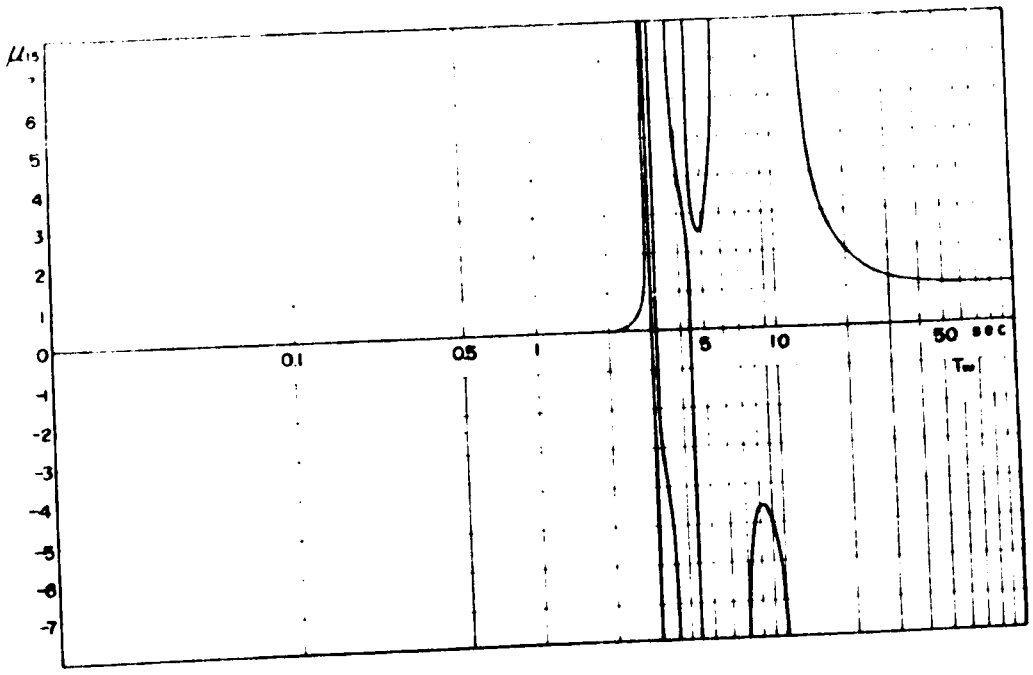

Fig. 111 (f) Resonance Curve
(section 15)

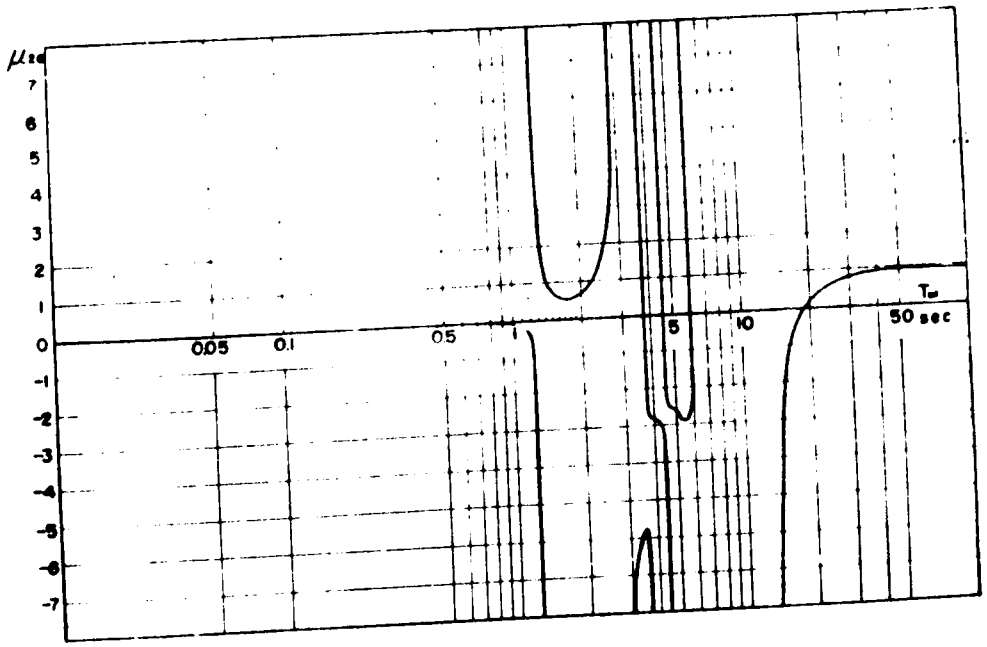

Fig. 111 (g) Resonance Curve
(section 28)

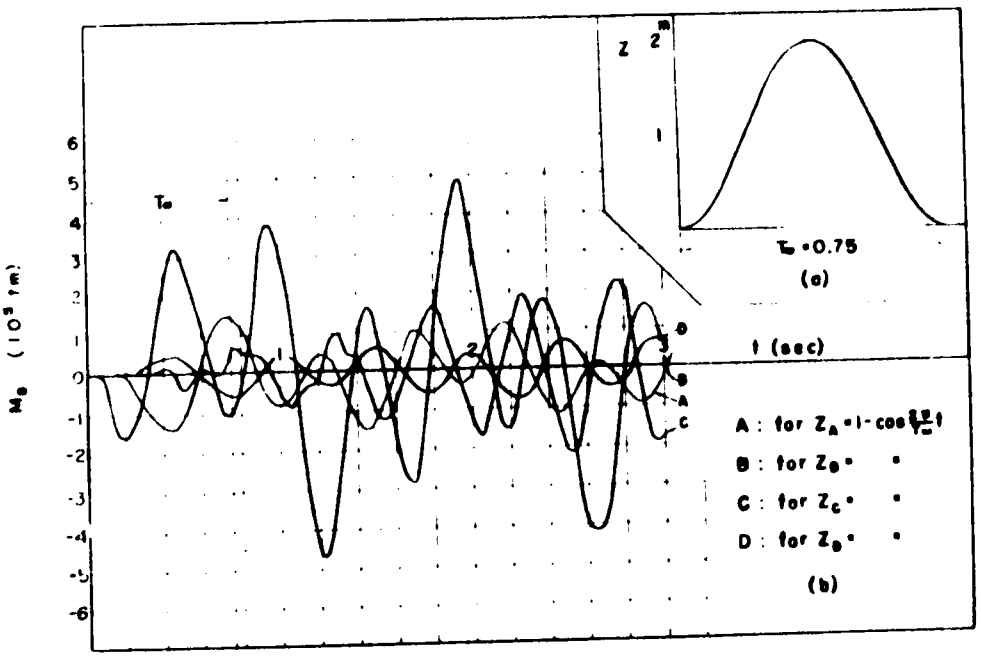

Fig. 113 Dynamic Response due to indivisual Ground Motion (M_B Curves)

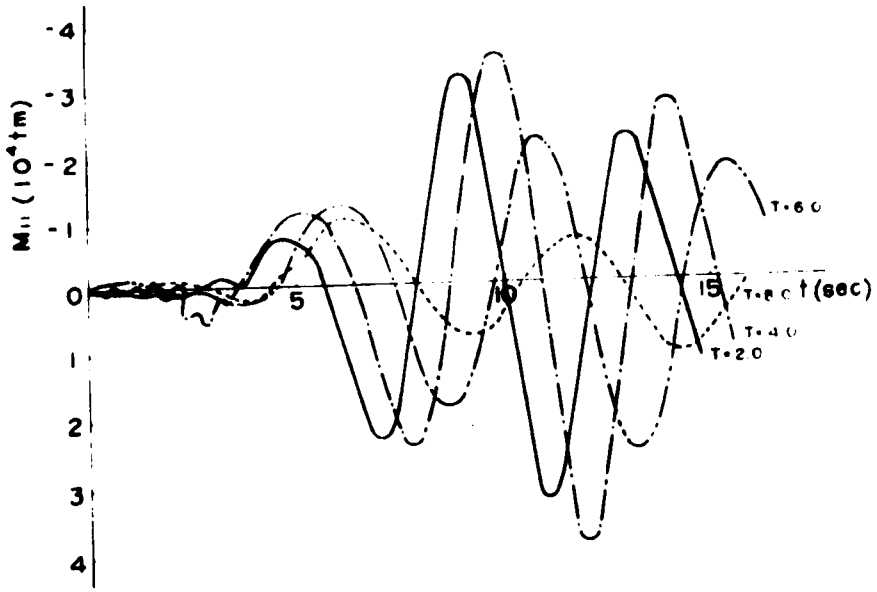

Fig. 115 Bending Moment-Time Curves (section 11, Approximation I)

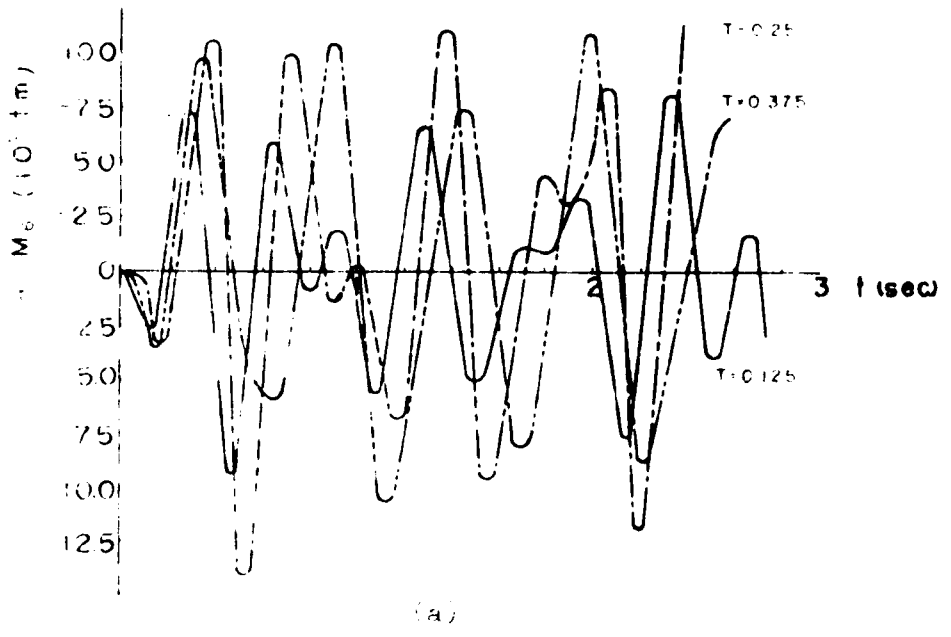

(a)

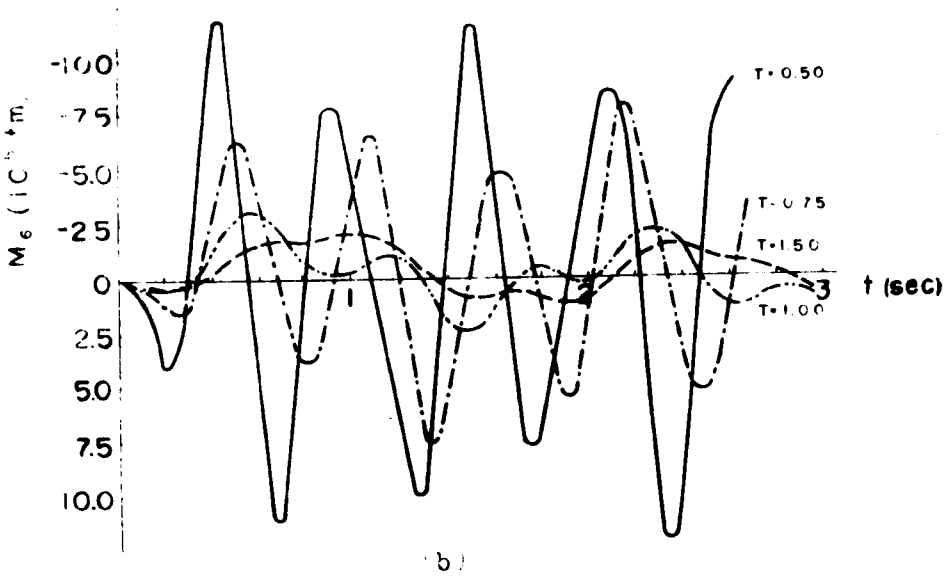

(b)

Bending Moment-Time Curves

(section 6, Approximation I)

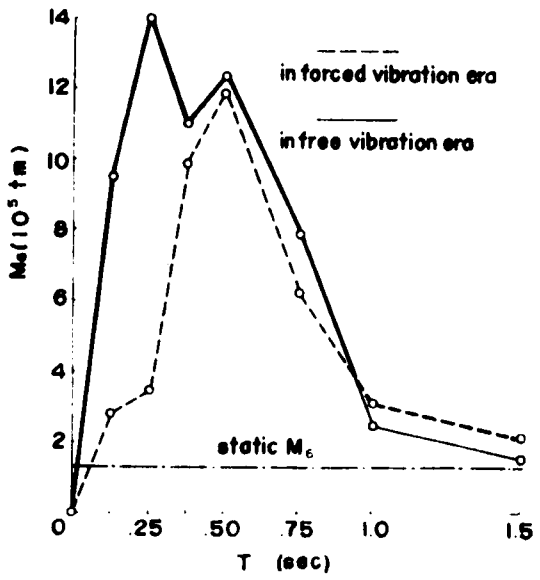

Fig. 11 Response Spectra
(section 6, Approx. I)

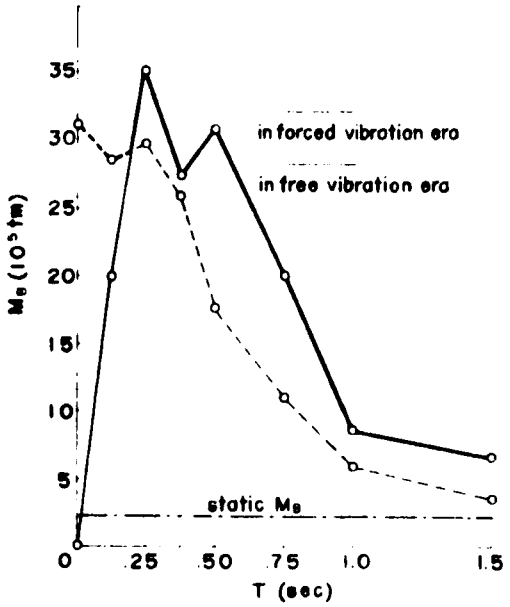

Fig. 117 Response Spectra
(section B, Approx. I)

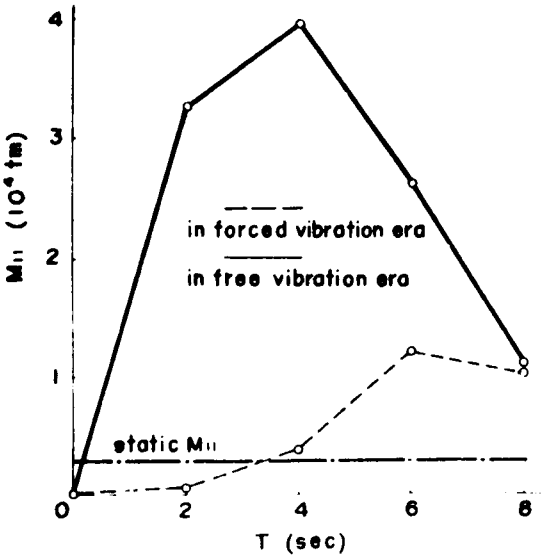

Fig. 118 Response Spectra
(section 11, Approx. I)

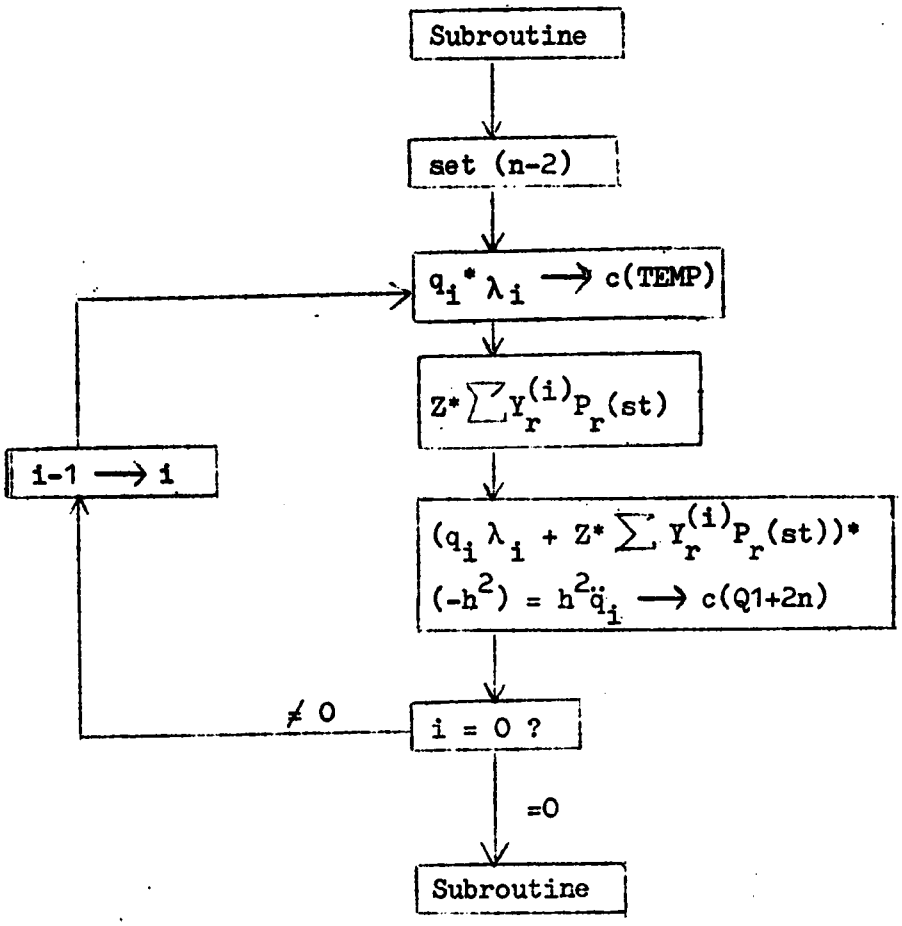

Fig. 119 Flow Diagram
Computation of $h^2\ddot{q}$ (AUX)

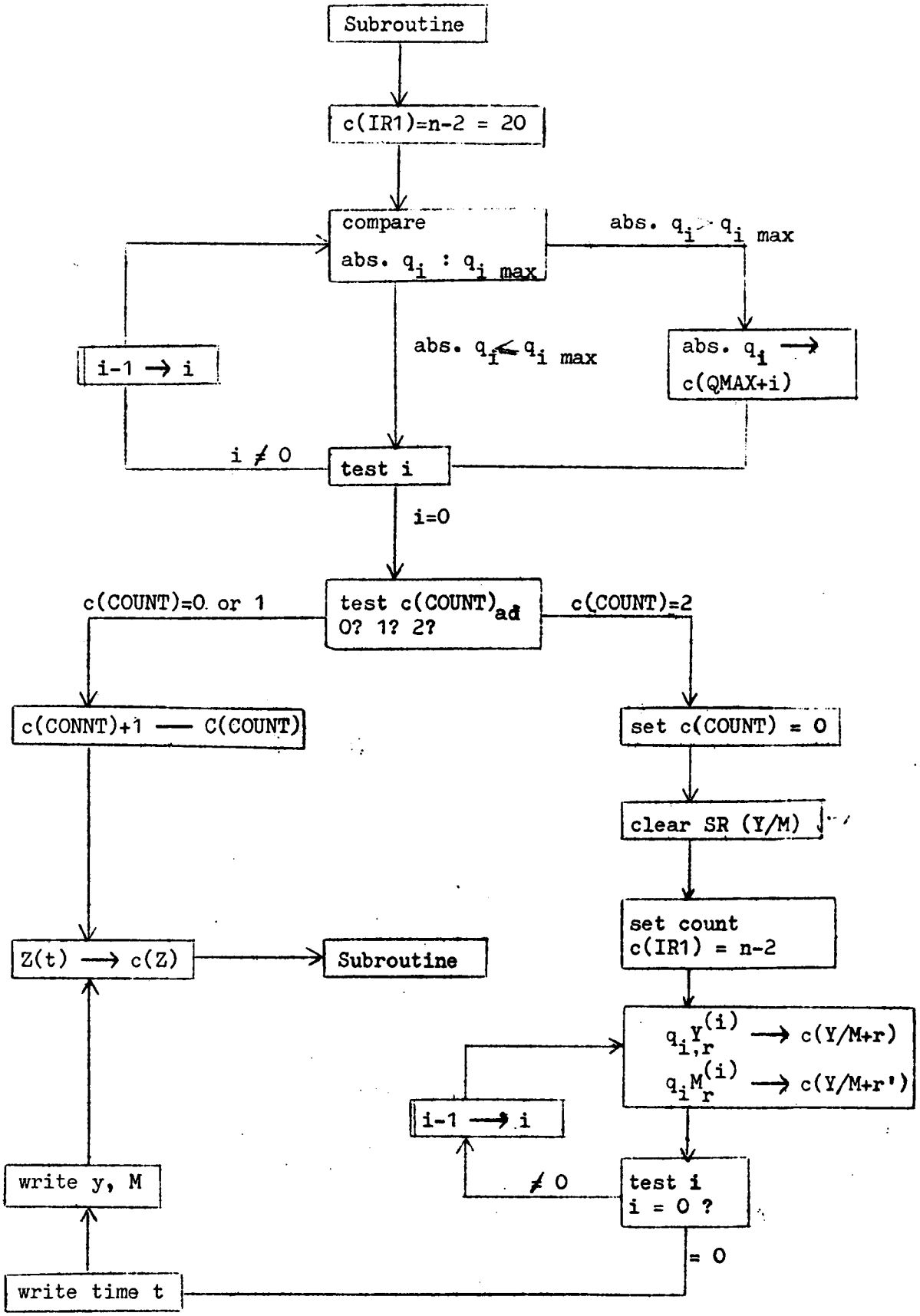

Fig. 120 Flow Diagram Print Time History (PRINT)

Program 101 Computation of $h^2\ddot{q}_i$ (AUX)

	LOC.	OPER.	XX	A	Remarks	DEC. CODE
4238	AUX	SEX	10	20	Set (n-2)	830 100 ω20"
	LOOP	LDM	10	Q1	$c(MD)=q_i$	320 100 ω4041"
4240		FMP/	10	LAMB	$c(AC)=\lambda_i q_i$	221 100 ω4172"
		STO	00	TEMP	$c(TEMP)=\lambda_i q_i$	300 000 ω4193"
		LDM	00	Z	$c(MD)=Z(t)$	320 000 ω4022"
		FMP/	10	ALPH	$c(AC)=\alpha_i * Z(t)$	221 100 ω4000"
		FAD	00	TEMP	$c(AC)=\alpha_i Z+ \lambda_i q_i$	200 000 ω4193"
4245		PAM	..			310 000 ω0"
		FMC/	00	SQH	$c(AC)=h^2 * \ddot{q}_i$	223 000 ω4021"
		STO	10	Q1+2n	$c(Q1+2n)=h^2\ddot{q}_i$	300 100 ω4085"
		JXL	10	LOOP	test i	850 100 ω4239"
		JMP	30	1	jump to subroutine	714 300 ω1"

4040	TIME	t	
4041	Q1	q_1	
	Q1+1	q_2	
	Q1+2	q_3	
	.	.	
	.	.	
	.	.	
4172	LAMB	fl(λ_1)	+29289+0"
		fl(λ_2)	+102074+1"
		fl(λ_3)	+19927+1"
		.	.
		.	.
		.	.
4000	ALPH	fl(α_1)	
		fl(α_2)	
		.	
		.	
4021	SQH	fl(h^2)	+35868572-3"
4022	Z	ground diswlacement Z(t)	

Program 102 Select maximum q_i
Print y_r and M_r
Load Ground Motion Z(t)
(PRINT)

	LOC.	OPER.	XX	A	Remarks	DEC. CODE
2000	PRINT	SEX	10	20	set (n-2)	830 100 ω20"
	LOOP	FAA/	10	Q1	c(AC) = $\|q_i\|$	203 100 ω4041"
		PAM			c(MD)= $\|q_i\|$	310 000 ω0"
		CMP	10	QMAX	$\|q_i\| \geq q_{imax}$?	324 100 ω2200"
		JMP		NEXT	jump to NEXT if >	714 000 ω2005"
2005		NOP				514 000 ω0"
		JMP		NEXT+1	jump to NEXT+1 if ≤	714 000 ω2008"
	NEXT	STO	10	QMAX	q_i -> c(QMAX+i)	300 100 ω2200"
		JXL	10	LOOP	test i	850 100 ω2001"
		SEX	10	2		830 100 ω2"
2010		LXA	20	COUNT		820 200 ω2076"
		JXU	20	UNE	jump to UNE if t≠3mh	854 200 ω2013"
		JMP		EQU	jump to EQU if t=3mh	714 000 ω2016"
	UNE	NOP				514 000 ω0"
		STX	20	COUNT	store counter	822 200 ω2076"
2015		JMP		LOAD	jump to LOAD	714 000 ω2070"
	EQU	STA/		COUNT	clear counter	307 000 ω2076"
		SEX	10	11	set No. of variables	830 100 ω11"
	LOOP2	STO/	10	Y/M	clear SR for part. sum	301 100 ω2230"
		JXL	10	LOOP2		850 100 ω2018"
2020		SEX	10	20	set (n-2)	830 100 ω20"
	LOOP3	LDM	10	Q1	c(MD)=q_i	320 100 ω4041"
		FMP/	10	Y2	c(AC)=$q_i * Y_2^{(i)}$	221 100 ω2300"
		FAD		Y/M	add to part. sum	200 000 ω2230"
		STO		Y/M	store part. sum	300 000 ω2230"
2025		FMP/	10	Y4	c(AC)=$q_i * Y_4^{(i)}$	221 100 ω2321"
		FAD		Y/M+1	add to paft. sum	200 000 ω2231"
		STO		Y/M+1	store part. sum	300 000 ω2231"
		FMP/	10	Y6	c(AC)=$q_i * Y_6^{(i)}$	221 100 ω2342"
		FAD		Y/M+2	add to part. sum	200 000 ω2232"
2030		STO		Y/M+2	store part. sum	300 000 ω2232"

2031		FMP/	10	Y8	$c(AC)=q_i*Y_8^{(i)}$	221 100 ω2363"
		FAD		Y/M+3	add to part. sum	200 000 ω2233"
		STO		Y/M+3	store part. sum	300 000 ω2233"
		FMP/	10	Y10	$c(AC)=q_i*Y_{10}^{(i)}$	221 100 ω2384"
2035		FAD		Y/M+4	add to part. sum	200 000 ω2234"
		STO		Y/M+4	store part. sum	300 000 ω2234"
		FMP/	10	Y15	$c(AC)=q_i*Y_{15}^{(i)}$	221 100 ω2405"
		FAD		Y/M+5	add to part. sum	200 000 ω2235"
		STO		Y/M+5	store part. sum	300 000 ω2235"
2040		FMP/	10	Y11	$c(AC)=q_i*Y_{11}^{(i)}$	221 100 ω2426"
		FAD		Y/M+6	add to part. sum	200 000 ω2236"
		STO		Y/M+6	store part. sum	300 000 ω2236"
		FMP/	10	M2	$c(AC)=q_i*M_2^{(i)}$	221 100 ω2447"
		FAD		Y/M+7	add to part. sum	200 000 ω2237"
2045		STO		Y/M+7	store part. sum	300 000 ω2237"
		FMP/	10	M6	$c(AC)=q_i*M_6^{(i)}$	221 100 ω2468"
		FAD		Y/M+8	add to part. sum	200 000 ω2238"
		STO		Y/M+8	store part. sum	300 000 ω2238"
		FMP/	10	M8	$c(AC)=q_i*M_8^{(i)}$	221 100 ω2489"
2050		FAD		Y/M+9	add to part. sum	200 000 ω2239"
		STO		Y/M+9	store part. sum	300 000 ω2239"
		FMP/	10	M10	$c(AC)=q_i*M_{10}^{(i)}$	221 100 ω2510"
		FAD		Y/M+10	add to part. sum	200 000 ω2240"
		STO		Y/M+10	store part. sum	300 000 ω2240"
2055		FMP/	10	M15	$c(AC)=q_i*M_{15}^{(i)}$	221 100 ω2531"
		FAD		Y/M+11	add to part. sum	200 000 ω2241"
		STO		Y/M+11	store part. sum	300 000 ω2241"
		JXL	10	LOOP3	test i	850 100 ω2021"
		SEL		0111	select PR	630 000 ω111"
2060		WSP		1401	CR	636 000 ω1401"
		FAD/		TIME	c(AC)=t	201 000 ω4040"
		FWR			write t	638 000 ω0"
		WSP		1401	CR	636 000 ω1401"
		SEX	10	11	set No. of variables	830 100 ω11"
2065		SEX	20	0		830 200 ω0"
	LOOP4	FAD/	20	Y/M	c(AC)=y or M	201 200 ω2230"
		FWR			write y or M	638 000 ω0"
		WSP		1301	SP	636 000 ω1301"
		JXU	20	LOOP4	test j=11 ?	854 200 ω2066"

```
2070  LOAD    FAD/      ZZER    c(AC)=Z(t)          200 000 @400"
              STO       Z       c(Z)=Z(t)           300 000 @4022"
              LDA/      LOAD                        320 000 @2070"
              RAA       1       raise c(LOAD)_old 1 100 000 @1"
              STA       LOAD                        300 000 @2070"
2075          JMP   30  1       jump to subroutine  714 300 @1"
      COUNT                                         0000"

2200  QMAX              q1max
                        q2max
                         .
                         .
                         .
2230  Y/M               y2
      Y/M+1             y4
      Y/M+2             y6
      Y/M+3             y8
      Y/M+4             y10
2235  Y/M+5             y15
      Y/M+6             y11
      Y/M+7             M2
      Y/M+8             M6
      Y/M+9             M8
2240  Y/M+10            M10
      Y/M+11            M15

2300        Matrix of Y_x^(i) in the following sequence.
  .
  .         (Y2) Y_2^(1), Y_2^(2), Y_2^(3), ..... (Y4) Y_4^(1), Y_4^(2), Y_4^(3),.....
  .         (Y6) ....., (Y8)....., (Y10)....., (Y15).....,
  .         (Y11)....., (M2)....., (M6)....., (M8).....,
  .         (M10)....., (M15).....,
2551
```

Table 111 Maximum Responses

	1957 So. Calif. E.Q. is applied to the Anchorage		to the Tower Base	
	Max. Response	$\sqrt{\sum(\text{Modal Maxima})^2}$	Max. Response	$\sqrt{\sum(\text{Modal Maxima})^2}$
Displacements (cm)				
y_2	0.423	0.501	0.163	0.093
y_4	1.143	0.579	1.573	1.786
y_6	1.233	0.796	3.533	2.484
y_8	0.852	0.701	2.934	1.884
y_{10}	0.388	0.312	1.683	1.024
y_{15}	0.268	0.213	0.045	0.061
Bending Moments (ton-m)				
M_2	23.9	19.5	2.1	3.3
M_6	1730	1524	6551	6975
M_8	2629	2240	8239	11385
M_{10}	2525	2618	11219	10029
M_{15}	11.5	16.2	0.3	0.3

Table 112 **Modal Maxima** $q_{i,\max}$

Modes	1957 So. Calif. E.Q. is applied to the Anchorage	to the Tower Base
Symmetric Modes		
1st	0.029297	0.005812
2nd	0.030758	0.001412
3rd	0.124728	0.000048
5th	0.032289	0.000524
6th	0.026943	0.000722
8th	0.068214	0.328535
9th	0.042121	0.234794
10th	0.016486	0.101691
11th	0.012064	0.056358
12th	0.011210	0.043061
13th	0.004076	0.046382
14th	0.000390	0.044899
Asymmetric Modes		
2nd	0.004761	0.006407
6th	0.000205	0.001518
7th	0.138783	0.324120
8th	0.090740	0.231129
9th	0.041777	0.104206
10th	0.020707	0.063494
11th	0.008615	0.050321
12th	0.002552	0.049701
13th	0.000303	0.044987

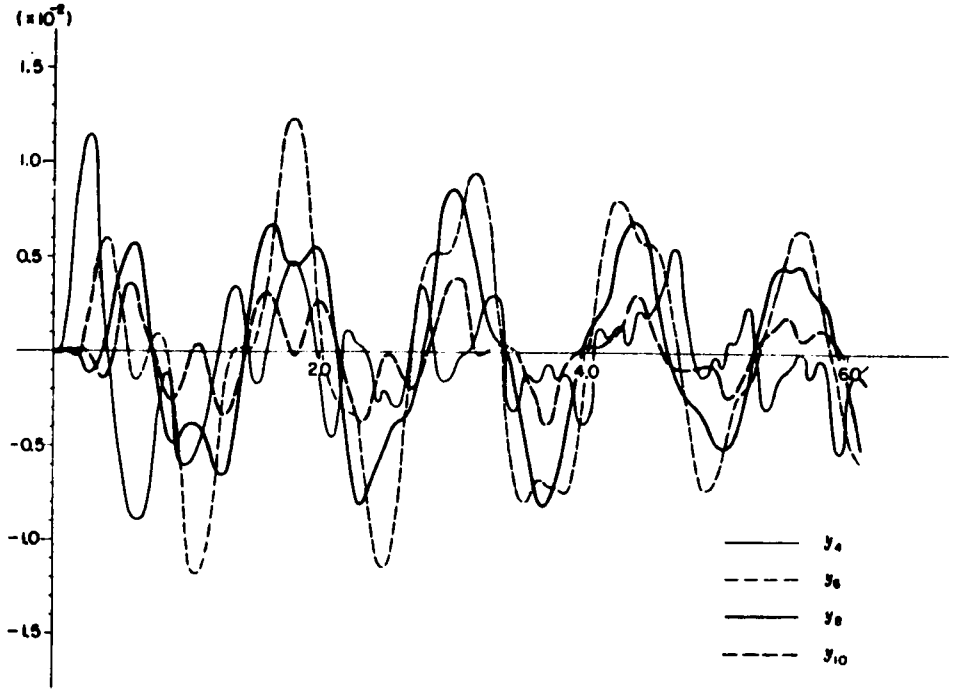

Fig. 121 (a) Deflection-Time Curves
(Tower)

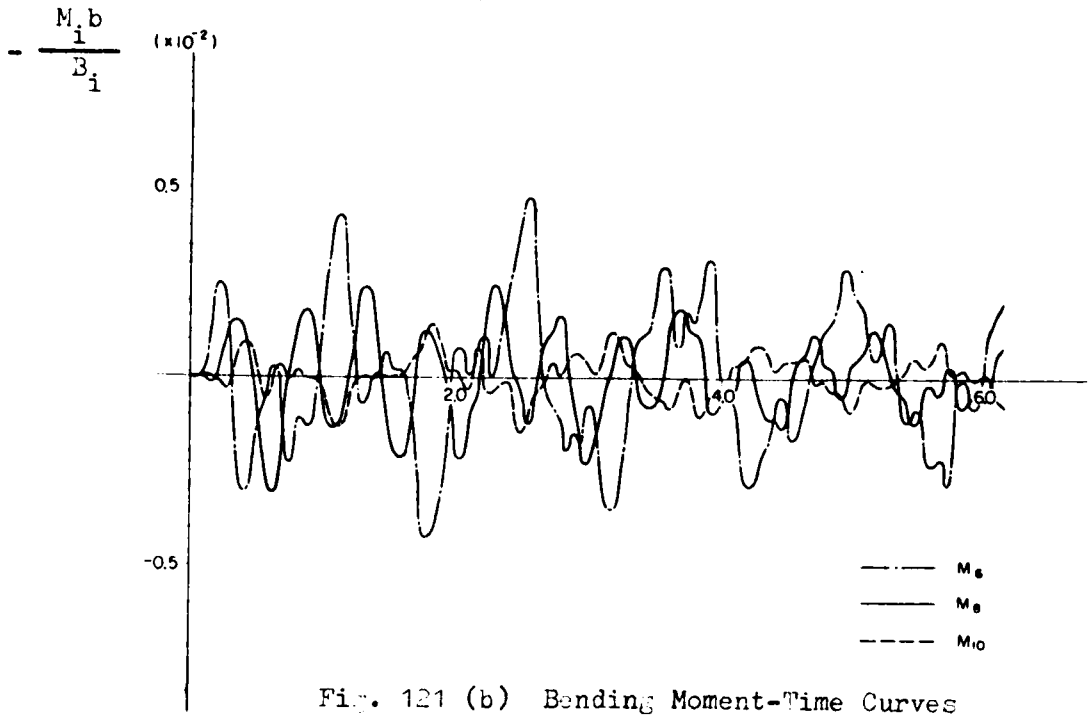

Fig. 121 (b) Bending Moment-Time Curves
(Tower)

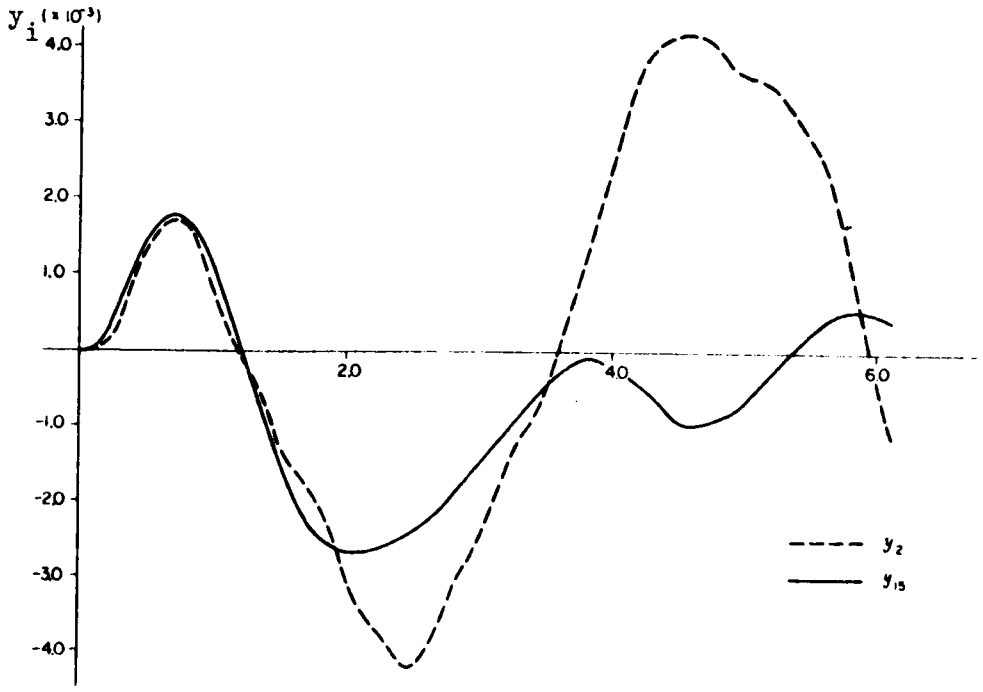

Fig. 121 (c) Deflection-Time Curves
(Suspended Structures)

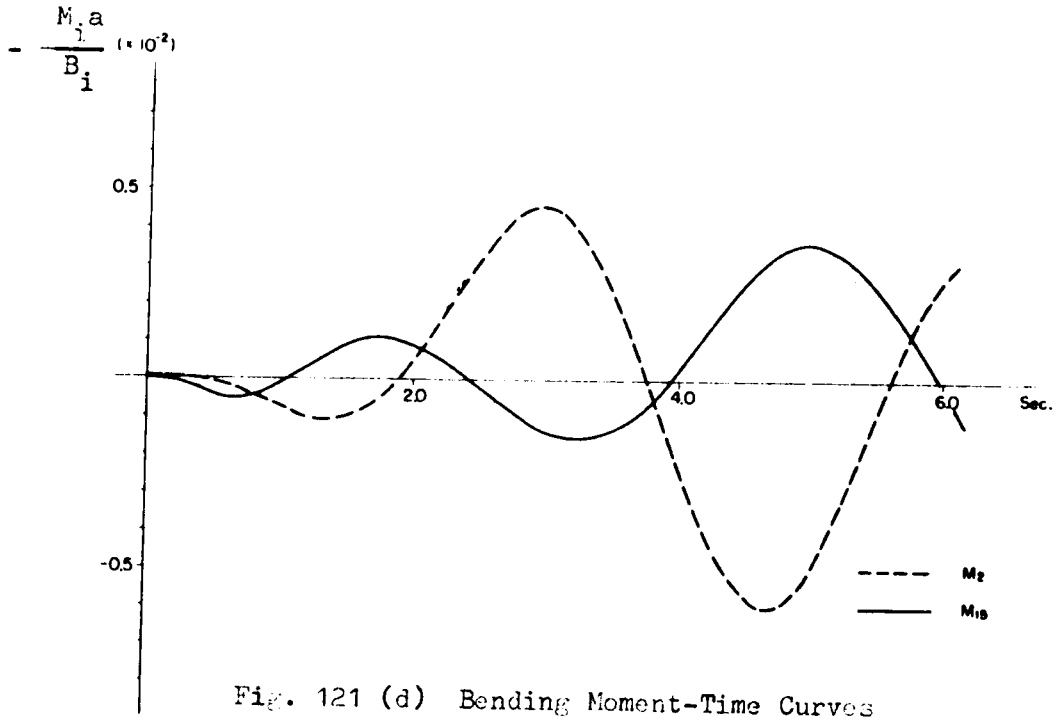

Fig. 121 (d) Bending Moment-Time Curves
(Suspended Structures)

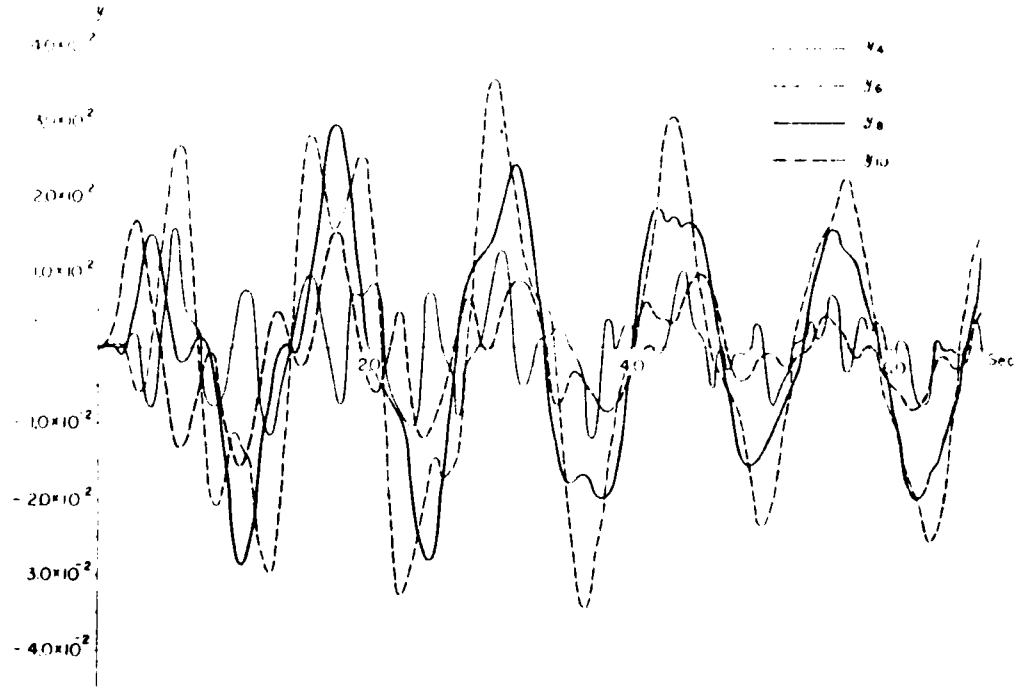

Fig. 122 (a) Deflection-Time Curves
(Tower)

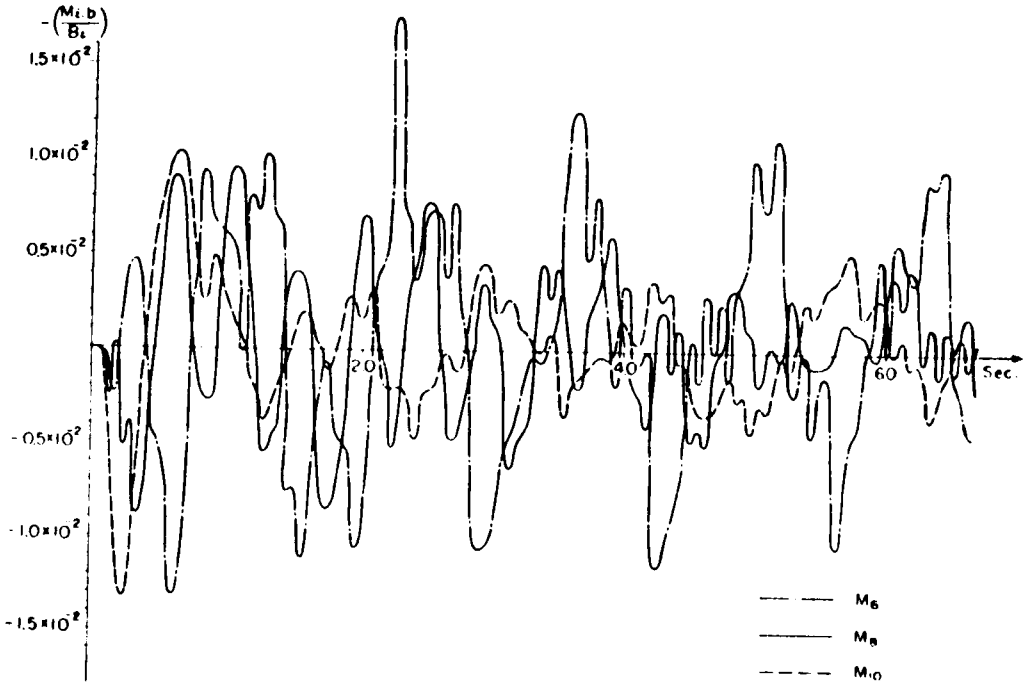

Fig. 122 (b) Bending Moment-Time Curves
(Tower)

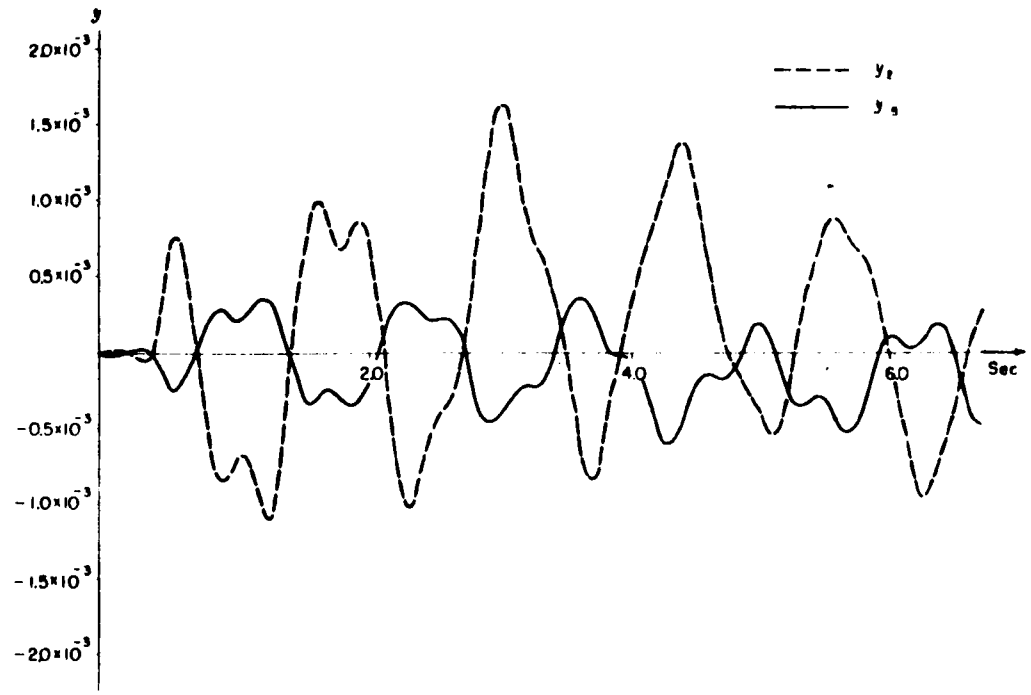

Fig. 122 (c) Deflection-Time Curves
(Suspended Structures)

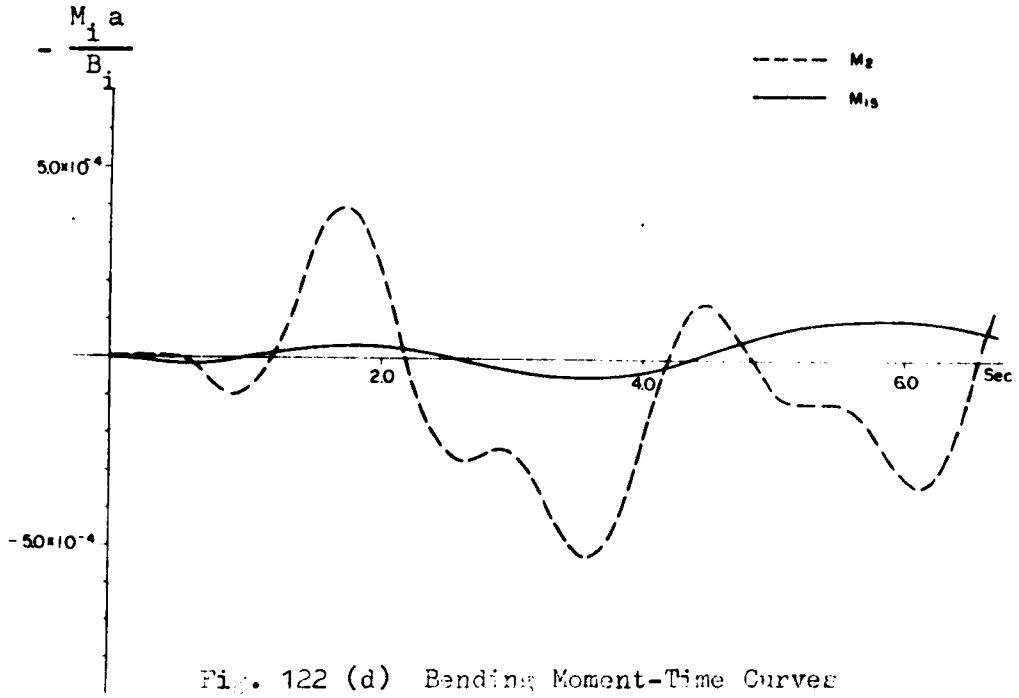

Fig. 122 (d) Bending Moment-Time Curves
(Suspended Structures)

IV CONCLUSION

122. Investigation for the Results Obtained

The method of analysis of the response of the suspension bridge subjected to ground motions with the direction of the bridge axis was derived by adopting the simplified structural system with finite degrees of freedom.

The responses due to static and dynamic ground motions were obtained by using modal analysis of linear structures. To apply the modal analysis to the problems of the static and dynamic responses, the natural frequencies and modes of the system were obtained on the high speed computer. Some investigations on the natural vibration were done already, and will not be repeated again here.

As it is clear from the response spectra, motions of towers subjected to an earthquake are more significant than those of the suspended structures, and the stiffness and masses of the towers have to be taken into account in the analysis of earthquake response of suspension bridges.

From the earthquake response for 1957 So. Calif. Earthquake shown in Table 111, the incremental stresses due to the earthquake are computed as shown in Table 113.

Table 113 Earthquake Stresses (kg/cm^2)

sections	Stresses due to Z_A ,	Stresses due to Z_B,	Total
2 (side span)	3	<1	3
6 (tower)	51	195	246
8 (tower)	41	129	170
10 (tower)	23	104	127
15 (center span)	1	<1	1
cable (side span)			90

It is clear from Table 113 that the stresses in the suspended structures are not important. The stress in the cable is not very small compared to the stresses in the suspended structures, but the allowable stress of the cable is very large compared to that of the ordinary structural steel. The stresses in the tower are comparatively large.

123. Suggestible Problems and Scope on Progressive Investigation

The following theoretical and experimental investigations are necessary to obtain clear understanding on the problem and practical design of suspension bridges.

(1) Although the responses for the 1957 So. California Earthquake were obtained, this earthquake is not the best one for the analysis of earthquake response because of its moderate magnitude. In the practical design the responses due to other large earthquakes are necessary and may be obtained in the further work by using the method of analysis obtained and the computer program obtained in this paper.

(2) The effects of the higher mode vibrations to the bending moment of the tower were significant according to the numerical results obtained. Damping and other properties of higher mode vibrations have to be clarified to obtain better information on the earthquake response.

(3) Model test on the tower has to be done to obtain the experimental results on earthquake response and damping constants, and it will be done in PART III.

(4) Analysis upon the deflection theory and the earthquake response with plastic deformations of the suspension bridge must be made clear. Elastic-plastic analysis of suspension bridge tower will be done in the following part of this paper.

(5) Response due to earthquake with any directions of motion must be investigated.

PART II ELASTIC-PLASTIC ANALYSIS OF SUSPENSION BRIDGE TOWER

I. ELASTIC-PLASTIC ANALYSIS

201. Introduction

The method of analysis described in the previous part makes the analysis of the earthquake response of a suspension bridge possible, and provides a complete method of the analysis of dynamic response due to any kinds of disturbances.

Some fundamental numerical analyses done in the previous studies indicated remarkable conclusions; i.e. (1) the motions of the tower subjected to an earthquake are more significant than those of the other parts of a suspension briedge. (2) the natural frequencies of the vibration modes with predominate displacements of the towers are between the vibration frequencies of earthquake motions and an earthquake disturbance may possibly be resonant with some of the natural vibrations of the suspension bridge. Big earthquakes, therefore, produce considerable amount of deformations which exceed the elastic limit of the material. The methods adoptable to prevent undesirable vibration of mechanical systems are to introduce some damping devices to the structures or to use enough materials to limit the acting stresses within the elastic limit of the material. The method of introducing some damping devices to the structure is quite common to avoid dynamic destruction of mechanical structures. For civil engineering structures, however, this method is not suitable as they are always exposed to the weather, and also as the construction and maintenance costs of such devices are very high. For economical reason, using enough cross sectional area to limit the working stresses within elastic limit is not adoptable in this case, because a destructive earthquake may arise in once a century or less.

It has been recognized, according to inelastic analysis of earthquake resistance of building which have been done during this decade, that the inelastic deformations absorb a large amount of the vibration energy of the structures. On these bases, it is clear that in elastic deformations of the structures there is a predominate factor in limiting the forces developed in a structure by a big earthquake.(201) (202) (203)

In the design of a suspension bridge, however, the basic structural characteristics are different from the ordinary building designs. Collapse

of a tower causes a catastrophic destruction of the bridge. Plastic deformations, residual deformation, must, therefore, be restricted within the magnitude which garuntee the safety of the bridge after destructive earthquake motion.

In this paper, an approximate method of elastic-plastic analysis of a suspension bridge tower will be firstly discussed employing the same kind of physical system used in Part I. As the process of the numerical integrations of such system are of quite a time consuming, a computer program for such solution on KDC-I, Kyoto University High Speed Digital Computer, will be provided, and numerical calculations will be done on the computer. Some considerations on allowable displacements and on static stability after the plastic displacement will be done at the conclusion of the part because such considerations, as mentioned already, are quite important especially in the analysis of suspension bridge.

The effects of the local instability of the tower members are also very important, but these are disregarded in this paper.

202. Simplification of Properties of a System

In the inelastic analysis of structures, the first consideration will be the material properties such as yield stress and ultimate strength especially, in dynamic analysis, for rapidly applied loads. Some of the experimental results on these are available but they should not be considered as precise. In the following analysis, therefore, the value of yield stresses considered as dynamic yield stress, and an idealized stress-strain curve for structural steel as shown in Fig. 201 will be employed.

(a) Bending Moment-Curvature Relationship for Bending Members. (204)

When the idealized stress-strain relation of Fig. 201 is assumed for a bending member, bending moment-curvature relationship shown by solid line in Fig. 202 is given theoretically. Curvature is defined as the angle change per unit length. The member bends elastically until the fiber stress of the section reaches its yield value. The curvature increases rapidly as the moment approaches the ultimate capacity M_p. For analytical design purpose, it is recommended that a reduced capacity should be used because considerable curve is required for the section to reach its ultimate capacity.

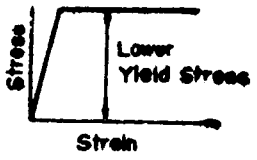

Fig. 201

The ultimate moment capacity, in this analysis, will be computed as

$$M_p = \frac{1}{2}(M_y + M'_p) \qquad (201)$$

$$M_y = \sigma_{dy} W$$

$$M'_p = \sigma_{dy} W_p$$

where

σ_{dy} = dynamic yield stress to be selected as equal to static yield stress,

W = section modulus,

W'_p = plastic modulus of the section.

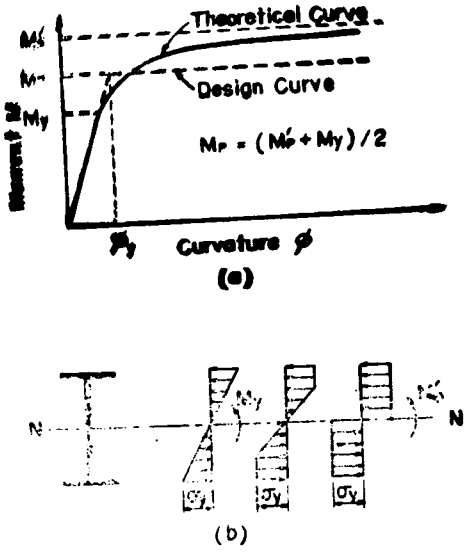

Fig. 202

The moment curvature relation in dotted line in Fig. 202 (a) will be used in the analysis.

For such a simplified curve, similar to the design curve for limit analysis of structures, the plastic hinges form at discrete points at which all plastic rotation occurs. In actuality the hinge extends over a length of the member, and such effect to response calculations will not be a problem to be discussed.

(b) Effect of Axial Force to Plastic Moment (205) (206)

The towers of the suspension bridge are subjected to a large amount of axial forces. Ultimate bending capacity of the tower will considerably be affected by the axial force due to dead load and to incremental vibration. The interaction curve between the moment capacity M and axial load P is shown in Fig. 203, in which P_Y indicates the yielding capacity due to axial force only.

In order to avoid the complexity of the analysis, the relation shown by the dotted line in Fig. 203 will be adopted in the analysis. The analytical method of introducing such relation into the analysis will be given later.

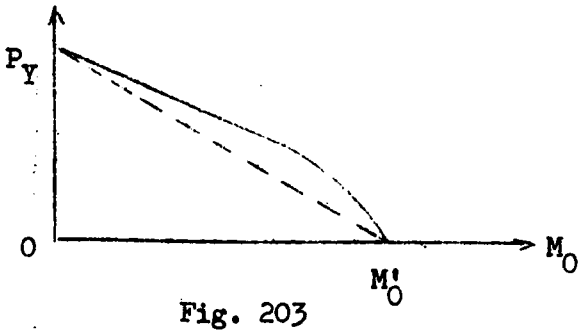

Fig. 203

II METHOD OF ELASTIC-PLASTIC ANALYSIS OF SUSPENSION BRIDGE TOWER

203. Physical System Considered

The system considered is the same as the system in the previous linear analysis. If the system of the previous study is used in inelastic analysis as it is, a great number of second order non-linear differential equations have to be solved simultaneously, for example for the system of Fig. 105, 21 equations, for the system of Fig. 106, 29 equations. If the system is a linear system, as in the previous analysis, the equations can be solved independently by using modal analysis. For the system having inelastic properties, however, the modal analysis is not applicable and numerical step-by-step method may be only the method of numerical analysis.

Although general mathematical principles have not yet been established increasing a number of equations causes decreasing the convergency and the stability of numerical integration, and a smaller time interval of each integration step is required. The number of equations, the same as the number of discrete points, therefore have to be determined by the following considerations. (1) Capacity and computing speed of a computer, (2) Importance of the analytical results, (3) Characteristics of the problem, and (4) Necessary accuracy for the results.

Considering these points, a single tower including some parts of suspended structures, shown in Fig. 204 is the system considered in the beginning of the analysis. With the derivation of the analysis, the motion of suspended structures is neglected.

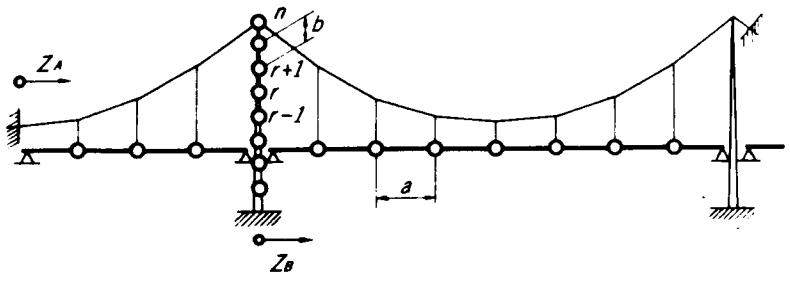

Fig. 204 Physical System Considered

204. Equations of Motion

Since the motion of the tower due to earthquake disturbance is of more inportance than that of the suspended structures, the equations of motion of the tower of the system of Fig. 204 will be discussed.

Assuming the same assumptions on the system as before, the equations of motion are given as follows.

At an inner points of the tower,

$$\frac{W_r}{g}\ddot{y}_r = \frac{1}{b}(M_{r-1}-2M_r+M_{r+1}) - \frac{1}{b}(P_{gr}+P_p)(y_{r-1}-2y_r+y_{r+1}) \tag{202}$$

At the top of the tower,

$$\frac{W_n}{g}\ddot{y}_n = \frac{1}{b}M_{n-1} - \frac{1}{b}(P_{gn}+P_p)(-y_n+y_{n-1}) + \Delta H \tag{203}$$

where,

W_r = dead load concentrated at the point r,

g = gravitational acceleration,

y_r = displacement of the point r,

b = length of a segment of the tower,

M_r = bending moment at the section of the point r,

P_{gr} = axial force due to dead load acting to the section r,

P_p = increment to the axial force due to inertia force,

ΔH = horizontal force acting to the top of the tower during vibration.

In Eqs. (202) and (203), ΔH and P_p are due to cable tension and can be determined from the cable equations,

$$\begin{aligned} u_1 &= \frac{H_{p1}L_{E1}}{E_cA_c} - \frac{W_r}{H_g}\sum y_r \\ u_c &= \frac{H_{pc}L_{Ec}}{E_cA_c} - \frac{W_r}{H_g}\sum y_r \end{aligned} \tag{204}$$

where,

u_1 = horizontal component of total elongation of the cable of the side span,

u_c = horizontal component of total elongation of the cable of the center span,

H_{p1} = increment to the horizontal component of the side span cable tension,

H_{pc} = increment to the horizontal component of the center span cable tension,

$L_{E1} = \sum (e/\cos^3\alpha_{r,r+1})$ (side span)

$L_{Ec} = \sum (a/\cos^3\alpha_{r,r+1})$ (center span)

H_g = horizontal component of dead load cable tension,

W_r = dead load concentrated at a point in suspended structures.

A period of the fundamental natural vibration, in which the vibration of the suspended structures are predominant, of a long span suspension bridge is about 10 sec. as shown in the previous study, then the suspended structures are considered to be of flexible type structures already introduced. The vibration amplitudes of such structures subjected to earthquake are not large or rather stand still like a mass of a displacement vibrograph.

Accordingly one assumes,

$$y_r = 0 \quad \text{(for suspended structures)} \tag{205}$$

Then,

$$u_1 = \frac{H_{p1} L_{E1}}{E_c A_c}$$
$$u_c = \frac{H_{pc} L_{Ec}}{E_c A_c} \tag{206}$$

The horizontal components of cable tension are

$$H_{p1} = \frac{E_c A_c u_1}{L_{E1}}$$
$$H_{pc} = \frac{E_c A_c u_c}{L_{Ec}} \tag{207}$$

And the horizontal force acting to the top of the tower is

$$\Delta H = H_{pc} - H_{p1} = E_c A_c \left(\frac{u_c}{L_{Ec}} - \frac{u_1}{L_{E1}}\right) \tag{208}$$

If the cable of both sides of the tower are fixed at their ends

$$u_c = -y_n \qquad u_1 = y_n$$

Then

$$\Delta H = - E_c A_c \left(\frac{1}{L_{Ec}} + \frac{1}{L_{E1}}\right) y_n \tag{209}$$

The incremental axial force acting to the top of the tower is

$$P_p = (H_{pc} + H_{p1}) \tan \alpha$$

$$= E_c A_c \left(\frac{1}{L_{E1}} - \frac{1}{L_{Ec}}\right) y_n \tan \alpha \tag{210}$$

If the ground motion of the left side anchorage Z_A is taken into consideration Eqs. (209) and (210) are modified as follows.

$$\Delta H = -E_c A_c \left(\frac{y_n - Z_A}{L_{E1}} + \frac{y_n}{L_{Ec}}\right) \tag{211}$$

$$P_p = E_c A_c \left(\frac{y_n - Z_A}{L_{E1}} + \frac{y_n}{L_{Ec}}\right) \tan \alpha \tag{212}$$

Bending moment in Eqs. (202) and (203) can be obtained by the following equation.

$$M_r = - \frac{B_r}{b} (y_{r-1} - 2y_r + y_{r+1}). \tag{213}$$

where,

B_r = bending stiffness at the section r in the tower.

Inelastic properties of the bending moment are also taken into consideration and will be discussed lately.

205. Considerations on Inelastic and Non-linear Properties

Using Eq. (210) or (212) into Eq. (202), non-linear properties due to axial force are taken into consideration.

To avoid the complexity of numerical computation, the cable tensions are assumed to be always within the elastic limit. When the computation was carried out, it must be verified whether this condition is satisfied or not.

The elastic-plastic properties of the bending moment of the tower are considered to be concentrated at each hinged point considered. Since the plastic hinges occur at discrete points, under the assumed

elastic-plastic relation, this assumption restricts these discrete points to the hinged points considered. Dividing the tower into a sufficiently large number of segments, highly accurate analogy to the tower can be accomplished, and the positions in which the plastic hinges are yielded can be precisely determined. If a number of the divided segments is not large enough, the accuracy of the analysis might be more or less unsatisfactory. Because the plastic hinges of structures are generally yielded only at a few point, effects of fundamental properties on inelasticity of the tower may approximately be studied.

The bending moment considered does not always retrace its values when the system displaces with velocities of opposite signs. Fig. 205 shows this relation, hysteretic relation, between angle change and the bending moment M_r. The moment in Eqs. (202) and (203) have this elastic-plastic hysteretic property, and this relation can easily be considered in the computer program.

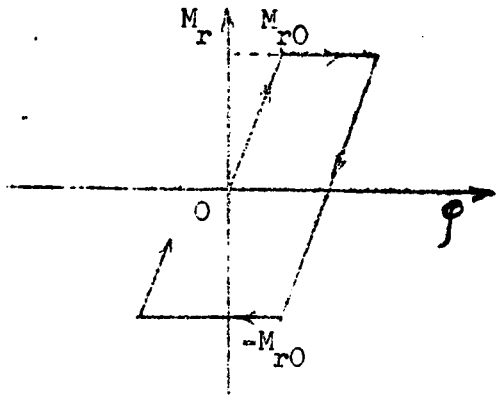

Fig. 205

Considering these relations the restoring moment M_r must be less than M_{r0}, yield moment. Using the following considerations in the calculation, the inelastic histeretic relations on the restoring moment M_r are taken into the analysis.

$$\text{If} \quad (M_{r,i-1} + \Delta M_{r,i}) \geqq M_{r0} \quad \text{then} \quad M_{r,i} = M_{r0}$$

$$\text{or} \quad \text{if} \quad (M_{r,i-1} + \Delta M_{r,i}) \leqq -M_{r0} \quad \text{then} \quad M_{r,i} = -M_{r0}$$

$$\text{or} \quad \text{if} \quad |M_{r,i-1} + \Delta M_{r,i}| < M_{r0} \quad \text{then} \quad M_{r,i} = M_{r,i-1} + \Delta M_{r,i}$$

..... (214)

The relation between the axial force and yield moment M_{r0} is given as the following equation under the assumption already given.

$$M_{r0} = M'_{r0} \left(1 - \frac{P_{gr} + P_r}{P_{Yr}}\right) \qquad (215)$$

where,

M'_{r0} = yield moment of the section r under no axial loads,

P_{Yr} = axial force which produce yield stress.

206. Method of Numerical Integration

The analysis was performed on the Kyoto University High Speed Digital Computer, KDC-I, using a numerical method of integration described by Prof. Newmark. (105) (106)

For the second order differential equation of motion the procedure of integration is shown in the following equations.

$$y_{r,i+1} = y_{r,i} + \dot{y}_{r,i} h + (\frac{1}{2} - \beta) \ddot{y}_{r,i} h^2 + \beta \ddot{y}_{r,i+1} h^2 \qquad (216)$$

$$\dot{y}_{r,i+1} = \dot{y}_{r,i} + \frac{1}{2} (\ddot{y}_{r,i} + \ddot{y}_{r,i+1}) h \qquad (217)$$

Steps of calculations are as follows.

(1) Assume values of the acceleration of each mass at the time $t = (i+1) h$, i.e. assume $\ddot{y}_{r,i+1}$.

(2) Compute the velocity and the displacement of each mass at the time $t = (i+1) h$ from Eqs. (216) and (217).

(3) For the computed velocities and displacements compute the accelerations from the fundamental equations of motion, Eqs. (202) and (203).

(4) Compare the derived acceleration with the assumed acceleration. If these are different, repeat the calculation with the derived acceleration as the new assumed acceleration.

(5) If the differences of these accelerations are less than a specified error criterion, the computation of the considering step is completed, then advance to the next step.

III COMPUTER PROGRAM

207. Description of Programs for the Solution on KDC-I

The method described in the preceding chapter has been programmed for the solution on the KDC-I, the Digital Computer of Kyoto University.

The method of numerical integration by Newmark is applicable to any kinds of the system of second order differential equations, and the program of "Solution of n-Simultaneous Second Order Differential Equations by Newmark's β Method (NEWM)" was programmed by the author of this paper and listed as one of the KDC-I Subroutines.[207] This Subroutine is given in Appendix of this paper.

The subroutine (NEWM) includes the steps (1), (2), and (4) given in the previous article 206 and requires two auxiliary routines. One is the routine of computing the accelerations from the fundamental equations of motion, step (3), and the other is the routine of printing the computed results in the given format.

Two different programs have been prepared as the routine of printing the computed results. The first provides results for the complete history of the dynamic response of the system, while the other can be used to determine only the maximum and minimum responses during the time history of the system.

The computer programs for the computation of either the complete history of the response or the maximum and minimum dynamic responses consists of four parts of instructions and two parts of data as follows.

(I) Main Controlling Routine (MAIN) -Program 201-

(II) Subroutine of the Solution of Simultaneous 2nd Order Differential Equations (NEWM) -Appendix-

(III) Auxiliary Routine I (AUX) -Program 202- Computation of accelerations from the fundamental equations of motion.

(IV) Auxiliary Routine II (PRINT)

Type A -Program 203 (a)- Printing the results at the end of each step and storing the external disturbance necessary to the advanced step of calculation.

Type B -Program 203 (b)- Selecting the maximum and minimum responses at the end of each step and storing the external disturbance necessary at the advanced step. When the computation is finished, print the maximum and minimum dynamic responses.

(V) Data showing the structural properties (DATAI) -included in Program 202-.

(VI) Data of ground motion (DATAII) -included in Program 203 (a), (b).

In Fig. 206 is shown a general flow diagram of the computation. Program 201 through 203 show the write up the complete program, and Figs. 207 and 208 are their flow diagrams.

Program 202 (a) provided for the solution of the dynamic response of the suspension bridge tower subjected to the ground motion acting only to the tower base. Effects of the motion of the left side anchorage, Eqs. (211) and (212), can be considered by slight modifications of the program. The modified program is shown in Program 202 (b). Because of the long span length of the suspension bridge, any phase differences between the disturbances are possible. In program 202 (b), the ground motions are assumed to have opposite directions, i.e.

$$Z_A = - Z_B$$

The method of summing up the effects which was used in the linear analysis may not be applied to this analysis because of non-linearity of the stetem.

The complete time history of the dynamic response was printed out in the format of Table 201. In the case of the maximum and minimum dynamic response computation the computed results were given in the form of Table 202. In Table 202, the following notations are used.

Y MAX = the maximum dynamic response of the absolute value of displacements.

M MAX = the maximum dynamic response of bending moments,

M MIN = the minimum dynamic response of bending moments,

FIMAX = the maximum dynamic response of curvatures multiplied by b , i.e. the maximum $(-y_{r-1}+2y_r -y_{r+1})$,

FIMIN = the minimum dynamic response of curvatures multiplied by b , i.e. the minimum $(-y_{r-1}+2y_r -y_{r+1})$.

If there are no plastic deformations yielded the maximum and minimum bending moments are proportional to the maximum and minimum curvatures respectively.

208. Time Required for Solution of a Program

Required computation time for one step of computation during $t = n\,h$ and $t = (n+1)\,h$ is about by using the program of time history, Program Type A,

$$1\,000\,s + 21\,000 \quad (ms)$$

in which 1000 s is the computation time and 21000 is the printing time, and s indicates the number of iterations. The value of s varies according to the error criterion δ specified in the subroutine, and it is preferably selected as 5 or 6. Substituting $s = 5$ into the above expression, the average computation time of each time interval is about 5 sec. and the printing time is about 21 sec. If the complete time history is required, the printing time is therefore about four times greater than the computing time. In order to save the computing time, the computer program to obtain only the maximum and minimum dynamic responses, Program Type B, was programmed, and the complete time history of dynamic response was obtained for only limited cases. By using the modified program the average total computing time of each step decreased to about 10 sec.

If 400 steps are computed, the total time required are for Type A program,

400 x 26 sec = 10400 sec = 2.9 hour,

and for Type B program,

400 x 10 sec = 4000 sec = 1.1 hour.

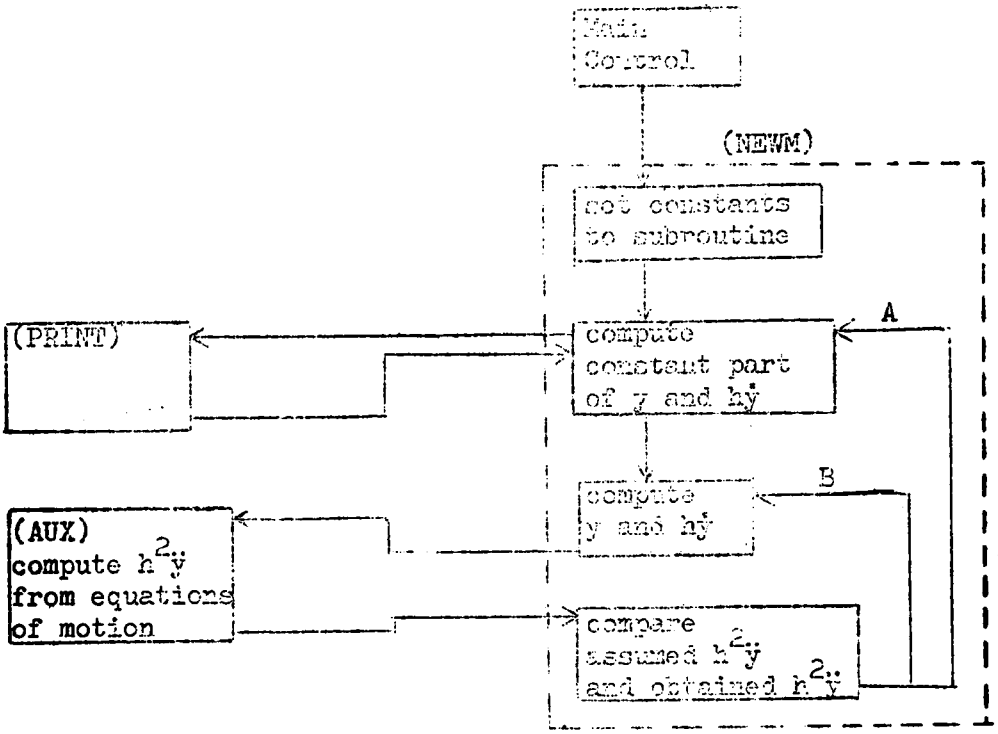

A : step to the next time interval

B : iteration

Fig. 206 Main Diagram

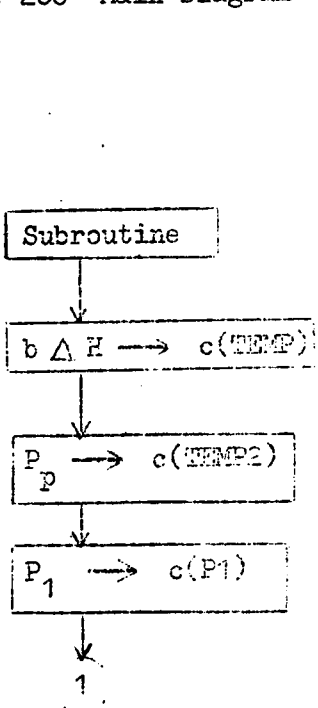

Fig. 207 Flow Diagram (AUX) (1)

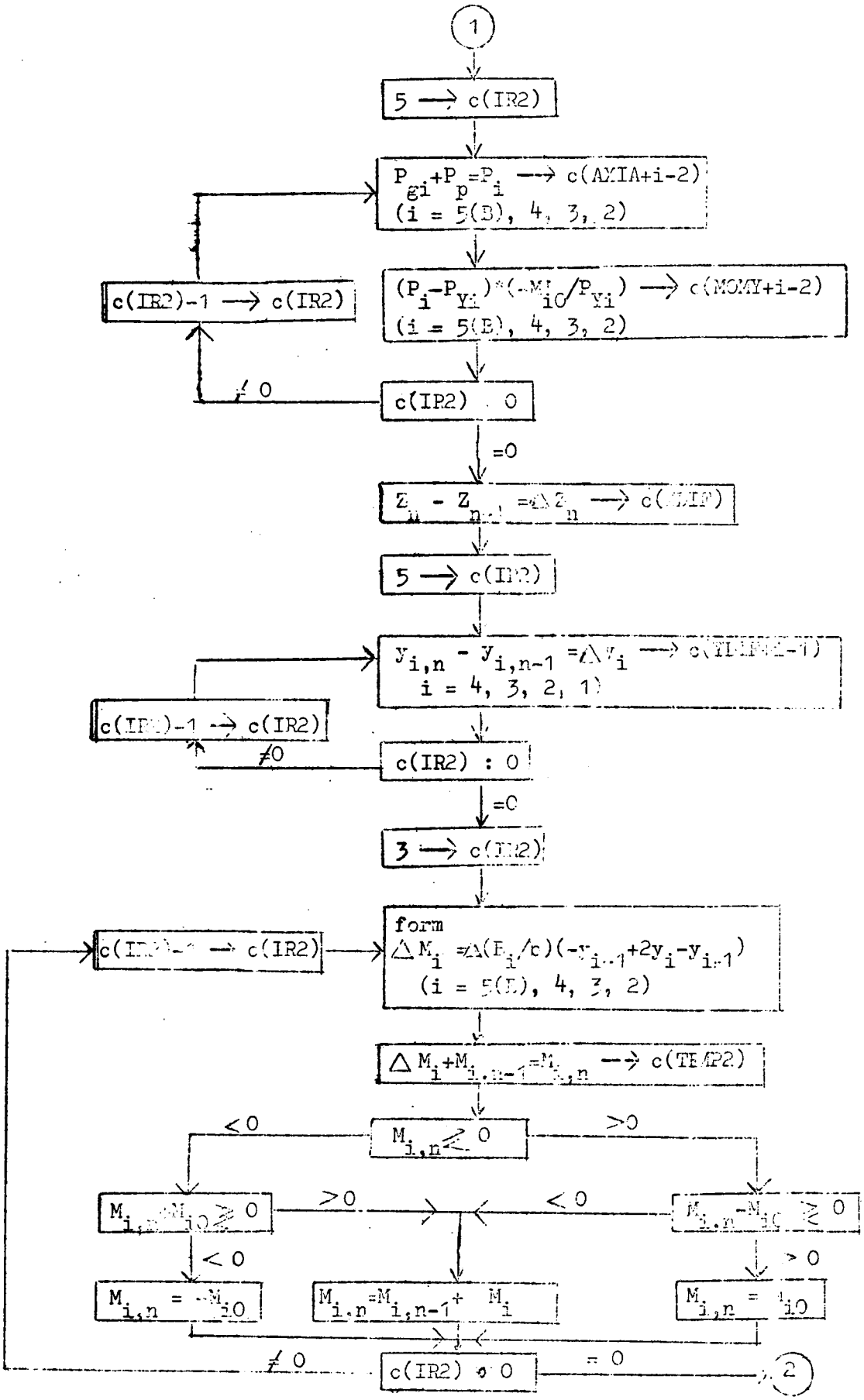

Fig. 207 Flow Diagram (AUX) (2)

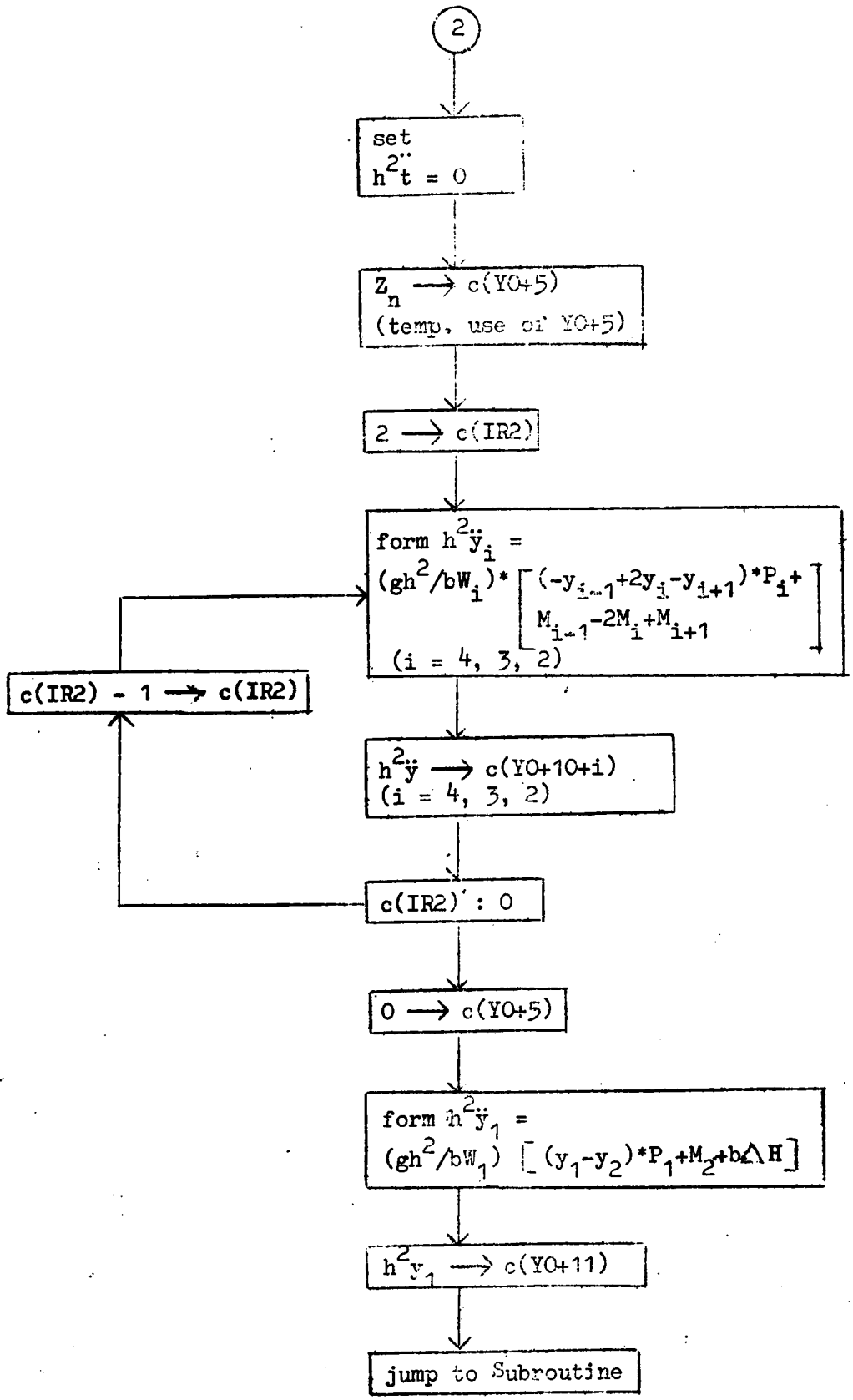

Fig. 207 Flow Diagram (AUX) (3)

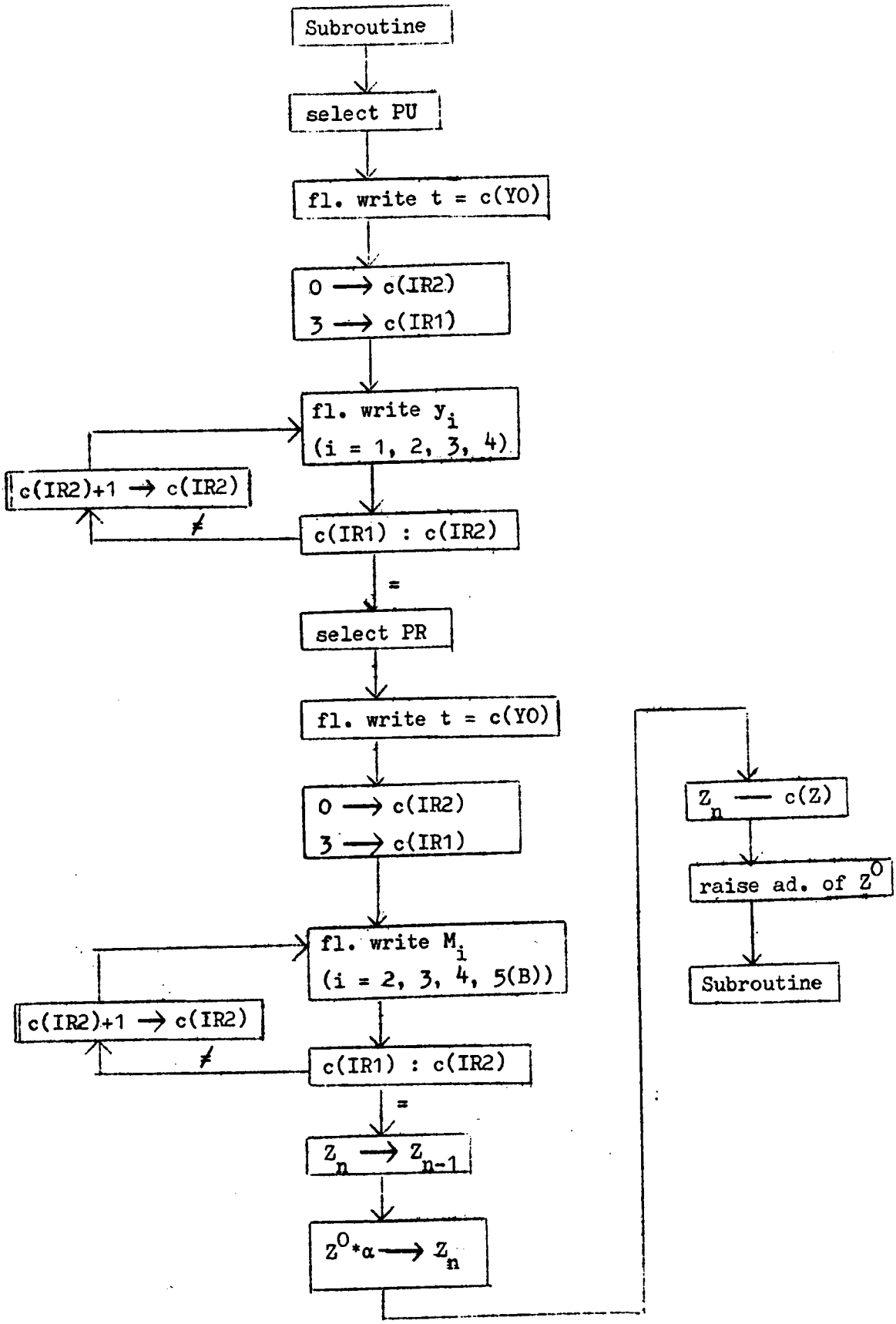

Fig. 208 (a) Flow Diagram (PRINT) Type I

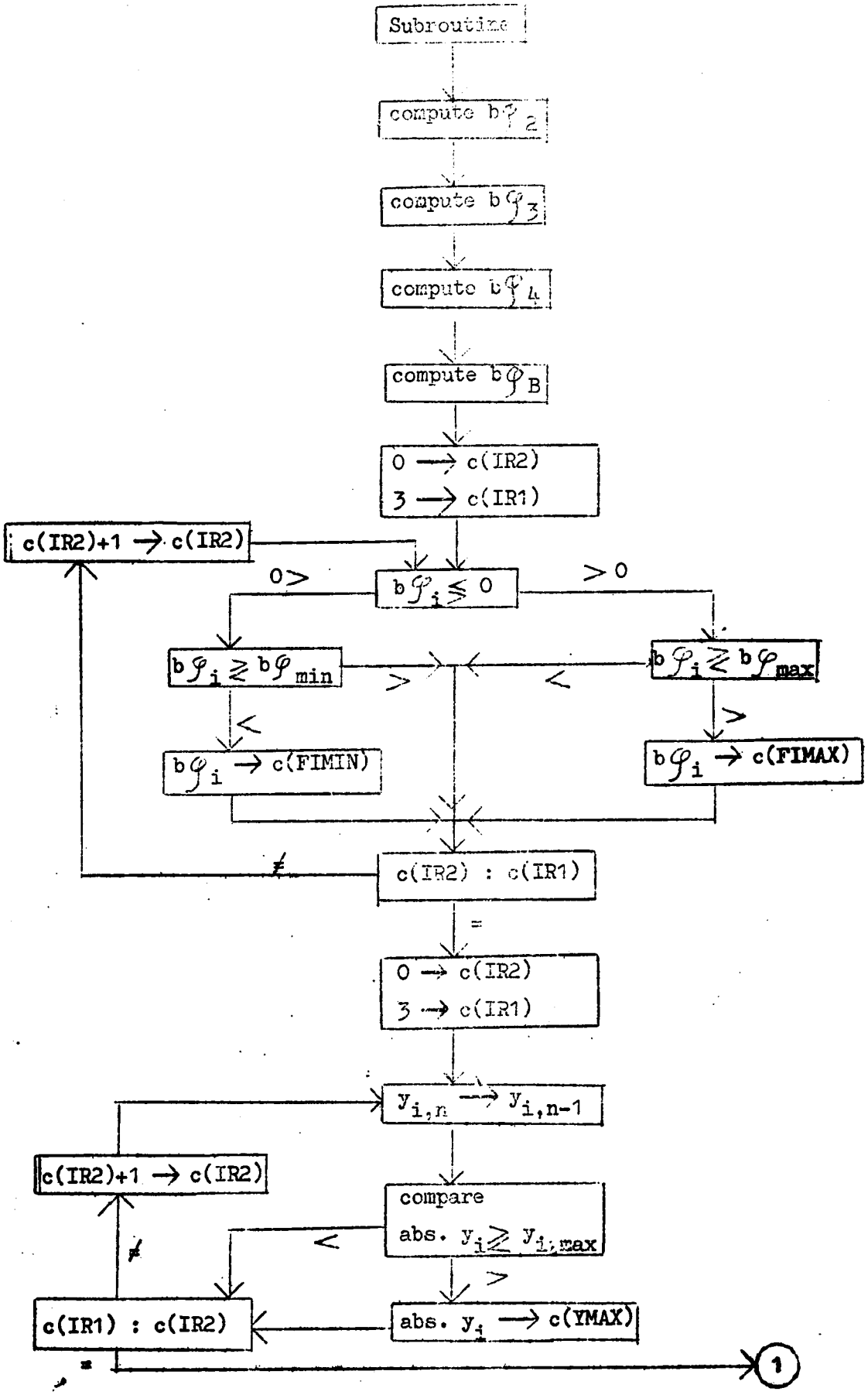

Fig. 208 (b) Flow Diagram (PRINT) Type II (1)

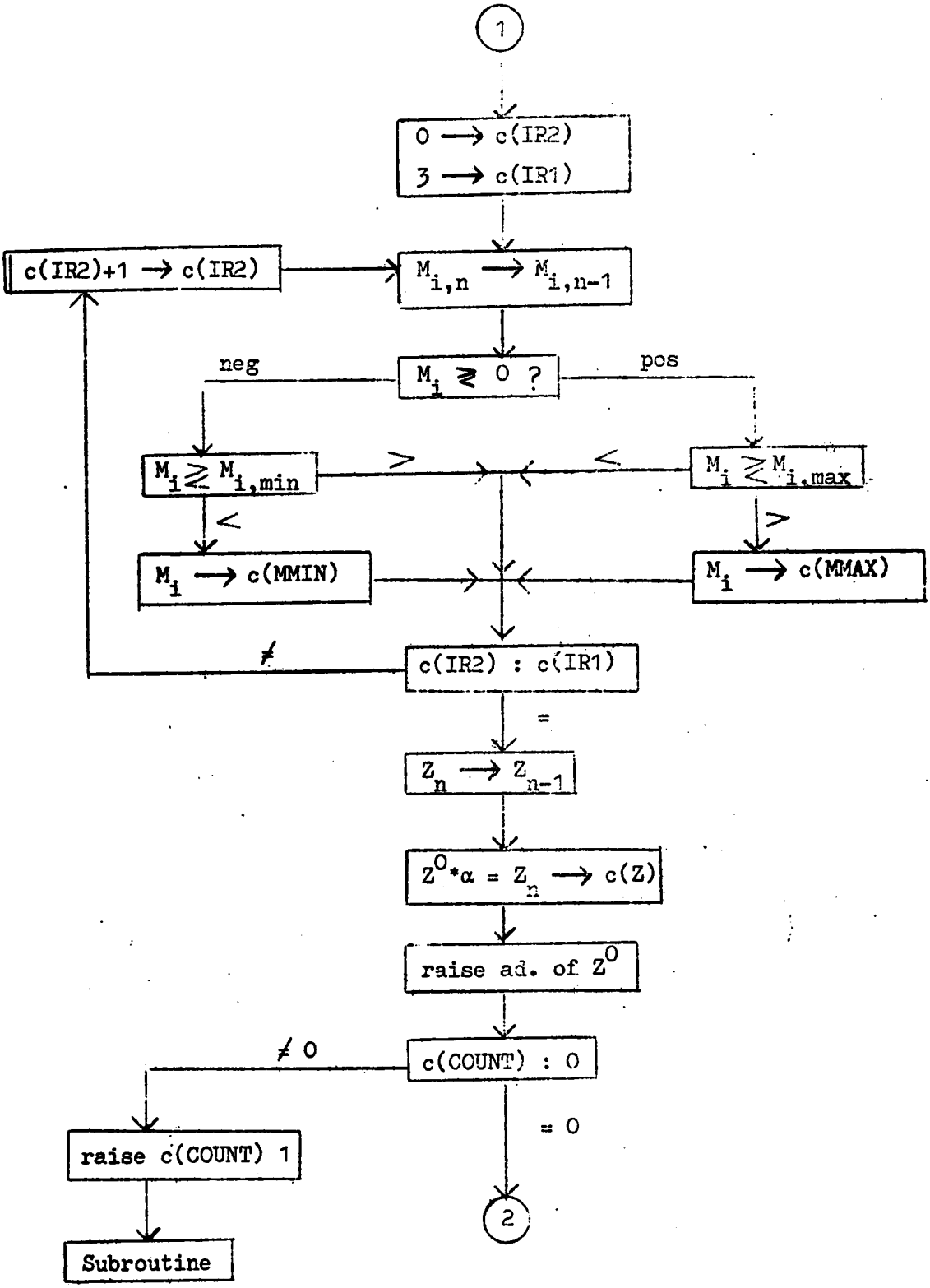

Fig. 208 (b) Flow Diagram (PRINT) Type II (2)

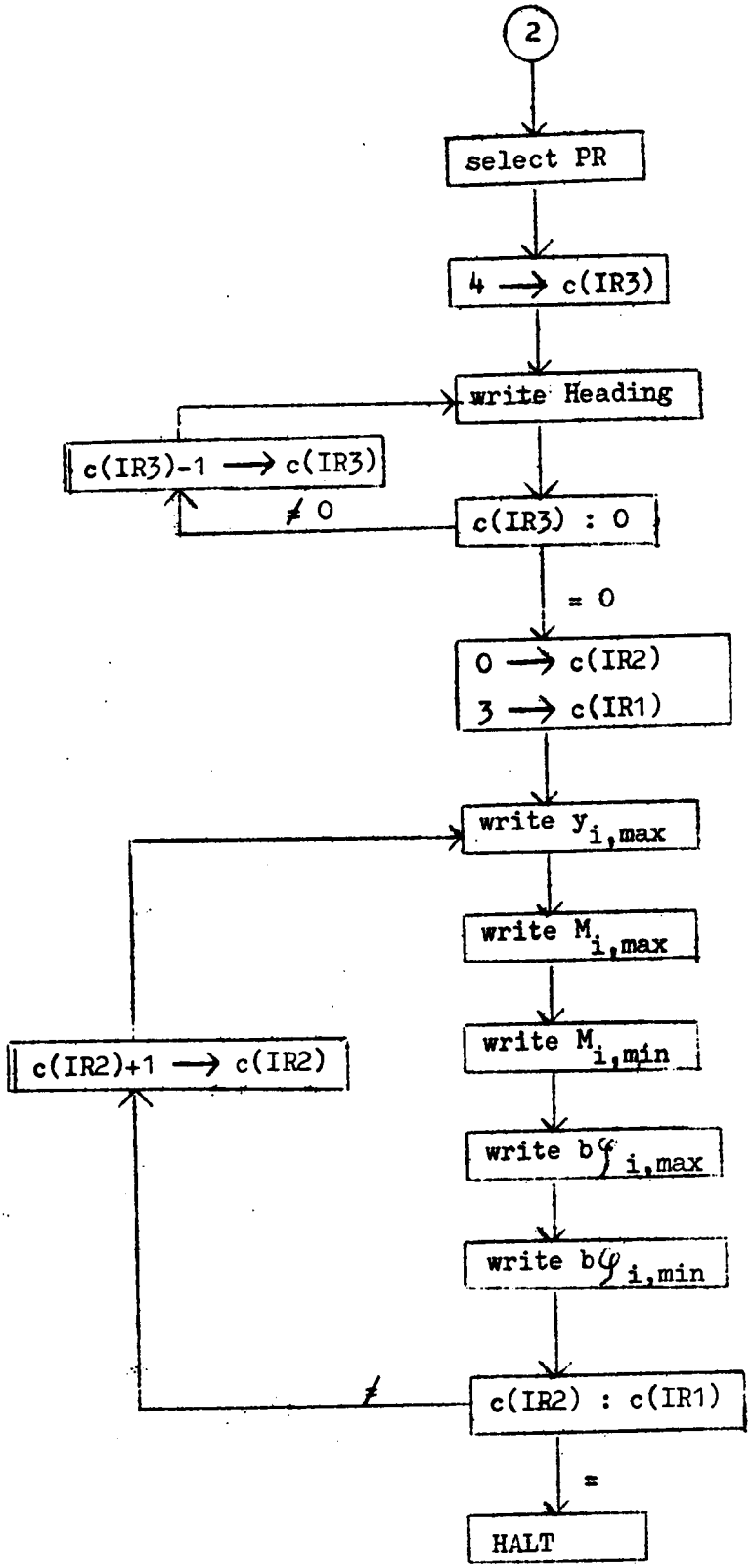

Fig. 208 (b) Flow Diagram (PRINT) Type II (3)

Program 201 Main Control

	LOC.	OPER.	XX	A	Remarks	DEC. CODE
200		SEL		0111	select PR	630 000 ω111"
		WSP		1401	CR	636 000 ω1401"
		SEX	30	4		830 300 ω4"
	TITL	ADD/	03	HEAD		101 030 ω221"
		WRT		1005	write heading	634 000 ω1005"
205		JXL	30	TITL		850 340 ω9998"
		WSP		1402	CR:2	636 000 ω1402"
		WSP		1306	SP:6	636 000 ω1306"
		WSP		3701	write T	636 000 ω3701"
		WSP		1333	SP:33	636 000 ω1333"
210		WSP		3001	write M	636 000 ω3001"
		WSP		1401	CR	636 000 ω1401"
		SEX	30	4		830 300 ω4"
	INIT	STO/	30	YO	set initial condition y=0	301 300 ω4040"
		JXL	30	INIT		850 340 ω9999"
215		JSX	30	NEWM	jump to subroutine NEWM	856 300 ω300"
		(AD)		AUX		4120"
		(AD)		YO		4040"
		(AD)		n		5"
		(FL)		δ		+25-8"
220		(AD)		PRINT		230"
	HEAD	31 32 54 14 14			N O . CR CR	3132541414"
		35 32 24 54 13			R O G . SP	3532245413"
		18 37 22 14 33			A T E CR P	1837221433"
		18 21 18 14 21			A D A CR D	1821181421"
225		42 13 42 18 30			Y SP Y A M	4213421830"
	ALPH.	(FL)		α	load factor	"

Program 202 (a) Aux. Routine (AUX)

	LOC.	OPER.	XX	A	Remarks	DEC. CODE
4120	AUX	LDM		YO+1	$c(MD)=y_1$	320 000 ω4041"
		FMC/		HORI	$c(AC)=\Delta H$	223 000 ω4038"
		STO		TEMP1	$c(TEMP1)=\Delta H$	300 000 ω4197"
		FMP/		VERT	$c(AC)=P_p$	221 000 ω4039"
		STO		TEMP2	$c(TEMP2)=P_p$	300 000 ω4198"
4125		FAD		AXIG	$c(AC)=P_p+P_{g1}=P_1$	200 000 ω4078"
		STO		P1	$c(P1)=P_1$	300 000 ω4199"
		SEX	20	3		830 200 ω3"
	LOOP1	FAD/		TEMP2		201 000 ω4198"
		FAD	20	AXIG+1	form P_i	200 200 ω4079"
4130		STO	20	AXIA		300 200 ω4116"
		FSB	20	AXIY	$c(AC)=P_i-P_{Yi}$	204 200 ω4083"
		PAM				310 000 ω0"
		FMP/	20	MOMYC	$c(AC)=-(M'_{iO}/P_{Yi})*c(MD)$	221 200 ω4087"
		STO	20	MOMY	$c(MOMY+c(IR2))=M_{iO}$	300 200 ω4112"
4135		JXL	20	LOOP1	test i	850 200 ω4128"
		FAD/		Z		201 000 ω4096"
		FSB		ZMIN	$c(AC)=Z_n-Z_{n-1}=\Delta Z$	204 000 ω4095"
		STO		ZDIF	store ΔZ	300 000 ω4101"
		SEX	20	3		830 200 ω3"
4140	LOOP2	FAD/	20	YO+1	$c(AC)=y_i$	201 200 ω4041"
		FSB	20	YMIN	$c(AC)=y_{i,n}-y_{i,n-1}=\Delta y_i$	204 200 ω4091"
		STO	20	YDIF	store Δy_i	300 200 ω4097"
		JXL	20	LOOP2	test i	850 200 ω4140"
		FAD/		YDIF+3	$c(AC)=\Delta y_4$	201 000 ω4100"
4145		STO		ZDIF+1	set bound. condi.	300 000 ω4102"
		SEX	20	3		830 200 ω3"
	LOOP3	FAD/	20	YDIF+1	$c(AC)=\Delta y_i$	201 200 ω4098"
		FAD	20	YDIF+1	$c(AC)=2\ \Delta y_i$	200 200 ω4098"
		FSB	20	YDIF	$c(AC)=2\ \Delta y_i - \Delta y_{i-1}$	204 200 ω4097"
4150		FSB	20	YDIF+2	$c(AC)=-\Delta y_{i+1} \rightarrow c(AC)$	204 200 ω4099"
		PAM				310 000 ω0"
		FMP/	20	STIF	$c(AC)=\Delta M_i$	221 200 ω4074"
		FAD	20	MMIN	$c(AC)=M_{i,n-1}+\Delta M_i$	200 200 ω4103"
		STO		TEMP2		300 000 ω4198"

	LOC.	OPER.	XX	A	Remarks	DEC. CODE
4155		JMI		MINUS	jump to MINUS if $M_{i,n}<0$	750 000 ω4162"
		FSB	20	MOMY	$c(AC)=M_{i,n}-M_{i0}$	204 200 ω4112"
		JMI		PLUS	jump if $M_{i,n}<M_{i0}$	750 000 ω4160"
		FAD/	20	MOMY	$c(AC)=M_{i0}$	201 200 ω4112"
		JMP		SHIM		714 000 ω4166"
4160	PLUS	FAD/		TEMP2	$c(AC)=M_{i,n}$	201 000 ω4198"
		JMP		SHIM		714 000 ω4166"
	MINUS	FAD	20	MOMY	$c(AC)=M_{i,n}+M_{i0}$	200 200 ω4112"
		JMI		YELD	jump if $\|M_{i,n}\|>M_{i0}$	750 000 ω4165"
		JMP		PLUS	jump if $\|M_{i,n}\|<M_{i0}$	714 000 ω4160"
4165	YELD	FSB/	20	MOMY	$c(AC)=-M_{i0}$	205 200 ω4112"
	SHIM	STO	20	MOME+1	store M_i	300 200 ω4108"
		JXL	20	LOOP3	test i	850 200 ω4147"
		STO/		YO+10	$h^2\ddot{t}=0$	301 000 ω4050"
		FAD/		Z	$c(AC)=Z_n$	201 000 ω4096"
4170		STO		YO+5	(YO+5 for temp. use)	300 000 ω4045"
		SEX	20	2		830 200 ω2"
	LOOP4	FAD/	20	YO+2	$c(AC)=y_i$ (i=4,3,2)	201 200 ω4042"
		FAD	20	YO+2	$c(AC)=2y_i$	200 200 ω4042"
		FSB	20	YO+3	$c(AC)=2y_i-y_{i+1}$	204 200 ω4043"
4175		FSB	20	YO+1	$c(AC)=-y_{i-1}+2y_i-y_{i+1}$	204 200 ω4041"
		PAM				310 000 ω0"
		FMP/	20	AXIA	$c(AC)=P_i*c(MD)$	221 200 ω4116"
		FSB	20	MOME+1	$c(AC)=P_i(-y_{i-1}+2y_i-y_{i+1})+M_{i-1}-2M_i+M_{i+1}$	204 200 ω4108"
		FSB	20	MOME+1		204 200 ω4108"
4180		FAD	20	MOME		200 200 ω4107"
		FAD	20	MOME+2		200 200 ω4109"
		PAM				310 000 ω0"
		FMP/	20	WEIG+1	$c(MD)*(gh^2/bW_i)\rightarrow c(AC)$	221 200 ω4071"
		STO	20	YO+12	$h^2\ddot{y}_i \longrightarrow c(YO+10+i)$	300 200 ω4052"
4185		JXL	20	LOOP4	test i	850 200 ω4172"
		STO/		YO+5	clear temp. use	301 000 ω4045"
		FAD/		YO+1	$c(AC)=y_1$	201 000 ω4041"
		FSB		YO+2	$c(AC)=y_1-y_2$	204 000 ω4042"
		PAM				310 000 ω0"

	LOC.	OPER.	XX	A	Remarks	DEC. CODE
4190		FMP/		P1	$c(AC)=P_1(y_1-y_2)$	221 000 ω4119"
		FAD		MOME+1	$c(AC)=P_1(y_1-y_2)+M_2$	200 000 ω4108"
		FAD		TEMP1	$c(AC)=P_1(y_1-y_2)+M_2+\Delta H$	200 000 ω4197"
		PAM				310 000 ω0"
		FMP/		WEIG	$c(AC)=h^2\ddot{y}_1$	210 000 ω4070"
4195		STO		YO+11	$c(YO+11)=h^2\ddot{y}_1$	300 000 ω4051"
		JMP	30	1	jump to subroutine	714 300 ω1"
	TEMP1					0000"
	TEMP2					0000"

Constants and Working Space

4038	HORI	(FL)	$b(E_cA_c/L_{E1}+E_cA_c/L_{Ec})$
4039	VERT	(FL)	$(E_cA_c/L_{E1}-E_cA_c/L_{Ec})\tan\alpha$
4040	YO		Working space specified by Subroutine (NEWM)
•			
•			
4069	YO+29		
4070	WEIG	(FL)	gh^2/bW_i (i=1, 2, 3, 4)
•			
4073			
4074	STIF	(FL)	B_i/b (i=2, 3, 4, B)
•			
4077			
4078	AXIG	(FL)	P_{gi} (i=1, 2, 3, 4, B)
•			
4082			
4083	AXIY	(FL)	P_{Yi} (i=2, 3, 4, B)
•			
4086			
4087	MOMYC	(FL)	$-M'_{iO}/P_{Yi}$ (i=2, 3, 4, B)
•			
4090			

4091	YMIN		
•		$y_{i,n-1}$	(i=1, 2, 3, 4) **(initially set zeros)**
4094			
4095	ZMIN	Z_{n-1}	(initially set zero)
4096	Z	Z_n	
4097	YDIF		
•		$y_{i,n}-y_{i,n-1}$	(i=1, 2, 3, 4)
4100			
4101	ZDIF	Z_n-Z_{n-1}	
4102		$y_{4,n}-y_{4,n-1}$	
4103	MMIN		
•		$M_{i,n-1}$	(i=2, 3, 4, B)
4106			
4107	MOME		
•		M_i	(i=1, 2, 3, 4, B)
4111			
4112	MOMY		
•		M_{i0}	(i=2, 3, 4, B)
4115			
4116	AXIA		
•		P_i	(i=2, 3, 4, B)
4119			
4199	P1	P_1	

Program 202 (b) Modification of (AUX)

Modification

	LOC.	OPER.	XX	A	Remarks	DEC. CODE
4125		JMP		MODI		714 000 ω4200"

New Addition

4200	MODI	LDM		Z		320 000 ω4096"
		FMC/		CONST1		223 000 ω4209"
		FAD		TEMP1	correction for ΔH	200 000 ω4197"
		STO		TEMP1		300 000 ω4197"
		FMP/		CONST2		221 000 ω4210"
4205		FAD		TEMP2	correction for P_p	200 000 ω4198"
		STO		TEMP2		300 000 ω4198"
		FAD		AXIG	(same as 4125 of orig. Pgr)	200 000 ω4078"
		JMP		4126		714 000 ω4126"
	CONST1			$b*(E_cA_c/L_{E1})$		
4210	CONST2			$(E_cA_c/L_{E1})\tan\alpha$		

Program 203 (a) Print Time History (PRINT)

	LOC.	OPER.	XX	A	Remarks	DEC. CODE
230	PRINT	SEL		0112	select PU	630 000 ω112"
		WSP		1401	CR	636 000 ω1401"
		FAD/		YO	c(AC)=t	201 000 ω4040"
		FWR			write t	638 000 ω0"
		SEX	20	0		830 200 ω0"
235		SEX	10	3		830 100 ω3"
	LOOP	FAD/	20	YO+1	$c(AC)=y_i$ (i=1, 2, 3, 4)	201 200 ω4041"
		STO	20	YMIN	store y_i	300 200 ω4091"
		FWR			write y_i	638 000 ω0"
		WSP		1301	SP	636 000 ω1301"
240		JXU	20	LOOP	test i	856 240 ω9996"
		SEL		0111	select PR	630 000 ω111"
		WSP		1401	CR	636 000 ω1401"
		FAD/		YO	c(AC)=t	201 000 ω4040"
		FWR			write t	638 000 ω0"
245		WSP		1301	SP	636 000 ω1301"
		SEX	20	0		830 200 ω0"
		SEX	10	3		830 100 ω3"
	LOOP2	FAD/	20	M1	$c(AC)=M_i$ (i=2,3,4,B)	201 200 ω4108"
		STO	20	MMIN	store M_i	300 200 ω4103"
250		FWR			write M_i	638 000 ω0"
		WSP		1301	SP	636 000 ω1301"
		JXU	20	LOOP2	test i	854 240 ω9996"
		FAD/		Z		201 000 ω4096"
		STO		ZMIN		300 000 ω4095"
255	EXT	LDM		(ZZER)		320 000 ω400"
		FMP/		ALPHA	multipl. load factor	221 000 ω226"
		STO		Z		300 000 ω4096"
		LDA/		EXT		323 000 ω255"
		RAA		1	raise $c(EXT)_{ad}$ 1	130 000 ω1"
260		STA		EXT		306 000 ω255"
		JMP	03	1	jump to subroutine	714 030 ω1"

400	ZZER				displacement records of ground motion
⋮					

Program 203(b) Select Max Y_i, M_i, and φ_i (PRINT)

	LOC.	OPER.	XR	A	Remarks	DEC. CODE
230	PRINT	FAD/		YO+2	$c(AC)=y_2$	201 000 ω4042"
		FAD		YO+2	$c(AC)=2y_2$	200 000 ω4042"
		FSB		YO+1	$c(AC)=2y_2-y_1$	204 000 ω4041"
		FSB		YO+3	$c(AC)=-y_1+2y_2-y_3$	204 000 ω4043"
		STO		FI	$c(FI)=b\varphi_2$	300 000 ω1020"
235		FAD/		YO+3		201 000 ω4043"
		FAD		YO+3		200 000 ω4043"
		FSB		YO+2		204 000 ω4042"
		FSB		YO+4		204 000 ω4044"
		STO		FI+1	$c(FI+1)=b\varphi_3$	300 000 ω1021"
240		FAD/		YO+4		201 000 ω4044"
		FAD		YO+4		200 000 ω4044"
		FSB		YO+3		204 000 ω4043"
		FSB		Z		204 000 ω4096"
		STO		FI+2	$c(FI+2)=b\varphi_4$	300 000 ω1022"
245		FAD/		Z		201 000 ω4096"
		FAD		Z		200 000 ω4096"
		FSB		YO+4		204 000 ω4044"
		FSB		YO+4		204 000 ω4044"
		STO		FI+3	$c(FI+3)=b\varphi_5$	300 000 ω1023"
250		SEX	20	0		830 200 ω0"
		SEX	10	3		830 100 ω3"
	LOOP	FAD/	20	FI	$c(AC)=b\varphi_i$	201 200 ω1020"
		PAM				310 000 ω0"
		JMI		NUS	jump to NUS if $b\varphi_i < 0$	750 000 ω259"
255		CMP	20	FIMAX	$b\varphi_{max} \geq b\varphi_i$	324 200 ω1012"
		STO	20	FIMAX	$b\varphi_i \longrightarrow c(FIMAX)$ if $<$	300 200 ω1012"
		NOP				514 000 ω0"
		JMP		TEST		714 000 ω263"
	NUS	CMP	20	FIMIN	$b\varphi_{min} \leq b\varphi_i$	324 200 ω1016"
260		NOP				514 000 ω0"
		JMP		TEST		714 000 ω263"
		STO	20	FIMIN	$b\varphi_i \longrightarrow c(FIMIN)$ if $>$	300 200 ω1016"
	TEST	JXU	20	LOOP	test i	854 200 ω252"
		JMP		PRINT2		714 000 ω1100"

	LOC.	OPER.	XX	A	Remarks	DEC. CODE
1100	PRINT2	SEX	20	0		830 200 ω0"
		SEX	10	3		830 100 ω3"
	LOOP1	FAD/	20	YO+1	c(AC)=y_i	201 200 ω4041"
		STO	20	YMIN	$y_{i,n} \rightarrow y_{i,n-1}$	300 200 ω4091"
		SSP			set absolute y_i	510 000 ω0"
1105		PAM				310 000 ω0"
		CMP	20	YMAX	abs. $y_i \gtrless$ abs. y_{max}	324 200 ω1000"
		STO	20	YMAX	store abs. y_i if $>$	300 200 ω1000"
		NOP				514 000 ω0"
		JXU	20	LOOP1	test i	854 200 ω1102"
1110		SEX	20	0		830 200 ω0"
		SEX	10	3		830 100 ω3"
	LOOP2	FAD/	20	MOME+1	c(AC)=M_i (i=2,3,4,5)	201 200 ω4108"
		STO	20	MMIN	$M_{i,n} \rightarrow M_{i,n-1}$	300 200 ω4103"
		PAM				310 000 ω0"
1115		JMI		NEG	jump to NEG if $M_i < 0$	750 000 ω1120"
		CMP	20	MMAX	$M_i \gtrless M_{max}$	324 200 ω1004"
		STO	20	MMAX	store M_i if $>$	300 200 ω1004"
		NOP				514 000 ω0"
		JMP		SKIP		714 000 ω1124"
1120	NEG	CMP	20	MSML	$M_i \gtrless M_{min}$	324 200 ω1008"
		NOP				514 000 ω0"
		JMP		SKIP		714 000 ω1124"
		STO	20	MSML	store M_i if $<$	300 200 ω1008"
	SKIP	JXU	20	LOOP2	test i	854 200 ω1112"
1125		FAD/		Z	c(AC)=Z	201 000 ω4096"
		STO		ZMIN	$Z_n \rightarrow Z_{n-1}$	300 000 ω4095"
	EXT	LDM		(ZZER)		320 000 ω400"
		FMP/		ALPHA	multipl. load factor	221 000 ω226"
		STO		Z		300 000 ω4096"
1130		LDA/		EXT		323 000 ω1127"
		RAA		1	raise $c(EXT)_{ad}$ 1	130 000 ω1"
		STA		EXT		306 000 ω1127"
		LXA	20	COUNT		320 200 ω1169"
		JXL	20	SKIP1	if c(COUNT)≠0 next step	850 200 ω1136"

	LOC.	OPER.	XX	A	Remarks	DEC. CODE
1135		JMP		SKIP2	if c(COUNT)=0 print	714 000 ω1138"
	SKIP1	STX	20	COUNT		822 200 ω1169"
		JMP	03	1	jump to subroutine	714 030 ω1"
	SKIP2	SEL		0111	select PR	630 000 ω111"
		SEX	30	4		830 300 ω4"
1140	LOOP3	ADD/	03	HEAD		101 030 ω1164"
		WRT		1005	write HEAD	634 000 ω1005"
		WSP		1309	SP:9	636 000 ω1309"
		JXL	30	LOOP3	test i	850 300 ω1140"
		WSP		1401	CR	636 000 ω1401"
1145		SEX	20	0		830 200 ω0"
		SEX	10	3		830 100 ω3"
	LOOP4	FAD/	20	YMAX		201 200 ω1000"
		FWR			write y_{max}	638 000 ω0"
		WSP		1301	SP	636 000 ω1301"
1150		FAD/	20	MMAX		201 200 ω1004"
		FWR			write M_{max}	638 000 ω0"
		WSP		1301	SP	636 000 ω1301"
		FAD/	20	MSML		201 200 ω1008"
		FWR			write M_{min}	638 000 ω0"
1155		WSP		1301	SP	636 000 ω1301"
		FAD/	20			201 200 ω1012"
		FWR			write φ_{max}	638 000 ω0"
		WSP		1301	SP	636 000 ω1301"
		FAD/	20	FIMIN		201 200 ω1016"
1160		FWR			write φ_{min}	638 000 ω0"
		WSP		1401	CR	636 000 ω1401"
		JXU	20	LOOP4	test i	854 200 ω1147"
		HJM		0	halt	710 000 ω0"
	HEAD	23 26 30 26 31			F I M I N	2326302631"
1165		23 26 30 18 41			F I M A X	2326301841"
		30 13 30 26 31			M SP M I N	3013302631"
		30 13 30 18 41			M SP M A X	3013301841"
		42 13 30 18 41			Y SP M A X	4213301841"
	COUNT	(AD)			initialle set the number of steps	"

Working Space for Modified (PRINT)

1000	YMAX	y_{max}
•		
1003		
1004	MMAX	M_{max}
•		
1007		
1008	MSML	M_{min}
•		
1011		
1012	FIMAX	$b\varphi_{max}$
•		
1015		
1016	FIMIN	$b\varphi_{min}$
•		
1019		
1020	FI	$b\varphi_i$
•		
1023		

400	ZZER	displacement records of ground motion
•		
•		
•		
•		

Table 201

T	M			
+000000000-00	+000000000-00	+000000000-00	+000000000-00	+000000000-00
+189390000-01	+26127454 2+01	-423585878+01	-505661679+03	+185759156+04
+378780000-01	+359161947+02	-584986620+02	-396975521+04	+147385888+05
+568170000-01	+2063991 50+03	-338847914+03	-108841250+05	+415158073+05
+757560000-01	+629413989+03	-113058131+04	-151414525+05	+618933725+05
+946950000-01	+1543778 54+04	-262405558+04	-175607009+05	+802439014+05
+1136340000+00	+2785096611+04	-486912812+04	-161366484+05	+900654925+05
+1325730000+00	+4246185 34+04	-773450678+04	-128926172+05	+985804103+05
+1515120000+00	+5718448 26+04	-1096386 10+05	-701652467+04	+1021002 27+06
+1704510000+00	+6927342 99+04	-1418728 16+05	+1008708 61+04	+1011034 89+06
+1893900000+00	+7591246 72+04	-1695078 47+05	+1145946 59+05	+9272780 35+05
+2083290000+00	+7428862 57+04	-1870954 65+05	+2735685 29+05	+6346696 96+05
+2272680000+00	+6144354 29+04	-1878897 09+05	+4387514 54+05	+2713427 08+05
+2462070000+00	+3539678 30+04	-1656191 33+05	+5912881 61+05	-1331672 76+05
+2651460000+00	-4222039 45+03	-1156745 88+05	+7338854 68+05	-6238868 34+05
.....	.....	.....	.....	.....

Table 202

H = +189390000-01 α = +500000000-01

Y MAX	M MAX	M MIN	FIMAX	FIMIN
+435148534-01	+290362893+05	-315517497+05	+314531489+00	-341779858+00
+219110841+00	+540615584+05	-536588870+05	+251402333+00	-249529797+00
+175356013+00	+5743817 52+05	-559699395+05	+132929196+00	-129531261+00
+910706716-01	+1777039 32+06	-1363161 04+06	+227060530+00	-174177395+00

IV NUMERICAL ANALYSIS

209. Numerical Example and its Physical Constants

To facilitate numerical computations the Akashi Straits Bridge Plan II, used in the previous study was adopted. A seismic design of the towers of this bridge was primarily done by the classical seismic coefficient method using the seismic coefficient k = 0.2. The steel weight of these towers are considerably large compared to those of a modern suspension bridge, Mackinac Bridge, to which no precautions against earthquake were paid.

The main dimensions and physical constants of the towers are shown in Fig. 209 and Table 203. The following simplifications of the structure necessary to carry the computer analysis derived were assumed.

(1) The tower was devided into four segments as shown in Fig. 210.

(2) Physical constants of this simplified system were assumed as shown in Table 204.

210. Ground Motion

As already mentioned the earthquake motions are quite complicated and it is quite difficult to predict future strong earthquakes. Since no strong motion records are available in Japan, the ground motion used in this numerical analysis are (a) a simple harmonic motion, and (b) 1957 So. California Earthquake.

(a) Ground motion with simple harmonic shape

The purpose of the numerical analysis for the ground motion with simple shape is to study the fundamental characteristics of the dynamic response.

Ground motion used is one which has the following shape.

$$\begin{aligned} Z &= A \sin \omega t && 0 \leqq t \leqq T \\ &= 0 && t > T \end{aligned} \qquad (218)$$

where $\omega = \frac{2\pi}{T}$

Numerical calculation have been done for the ground motion with the period T = 0.6 sec. and T = 1.2 sec. Displacement amplitudes A were selected as A = 10, 20, 30, and 40 cm, and corresponding maximum accelerations are

In the case of	T = 0.6 sec	T = 1.2 sec
A = 10 cm	1.119 g	0.280 g
A = 20 cm	2.238 g	0.560 g
A = 30 cm	(3.357 g) *	0.893 g
A = 40 cm	4.476 g	1.119 g

(b) 1957 So. California Earthquake

1957 So. California Earthquake is already given previously.

The ground motion of 1957 So. California Earthquake, however, is not large enough to apply to the elastic-plastic analysis of the suspension bridge tower, and the ground motions multiplied by load factors were used in the numerical analysis. These factors are varied as α = 1, 5, 10, 15, 20, 30, and 40.

211. Numerical Computation

The numerical computations were, as already mentioned, done on KDC-I using the program previously given.

The time intervals h of numerical integration were selected, considering the accuracies of the process, as follows.

For the ground motion of

Sine curve with the period T = 0.6 sec	h = 0.01 sec
Sine curve with the period T = 1.2 sec	h = 0.02 sec
The ground motion of 1957 So. California E.Q.	h = 0.018939sec

The value of δ which specifies the accuracy of the iterative process is selected, for all cases, as

$$\delta = 0.25 \times 10^{-8} \quad (m)$$

Taking this value, the iteration of each step repeated ablut five times and δ is considered to be adequate.

---

* Computation for T = 0.6 sec and A = 30 cm was omitted.

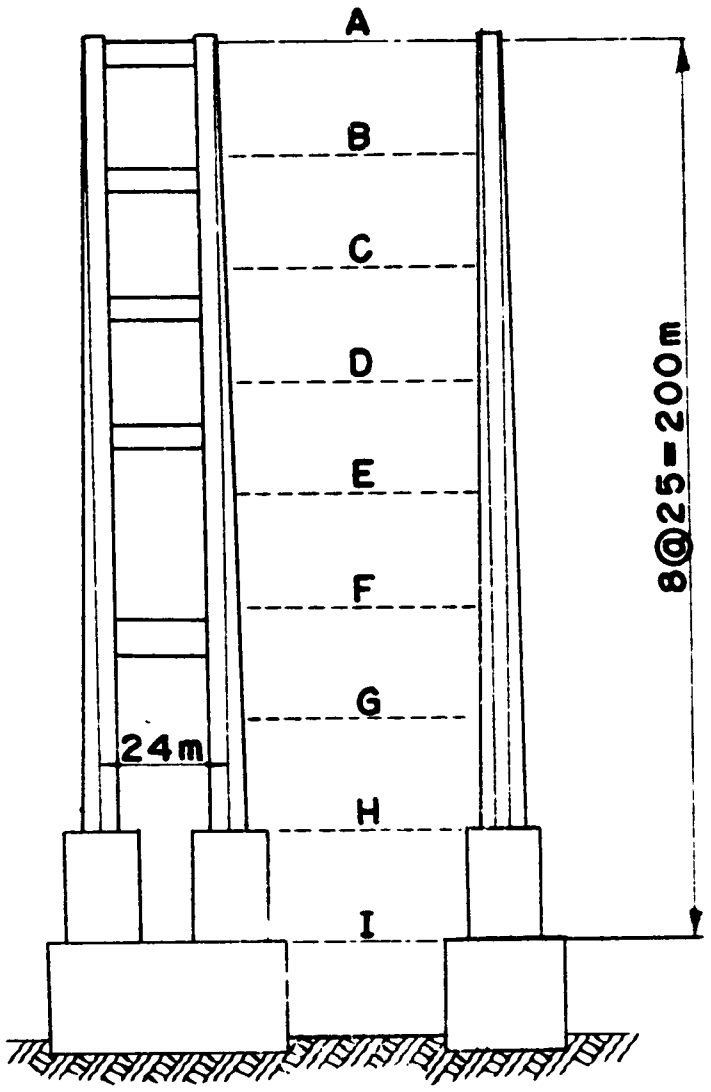

PROTOTYPE

Fig 209

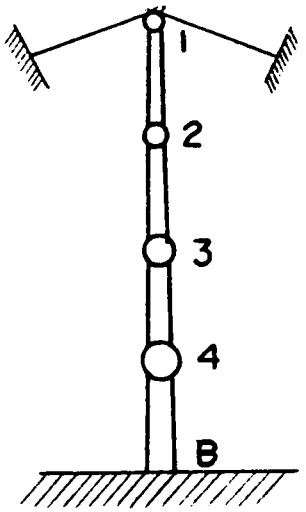

Fig. 210

Table 203 Dimensions of Towers

Section	b (m)	h (m)	A (m^2)	I (m^4)	W (ton)
A	3.00	5.00	1.62	3.75	177
B	3.50	5.75	2.25	6.65	455
C	4.00	6.50	2.70	10.99	585
D	4.50	7.25	3.15	17.15	731
E	5.00	8.00	3.60	25.60	893
F	5.50	8.75	4.07	36.85	1071
G	6.00	9.50	4.50	51.44	1266
H	6.50	10.3	4.95	70.00	1476
I	7.00	11.0	5.40	93.17	

b, h = width and height of sections, A = cross sectional area
I = sectional moment of inertia, W = dead weight

Table 204 Dimensions of Physical System

Section	W_r (ton)	M_{r0} (t-m)	P_{gr} (ton)	P_{Yr} (ton)	B_r/b (ton)
1	340		11375		
2	1165	85135	11715	64800	92316
3	1978	161538	12880	86400	215040
4	2521	273022	14658	108000	432096
B		427118	17179	129600	782628

212. Representative History Curves

As already mentioned in the previous chapter, the history curves were obtained for limited cases. The results of the solution are presented in Figs. 211 through 214. A history curve is a plot of the variation of displacement or moment as a function of time. The curves in Figs. 211 (a) and (b) are for displacements and moments due to the simple harmonic ground motion with the period T = 0.6 sec. and the amplitude 10 cm. The curves in Figs 212 (a) and (b) are due to the simple harmonic ground motion with the period T = 1.2 sec. and the amplitude A = 40 cm. The curves in Figs. 213 (a) and (b), and 214 (a) and (b) are due to 1957 So. California Earthquake magnified by the load factors 10 and 40 respectively. In these curves are plotted the dynamic response given by the computer in the format of Table 201. The specific curves shown by a series of small open circles in these response history curves, y_2 curves and M_2 curves, show direct plotting of obtained values.

213. Maximum and Minimum Dynamic Responses

Maximum dynamic responses obtained on the KDC-I using Program 203 (b) are summarized in Tables 205 through 207. In these tables maximum bending moment and maximum curvature are the maximum dynamic responses of their absolute value.

These maximum values are the maximum dynamic response during the first few seconds of dynamic history specified by the number of total steps of time intervals. For simple harmonic ground motion T = 0.6 sec. T = 1.2 sec. and 1957 So. California Earthquake, these number of the steps were chosen as 130 steps (1.3 sec), 130 steps (2.6 sec) and 380 steps (7.2 sec) respectively.

Fig. 215 shows the relations of the maximum displacements and the load factors, and Fig. 216 shows the relations of the maximum moments or maximum curvatures and the load factors for the 1957 So. California Earthquake.

214. Bending Moment-Curvature Relation

As already mentioned, the maximum and minimum bending moments

and the corresponding curvatures were obtained on KDC-I in the format of Table 202. Although the complete response time history curves are necessary to obtain the complete bending moment-curvature relations, the outlines of these relations can be roughly estimated from the maximum and minimum dynamic responses obtained.

Figs. 217 (a) through (c) are the bending moment-curvature relations obtained from the complete time history curves due to the simple harmonic ground motion with the period T = 0.6 sec. Figs. 218 and 219 are the rough curves obtained from the maximum and minimum outputs. The open circles in Figs. 218 and 219 were the values of outputs of the computer, and the hysteresis curves were estimated from these points. Figs. 218 are for the simple harmonic motion with the period T = 1.2 sec. and Figs. 219 are for the 1957 So. California Earthquake.

The yield line of these figures are not the straight lines but the function of axial forces. Influences of incremental axial force, however, is quite small, and these effects were disregarded in these figures.

215. Effects of Motion of Anchorage

In the numerical computation described thus far, the ground motions were considered to act to only the base of the tower, and the left side anchorage was assumed to stand still.

Using the modified program, Program 202 (b), the effects of the motion of the anchorage can be taken into the numerical analysis.

Using the modified program and assuming the relative phase difference $Z_A = -Z_B$, time history curves due to 1957 So. California Earthquake were obtained as shown in Figs. 220 (a) and (b). The maximum dynamic responses obtained under the same assumption are tabulated in Table 208.

To indicate the manner in which the dynamic response is influenced by the disturbance from the anchrage, the history curves in Figs. 220 (a) and (b) are compared to corresponding curves in Figs. 213 (a) and (b) and shown in Figs. 221 and 222.

It can be seen from this comparison that the dynamic response curves of two cases are quite similar, except the response of the displacement at the top of the tower. The maximum dynamic responses shown in Table 208 appears to be slightly greater or less than the values in Table 207 except the response at the top of the tower.

216. Investigations on the Results Obtained

Some of the remarkable conclusions derived directly from the numerical computations will be summarized as the following.

(1) The large energy discipation due to plastic deformations affects the maximum dynamic responses which do not proportionally increase with the ground motion. Although some considerations on allowable plastic deformations of the tower are necessary, the effects of plastic deformations of the tower are significantly effective not only to the design of the towers but to the desigh of substructures.

(2) Influence of incremental axial force to elastic response given in the form of $P_p (y_{r-1}-2y_r+y_{r+1})$ is not important since the maximum dynamic response within an elastic range is approximately on a straight line.

(3) In the analysis given, the yield moments of the cross sections were considered to vary with the axial force. Numerical values of yield moments obtained from the dynamic response of the bending moments indicated a slight variation in those values, and they are approximately considered to be invariable and plotted on straight lines in the figures.

(4) In Figs. 223 (a) through (d) are compared the dynamic response history curves due to the ground disturbances with different periods but with the same maximum acceleration. This comparison indicates that the maximum ground acceleration is no longer a proper indication of the earthquake intensity for the suspension bridge analysis. In Figs. 224 (a) and (b) are compared the curves due to the ground motions with different periods but with the same amplitude. It seems to be able to conclude from this comparison that the suspensionbridge towers are structures of flexible type specified already. This comparison is done only for the special cases, T = 0.6 and 1.2 sec and more investigations are, therefore, necessary to obtain general conclusions on the effects of the periods of external disturbances.

(5) As shown in the preceding article, the effects of the motion of the anchorage are not significant in the analysis of the tower, and can be approximately possible to disregard the effects.

According to the results obtained, the tower is still stable even under the action of the large earthquake, 1957 So. California Earthquake multiplied the load factor 40, though plastic deformations of the tower are yielded. If a extremely large ground motion is acted to the base of the tower, such as the case of load factor more than

300, the tower becomes under the condition of instability, and the displacements increase infinitively. These actions are illustrated in Figs. 225 (a) and (b) for the load factors 300 and 600.

Elastic-plastic analyses of structures by finite difference method or the model expression have been done recently [208][209] and will be applied to the analyses of dynamic problems of the structures although more mathematical verifications are necessary.

Table 205 Maximum Response due to the Ground Motion

$Z_B = A \sin (2\pi/0.6)t \qquad 0 \leq t \leq 0.6$

A (m)	Response			
	Maximum Displacement (m)			
	y_1	y_2	y_3	y_4
0.1	0.06950	0.29515	0.15818	0.16435
0.2	0.12919	0.48090	0.27989	0.24551
0.4	0.16844	0.86065	0.55976	0.47640
	Maximum Bending Moments (ton-m)			
	M_2	M_3	M_4	M_B
0.1	54678.18	87485.34	75457.37	257245.61
0.2	69960.80*	137750.37*	153668.49	370240.31*
0.4	69690.99*	137790.00*	236288.50*	370942.54*
	Maximum Curvatures (multiplied by b m)			
	$\varphi_2{}^b$	$\varphi_3{}^b$	$\varphi_4{}^b$	$\varphi_B{}^b$
0.1	0.59229	0.40683	0.17782	0.32870
0.2	0.66861*	0.51249*	0.35564	0.49102*
0.4	1.81452*	1.20352*	0.68391*	0.72526*

* sections where the plastic hinges are yielded

Table 206 Maximum Response due to the Ground Motion

$Z_B = A \sin (2\pi/1.2)t \qquad 0 \leq t \leq 1.2$

A (m)	Response			δ
	Maximum Displacements (m)			
	y_1	y_2	y_3	y_4
0.1	0.038829	0.312723	0.250845	0.108106
0.2	0.077416	0.625976	0.484436	0.216213
0.3	0.116371	0.773533	0.644242	0.324319
0.4	0.136554	0.844889	0.606817	0.432424
	Maximum Bending Moments (ton-m)			
	M_2	M_3	M_4	M_B
0.1	36949.98	45210.25	67619.10	167156.60
0.2	69560.96*	89249.75	135213.92	334295.54
0.3	69943.25*	109958.54	185490.05	369887.11*
0.4	69975.85*	127908.24	204575.99	369636.36*
	Maximum Curvatures (multiplied by b m)			
	$\varphi_2 b$	$\varphi_3 b$	$\varphi_4 b$	$\varphi_B b$
0.1	0.400255	0.210241	0.156961	0.213584
0.2	0.802689*	0.415038	0.312926	0.427145
0.3	1.009824*	0.511340	0.429280	0.473491*
0.4	1.393774*	0.594811	0.473450	0.483583*

* sections where the plastic hinges are yielded

Table 207 Maximum Earthquake Response

Standard Earthquake : 1957 So. California Earthquake

Load Factor	Response			
	Maximum Displacements (m)			
	y_1	y_2	y_3	y_4
1	0.008696	0.043824	0.035070	0.018215
5	0.043515	0.21911	0.17536	0.09107
10	0.087116	0.43819	0.35073	0.18212
15	0.11664	0.64353	0.43419	0.24293
20	0.13238	0.85599	0.49891	0.32391
30	0.17243	1.20856	0.67451	0.48615
40	0.17649	1.48928	0.86365	0.63521
	Maximum Bending Moments (ton-m)			
	M_2	M_3	M_4	M_B
1	6311.45	10812.34	11487.72	27261.96
5	31551.75	54061.56	57438.18	177703.93
10	63089.32	108121.04	114869.73	272641.52
15	69998.95*	137332.84*	164109.12	344732.91
20	70050.22*	137663.69*	178498.82	345871.69
30	70140.29*	137769.24*	236130.87*	370804.85*
40	70143.31*	137838.01*	236175.79*	370996.71*
	Maximum Curvatures (multiplied by b m)			
	$\varphi_2{}^b$	$\varphi_3{}^b$	$\varphi_4{}^b$	$\varphi_B{}^b$
1	0.068368	0.050281	0.026586	0.034834
5	0.34178	0.25140	0.13293	0.22726
10	0.68341	0.50280	0.26594	0.34837
15	1.01864*	0.65397*	0.37980	0.44048
20	1.49461*	0.81745*	0.41310	0.44193
30	1.93737*	1.07380*	0.57448*	0.56058*
40	2.29241*	1.25193*	0.72752*	0.82444*

* sections where the plastic hinges are yielded

Table 208 Maximum Earthquake Response

Standard Earthquake : 1957 So. California Earthquake (including the effects of the motion of the left side anchorage) $Z_A = -Z_B$

Load Factor	Response			
	Maximum Displacements (m)			
	y_1	y_2	y_3	y_4
10	0.17449	0.39172	0.31017	0.17986
20	0.32362	0.72961	0.39808	0.33033
40	0.51506	0.88772	0.76559	0.64628
	Maximum Bending Moments (ton-m)			
	M_2	M_3	M_4	M_B
10	61887.18	111467.92	111612.81	271970.51
20	70219.92*	137898.89	159828.98	347521.17
40	70837.37*	139033.51*	238376.34*	369794.40*
	Maximum Curvatures (multiplied by b m)			
	$\varphi_2{}^b$	$\varphi_3{}^b$	$\varphi_4{}^b$	$\varphi_B{}^b$
10	0.67038	0.51836	0.25831	0.34751
20	1.38915*	0.85358	0.36989	0.44404
40	1.41968*	1.42920*	0.72907*	0.88568*

* sections where the plastic hinges are yielded

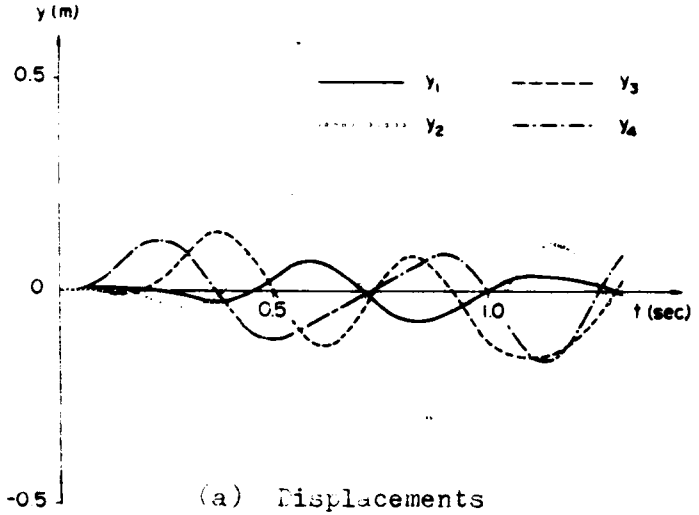

(a) Displacements

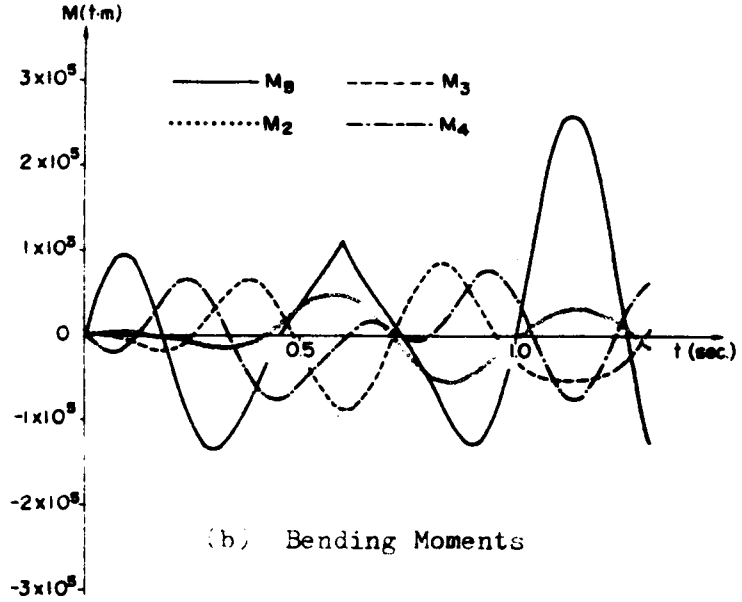

(b) Bending Moments

Fig. 211 Time History Curves due to the Ground Motion

$Z_B = A \sin \omega t$ $\omega = \frac{2\pi}{C\zeta}$ (sec^{-1})

A = 10 cm

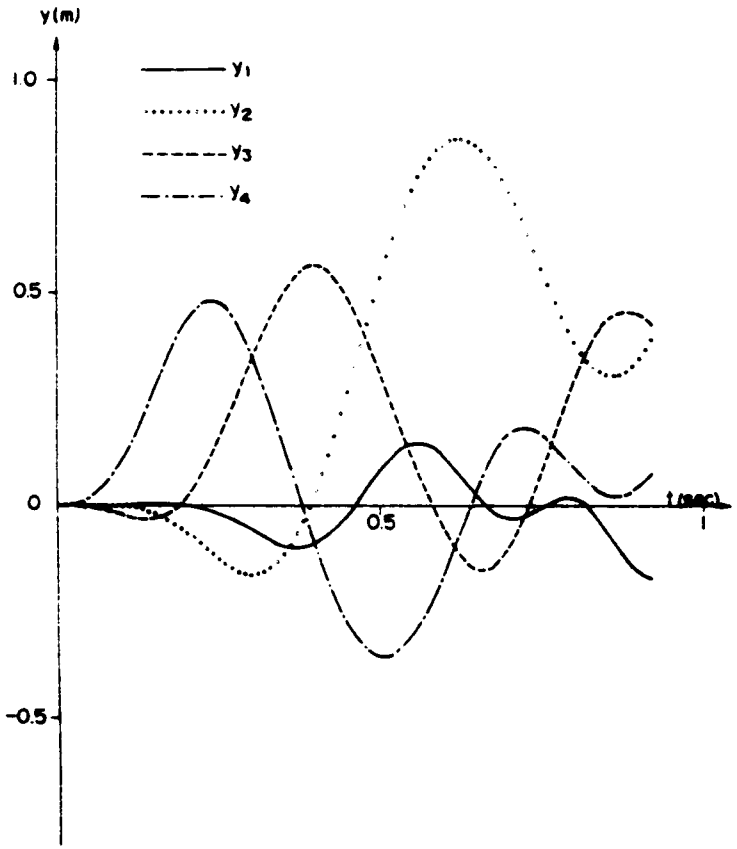

(a) Displacements

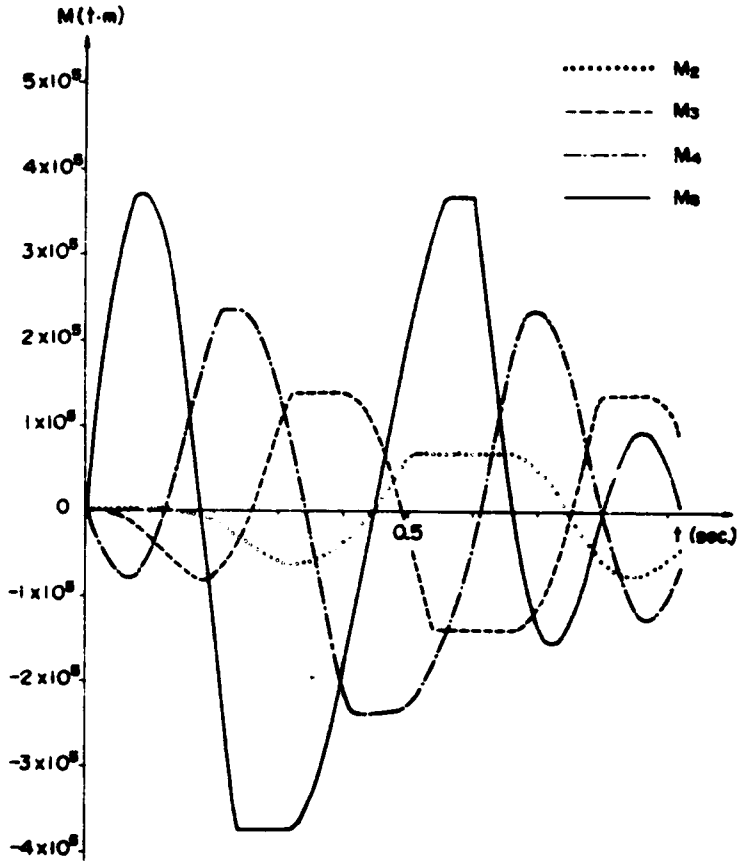

(b) Bending Moments

Fig. 212 Time History Curves due to the Ground Motion

$Z_B = A \sin \omega t$ $\qquad \omega = \frac{2\pi}{1.2}$ sec^{-1}

A = 40 cm

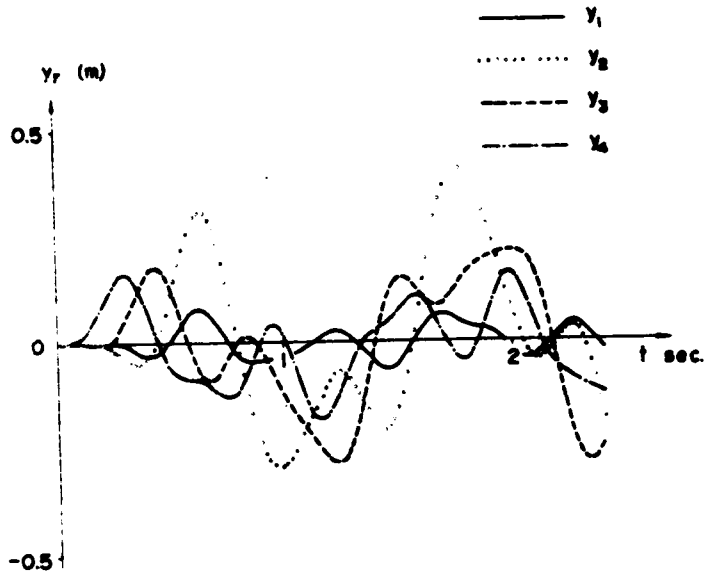

(a) Displacements

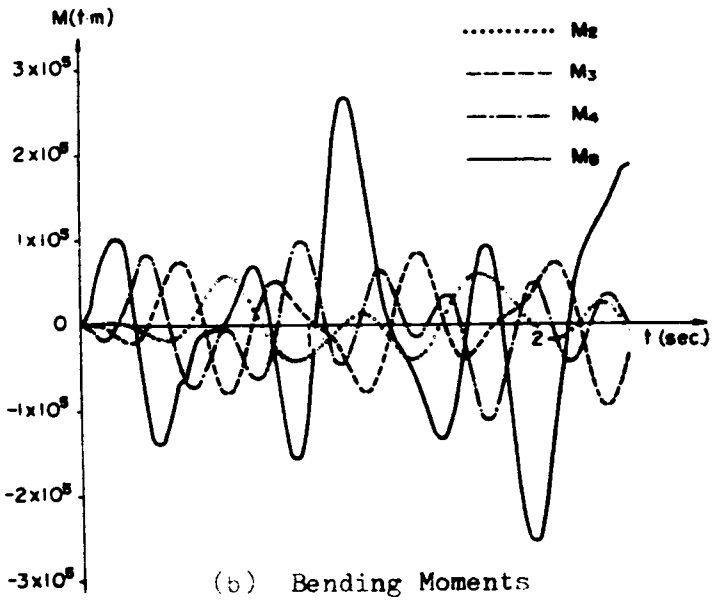

(b) Bending Moments

Fig. 213 Time History Curves due to 1957 So. Calif. E.Q. x 10

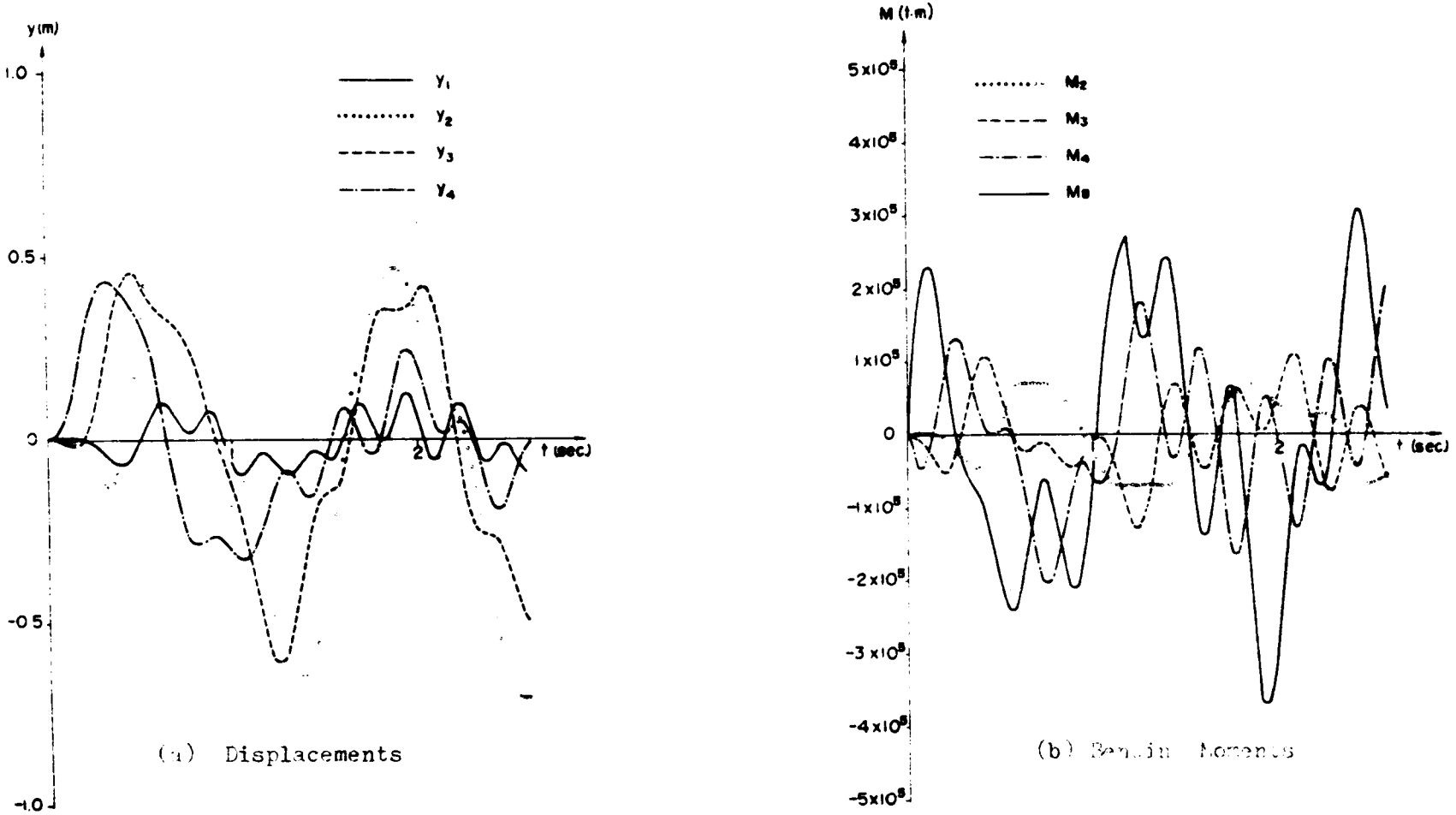

(a) Displacements

(b) Bending Moments

Fig. 214 Time History Curves due to 1952 So. Calif. E.Q. x 40

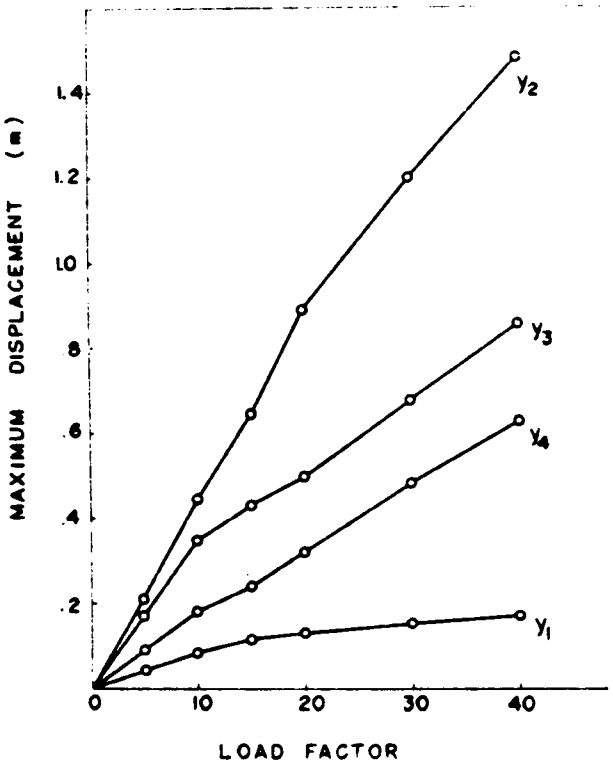

Fig. 215

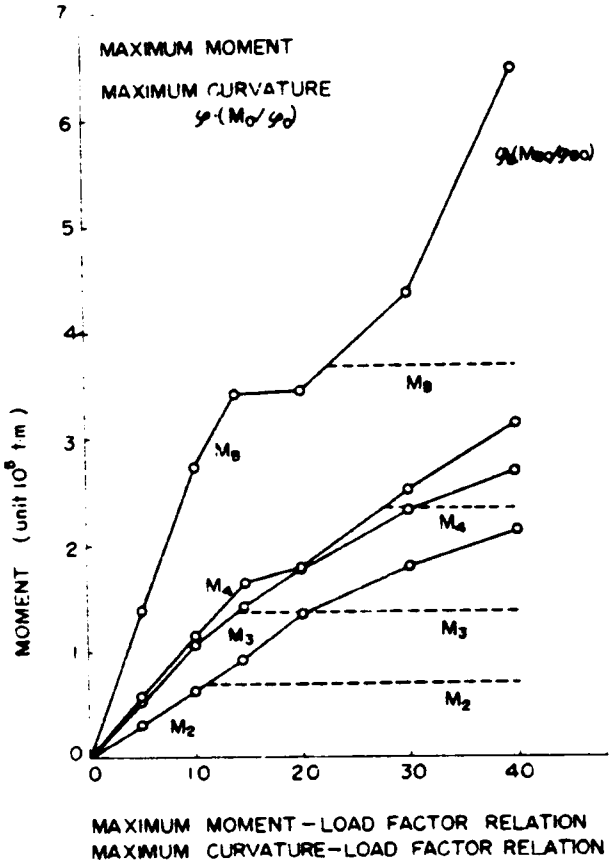

Fig. 216

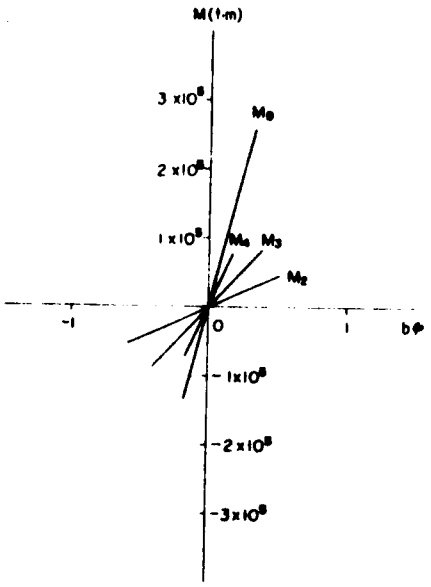

(a) A = 10 cm

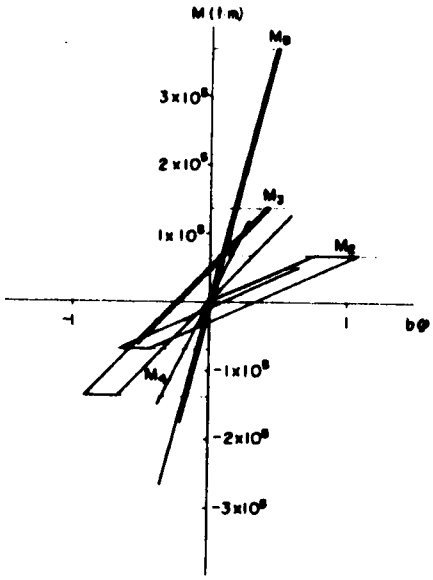

(b) A = 20 cm

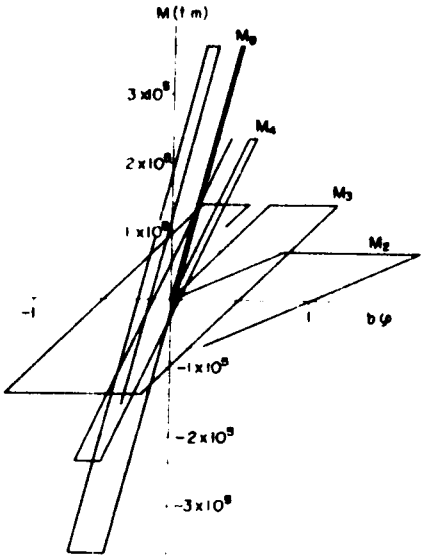

(c) A = 40 cm

Fig. 217 Moment-Curvature Relations due to the Ground Motion

$Z = A \sin \omega t$ $\omega = \frac{2\pi}{0.6}$ sec^{-1}

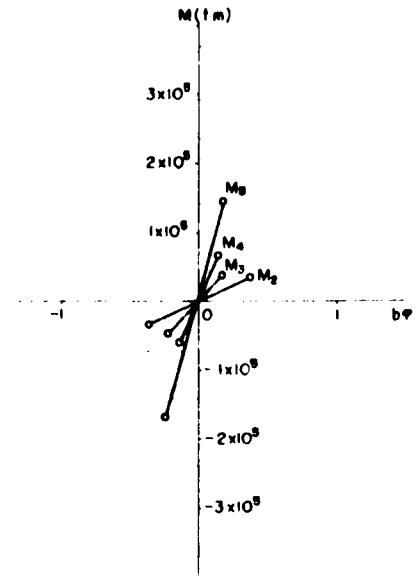

(a) A = 10 cm

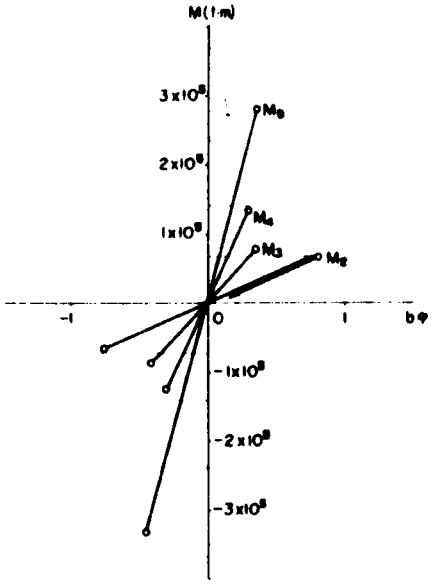

(b) A = 20 cm

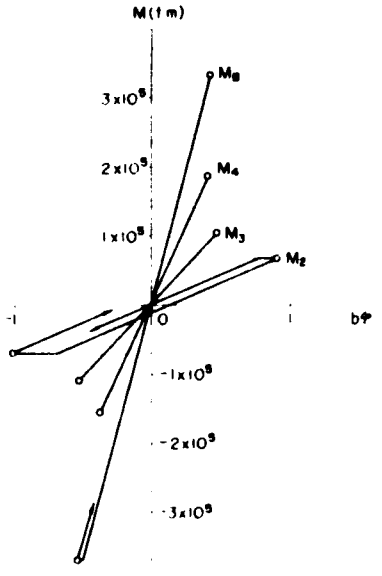

(c) A = 30 cm

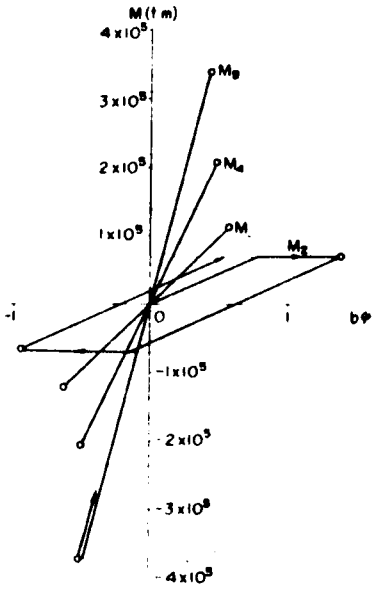

(d) A = 40 cm

Fig. 21 Moment-Curvature Relations due to the Ground Motion

$Z_B = A \sin \omega t$ $\omega = \frac{2\pi}{1.2}$ sec^{-1}

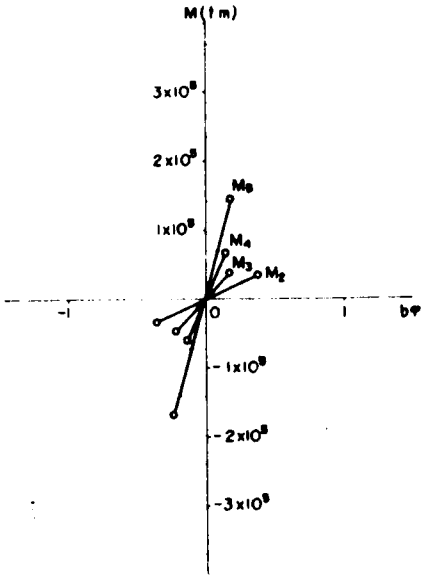

(a) $\alpha = 5$

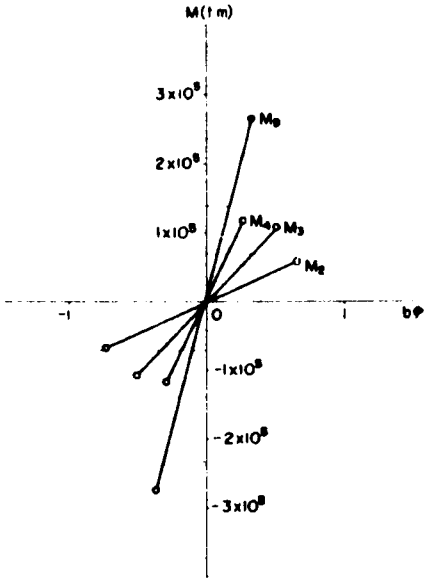

(b) $\alpha = 10$

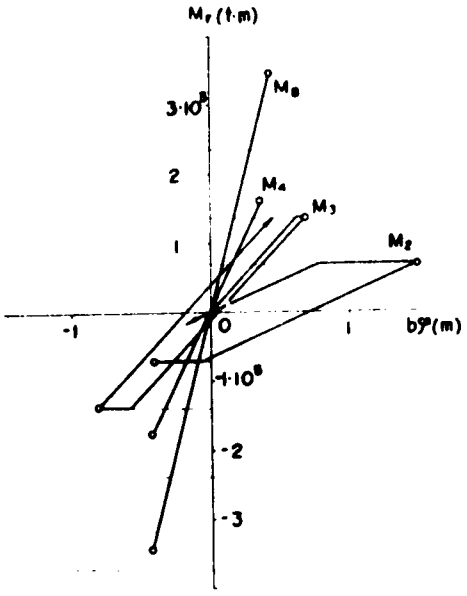

(c) $\alpha = 20$

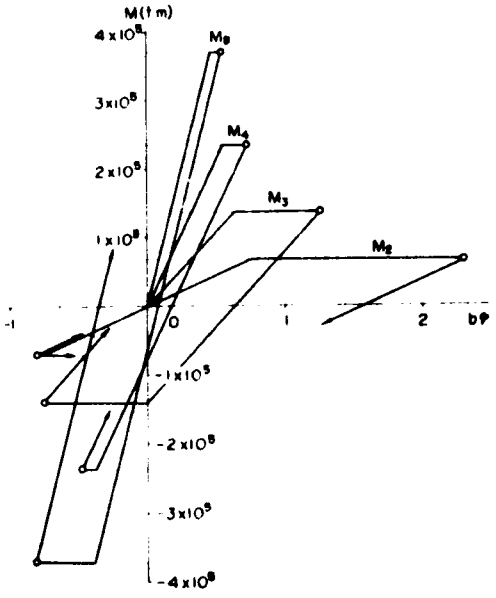

(d) $\alpha = 40$

Fig. 219 Moment-Curvature Relations due to 1957 So. Calif. E.Q. x Load Factor α

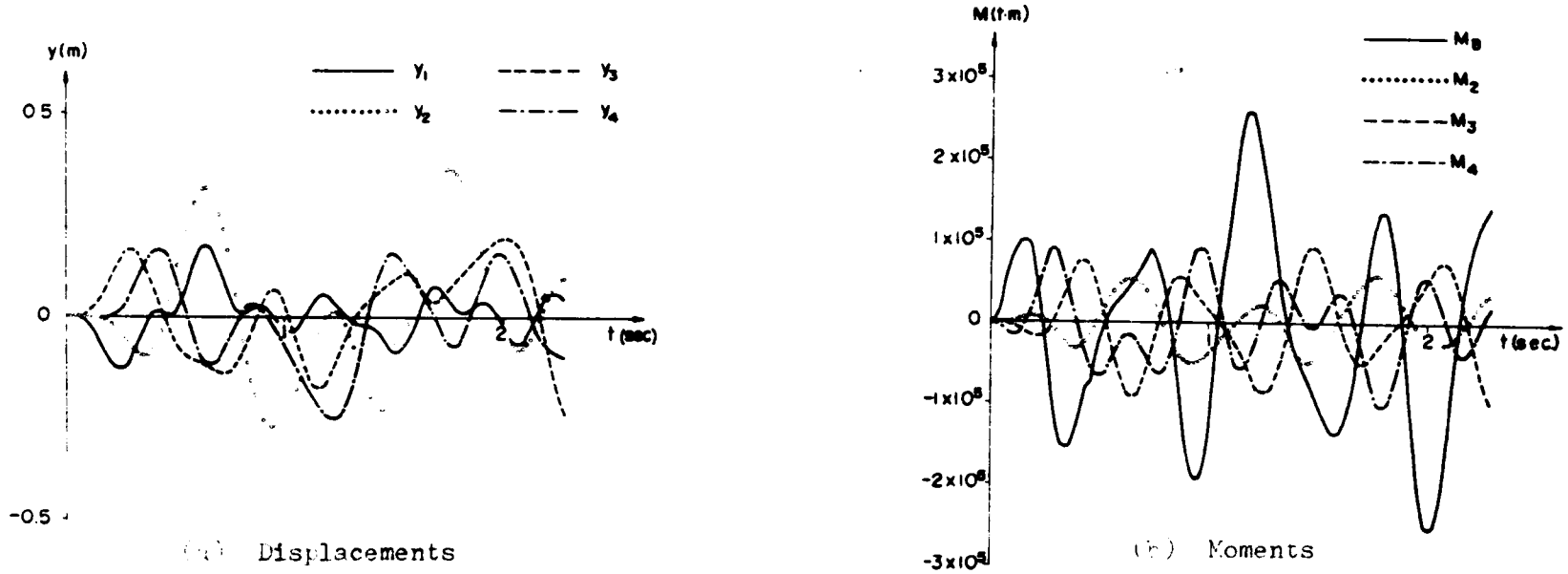

(a) Displacements (b) Moments

Fig. 220 Effects of the Motion of the Cable Anchorage
1957 So. Calif. Eqk. x 10

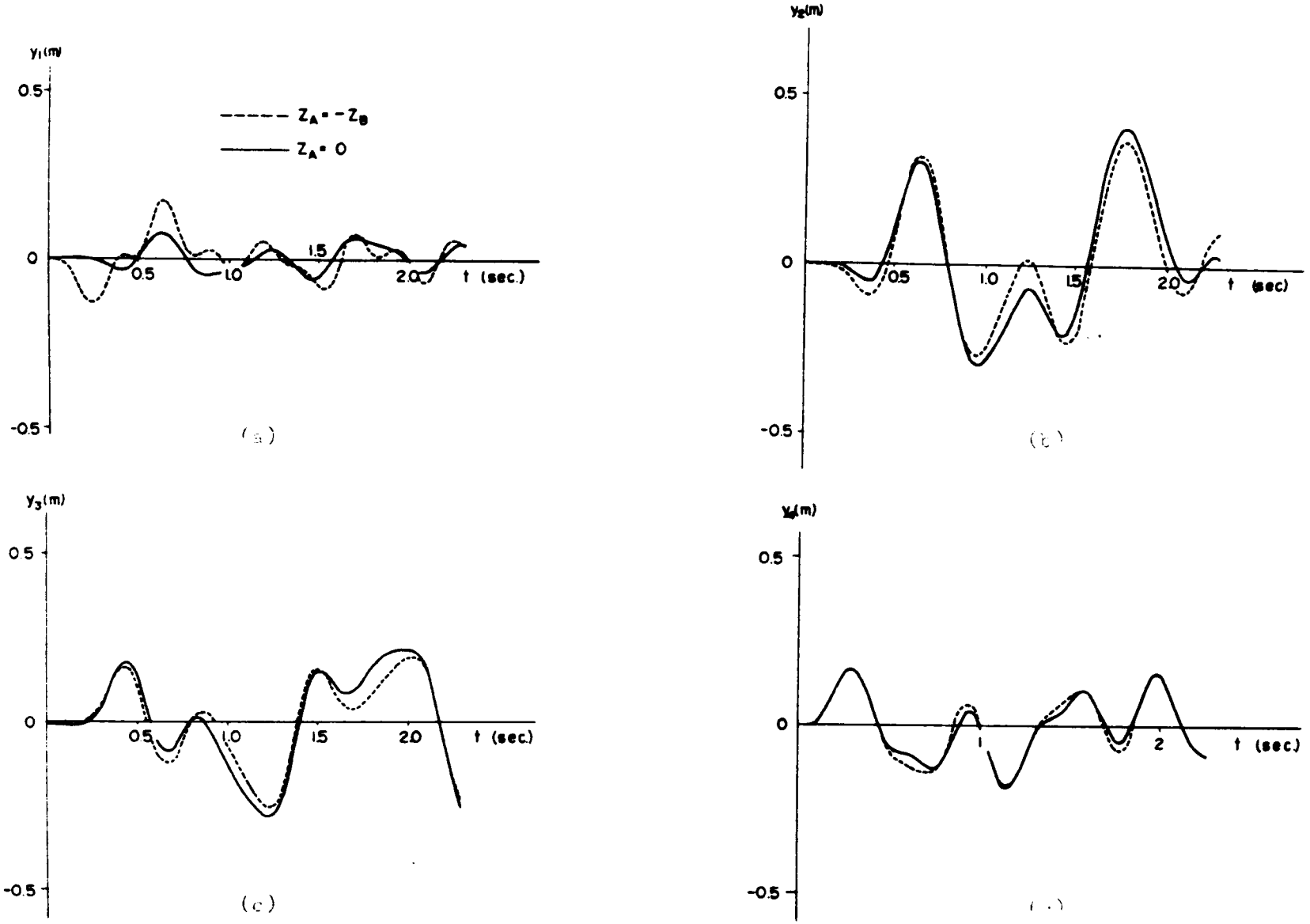
y_1(m)
0.5
0
-0.5
$Z_A = -Z_B$
$Z_A = 0$
0.5
1.0
1.5
2.0
t (sec.)
(a)
y_2(m)
0.5
0
-0.5
0.5
1.0
1.5
2.0
t (sec)
(b)
y_3(m)
0.5
0
-0.5
0.5
1.0
1.5
2.0
t (sec.)
(c)
y_4(m)
0.5
0
-0.5
1
2
t (sec.)
(d)

Fig. 21

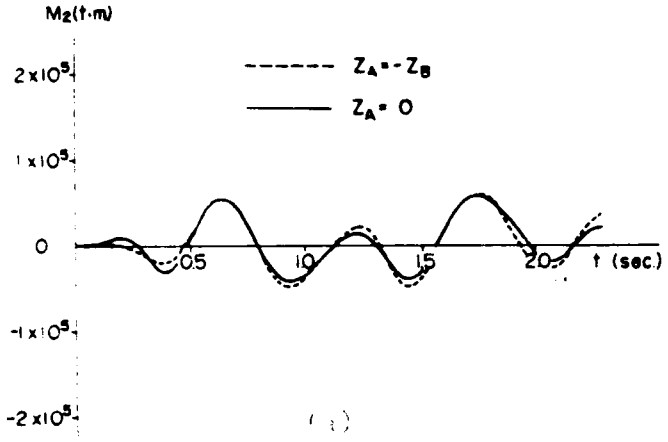
M2(t·m)
2x10^5
1x10^5
0
-1x10^5
-2x10^5
Z_A = -Z_B
Z_A = 0
0.5
1.0
1.5
2.0
t (sec.)

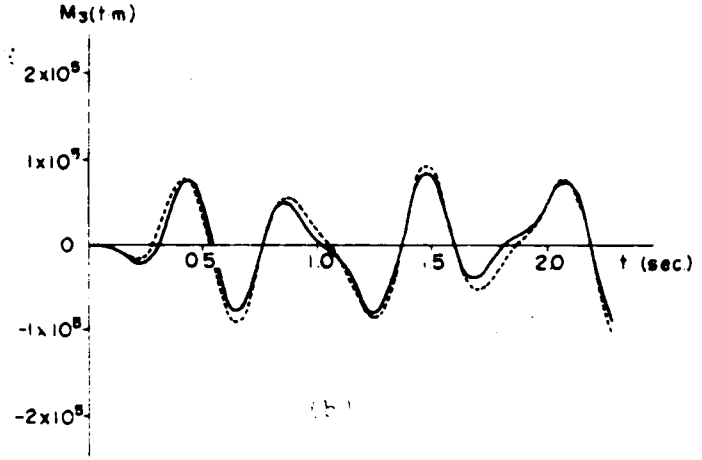
M3(t·m)
2x10^5
1x10^5
0
-1x10^5
-2x10^5
0.5
1.0
1.5
2.0
t (sec.)

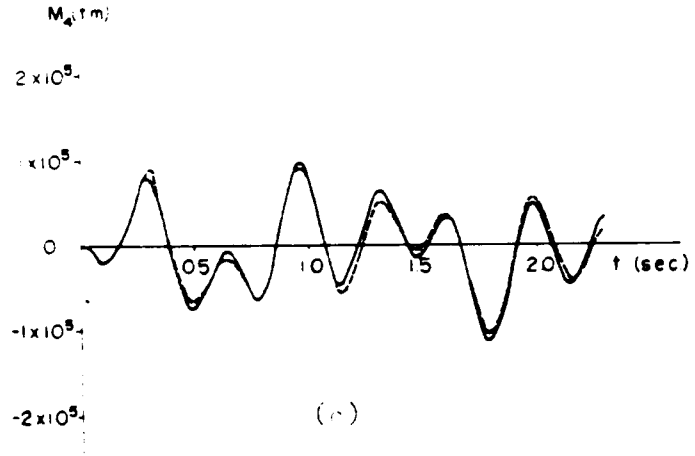
2x10^5
1x10^5
0
-1x10^5
-2x10^5
0.5
1.0
1.5
2.0
t (sec)

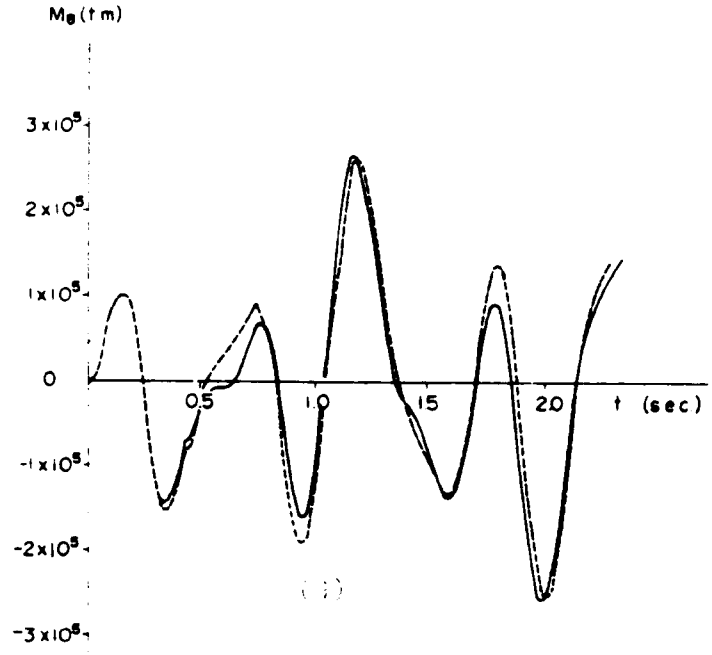
M8(t·m)
3x10^5
2x10^5
1x10^5
0
-1x10^5
-2x10^5
-3x10^5
0.5
1.0
1.5
2.0
t (sec)

Fig. 222

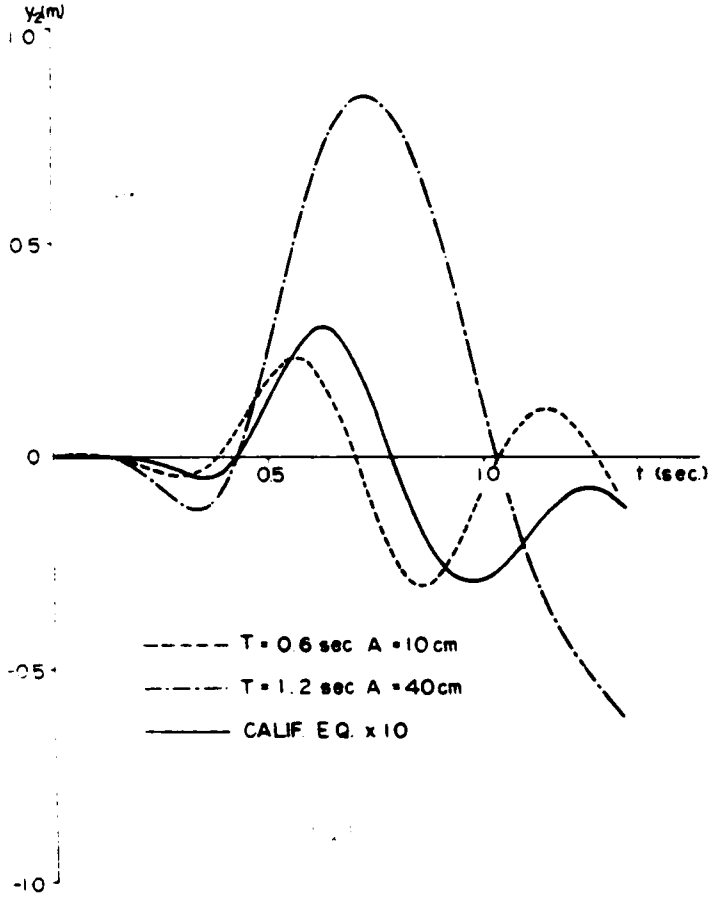
y_2(m)
1.0
0.5
0
-0.5
-1.0
0.5
1.0
t (sec.)
T = 0.6 sec A = 10 cm
T = 1.2 sec A = 40 cm
CALIF. EQ. x 10

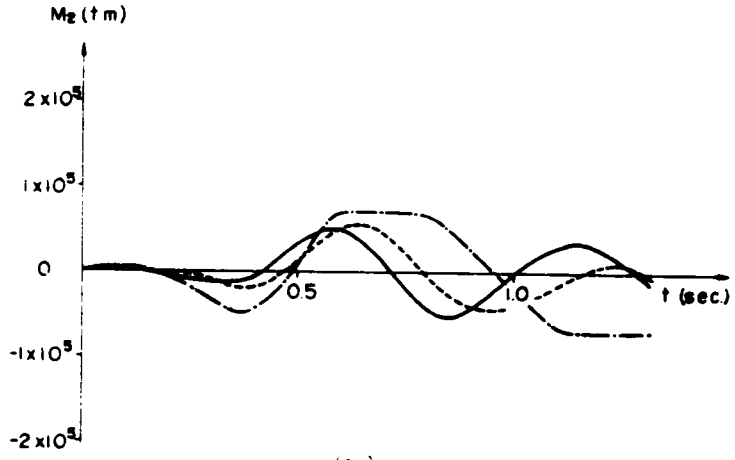
M_2 (t m)
2×10^5
1×10^5
0
-1×10^5
-2×10^5
0.5
1.0
t (sec.)

(b)

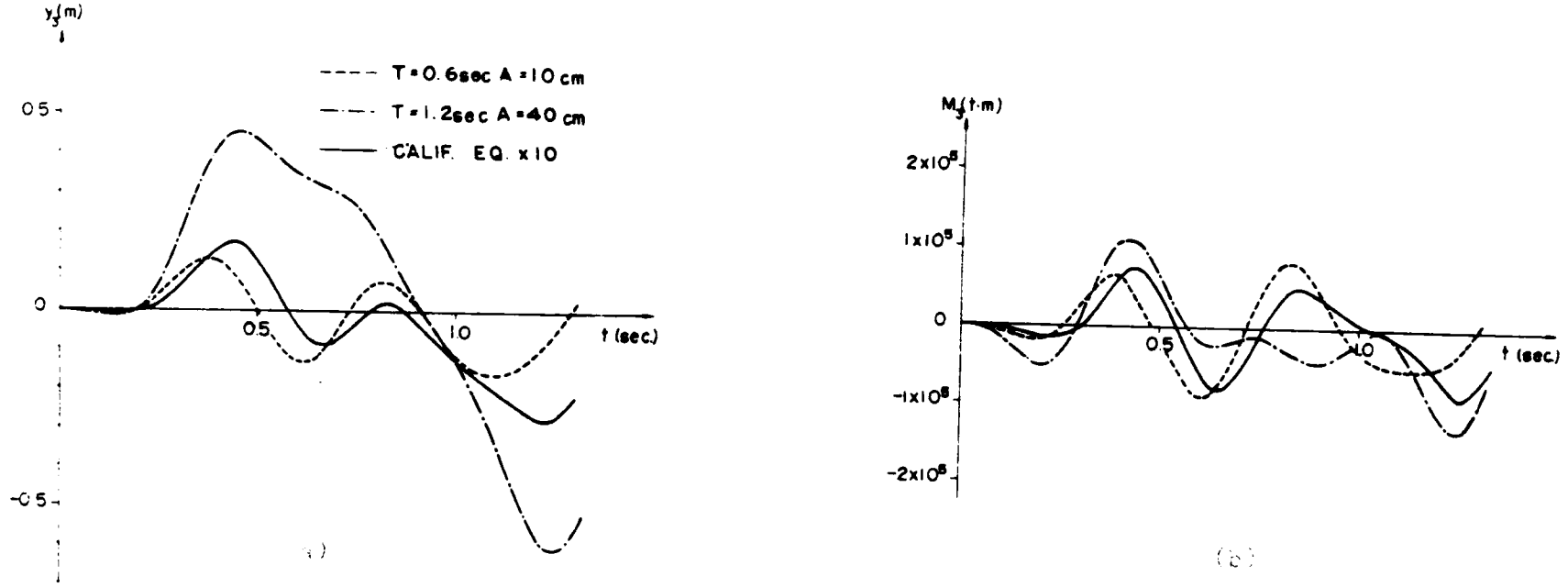
y_3(m)
T=0.6sec A=10 cm
T=1.2sec A=40 cm
CALIF. EQ. x10
0.5
0
-0.5
0.5
1.0
t (sec.)
(a)
M_3(t·m)
2x10^5
1x10^5
0
-1x10^5
-2x10^5
0.5
1.0
t (sec.)
(b)

Fig. 224

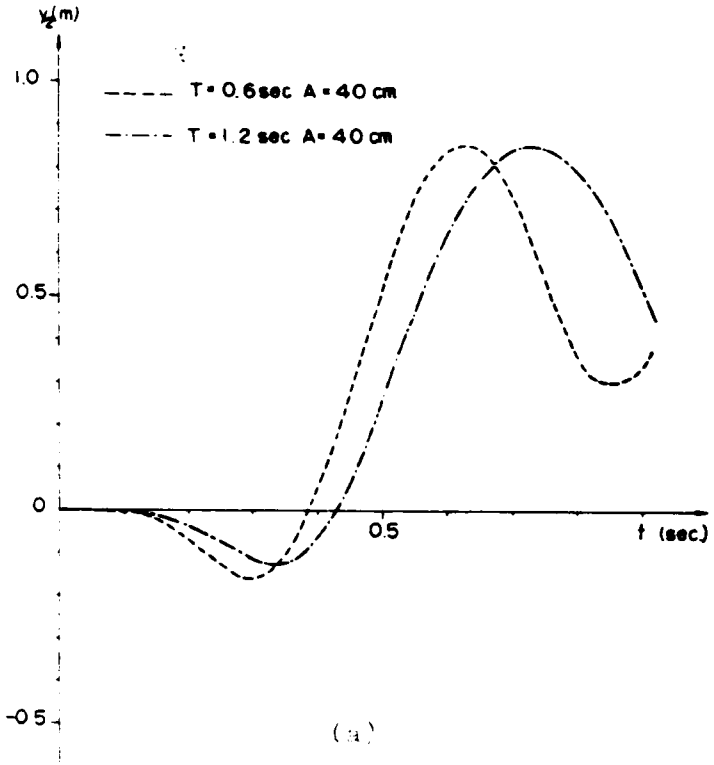
y_2(m)
T = 0.6sec A = 40 cm
T = 1.2 sec A = 40 cm
1.0
0.5
0
-0.5
0.5
t (sec)

(a)

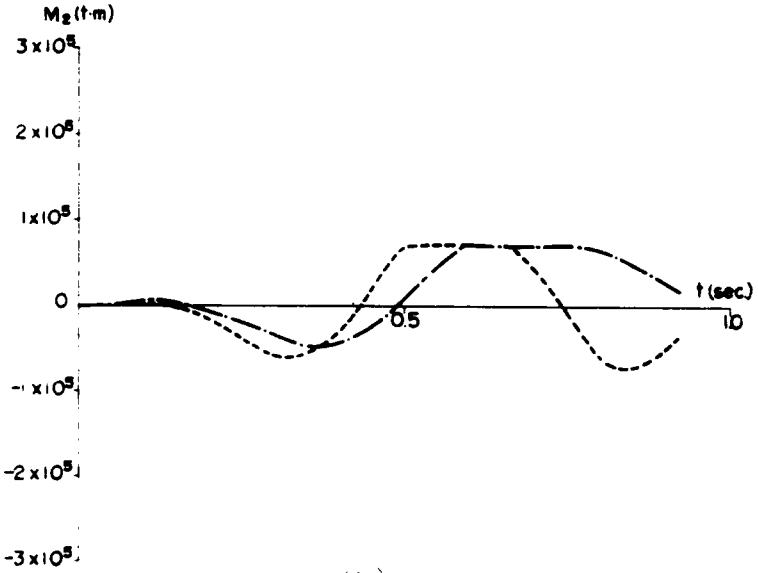
M_2(t·m)
3x10^5
2x10^5
1x10^5
0
-1x10^5
-2x10^5
-3x10^5
0.5
1.0
t (sec)

(b)

Fig. 225

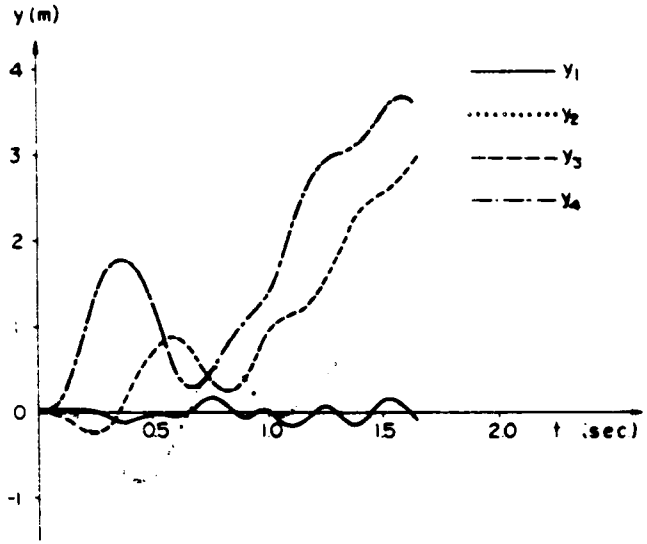

(a) $\alpha = 30^0$

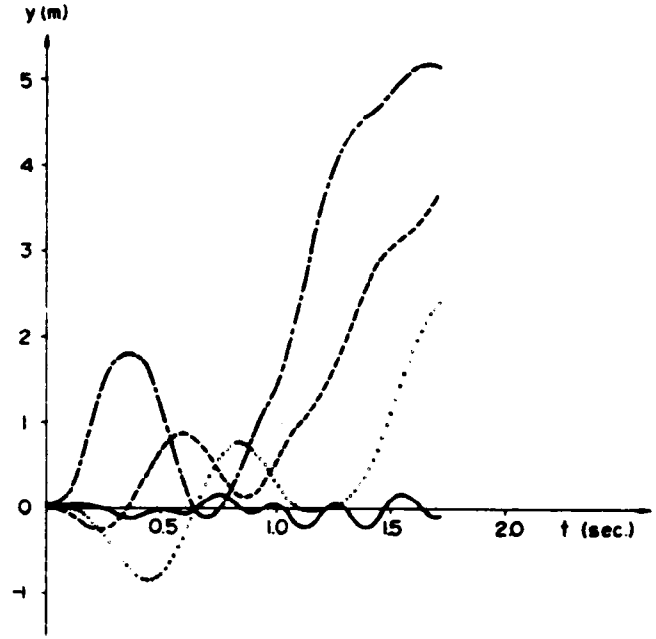

(b) $\alpha = 60^0$

Fig. 226

PART III EXPERIMENTAL ANALYSIS AND SOME CONSIDERATIONS ON STRUCTURAL DAMPING

I. INTRODUCTION

301. Introduction

Theoretical studies on earthquake response of suspension bridges were given in the previous parts of this paper. Experimental verification of these theories may be possible if the experiments were carried out for transient vibration on a shaking table. The shaking table now available is for merely steady forced vibration and no experimental studies are possible for transient vibration. The experimental studies given in the following chapters aim chiefly to obtain the fundamental properties of the suspension bridge subjected to steady forced or free vibrations.

Two kinds of models were constructed and tested. One is a full model with scale factor 1/1000, and the other is tower models with scale factor 1/100.

Since the scale factor of the full model was small, the investigations were limited to a few vibration modes of the suspension bridge, and the fundamental vibration characteristics of the suspension bridges were investigated. A larger scale model is then required for the investigations of earthquake response. It was found that framing such large scale full model, however, costs much and requires large space. For experimental studies on the behaviors of towers, so the tower models were made instead of full models for the large scale experiments.

In Chapters II and III, the experimental studies and their investigations on these full and tower models will be given.

To obtain the basic properties of actual suspension bridges, field tests were done on two comparatively small span suspension bridges. Vibration nature, such as natural frequencies, and damping properties, obtained on these bridges will be given in Chapter III.

Damping properties of bridges are quite important not only for the dynamic studies of suspension bridges but also for ordinary bridges. Some of the basic considerations on structural damping will be given in Chapter IV, refering to the steel beam models and the actual highway bridges.

II EXPERIMENT ON FULL MODEL

302. Design of Model

The main object of the experimental studies with the full model is to obtain basic vibration properties, such as natural periods, natural modes, and damping constants of the long span suspension bridge by means of model.

The scale factor of the full model was limited by the capacity of the shaking table and determined as 1/1000. This scale factor of the model is not large enough, rather too small to obtain the earthquake response. Complete similarity between the model and the prototype can not be obtained by such a small scale model, and some modifications of the conditions of perfect similitude are necessary.

The geometric and physical quantities which are necessary for dynamic analysis of suspension bridges are as follows.

l = span length

y = displacement of the suspended structures

f = sag

A_c = cross sectional area of the cables

E_c = Yound's modulus of the material of the cables

I = sectional moment of inertia of the suspended structures

E = Young's modulus of the material of the suspended structures

g = acceleration of gravity

w = dead weight of the suspended structures and the cables

H = horizontal component of the cable tension

t = time

The set of dimensionless products, π terms, that can be found from the given variables are the following.

$$f/l, \quad y/l, \quad A_c/l^2, \quad I/l^4, \quad w/El, \quad H/El^2,$$
$$E_c/E, \quad gt^2/l.$$

The values of g, E, and E_c are unchangeable if the experiments are conducted in the gravitational field and the material of the models is the same as that of the prototype.

Let primes refer to the model, and define the following scale factors.

$$K_l = l'/l, \quad K_f = f'/f, \quad K_I = I'/I, \quad K_A = A_c'/A_c,$$

$$K_w = w'/w, \quad K_H = H'/H, \quad K_y = y'/y, \quad K_t = t'/t.$$

In order to satisfy the conditions of similitude, the following relations must be satisfied.

$$K_f = K_l, \quad K_y = K_l, \quad K_I = K_l^4, \quad K_A = K_l^2, \quad K_w = K_l,$$

$$K_t = (K_l)^{1/2}$$

The prototype used in the experimental studies of the full model is the Akashi Straits Bridge, Plan I, and is somewhat different from the prototype used in the theoretical studies. This bridge has the following dimensions.

Total span length	2600 m
Center span length	1300 m
Side span length	650 m
Width of the Bridge	26 m
Center to center distance of the cables	30 m
Dead weight	30 ton/m
Height of the stiffening truss	15 m
Horizontal tension of the main cable due to dead load	58680 ton
Horizontal tension of the main cable due to live load	11430 ton

(a) Cross Sectional Area of the Cable, A_c

According to the model law,

$$K_A = (A_c'/A_c) = K_l^2 = (1/1000)^2$$

$$A_c' = A_c\ (1/1000)^2 = 1.232\ mm^2$$

Considering the maximum allowable dead weight of the model and minimum cable diameter to which strain gages are attachable, the diameter of the cable wire of the model was determined as $d = 1.00$ mm.
Then the linear reduction factor is

$$\alpha = 0.6375$$

(b) Dead Weight, w

Using the model law and the linear reduction factor α, dead weight of the model is obtained as follows.

$$K_w = (w'/w) = \alpha\ (K_1)$$

$$w' = w\ \alpha\ K_1 = 191.25\ \text{gr/cm}$$

Steel blocks with the dimensions 20 x 80 x 100 mm were required if the blodks were placed at distances of 32.5 mm. Fixing such size of blocks was practically impossible for the model, then the linear reduction factor of the dead weight was reduced to

$$\alpha = (1/4)\ 0.6375 = 0.1594.$$

Influences of such distortion of the model are not significant for the model according to theoretical investigations. The steel blocks of the size 20 x 20 x 100 mm were placed at the distances of 32.5 mm.

(c) Sectional Moment of Inertia of the Suspended Structures, I'

(i) Center Span

Using $\alpha = 0.6375$

$$K_I = (I'/I)\ \alpha\ K_1^4$$

$$I' = \alpha\ I\ K_1^4 = 5 \times 0.6375 \times (1/1000)^4\ (m)^4 = 3.1875\ (mm)^4$$

If the linear reduction factor is selected as

$$\alpha = (1/2)\ 0.6375$$

the sectional moment of inertia is

$$I' = 1.5938\ mm^4$$

Rounded bars with the diameter 2.4 mm were used as suspended structures of the model. Then the actual I' is

$$I' = 1.6286\ mm^4$$

(ii) Side Span

The sectional moment of inertia of the side spans is 1.4 times that of the center span, then the diameter of the rounded bars of the side spans is selected as

$$d_{side} = d_{center}\ (1.4)^{1/4} = 2.4\ (1,4)^{1/4} = 2.61\ mm$$

Actually 2.6 mm was used.

(d) Dead Weight of the Cable

Dead weight of w = 30 ton/m includes the weight of the suspended structures and that of the cables. For a close investigation on the effects of mass distribution, it is preferable to devide the dead load into two parts. The model weight was thus designed to be separable into the following two parts.

Block 20 x 13 x 100 mm (suspended structures)

Cylindrical Weight 2^4 (diameter) x 20 (cable)

The full model thus designed is given in Fig. 301. Experimental set up of the model and its detail were shown in Fig. 302 and Figs. 303 (a) through (d).

No specific considerations were paid on the similitude of the towers.

303. Natural Frequencies of the Model

Using the Bleich Method, the natural frequencies of the designed model are obtained as shown in Table 301. Since the model does not satisfy the conditions of perfect similitude, the natural frequencies thus obtained does not satisfy the similarity condition on time scale factor

$$K_t = (K_l)^{1/2}$$

The natural frequencies of an ideal model having perfect similitude to the prototype are shown in Table 301 and are compared to those of the approximate model. It might be concluded that there is not much difference between them.

304. Instrumentation

(a) Shaking Table

Steady forced vibration was applied by means of shaking table. The capacity of the table is as shown in Table 302. Two kinds of excitation, cam driving and unbalanced mass driving, are possible.

(b) Strain Measurement

Strains were measured by means of SR-4 Type Strain Gages. The location of the strain gages is shown in Fig. 304.

(c) Deflection Measurement

Inductance type deflection gages were used to record the deflections. The location of the deflection gages is also shown in Fig. 304.

Table 301 Natural Frequencies of the Model (Theoretical Values)

Modes	Freq. of Actral Model	Freq. of Perfect Model
Symmetric Mode		
1 st	165 cpm	158 cpm
2nd	324	308
Asymmetric Modes		
1 st (center span)	210	207
2 nd (side span)	215	208
3 rd (center span)	468	442
4 th (side span)	496	452
5 th (center span)	806	713
6 th (side span)	889	760

Table 302 Shaking Table (Type UBC-8)

Methods of Excitation	CAM	UNBALANCED MASS
Exciting Frequencies	0 - 600 cpm	300 - 3300 cpm
Maximum Amplitudes	10 mm	1 mm
Maximum Acceleration	2 g	7 g
Maximum Loading Capacity	80 kg	80 kg
Table Area	80 x 80 cm^2	

305. Test Procedure

(a) Free Vibration Tests

The procedures used are of exciting by hand the center of the center span or the side span for a symmetric mode of vibration, and of exciting the quarter point of the center span for an asymmetric mode of vibration. The outputs were recorded continuously by means of a magnetic oscillograph.

(b) Steady Forced Vibration

Steady forced vibrations in the vertical direction were conducted by means of the shaking table, and exciting amplitudes were varied as 0.29, 0.34, 0.48, 0.55, and 0.74 mm. The same method was applied to the horizontal vibration in the direction of the bridge axis, and

their amplitudes were varied as 0.46, 0.91, 1.42, and 1.91 mm.

306. Results and Investigations

Natural frequencies obtained from free vibration tests were 246 cpm for the 1st symmetric mode and 230 cpm for the 1st asymmetric mode.

Damping constants obtained from the free vibration tests are between 0.04 and 0.1, and these are considerably greater than those of actual suspension bridges. Some of the field tests on actual suspension bridges will be given in Chapter IV. Because the scale factor of the model is small, the model includes more sources of structural damping in comparison with its maximum energy storage capacity than those in the prototype. No specific correlations between the damping constants and vibration amplitudes can be obtained.

Typical amplitude-frequency relations, resonance curves, are given in Figs. 305 (a) through (c) for vertical excitation, and Figs. 306 (a) and (b) for horizontal excitation.

Resonant frequencies obtained from steady forced vibration are summarized in Table 303. The test results are comparatively in good agreement with the theoretical values given in the same table.

Because of the small scale factor of the model and the structural complexity of the suspension bridge, the steady forced vibrations obtained in these tests were rather irregular in comparison with other vibration test results, and large scale model are required for further investigations of the phenomenon.

Table 303 Resonant Frequencies (cpm)

Modes	Experimental	Theoretical
Symmetric		
1st		165
2nd	310 - 350	324
Asymmetric		
1st (center span)	230	210
2nd (side span)	240	215
3rd (center span)	490	468
4th (side span)	500	496

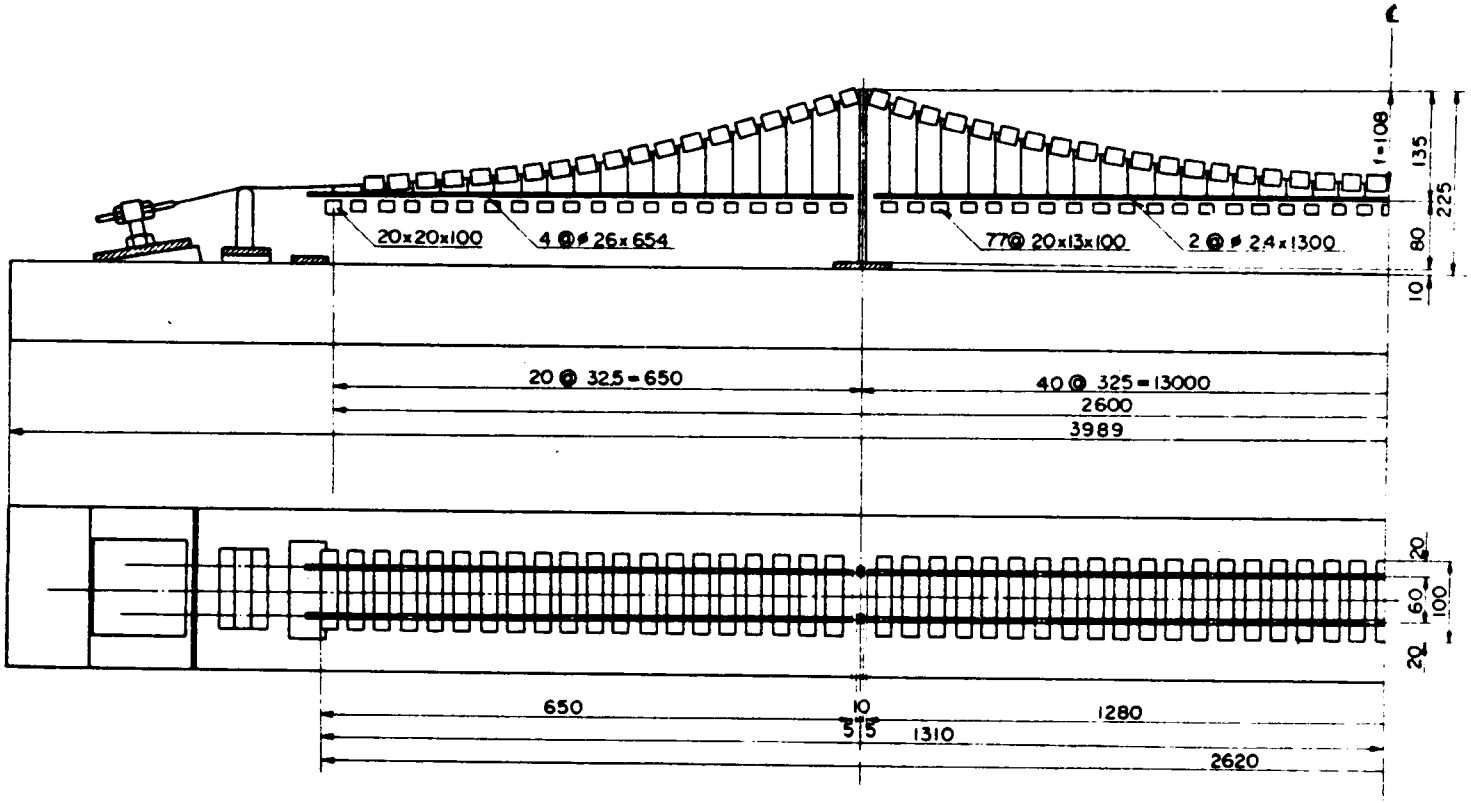

Fig. 301 Full Model

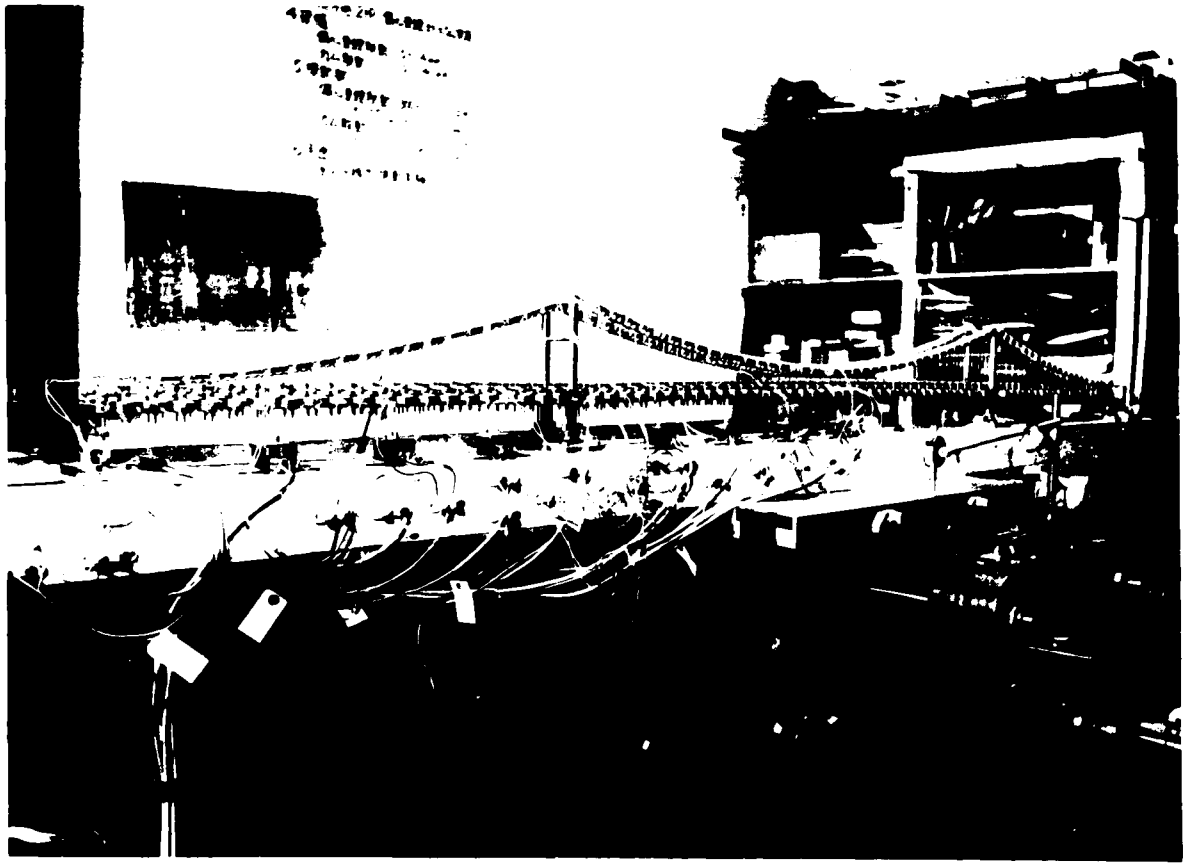

Fig. 302 Experimental Set-up

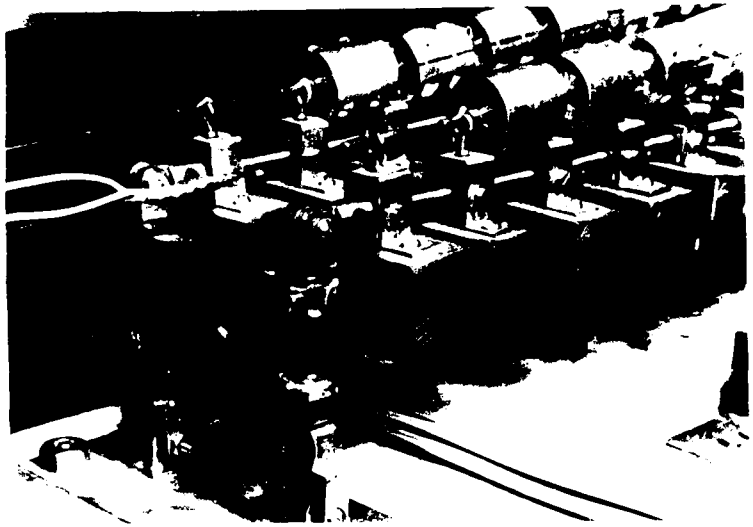

(a) End Support of the Side Span

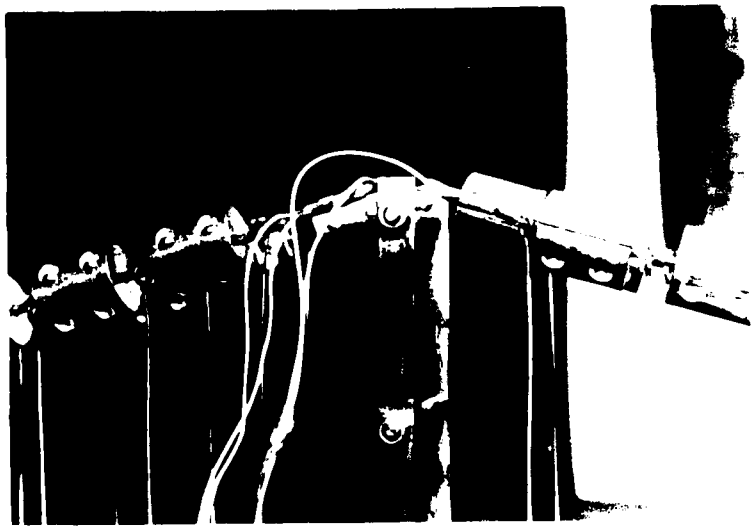

(b) Top of the Tower

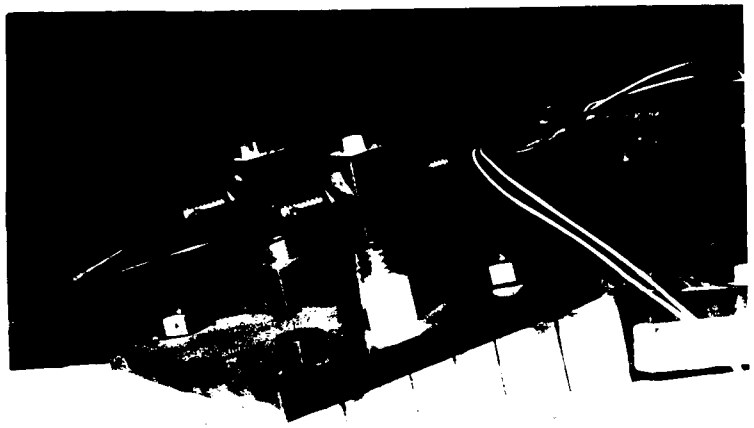

(c) Cable Anchorage

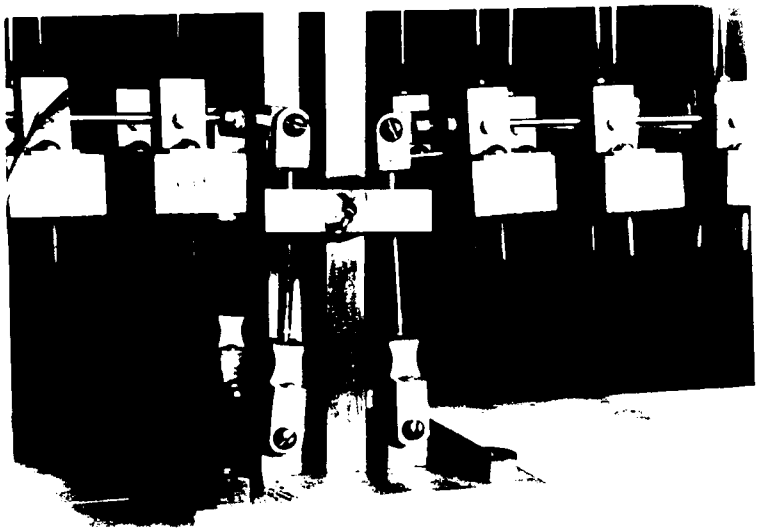

(d) Base of the Tower

Fig. 303

(a) Location of Deflection Gages

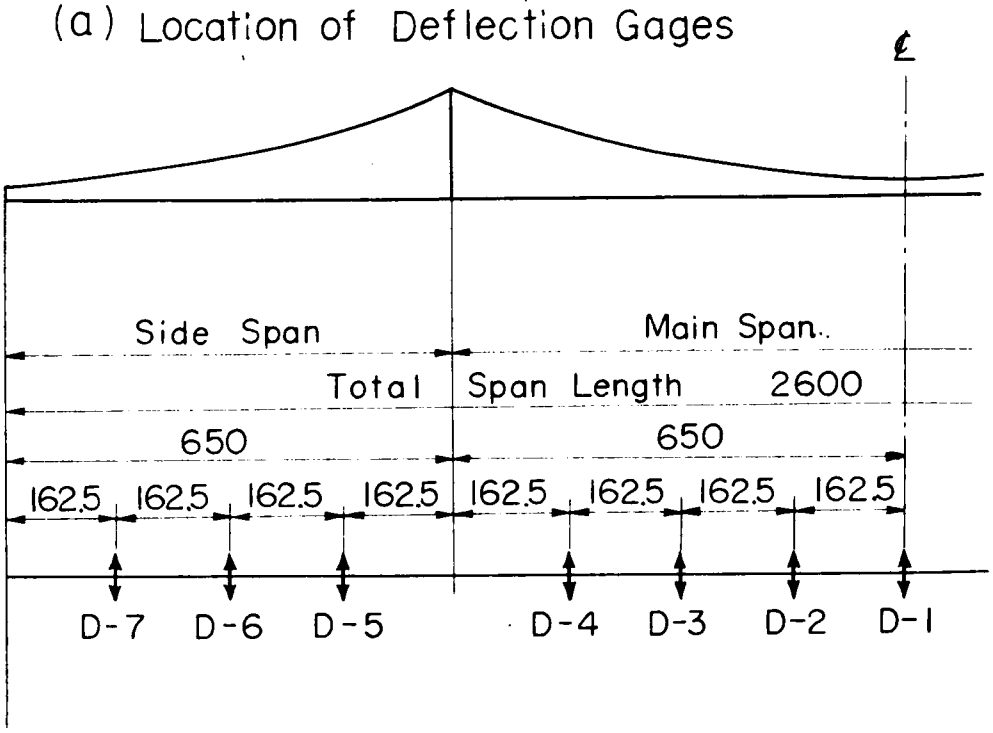

(b) Location of Strain Gages

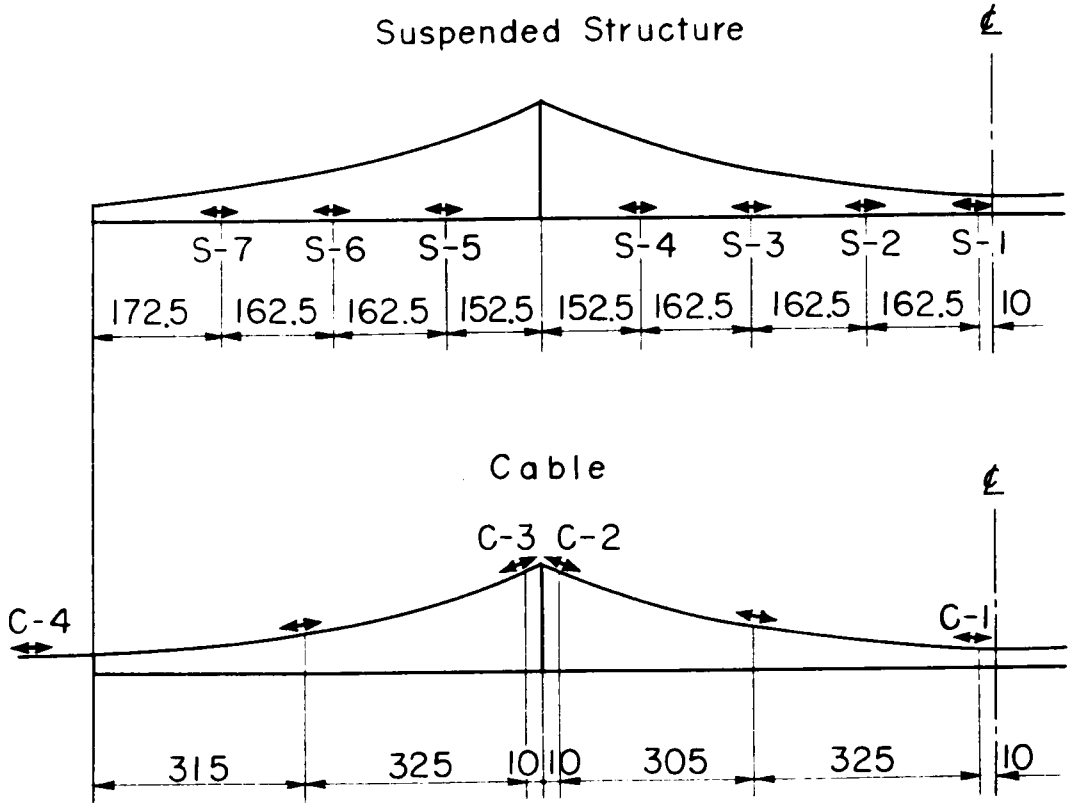

Fig. 304

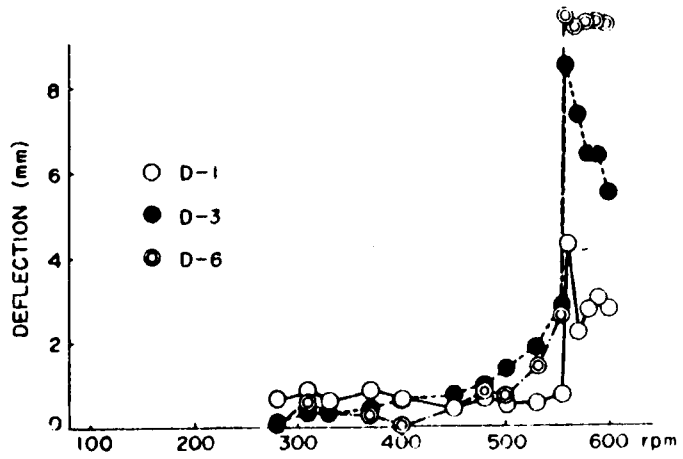

a) Deflections

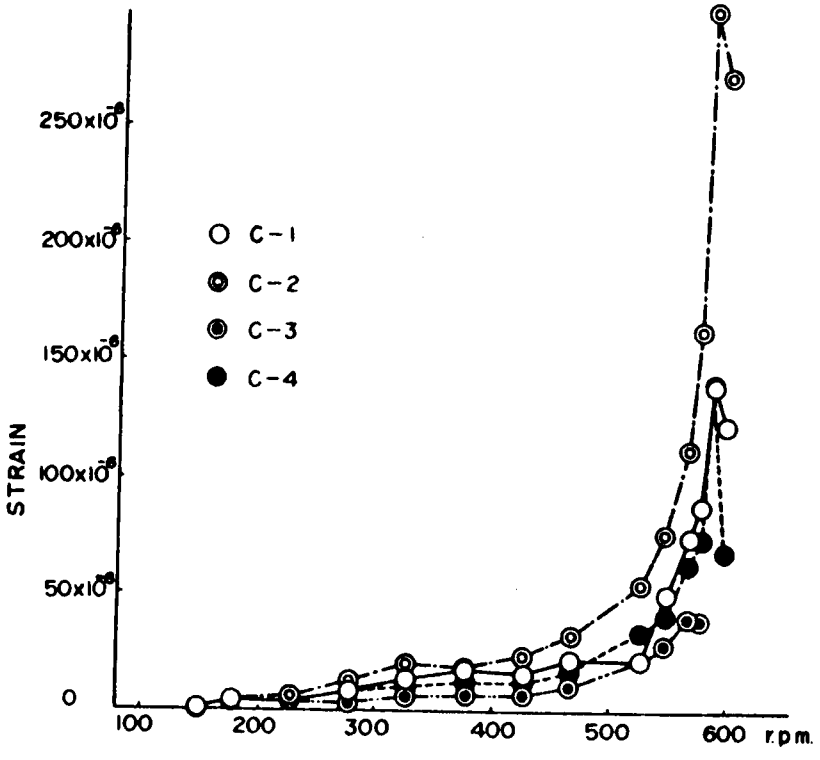

b) Cable Strains

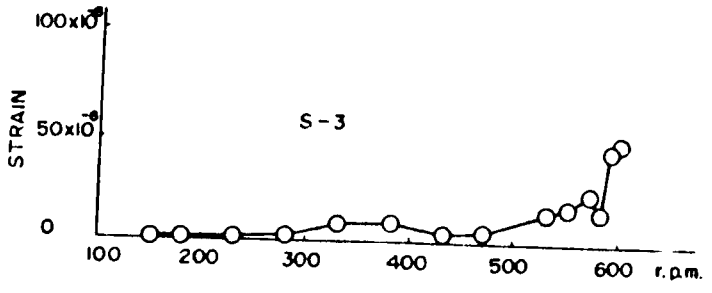

c) Strains in Suspended Structures

Fig. 305 Resonance Curves

(Table Amplitude, Vertical 0.73 mm)

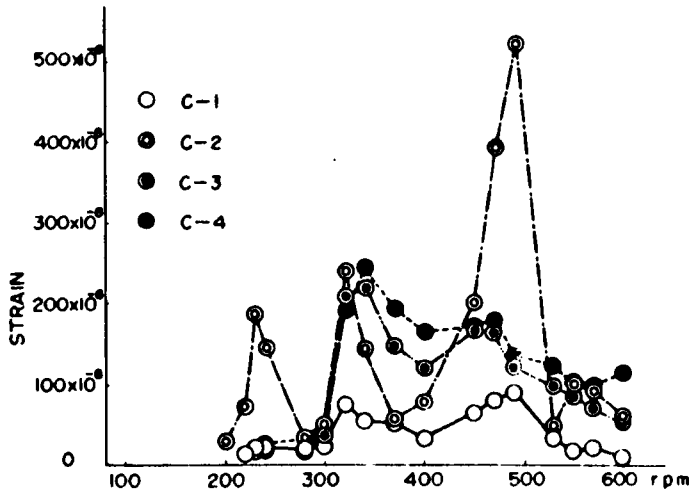

(a) Cable Strains

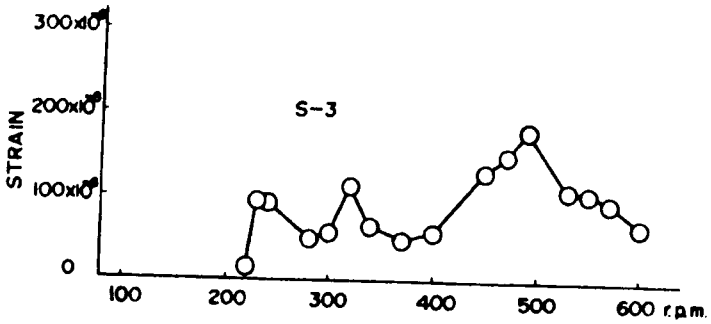

(b) Strains in Suspended Structures

Fig. 306 Resonance Curves
(Table Amplitude, Horizontal 1.42 mm)

III EXPERIMENTAL STUDIES ON SUSPENSION BRIDGE TOWER MODELS

307. Object and Scope

The scale factor of the full model used in Chapter II was not large enough to study the earthquake response of the suspension bridge, and the experiments were limited to verify only the basic vibration properties of a few vibration modes of the suspension bridge. A larger scale model, if possible a larger scale full model, is required for the studies on earthquake response.

According to the theoretical results obtained by the linear analysis on earthquake response of the suspension bridge, the effects of the high mode vibrations having predominate vibration amplitudes of the towers are significantly important. It was therefore concluded that in the experimental investigations of earthquake response, partial model tests in which the tower and some of the physically equivalent effects from the cables and the suspended structures are approximately possible.

In this investigation, model towers were designed and constructed under such bases. If possible, model experiments would rather be, like the theoretical studies described previously, done for transient vibration due to the ground motion. In this investigation, however, the experiment were limited to free and steady forced vibrations.

The main object of this experimental study is to clarify the following points.

(1) Effects of higher mode vibration to earthquake response.

(2) Effects of vibration damping to the higher mode vibrations.

(3) Fundamental characteristics of suructural damping, especially related to the structural connections.

The prototype of this experimental study is the Akashi Straits Bridge Plan I.

308. Design of Model

The model used in this study were designed and constructed using the ordinary theories of dynamic similitude.

The geometrical and physical quantities necessary in the design

of the tower model are the following.

L = height of the tower

B = width of a section of the tower

C = height of a section of the tower

y = horizontal displacement of the tower

A = cross sectional area of the tower

I = sectional moment of inertia of the tower

E = Young's modulus of the material of the tower

g = acceleration of gravity

W = dead weight of the tower

H = horizontal force acting to the top of the tower

P = vertical force acting to the top of the tower

M = bending moment on the tower section

T = time

The complete sets of dimensionless products, π terms, can be obtained from the given variable as the following.

$$A/L^2, \quad B/L, \quad C/L, \quad I/L^4, \quad W/(EL^2), \quad H/(EL^2),$$

$$P/(EL^2), \quad (T^2g)/L, \quad y/L, \quad M/(EL^3).$$

From the elementary considerations, the dimensionless products B/L, and C/L can be omitted because they have only an effect to bending stress which can be computed from bending moments. The dimensionless product A/L^2 is concerned primarily with the direct stresses of the tower, and it can be also omitted if the stress distribution in a section is out of question. The values of g and E are unchangeable if the experiments are conducted in the gravitational field and the material of the model is the same as that of the prototype.

Let primes refer to the model, and define the folloowing scale factors.

$$K_L = L'/L, \quad K_I = I'/I, \quad K_W = W'/W, \quad K_H = H'/H,$$

$$K_P = P'/P. \quad K_y = y'/y, \quad K_M = M'/M, \quad K_T = T'/T.$$

In order to satisfy the conditions of complete similitude, the following relations among these scale factors must be satisfied.

$$K_I = K_L^4, \quad K_W = K_H = K_P = K_L^2, \quad K_y = K_L, \quad K_T = (K_L)^{1/2}$$

To satisfy these conditions, one requires a large scale experimental

model. Some distortions, however, are possible in the model under the following considerations.

The fundamental equation of motion of the problem now considered is

$$E \frac{\partial^2}{\partial x^2}\left(I \frac{\partial^2 y}{\partial x^2}\right) + \frac{w}{g} \frac{\partial^2 y}{\partial t^2} + P \frac{\partial^2 y}{\partial x^2} = p(x,t) \qquad (301)$$

Then, the following relation between the physical quantities is derived. For the prototype,

$$EI \frac{y}{x^4} + \frac{W}{gL} \frac{y}{T^2} + P \frac{y}{x^2} = p(x,t) \qquad (302)$$

For the model,

$$EI' \frac{y'}{x'^4} + \frac{W'}{gL'} \frac{y'}{T'^2} + P' \frac{y'}{x'^2} = p'(x,t) \qquad (303)$$

These can be rewritten to the following non-dimensional equations.

$$\left(\frac{I}{L^4}\right)\left(\frac{y}{L}\right) + \left(\frac{W}{EL^2}\right)\left(\frac{L}{T^2 g}\right)\left(\frac{y}{L}\right) + \left(\frac{P}{EL^2}\right)\left(\frac{y}{L}\right) = \frac{p(x,t)}{E\,L} \qquad (304)$$

$$\left(\frac{I'}{L'^4}\right)\left(\frac{y'}{L'}\right) + \left(\frac{W'}{EL'^2}\right)\left(\frac{L'}{T'^2 g}\right)\left(\frac{y'}{L'}\right) + \left(\frac{P'}{EL'^2}\right)\left(\frac{y'}{L'}\right) = \frac{p'(x,t)}{E\,L'} \qquad (305)$$

Each term of these two equations must be equal or equally proportional to satisfy the condition of similitude on the vibration characteristics of the tower.

The value of (y/L) is the response which have to be obtained from the experiment. Then, to the condition

$$y/L = \beta\,(y'/L')$$

the relations

$$I/L^4 = \alpha\,(I'/L'^4)$$

$$W/EL^2 = \alpha_1\,(W'/EL'^2), \qquad L/T^2 g = \alpha_2\,(L'/T'^2 g), \qquad \alpha = \alpha_1\,\alpha_2,$$

$$P/EL^2 = \alpha\,(P'/EL'^2),$$

$$p/EL = \alpha\,\beta\,(p'/EL'),$$

where

α, α_1, α_2 = linear reduction factor,

β = distortion factor,

have to be satisfied.

In order to investigate the vibration characteristics of the suspension bridge tower, two models were designed and made. One is to have an uniform cross section, Model I, and the other is to have variable cross sections, Model II. Both models have a height of 2 m (scale factor $K_L = 1/100$). The top of the model is set up in such a way that the similitude of the dynamic end condition, given in Part II of this paper, is satisfied.

The main dimensions of the models are shown in Figs. 307 and 308.

Model I (Fig. 307) : The sectional moment of inertia of the prototype was assumed to be invariable and is $40.2\ m^4$. The cross section of the model was formed by using two strip steel bands as

$$B' = 19\ mm, \quad C' = 2 \times 6 = 12\ mm$$

Then, sectional moment of inertia of the model is obtained as

$$I' = 0.2376\ cm^4$$

and the linear reduction factor α is

$$\alpha = (I/I')(L'/L)^4 = 147$$

Dead weight of the model is

$$W' = 10.24\ kg\ (per\ tower).$$

Then, the linear reduction factor α_1 is

$$\alpha = (W/W')(L'/L)^2 = 146$$

Natural period of the model is, since $\alpha_2 = \alpha/\alpha_1 = 1$,

$$T' = T(K_L)^{1/2} = (1/100)^{1/2}\ T = 0.1\ T$$

Model II (Fig. 308) : The sectional moment of inertia at the point of the cross sections A, B, C, D, E, F, G, and H of the prototype (Refer Fig. 209. p. 107) is shown in Table 304. For the model design, the mean value of each interval of the segments A-B, B-C, ... is assumed to be the sectional moment of inertia of the prototype. The linear reduction factor α for each segment is given in the same table, Table 304.

The mean value of α is $\alpha = 176$.

The dead weight of the model are given in Table 304. Linear reduction factor for the dead weight is

$$\alpha_1 = (W/W')(K_L)^2 = 110.6$$

Linear reduction factor for the vibration period can then be computed as

$$\alpha_2 = \alpha/\alpha_1 = 176/110.6 = 1.59$$

Then,

$$T'/T = 1/7.9$$

Damping properties of the model have not been discussed yet, and are the important factors for the model design. The damping constant of the model were controlled by adjusting the torque of fastening the bolts of the models. Each model has different assembly of the members as shown in Fig. 307 and Fig. 308, and they have different damping properties.

309. Experimental Set-Up and Instrumentation

The general view of the experimental set-up is shown in Fig. 309.

(a) Shaking Table

Steady forced excitation was conducted by means of shaking table. The shaking table used in this experiment is that used in the full model test.

(b) Cable Supporting Frame

To connect cables, necessary to satisfy the end condition at the top of the tower model, a frame was arranged around the shaking table and the model. Fig. 309 illustrates the frame. Two ball bearing wheels were fixed to the frame to bend the cables. (Fig. 310). The bended cables are elastically fixed to the frame.

(c) Strain Measurments

Strains were measured by means of SR-4 Type strain gages. These were placed in pairs to boost the output from each location. Figures 1, 2, 3, ..., 7 in Fig. 312 show the locations of strain gages.

The output was recorded by means of a magnetic oscillograph.

(d) Strobo Flush Unit

Vibration modes at the resonant states with the steady forced excitation were measured by means of a multiple strobo flush and a camera.

310. Description of Test Procedure

Vibration tests were conducted with the free vibration and the steadu forced vibration by means of shaking table,

(a) Free Vibration Tests

Free vibration tests were conducted under two different supporting conditions at the top of the tower model. One is freely supported and the other is supported by the cables as shown in Fig. 311.

Vibration damping of the model was controlled by fastening the bolts of the model with different torque. For Model I, the torque was varied as 2, 5, 10, 20, and 30 kg-cm. For Model I no variations on the vibration damping of the model were found for bolt fastening over these values.

For Model II, the torque was varied as 30, 60, and 100 kg-cm. No experiment over these torque indeces were done because of the yielding of the bolt material.

The procedure used in the free vibration tests consisted of deforming the model by hand and releasing it suddenly, where upon strains were recorded by means of the oscillograph.

(b) Steady Forced Vibration Tests

Steady forced vibration tests were conducted by means of shaking table, and the dynamic strains induced in the tower model were recorded by means of the dynamic strain amplifier and the electro-magnetic oscillograph.

The frequency of exciting force was varied from 250 cpm to 3000 cpm, and the shaking table was controlled to vibrate with a constant vibration amplitude 0.1 mm.

Vibration modes at the resonant states were photographed by means of a strobo flush and a camera.

311. Representation of Results

(a) Free Vibration

Damping constants of the model were computed by the formura

$$\beta = \frac{1}{2\pi} \log_e \frac{\varepsilon_n}{\varepsilon_{n+1}} = \frac{1}{2\pi} \delta \qquad (306)$$

where

β = damping constant

ε_n = strain amplitude at the number n of cycles of vibration,

δ = logarithmic decrement.

In Fig. 313 (a), are plotted damping constants-strain amplitude relations obtained from the damped free vibration for the Model I fixed at its top by cables. Different relation curves as shown in Fig. 313 (b) were obtained depending upon the values of fastening torque. Fig. 314 through 316 are the damping constants-strain amplitude relations for the Model II. Table 305 shows the test conditions of these tests.

Table 305 Test Conditions

Figs.	End condition at the top	Vibration Modes
314	free	1st mode
315	free	2nd mode
316	supported by cables	1st mode

The second mode vibration could be obtained by applying the initial deformation similar to the second mode vibration by hand and by releasing it suddenly. The influences of the lower mode vibration included in the vibration thus obtained were quite small compared to the second mode vibration.

(b) Steady Forced Vibration

Steady forced vibration tests were done on the Model I and II.

According to the results obtained in the free vibration tests, the results obtained in the Model II were concluded to be more adequate than those on the Model I. The results obtained on the Model I are, therefore, omitted in this paper.

Fig. 317 (a) through (f) show the resonance curves obtained on the Model II. These tests were done under the end condition of fixing the top of the tower by the cables to satisfy the dynamic condition. The resonance curves with different amplitude were obtained with the variation of the values of fastening the bolts of the model. In Tables 306 and 307 are tabulated the maximum strain amplitudes at the resonant condition of steady forced vibration. Table 306 is for the end condition built-in at the base and free at the top. Table 307 is for the end conditions fixed at the top by the cables and is corelated with the resnannce curves of Figs. 317 (a) through (f).

Figs. 318 (a) and (b) show the vibration modes obtained by means of the strobo flush and a camera. Distributions of vibration amplitudes at the 1st and 2nd mode resonance are shown in these figures.

312. Investigation on the Results Obtained

Although the experiment was limited to free and steady forced vibration, the following conclusions were resulted.

(1) Employing the Model II in stead of the Model I, the damping force can be distributed along the whole length of the model, and the damping characteristics were considerably improved. This method of controlling the damping constants is applicable to the other kinds of model tests.

(2) The damping constants to higher mode vibrations are not always larger than those of lower mode vibration. Damping constants to the 2nd mode vibration were smaller than those of the 1st mode in the results obtained in this study.

(3) The similarity in vibration damping between a prototype and a model can be controlled by the method used in this study.

(4) The resonance amplitudes are changed remarkably with the variation of torque indeces of fastening the bolts of the model, and the effects of the high mode vibrations are not small in tall structures like suspension bridge towers.

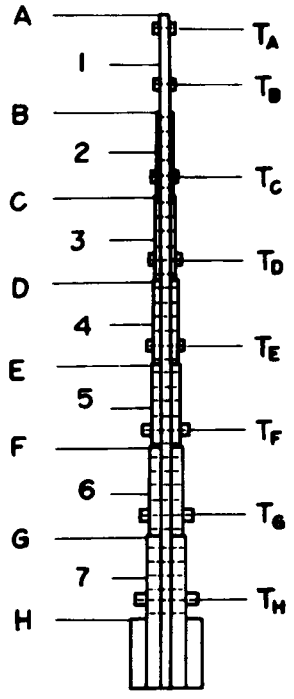

MODEL II

Table 304 Model II

Section		Prototype B (m)	H (m)	A (m^2)	I (m^4)	I (m^4)	w (ton)	Model II H' (mm)	I' (cm^4)	w' (kg)
A		3.00	5.00	1.62	3.75		177			0.419
	1					5.20		6.0	0.0288	
B		3.50	5.75	2.25	6.65		455			0.457
	2					8.82		0.6+6+0.6= 7.2	0.0498	
C		4.00	6.50	2.70	10.99		585			0.525
	3					14.07		1.2+6+1.2= 8.4	0.0790	
D		4.50	7.25	3.15	17.15		731			0.676
	4					21.38		1.8+6+1.8= 9.6	0.1180	
E		5.00	8.00	3.60	25.60		893			0.823
	5					31.23		2.4+6+2.4=10.8	0.1680	
F		5.50	8.75	4.07	36.85		1071			1.009
	6					44.15		3.2+6+3.2=12.4	0.2542	
G		6.00	9.50	4.50	51.44		1266			1.206
	7					60.72		3.8+6+3.8=13.6	0.3354	
H		6.50	10.3	4.95	70.00		1476			1.403
	8					81.58		B' = 16 mm const.		
I		7.00	11.0	5.40	93.17					

Table 306 Maximum Strain Amplitude ($x10^{-4}$)

Mode	Torque (kgcm)	Frequency (r.p.m.)	Section 7	6	5	4	3	2
	30	98	0.92	0.69	0.80	0.62	0.98	0.42
1 st	60	100	1.34	1.29	1.19	0.85	0.97	0.40
	100	101	2.20	1.78	1.46	1.18	0.96	0.45
	30	1085	2.22	1.42	3.55	1.18	3.48	5.04
2 nd	60	1170	3.69	1.70	5.00	1.93	4.87	6.56
	100	1205						
	30	2025	1.24	2.42	0.85	4.27	2.11	5.59
3 rd	60	2180	2.58	3.80	1.79	6.06	3.32	8.03
	100	2245						

(Built-in Free)

Table 307 Maximum Strain Amplitude ($x10^{-4}$)

Mode	Torque (kgcm)	Frequency (r.p.m.)	Section 7	6	5	4	3	2
	30	290	1.37	0.48	0.47	1.32	2.08	2.40
1 st	60	308	2.38	1.32	2.42	2.84	4.19	2.44
	100	312	4.02	1.26	11.62	4.43	2.18	6.74
	30	857	2.47	0.89	2.90	1.46	1.39	5.80
2 nd	60	900	5.93	2.15	10.00	3.12	2.80	6.42
	100	923	3.34	2.33	13.84	4.43	4.30	9.07
	30	1910	1.00	1.30	1.03	2.93	1.50	4.00
3 rd	60	1980	2.01	0.06	2.26	7.97	3.83	6.74
	100	2080	2.38	4.86	5.10	10.63	1.03	7.29

(Built-in Supported)

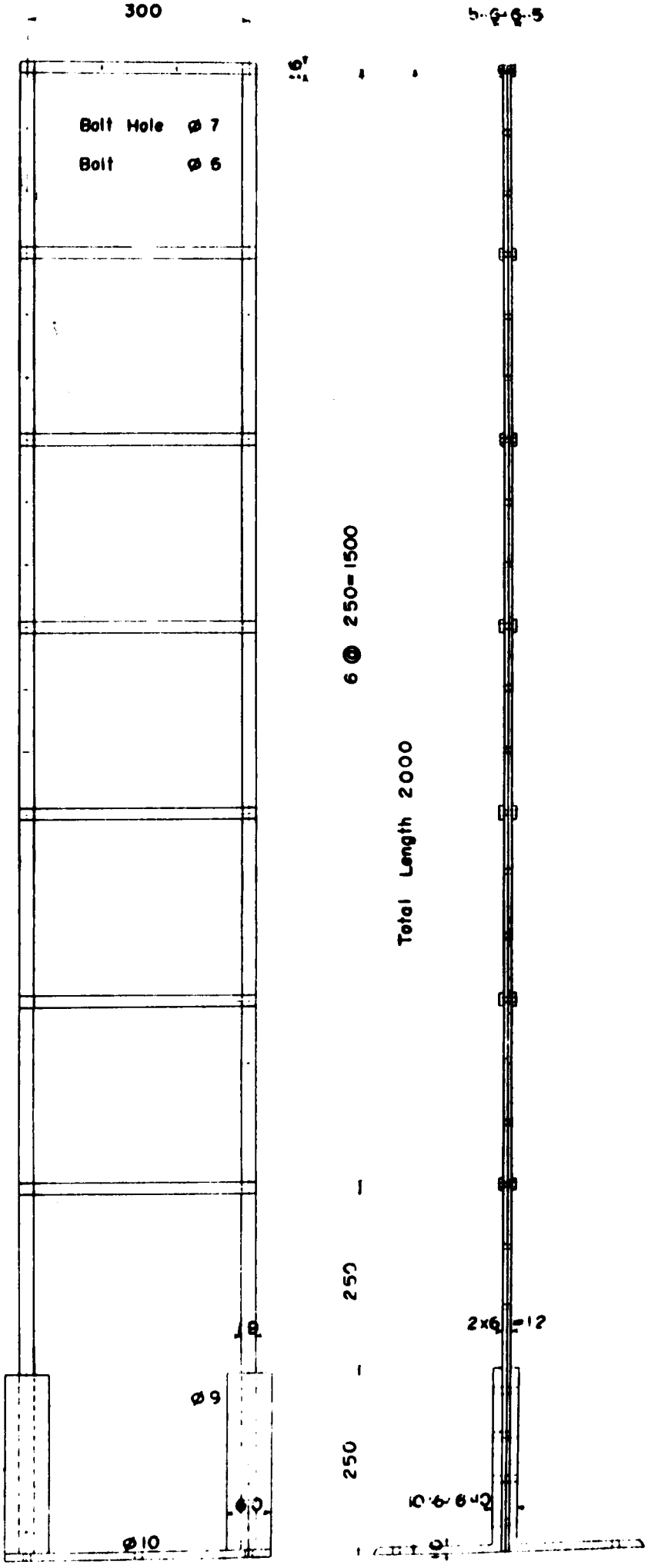

Fig. 307 Model I

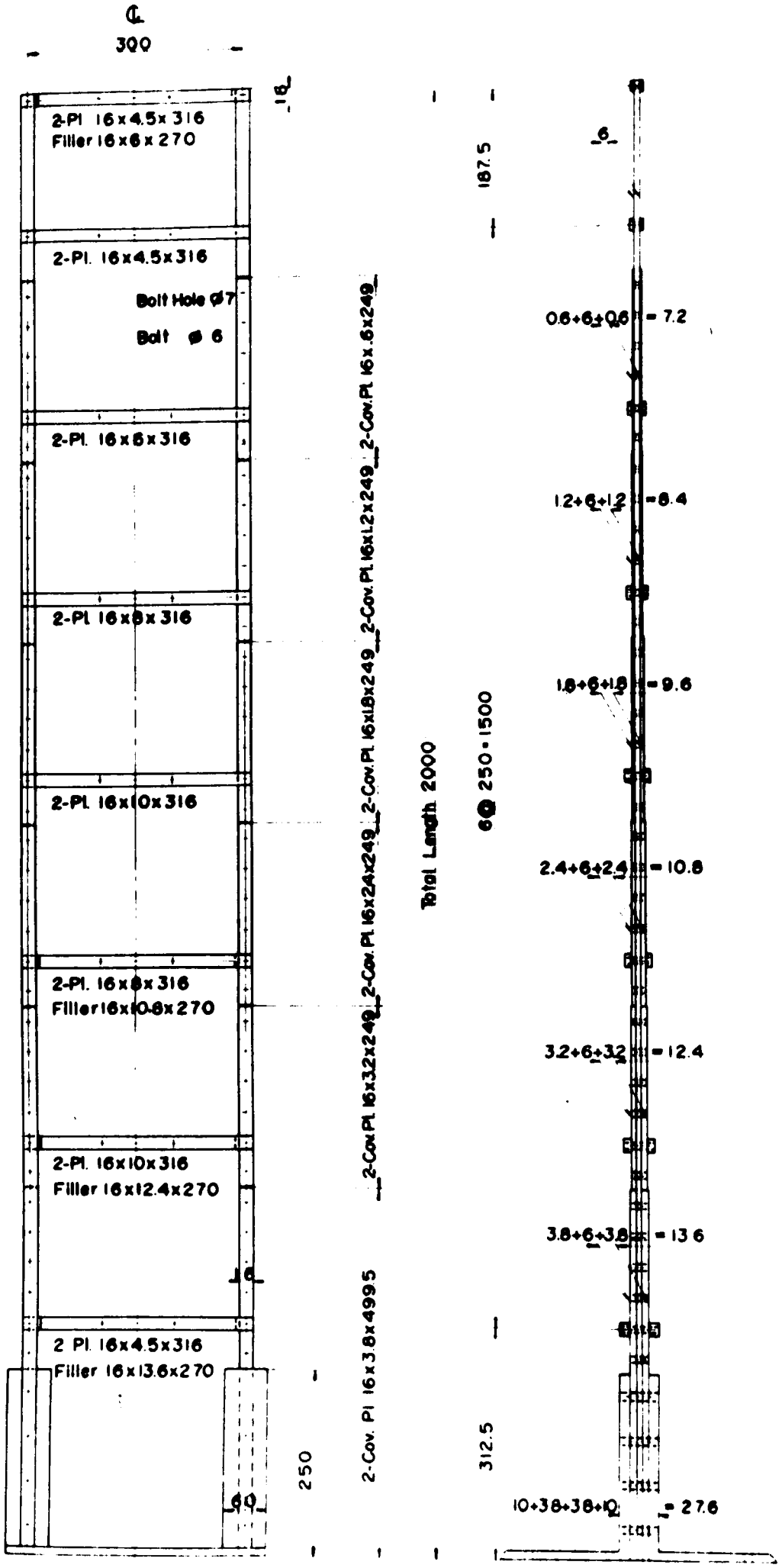

Fig. 303 Model II

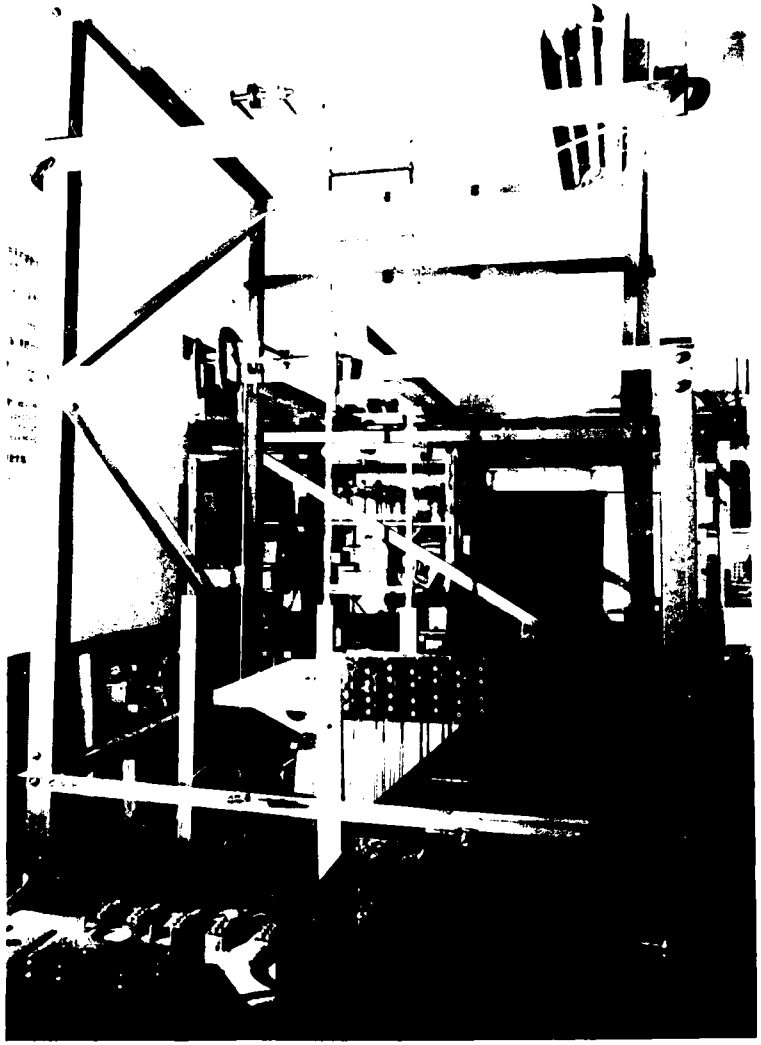

Fig. 309 Experimental Set-up

Fig. 311

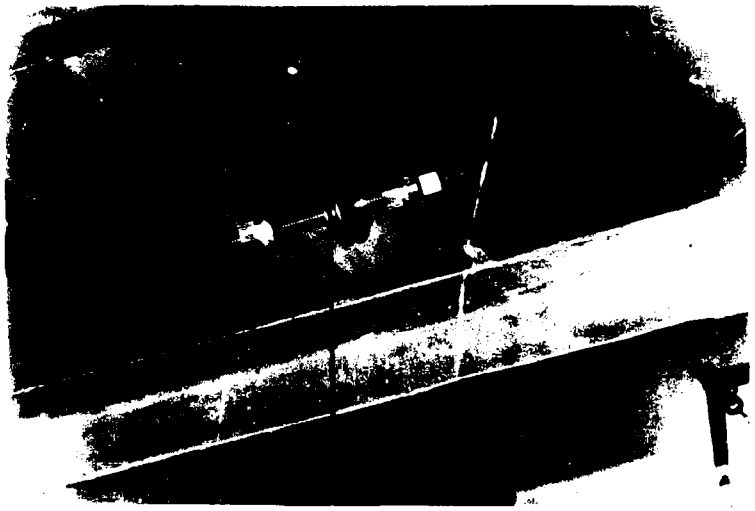

Fig. 310

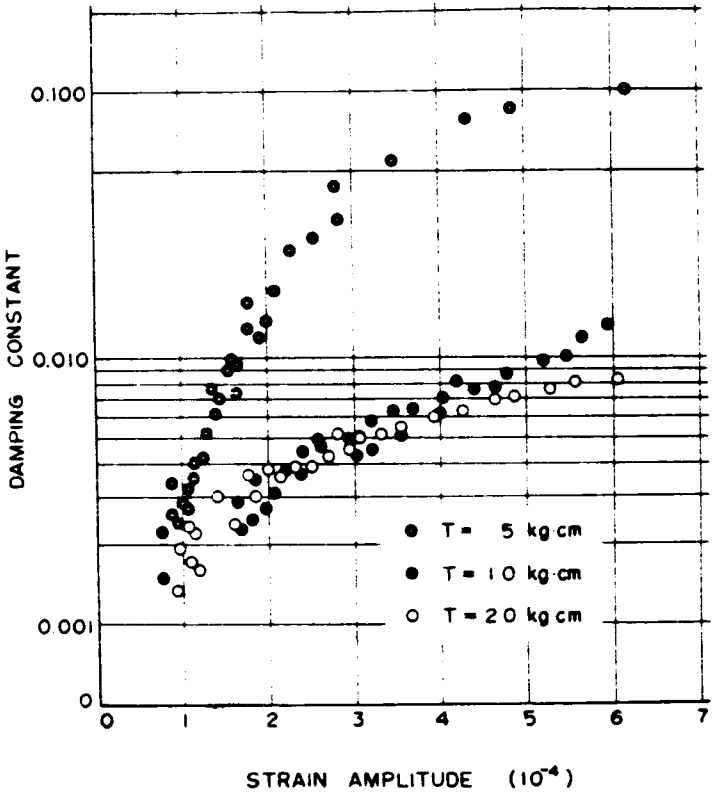

Fig. 7.13 (a) Damping Constant-Strain Amplitude Relations

(Model I)

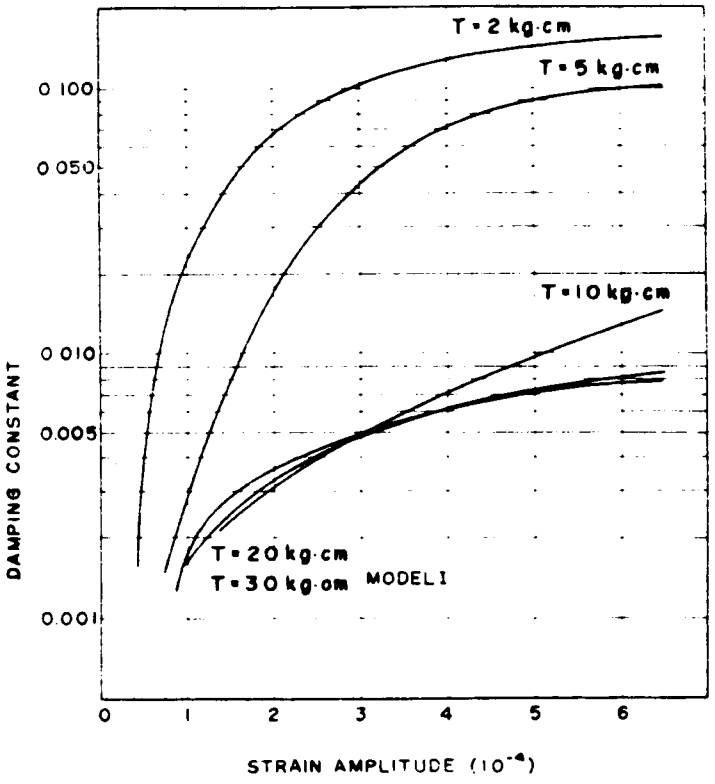

Fig. 7.13 (b) Summarized Curves of Damping Constant-Strain Amplitude Relations

(Model I)

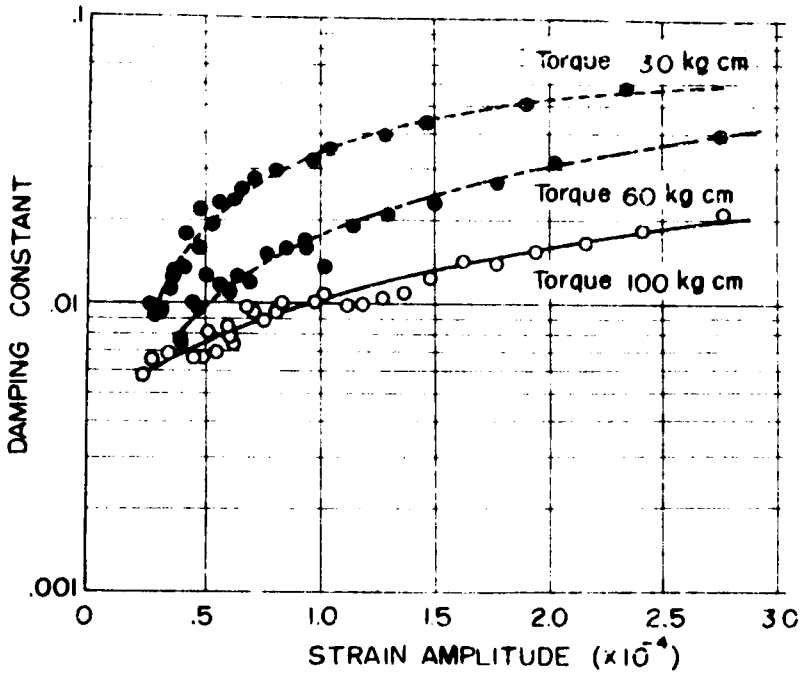

Fig. 314 Damping Constant-Strain Amplitude Relations

(Model II, free at the top 1 st mode)

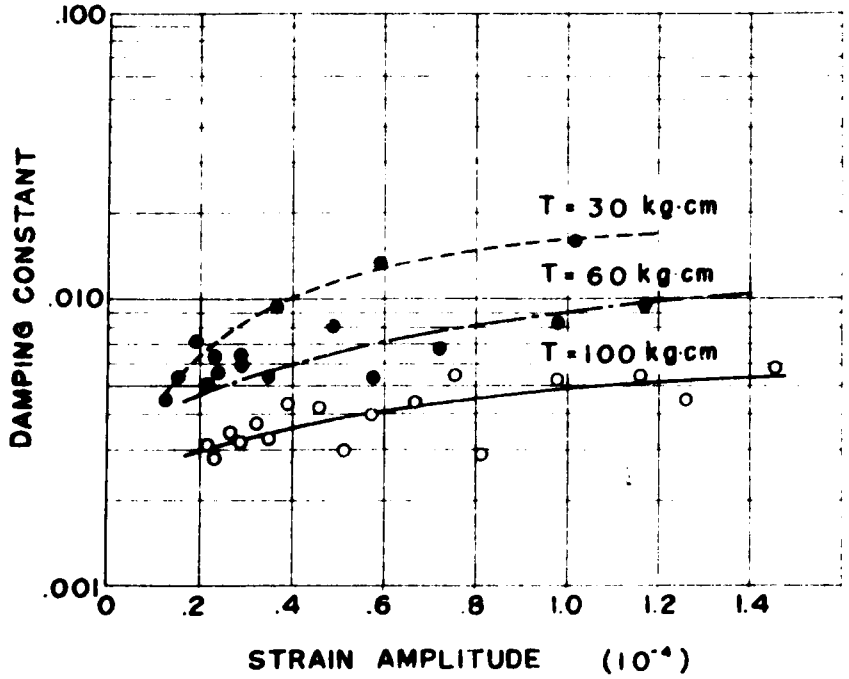

Fig. 315 Damping Constant-Strain Amplitude Relations

(Model II, free at the top 2 nd mode)

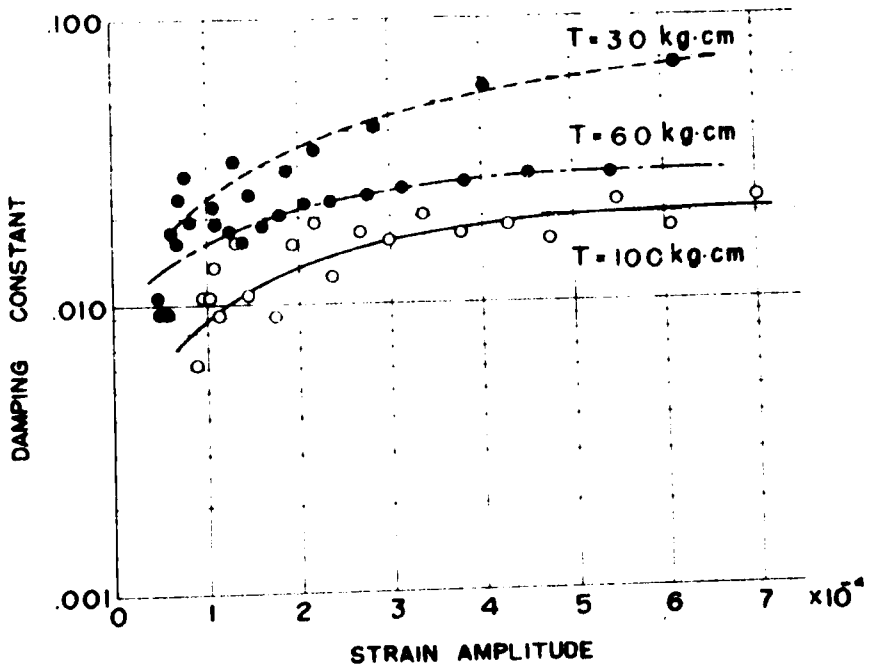

Fig. 316 Damping Constant-Strain Amplitude Relations

(Model II, fixed by the cables 1 st mode)

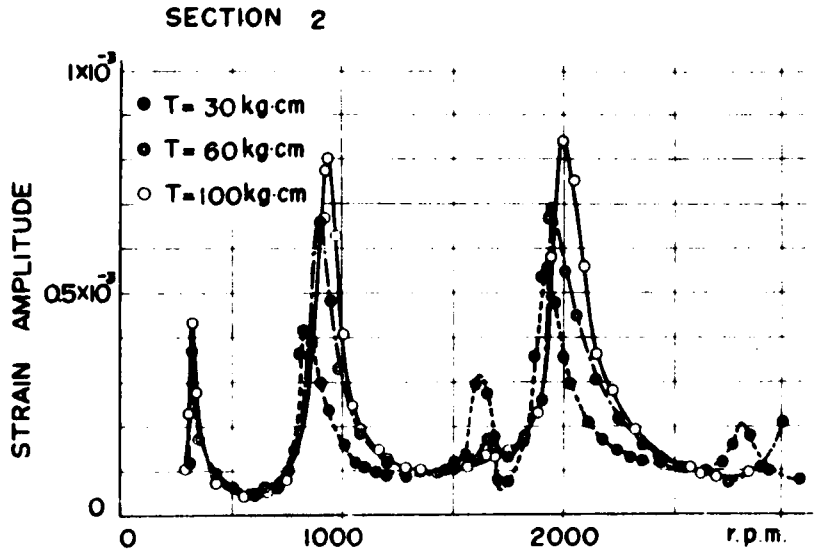

Fig. 317 (a)

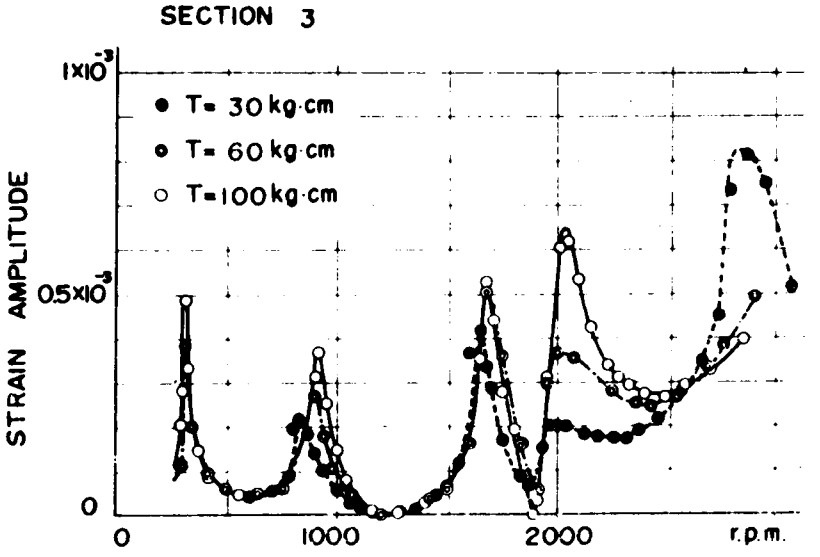

Fig. 317 (b)

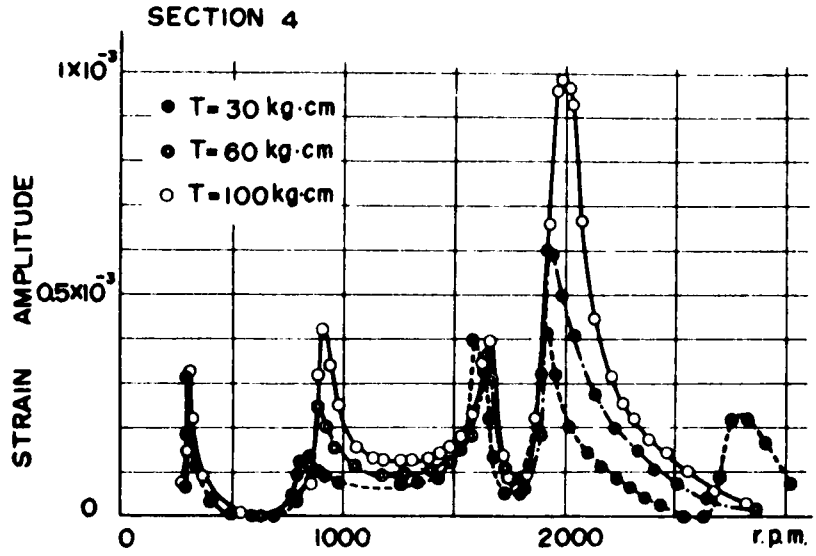

Fig. 317 (c)

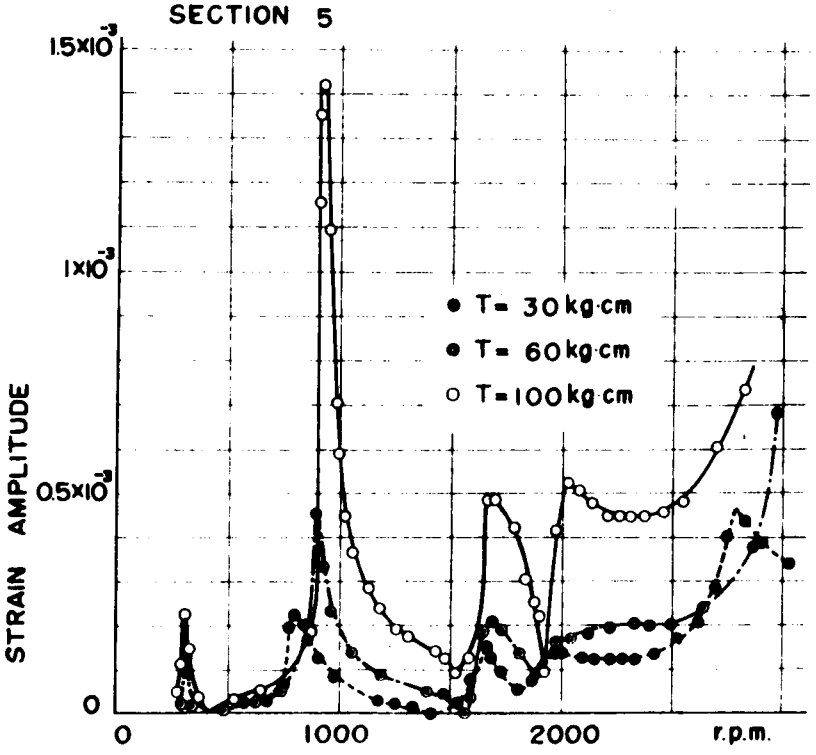

Fig. 317 (d)

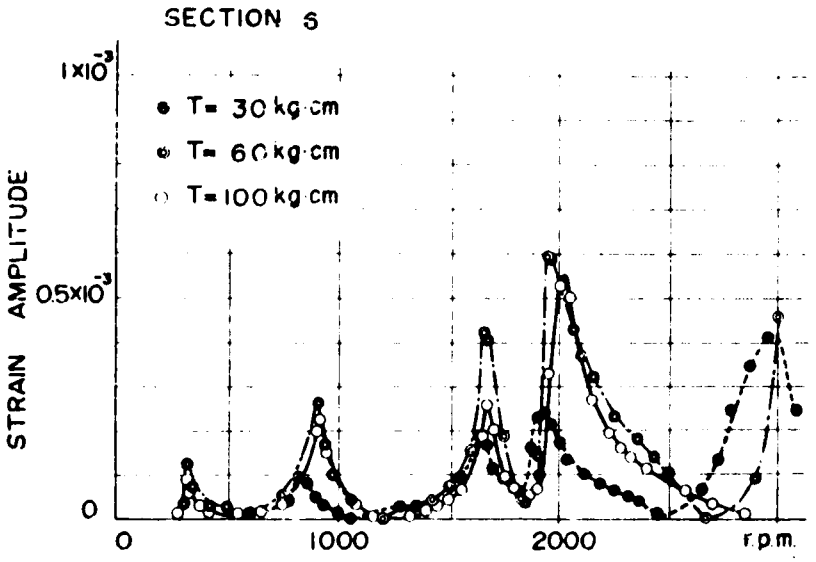

Fig. 317 (e)

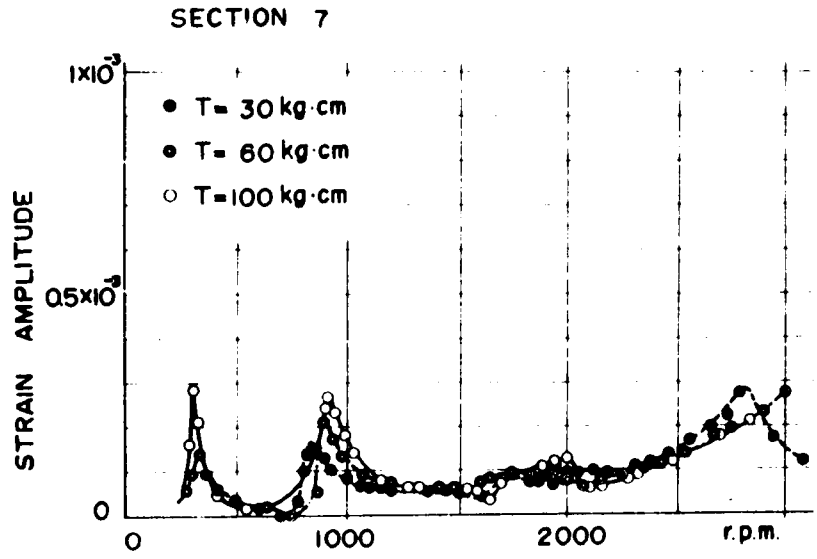

Fig. 317 (f)

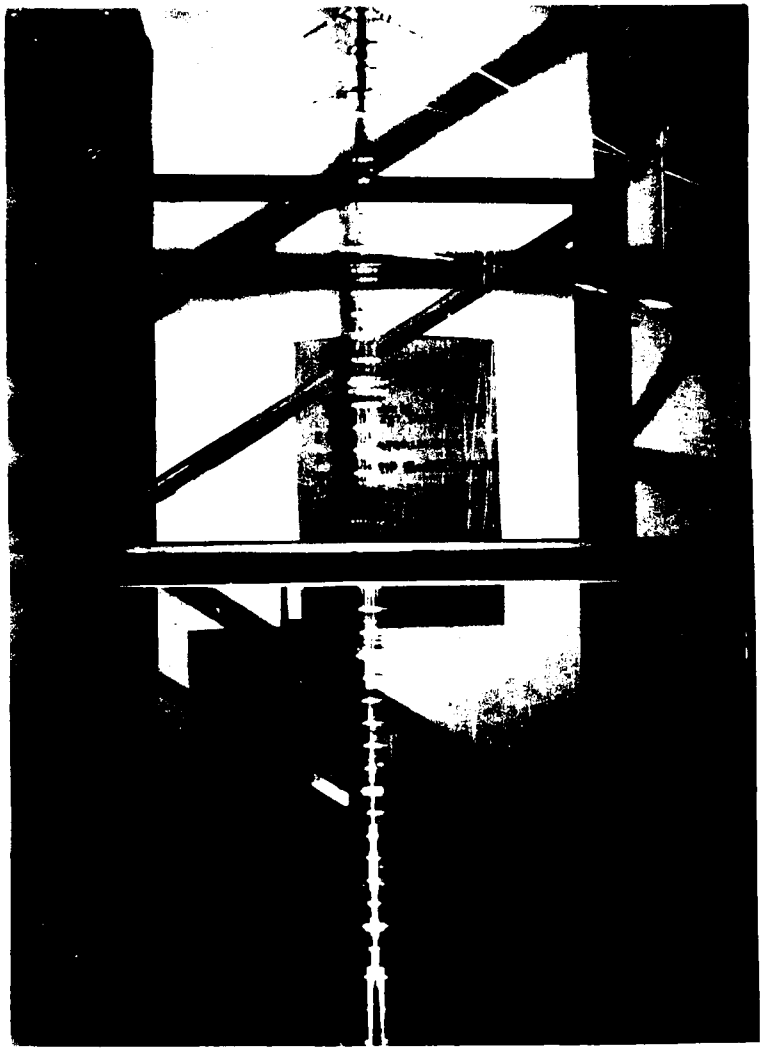

(a) First Mode Resonance

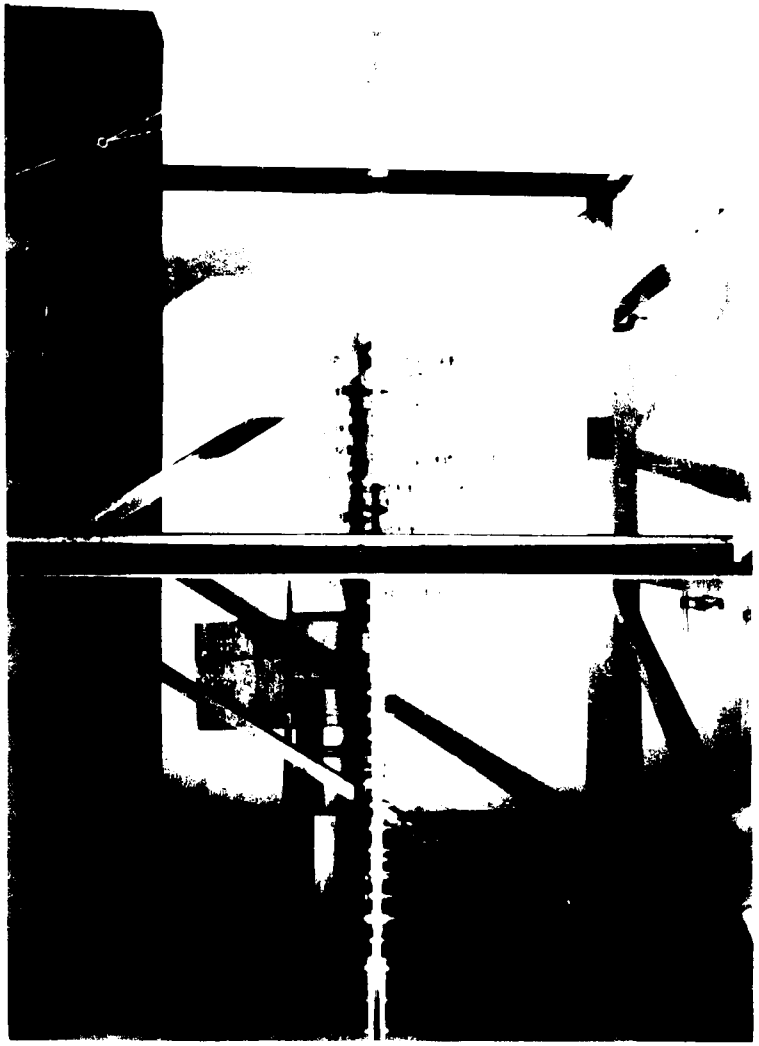

(b) Second Mode Resonance

Fig. 318

IV. FIELD MEASUREMENT OF VIBRATION OF SUSPENSION BRIDGES

313. Objective and Test Bridges

In the investigation of the aerodynamic stability and the earthquake response of suspension bridges, the basic dynamic behaviors of the structures, such as the natural periods, the natural modes, and the damping effect of the structures, are of great interest. In the preceding two chapters, the fundamental vibration behaviors of the suspension bridge and the suspension bridge tower were investigated by means of models. In this chapter the experimental studies on vibration of suspension bridges will be done employing two actual suspension bridge with comparatively small bridge spans.

The spans and other information of the bridges tested are given in Table. 308. Figs. 319 through 322 show the outline of these bridges.

One of these bridges, the Obata Bridge, was especially designed as a cable truss suspension bridge to resist to the wind action, while the other, the Monjigaichi Bridge, is an ordinary suspension bridge with floor stays. One of the objects of this field test is to verify the effects of cable truss to the vibration and the stiffness of the bridge.

Table 308 Test Bridges

Bridge Name	Monjigaichi Bridge	Obata Bridge
Length of Bridge	98.0 m	136.6 m
Span Length of Suspended Structure	97.5 m	136.0 m
Sag	8.5 m	8.5 m
Sag Ratio	1/11.5	1/13.7
Design load	200 kg/m^2	200 kg/m^2
Width of Bridge	1.2 m	1.2 m

314. Instrumentation

For the measurement of the vertical vibration mechanical deflection recorders designed by Dr. Tanabe were used. Using this type of deflection recorders, which was designed about fourty years ago which is of an old type, is considered to be the best method of vibration measurement of these bridges because of its excellent dynamic characteristics in range of comparatively low frequencies and of its simplicity. Setting of the deflection meter is shown in Fig. 323.

Vibfation with horizontal direction was measured by the method of the horizontal vibration pickups and electo-magnetic oscillograph. The horizontal vibration pickups shown in Fig. 324 were specially designed for this measurement and are having the natural period of 1.5 sec.

In Figs. 319 and 320 are shown the locations of these measuring instruments.

315. Method of Experiment

Vibration tests were performed by means of free vibration. It is preferable to obtain steady forced vibration or vibration due to wind action, but these were omitted in this investigation.

The following methods were used to start the free vibration.

Method I. First to pull the bridge in vertical or horizontal directions by means of the wire rope and a chain block with the force of about 500 kg, then to cut the wire rope suddenly and to make the free vibration.

Method II. First let some men jump with the natural frequency of the bridge, and to make a sudden stand still when the amplitude had its maximum value. The vibration amplitudes thus obtained were larger than those obtained in Method I.

316. Results of Experiments

Experimental results obtained are as follows.

(1) Vertical Vibration

Natural periods of vibfation produced by exciting the center of the bridges were given as shown in Table 309.

Table 309. Natural Period (Vertical Vibration)

Monjigaichi Bridge	T_v = 1.52 sec
Obata Bridge	T_v = 1.30 sec

A typical record obtained by a deflection recorder installed at the center of Monjigaichi Bridge is shown in Fig. 325. This record was recorded for the vibration due to Method II.

The relation between damping constants and displacement amplitudes of free vibration are given in Figs. 326 and 327 for the Monjigaichi and the Obata Bridge respectively. In Figs. 326 and 327 open circles are the values obtained by Method II, and closed circles are, by Method I.

The asymmetric vibration obtained by exciting a quarter point of the bridge showed quite a complicated motion in the first stage of vibration then turned into the symmetric vibration with the same period obtained by exciting the center or the bridge span. No typical asymmetric vibration with a node at the center of the span was therefore obtained.

(2) Torsional Vibration

A vibration was obtained by exciting a bridge side, but its amplitude were much smaller than those of pure vertical vibration. The natural period thus obtained are shown in Table 310.

Table 310. Natural Period (Torsional Vibration)

Monjigaichi Bridge	T_t = 0.438 sec
Obata Bridge	(T = 1.30 sec)

For the Monjigaichi Bridge vibration thus obtained was verified by vibration records as the torsional vibration, but for the Obata Bridge the natural period thus obtained is the same as that of the vertical vibration and no torsional vibration was recognized.

(3) Horizontal Vibration

Horizontal vibration was obtained by pulling the center of the span horizontally by Method I. It was checked from the records of the deflection recorders that there was no remarkable torsional vibration involved in the horizontal vibration thus obtained.

Natural periods of horizontal vibration are shown in Table 311. The relation between damping constants and recorded amplitudes are shown in Figs. 328 and 329.

Table 311. Natural Period (Horizontal Vibration)

Monjigaichi Bridge	T_h = 2.5 sec
Obata Bridge	T_h = 3.5 sec

317. Investigation on the Results Obtained

(1) Vertical Vibration

Employing the Bleich Method, the natural frequencies and modes of the bridges are obtained as shown in Table 312 and Figs. 330 and 331.

Table 312. Natural Period of Vertical Vibration (Theoretical)

Bridge	Symmetric Modes 1st	2nd	Asymmetric Modes 1st	2nd
Monjigaichi Bridge	1.94	1.43	2.55	1.17
Obata Bridge	1.98	1.48	2.60	1.24

The effects of floor stays were disregarded, and the cable truss members were replaced by ordinary suspension bridge hangers in the computation of these natural periods. Young's Modulus of cables were assumed as 1×10^6 kg/cm^2.

The measured natural periods are, as already given, for the Monjigaichi Bridge $T_v = 1.52$ sec and for the Obata Bridge $T_v = 1.30$ sec. These values are verified from the distribution of recorded deflections to correspond to the 1st symmetric mode of vibration.

The theoretical values, therefore, do not coincide well with the experimental values obtained especially for the natural periods of the Obata Bridge. The following are the reasons for these non-agreements. (1) Effects of the floor stays for the Monjigaichi Bridge, (2) Effects of truss cables for the Obata Bridge, (3) Incorrect assumption on Young's Modulus, and (4) Effects of initial tension of the cables.

According to the theoretical results obtained, the 1st asymmetric mode of vibration is the lowest mode of vibration of these bridges. Such vibration, however, is not remarkable in the experimental results obtained. The floor stays, the center stays, and the truss cables are also considered to be quite effective to prevent the first asymmetric mode of vibration.

Damping constants of vertical vibration are about 0.01 - 0.02 for the Monjigaichi Bridge and about 0.007 for the Obata Bridge. As will be seen from Figs. 326 and 327, the damping constants are quite scattered especially for small amplitudes. The damping constants increase a little with small amplitudes for the Monjigaichi Bridge. Some of the experimental results on the vibration damping of suspension bridges have been reported (301)(302), and almost the same results as in the experiments are given.

(2) Torsional Vibration

No torsional vibration is obtained in the Obata Bridge, and it might be expected that the cable truss suspension bridge has higher torsional rigidity than ordinary suspension bridges.

(3) Horizontal Vibration

Because the measured horizontal vibration periods are 2.5 sec. for the Monjigaichi Bridge and 3.5 sec. for the Obata Bridge, the horizontal vibrographs were employed as acceleration recorders. Since the free vibration periods are invariable during the experimental run, damping constants thus obtained are not so very different from correct values.

318. Conclusion

Some of the fundamental vibration behaviors of the actual suspension bridges were investigated. Comparing two tested bridges, it is clear that the cable truss suspension bridge has higher vibration and static rigidities than the suspension bridge with vertical hangers.

Some of the additional studies, theoretical and experimental, of cable truss suspension bridges are now being carried.

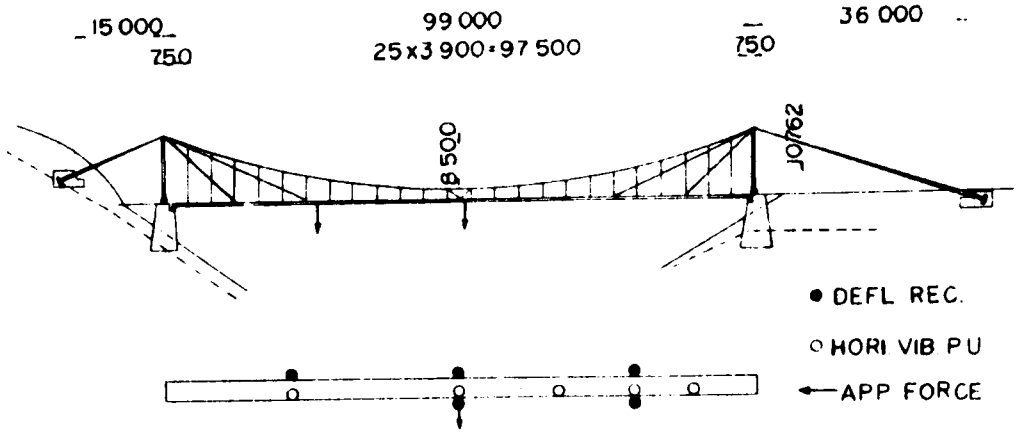

MONJIGAICHI BRIDGE

Fig. 319

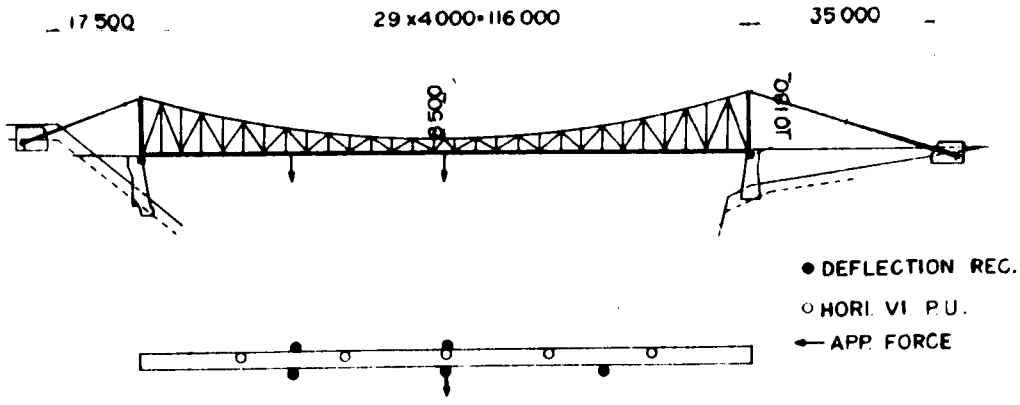

OBATA BRIDGE

Fig. 320

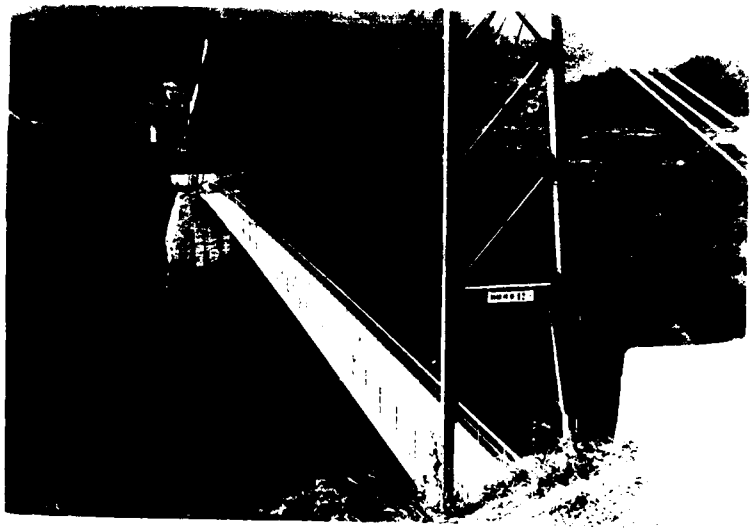

Fig. 321 Monjigaichi Bridge

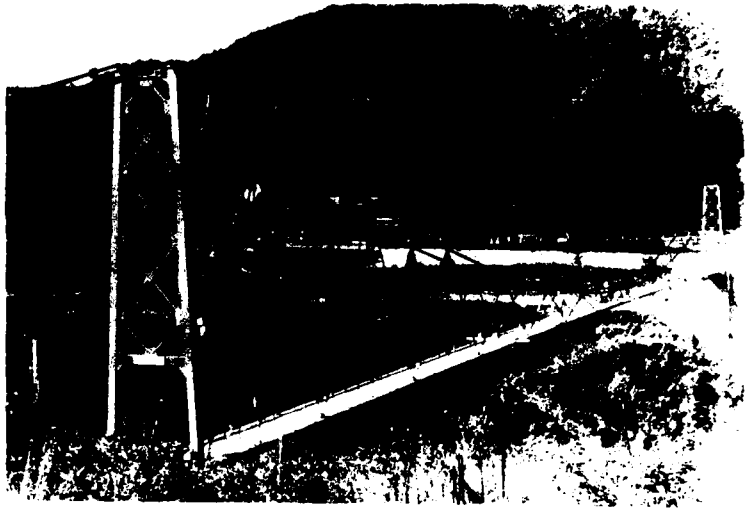

Fig. 322 Obata Bridge

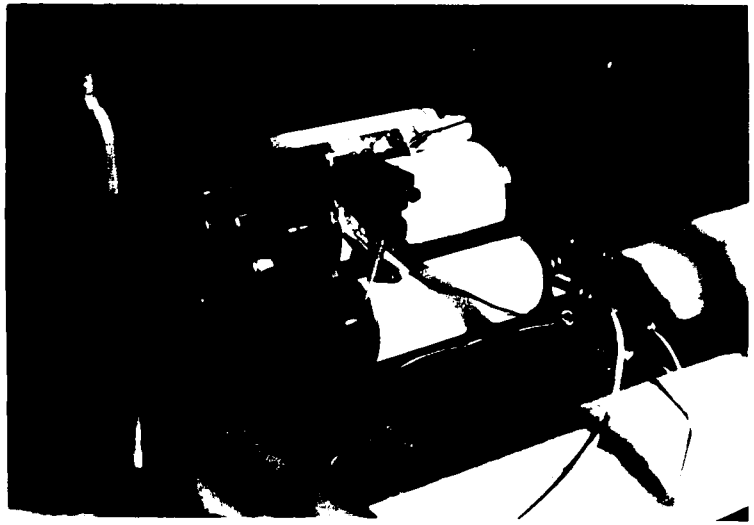

Fig. 323 Deflection Recorder

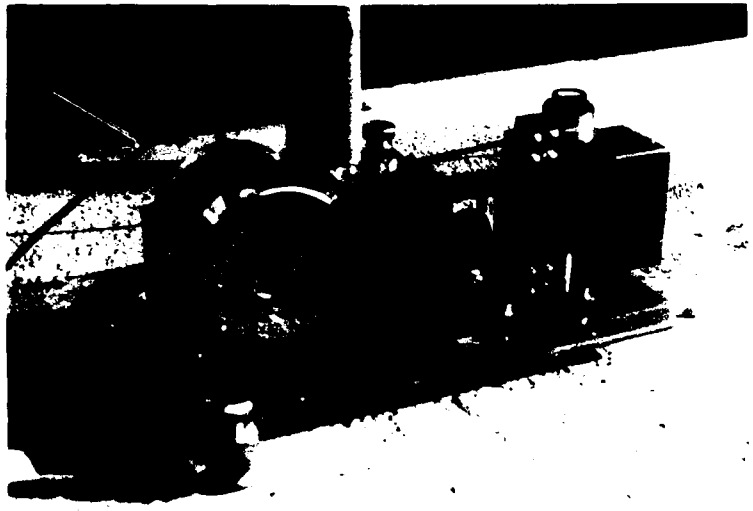

Fig. 324 Horizontal Vibration Pick-up

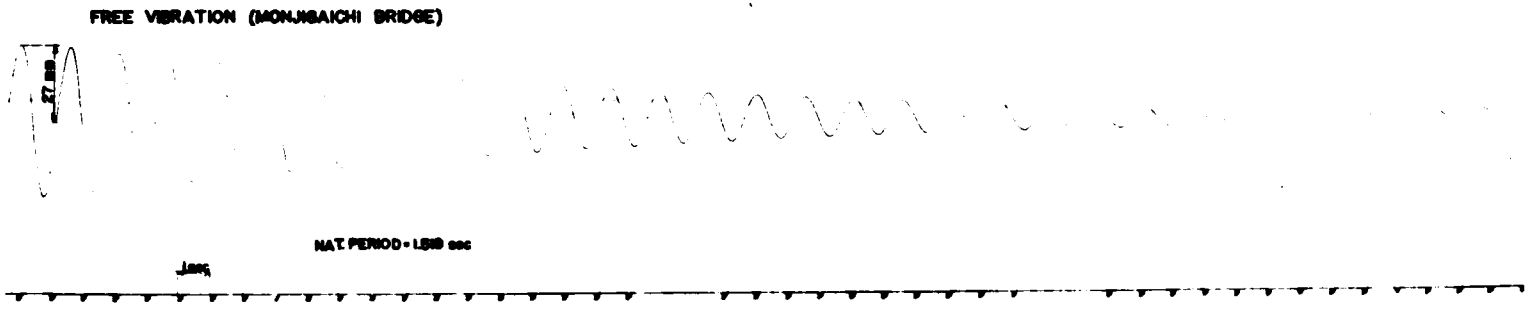

Fig. 325

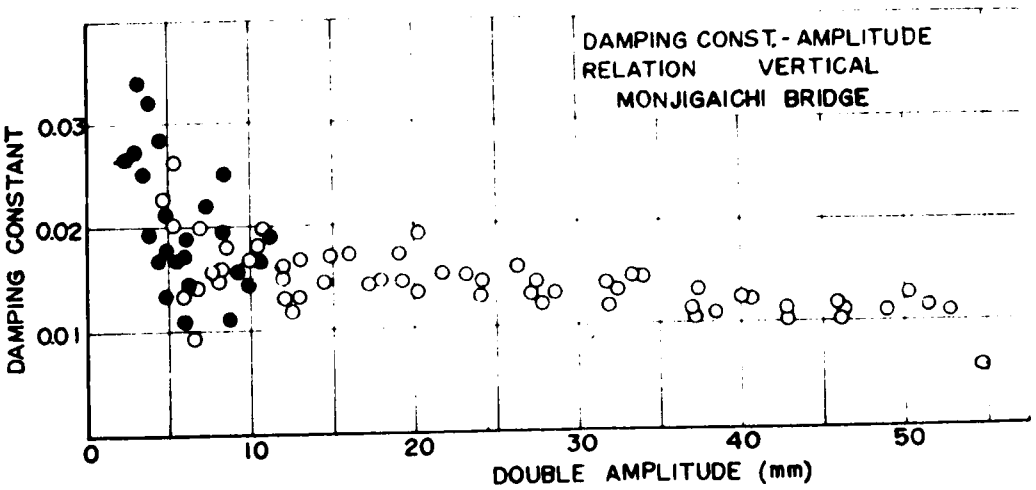

Fig. 326

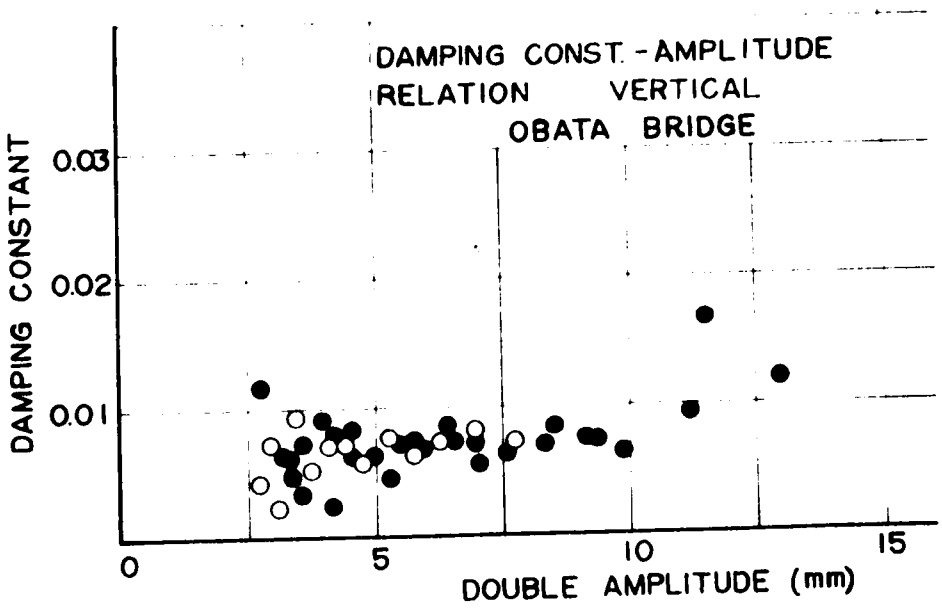

Fig. 327

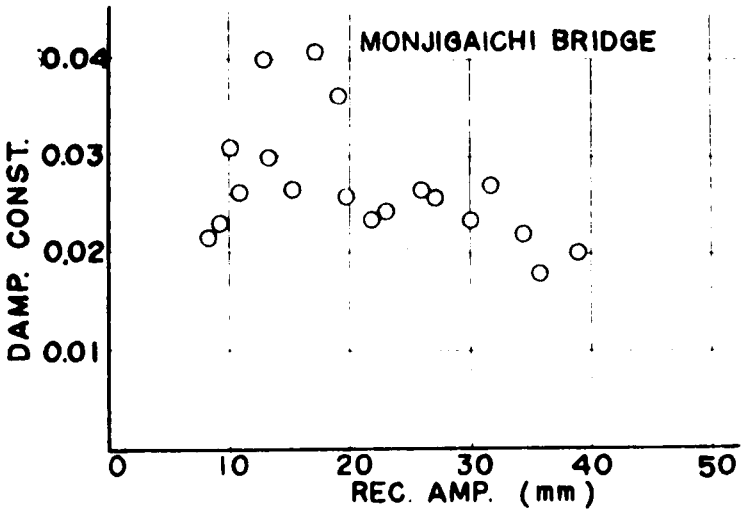

Fig. 328

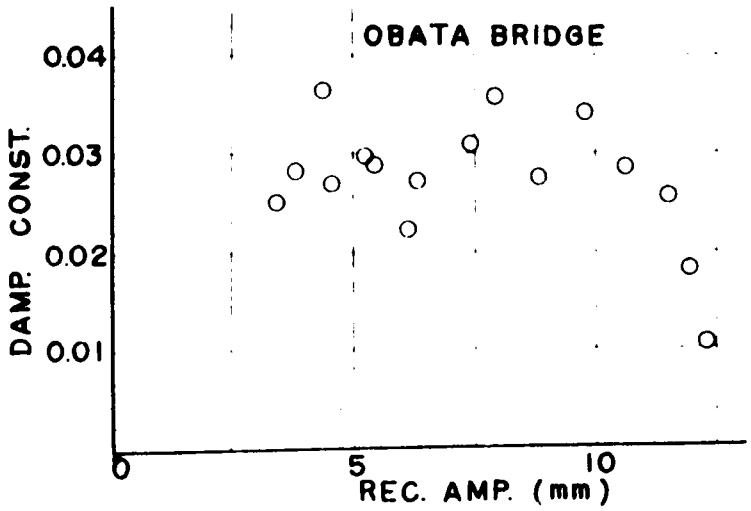

Fig. 329

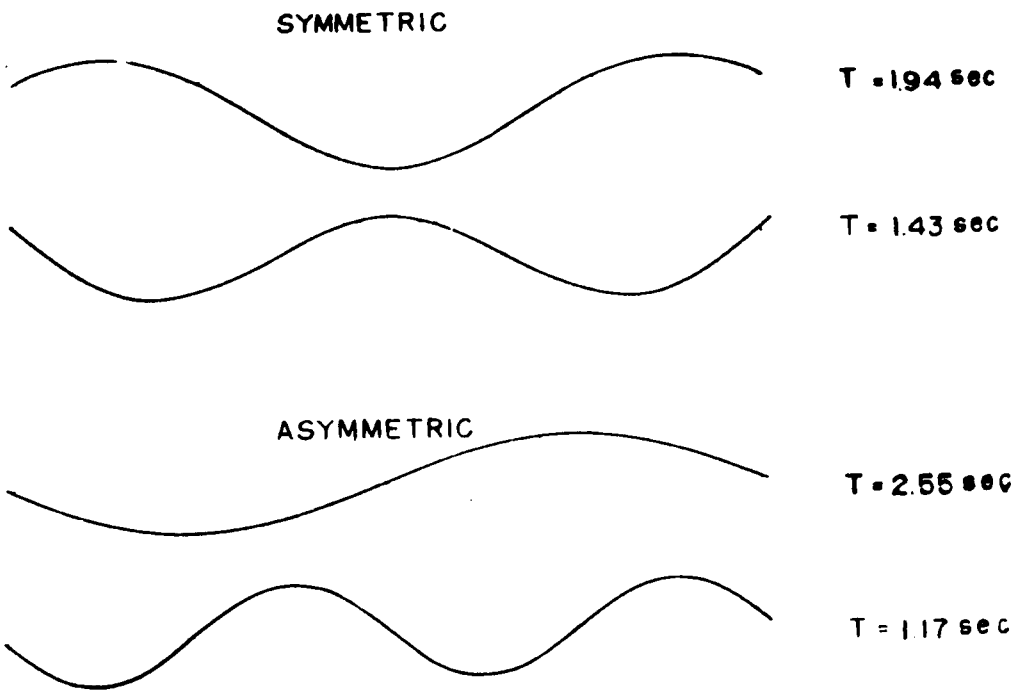

VIBRATION MODES (MONJIGAICHI BR.)

Fig. 330

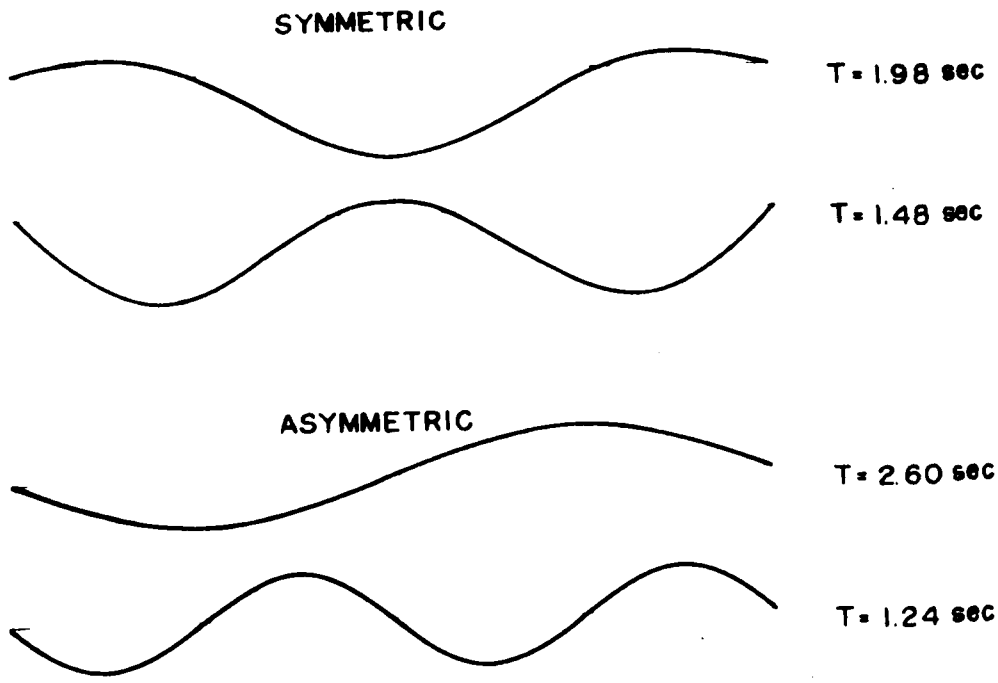

VIBRATION MODES (OBATA BR.)

Fig. 331

V. VIBRATION DAMPING OF BRIDGES

319. Introduction

In regard to the dynamic problems of bridges, such as the problems of aerodynamic stability and earthquake response of suspension bridges, the damping characteristics of vibration must be fully investigated.

In the theoretical analyses given in this paper, damping of the structures were mostly disregarded because the damping constants of ordinary steel structures are of quite small, say less than 5% the critical damping, and the effects of vibration damping to transient vibration are not significantly important as the effects to steady forced vibration. In some cases, such as dynamic resonance with external loads, damping characteristics of bridges are quite basic characteristics of vibfation.

In this chapter, some of the fundamental investigations on structural damping will be discussed in the first some articles, and the damping characteristics of several actual bridges, including some suspension bridges, will be given.

320. Classification of Damping Mechanisms of Structural Damping

Damping is the energy dissipation properties of a material or system under cyclic loading. As it is clear from the investigation of Part II of this paper, plastic deformation of the structure causes the large amount of energy dissipation and prevent the catastrophic destruction of the structures. The term damping used in this paper, however, defines the energy dissipation under cyclic loading of comparatively small stress level, say elastic limit.

Many types of damping are included in structural damping, but for convenience in the discussion damping of structures is classified as the following.

(1) Material Damping or Internal Friction Damping
(2) Interfacial Slip Damping
(3) Energy Dissipation at the Structural Supports
(4) Friction in the Main Expansion Joints
(5) Resistance of the Air or Water.

The damping effect caused by the damping influences of item (1), (2), and (3) may be discussed in the following three articles.

321. Material Damping

The dissipated energy lost from the internal friction of the material of structure is exhibited by the stress-strain curve for loading. The stress-strain curve for loading does not coincide with that for unloading, and neither of them is an exact straight line even within the elastic limit of the material. A hysteresis loop occurs as shown in Fig. 332, and the area A of the loop indicates the amount of energy dissipated during one cycle. That is

$$A = \Delta w = \oint \sigma \, d\varepsilon = \alpha_n \varepsilon_o^n \tag{307}$$

Δw shows the dissipated energy lost from the unit volume during one cycle, and

α_n = constant determined by the structural material,

ε_o = maximum strain.

The dissipation of energy caused by the elastic hysteresis of the steel is very small, because of the slight departure of the stress-strain curve from a strait line. The value of n is between 2 and 3 in the low intermediate stress region but much higher at the stress level beyond the critical stress.(303)

Elastic hysteresis in a wide range is nearly independent of the velosity of the vibration, and the internal damping capacity can be considered as being independent of the frequency of the vibrating structure.

If the stress-strain relation given in Eq. (307) and Fig. 332 is applied to the analysis of a bending member, the total energy dissipated within one cycle is obtained, by integrating Eq. (307) along the whole length and sectional area of the member, as

$$\Delta W = \int_{\ell} \iint_{A} \oint \sigma \, d\varepsilon \, dA \, dx = \alpha_n I_n \int \left(\frac{\partial^2 y}{\partial x^2}\right)^n dx \tag{308}$$

where,

$I_n = \int_A \xi^n dA$, sectional moment of nth order,

ℓ = length of the member,

A = sectional area

y = deflection of the member

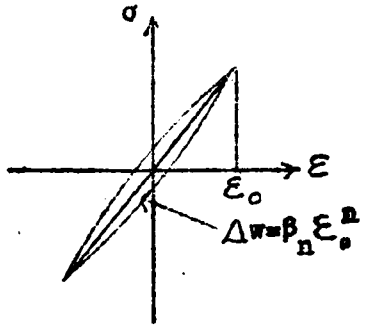

Fig. 332

x = coordinate along the length of the member

ξ = length from the center of gravity of the section to dA.

The maximum value of the potential energy of the member during the vibration is

$$W = \frac{EI}{2} \int_{\ell} \left(\frac{\partial^2 y}{\partial x^2}\right)^2 dx \qquad (309)$$

In the case of the free vibration, where the logarithmic decrement is very small compared to the unity, the terms of higher order of the series expansion of δ are neglected and the relation

$$\frac{\Delta W}{W} = 2\delta \qquad (310)$$

is obtained. From Eqs. (308) (309), and (310)

$$\delta f = \frac{\alpha_n I_n}{EI} \left\{ \int_{\ell} \left(\frac{\partial^2 y}{\partial x^2}\right)^n dx \Big/ \int_{\ell} \left(\frac{\partial^2 y}{\partial x^2}\right)^2 dx \right\} \qquad (311)$$

Assuming a simply supported beam at both ends , the distribution of the vibration amplitude is approximately assumed as

$$y = \eta \sin \frac{\pi x}{l}$$

then δ is obtained by

$$\delta = \frac{\alpha_n I_n}{EI} \left(\frac{\pi^2}{2l}\eta\right)^{n-2} \left\{ \Gamma\left(\frac{n+1}{2}\right) \Big/ \Gamma\left(\frac{n}{2}+1\right) \right\} \qquad (312)$$

Consequently, σ is proportional to (n-2)th power of η, and has no relation with the velocity of vibration.

When $n = 2$ α_n is shown by $\alpha_2 = E\delta$ using the logarithmic decrement δ, and in this case δ is a constant. When $n \neq 2$, the value δ is not only the function of the deflection but the value decided by the form and the dimensions of the structures.

The damping constant β is approximately expressed as the following using the logarithmic decrement δ.

$$\beta = \frac{\delta}{2\pi} \qquad (313)$$

322. Interfacial Slip Damping

Interfacial slip at any connection between distinct parts of a structure is an unavoidable source of hysteresis. It is clear from the experimental investigation on the suspension bridge tower given already and the experimental investigation on steel beams which will be given lately that large amount of energy is dissipated from the connection of the structures.

A theoretical and experimental investigation of the structural damping of simple built-up structures was made by Pian and Hallowell, (304)(305) (306) and they obtained a remarkable results.

According to their investigation the energy loss per cycle due to interfacial slip varies approximately as the third powdr of the load amplitude and is roughly in inverse proportion to the tightness of the fastening of the structural connections.

If the interfacial slip damping, which is concentrated at the connections of the structure, is considered to be distributed along the structure, the effects of slippage of structural parts are approximately expressed by letting n equal to or approximately equal to 3 in Eqs. (307), (308) (311), and (312) and by taking adequate constant α_n.

An analytical investigation of a system with damping mechanisms ununiformly distributed along the strudture is quite complicated because the effects of such damping source to vibration modes have not been made clear yet. The only method which is possible now is to use the vibration modes for the system without damping to the system with damping and to compute total dissipate energy during one cycle.

313. Energy Dissipation at Structural Supports

Large amount of vibration energy may be dissipated from the structural supports. Although the actual mechanisms of energy dissipation from the supports are very complicated, it is theoretically possible to consider to be Coulomb Friction.

The energy loss during one cycle of vibration is shown by $W = F\Delta s$, where the displacement of the support in one cycle is Δs, and the friction force of the support is F.

Taking the displacement of G as c (Fig.333) and the angle of rotation of the beam at the moving support as φ and taking into consideration the fact that an equal amount of rotation of the beam arises at the hinged support, the displacement of the supporting point in one cycle is shown as follows:

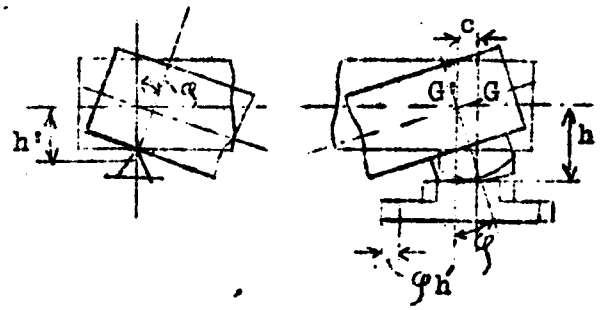

hinged support sliding support

Fig. 333

In case the beam displaces to the downward $\varphi h' + \varphi h - c$

In case the beam displaces to the upward $\varphi h' + \varphi h + c$

The displacement of the supporting point in one cycle is

$$\Delta s = 4 (\varphi h' + \varphi h)$$

Then, the energy dissipated through the support is

$$\Delta W = 4 \varphi (h + h') F$$

As φ and F are given by

$$\varphi = \left(\frac{dy}{dx}\right)_{x=0} = 2 \frac{\eta}{l} \pi \qquad F = \mu \frac{G}{2}$$

where,

η = maximum deflection of the beam,

l = span length of the beam,

μ = coefficient of friction of the sliding support,

G = total weight of the beam.

The energy loss during one cycle is

$$\Delta W = 2 \frac{h + h'}{l} \eta \pi \mu G \tag{314}$$

And as the W is shown in Eq. (309)

$$\frac{\Delta W}{W} = \frac{8 (h+h') \mu G l^2}{\pi^2 E I \eta} \tag{315}$$

is obtained.

For such damping, the damping capacity decreases hyperbolically as the amplitude increases. The amplitude decay curve is a straight line rather than an the expornential curve.

324. Damping Capacity of the Structure

Bridges or suspension bridges are built up of several structural elements, such as cables, suspended structures, towers, etc. Denoting the energy loss per cycle of the various elements and damping mechanisms by ΔW_1, ΔW_2, ..., respectively, the damping capacity of the whole system is given as

$$\psi = \frac{\Delta W_1 + \Delta W_2 + \cdots\cdots}{W} \tag{316}$$

The logarithmic decrement δ can be calculated by the following equation even when δ is comparatively large.

$$\delta = -\frac{1}{2} \log \left(1 - \frac{\Delta W_1 + \Delta W_2 + \cdots\cdots}{W}\right) \tag{317}$$

It is clear from Eq. (317), the free vibration does not arise when

$$\Delta W_1 + \Delta W_2 + \cdots\cdots > W$$

For example, if ΔW_1 is assumed to be the energy dissipated from the internal friction of the beam and ΔW_2 is that dissipated from the support, Eq. (317) can be given as the following when only these two mechanisms of dissipation are considered.

$$\delta = -\frac{1}{2} \log \left(1 - \frac{\Delta W_1 + \Delta W_2}{W}\right) \tag{318}$$

Substituting Eqs. (315) to Eq. (318)

$$\delta = -\frac{1}{2} \log \left(1 - \frac{8(h+h')\mu\, Gl^2}{\pi^3 E I \gamma} - 2\delta_1\right) \tag{319}$$

where δ_1 is the logarithmic decrement when only the effect of internal friction is considered.

325. Experimental Damping Studies on Steel Model Beams

To investigate the characteristics and the values of the vibration damping resulting from the different causes of damping mentioned previously model beams were made, and some experimental studies were done.

(a) Model Beams and Method of Experiment

The model beams used in this experiment are composed of two beams,

set in parallel, and they are of three kinds -- welded, riveted, and tolted beams. Fig. 334 shows schematically the main dimensions and the cross sections of these beams. Table 313 shows the data of these beams.

Table 313. Model Beams

Beams	Welded	Riveted	Bolted
Span Length (m)	6	6	6
Total Weight (kg)	196	207	210
Sectional Moment of Inertia (cm^4)	227	212	212
Free Vibration Frequency (Theoretical) (sec^{-1})	7.52	7.05	6.91
Free Vibration Frequency (Experimental) (sec^{-1})	7.67	7.18	6.95

For the support, ball-bearings are used as the hinge and rollers are used as the moving support. With these arrangements, the energy dissipated through the support can be disregarded almost completely. To investigate the effect of the supporting condition, sliding supports were used afterwards as the moving support.

Various different methods of experiment could be considered, but in this experiment, the damping free vibration was applied in order to obtain the damping characteristics exactly. As the means of vibrating, a method of vibrating by hand was adopted and the damping free vibration was recorded in Askania Vibrograph which was fixed on a supporting apparatus.

(b) Damping Behaviors of the Welded Beam and the Riveted Beam

The object of the experiments described in (b) and (c) is to investigate the energy which is dissipated by the internal friction of the beams. Then, a roller support has been used as the moving support.

Fig. 335 shows the amplitude decay curves for the riveted and the welded beams. It is clear from this figure that the condition of the decrement differs considerably depending upon the kinds of beams. The welded beam shows a smaller decrement than the riveted beam.

In the following damping constants are used instead of logarithmic decrements.

The relation between the damping constant and the vibration amplitude is illustrated in Fig. 336.

From Fig. 336 as far as this experiment is concerned, the following conclusion is obtained.

(1) The damping constant in the case of the welded beam is almost constant and its value is about $\beta = 0.00075$, and has no relation with the amplitude. This value is approximately equal to the damping constant of the material damping of the steel.

(2) In the case of the riveted beam, the damping constants increases as the beam has a larger amplitude. The effect of this goes to show the fact that the damping characteristics cannot be shown in a linear form even within the stress range of this experiment in which the Hooke's law can be applied. Expressing the function the logarithmic decrement of the riveted beam as

$$\beta = \beta_0 \, \delta^{\alpha} \tag{320}$$

and determining β_0 and α from the experimental data by the method of least squares,

$$\beta = 0.001907 \, \delta^{0.344} \tag{321}$$

is obtained. The curve shown by Eq. (321) is shown in Fig. 336 in a dotted line.

(c) <u>The Relations between Damping Behavior and Fastening of Bolts on the Bolted Beam</u>

The effect of fastening the connection of cross sections of a beam upon the damping characteristics is investigated by using the bolted beam.

The relation between the torque T for fastening the bolts and the tension P of the bolts is shown as follows.

$$T = C \, D \, P \tag{322}$$

where

D = the diameter of the bolts,

C = a constant (C = 0.2 is given by the experiment of H. Lenzen)

If the constant of C is chosen as C = 0.2, the relations between the torque and the stress of bolt δ are shown as follows for the bolts used in this beam.

$T = 50$ kg-cm $\quad \sigma = 370$ kg/cm^2

$T = 100$ kg-cm $\quad \sigma = 740$ kg/cm^2

$T = 400$ kg-cm $\quad \sigma = 2960$ kg/cm^2

As the yield point of the bolt is about 2600-30000 kg/cm^2, the torque T adopted in this experiment is 0-400 kg-cm. A torque wrench obtained in the market was used to fasten the bolts.

The amplitude decay curves of the free vibration are shown in Fig. 337 for several values of torque. And the relations between the amplitude and the damping constants are as shown in Fig. 338. From these figures the following conclusions are obtained.

(1) The damping constant is depended upon the tightness of the bolts, and almost the same characteristics of the damping as in the riveted beam is obtained.

(2) The fastening of the bolts as tight as to exceed $T = 100$ kg-cm has no effect on the damping.

(d) The Effects of the Types of the Moving Support

In order to investigate the effect of the types of the moving support, a sliding support was used. In this experiment the riveted beam was used. The amplitude decay curve in this experiment is as shown in Fig. 339.

It is clear from Fig. 339 that the effect of the Coulomb damping becames very remarkable when the roller support is replaced by the sliding support. The relation of the amplitude and the damping constant is shown in Fig. 340. The damping constant increases as the amplitude decreases, and this is nothing but a characteristics of the Coulomb damping.

The damping constant-amplitude relations calculated by using Eq. (319) are shown in Fig. 340, the dotted line is for $\mu = 0.1$ and the chain line for $\mu = 0.2$.

In Fig. 340 the theoretical line for $\mu = 0.1$ coincide well with the experimental results. The effect of the internal friction shown by $2\delta_1$ in Eq. (319) is disregarded in the computation because it is very small.

326. Vibration Damping of Actual Bridges

The vibration damping of actual suspension bridges was investigated in the preceding chapter. In this article vibration damping of ordinary bridges which were investigated by the author will be investigated for the purpose of reference of damping of structures.

The damping characteristics of actual bridges depend upon more

complicated mechanisms than those of the model beams. In the following some of the damping constants obtained by field tests will be given.

(a) Methods of measurement of a damping constant

Various methods can be applied to measure the vibration damping of a bridge. The following methods were used in this experiment:

Method I. Measure the amplitude of the damping free vibration after the moving load has passed.

Method II. Measure the amplitude of the damping free vibration arisen in the following manner. First let some men jump on the bridge so as to be resonant with the natural vibration period of the bridge until the bridge attains a considerable amplitude, then let these men stop jumping suddenly. The vibration amplitude thus obtained was larger than that obtained in the Method I.

Method III. Vibrate the bridge by using an oscillator and calculate the damping constant from a resonance curve using the following equation.

$$\beta = \frac{1}{4} \frac{\nu_1^2 - \nu_2^2}{\nu_r^2}$$

where, ν_1 and ν_2 are the circular frequency corresponding to the amplitude of 0.707 x (resonance amplitude) in resonance curve and ν_r is that of resonance amplitude.

A mechanical displacement vibrograph has been used as the measuring instrument and its natural period is 1.8 sec and the geometric magnification is about 15.

(b) Damping constants obtained

The amplitude used in the experiments was about 1 mm. The mean value of the damping constant obtained from the records of the damping free vibration is summerized in Table 314.

Fig. 341 illustrates the relation between the damping constant and the amplitude for three actual highway bridges. It is noticed that there is a tendency that the damping constant increases with the amplitude increase. The non-linear properties of the damping, however, are not remarkable in these cases, because the amplitude of vibration is comparatively small.

The damping constant obtained from the resonance curve are shown in parenthesis in Table 314. It seems that the value of the damping constant

obtained from the resonance curve in general is larger than the value obtained from damping free vibration.

The actual bridges show a rairly large damping constant than that of the model beams. The causes of this result are that in the case of actual bridges, the roadway slabs are made of concrete and they have a more complicated mechanism of damping than the model beams. However, the damping constant of the bridge is considerably small compared with other structures, such as building structures. This means that when the resonance amplitude is large, the damping ratio has a considerable effect on the dynamic behaviors of the bridges.

Table 3\4 Damping Constants of Actual Bridges

Name of Bridges	Types	Dimensions of Bridges	Natural Period (sec)	Damping Constants
Takakura	C.B. 2 spans	L = 45.15 m b = 11.125 m	0.290	0.0051
Shomen	Con. B. 3 spans	L = 75.80 m b = 6.00 m	0.304	0.0113 (0.029)
Kyokawa	C.B. 3 spans	L = 86.00 m b = 6.00 m	0.284	0.0095 (0.0162)
Taisho	Two Hinges Arch	l = 300 ft b = 21.92 m	0.405	0.0275
Masutani	Spandrel Brd. Arch	l = 77.2 m b = 6.00 m	0.334	0.0047 (0.0065)
Okawa	Warren Truss	l = 59.1 m b = 6.50 m	0.323	0.0107
Saijo	Box Gdr.	l = 36.30 m b = 5.5 m	0.285	0.0153
Morotomi	Warren Truss	l = 41.75 m b = 7.5 m	0.251	(0.03 - 0.05)
Yamasu	Box Gdr.	l = 36.30 m b = 4.5 m	0.368	0.0105
Hakuun	Box Gdr.	l = 28.00 m b = 6.0 m	0.194	0.0126
Kanaura	Box Gdr. (Steel Deck)	l = 40 m b = 8 m	0.412	0.01

C. B. = cantilever bridge, Con. B. = continuous bridge, Gdr. = girder

L = length of bridge, l = length of span, b = width of bridge

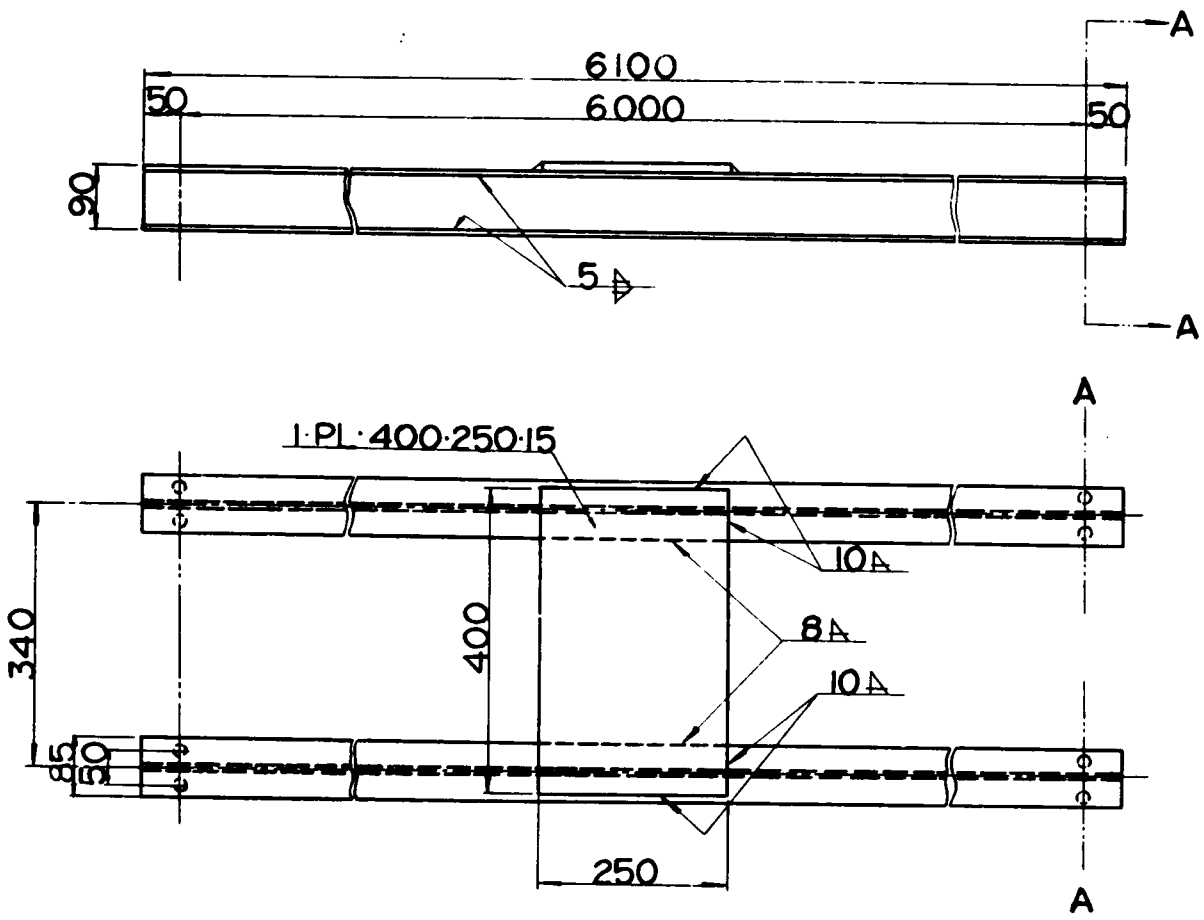

Welded Beam

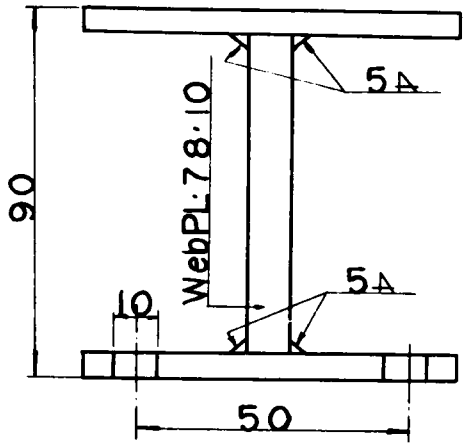

Section A A for Welded Beam

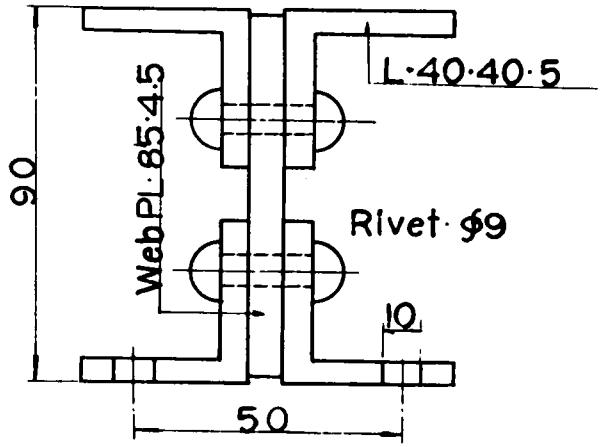

Section A A for Riveted and Bolted Beams

Fig. 334

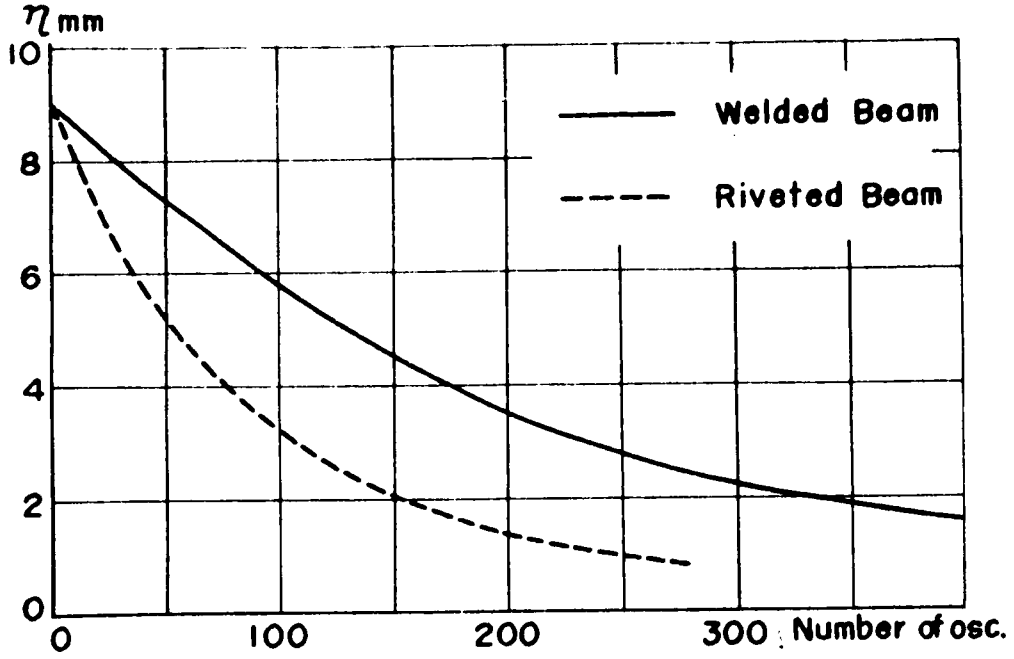

Fig. 335 Amplitude Decay Curves

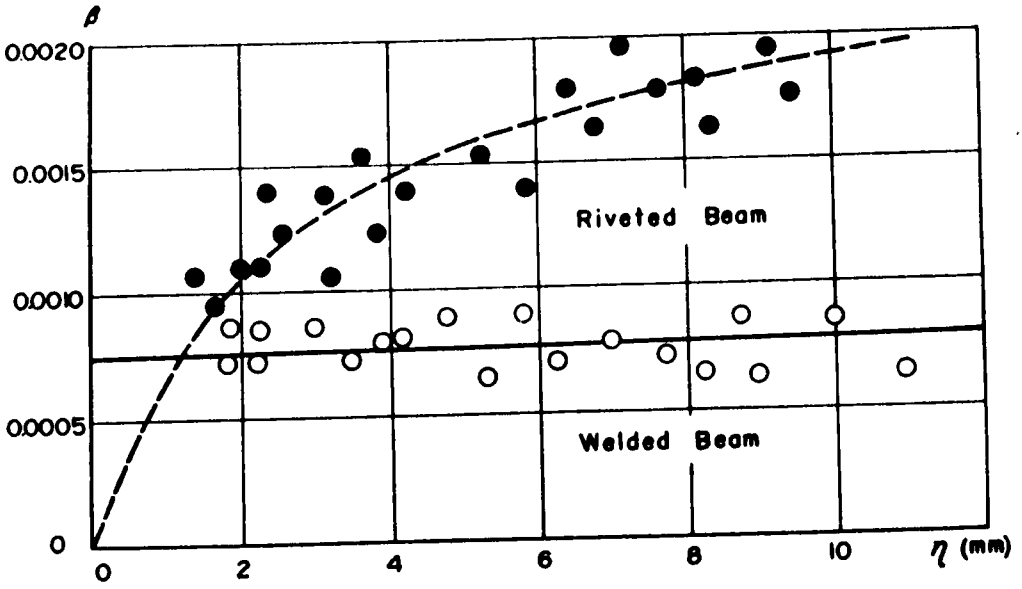

Fig. 336 Damping Constant-Amplitude Relations

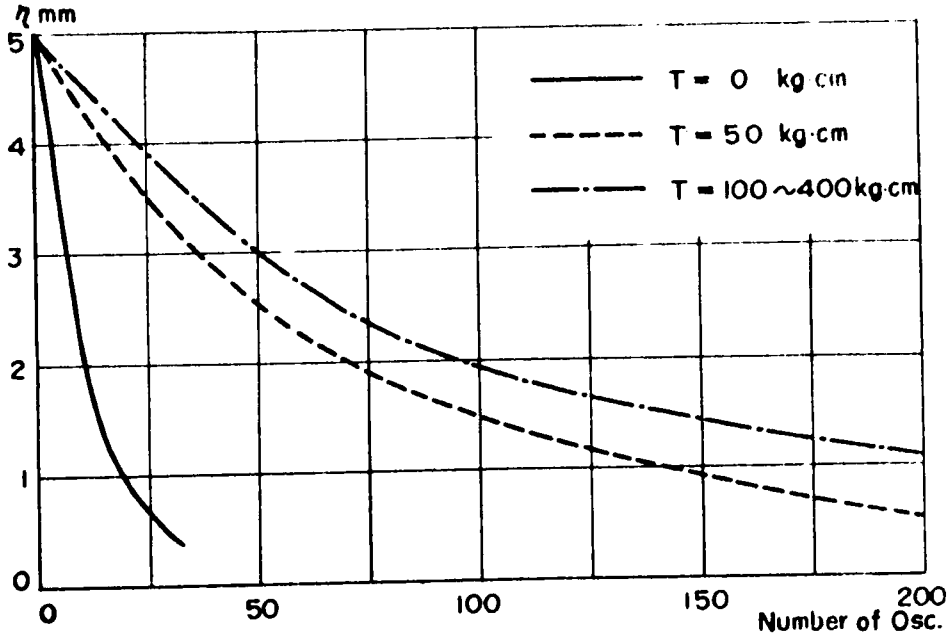

Fig. 337 Amplitude Decay Curves

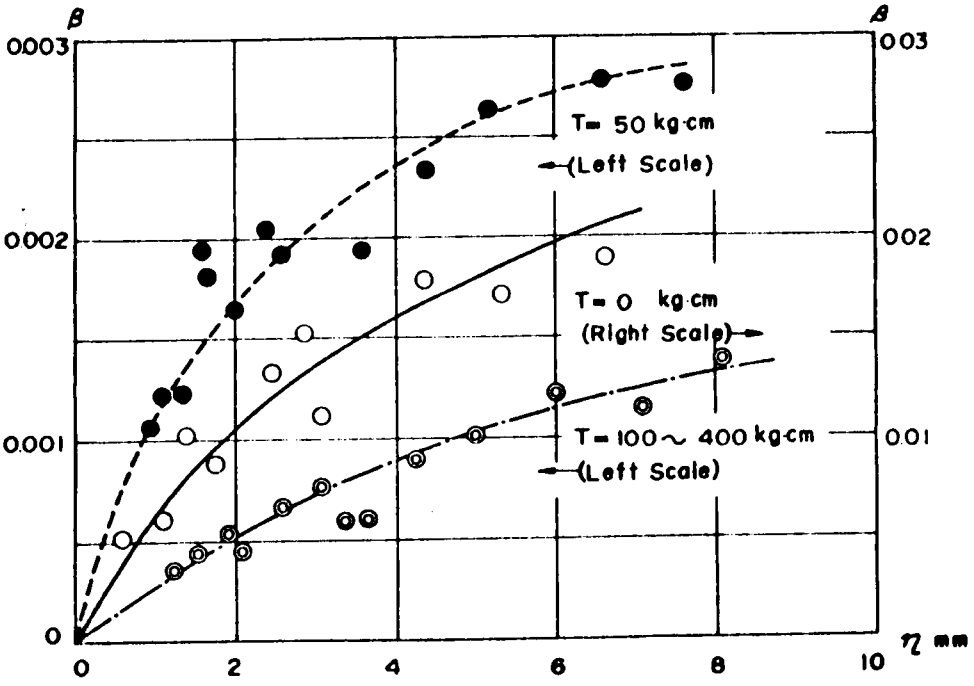

Fig. 338 Damping Constant-
Amplitude Relations

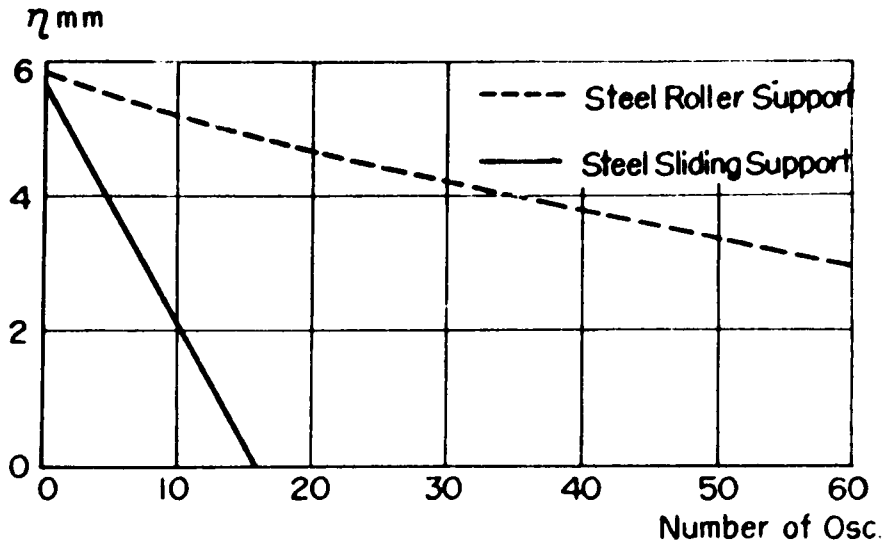

Fig. 339

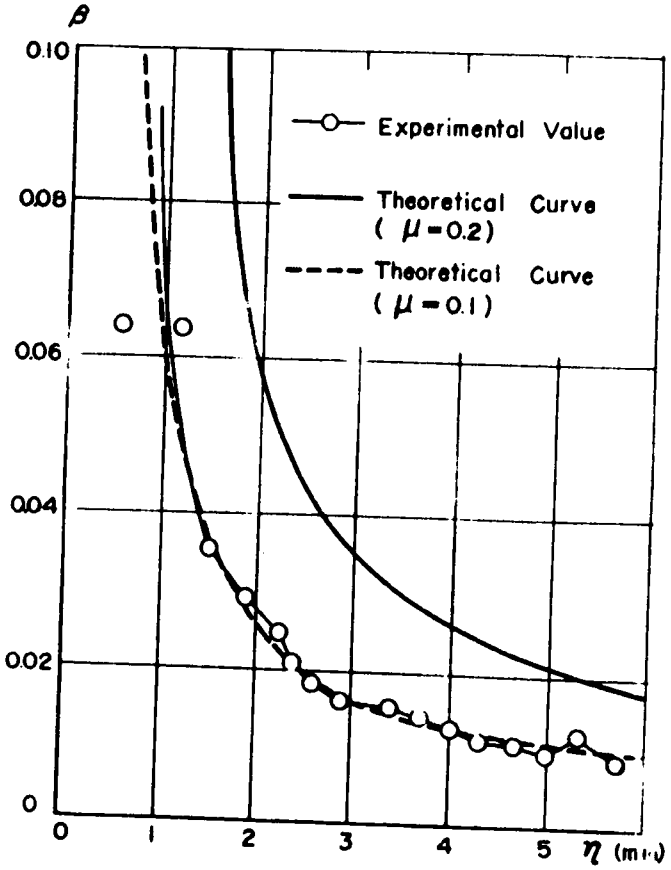

Fig. 340

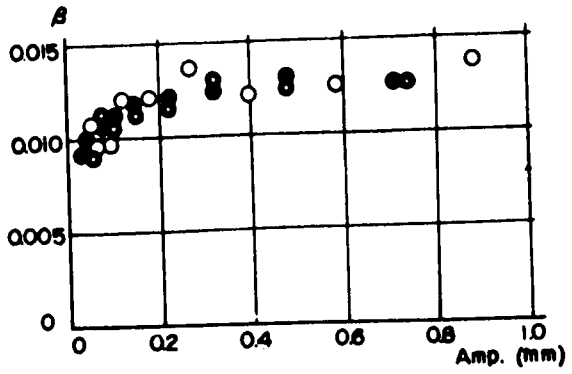

(a) Saomer Bridge

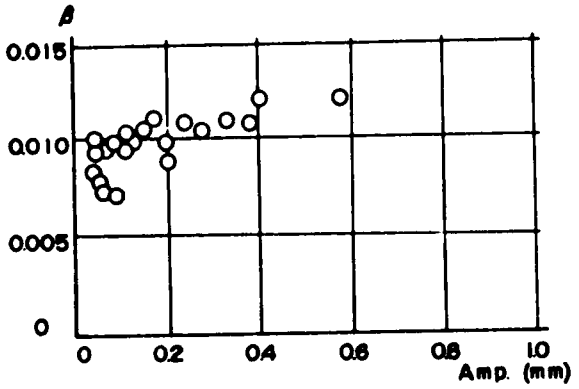

(b) Krokara Bridge

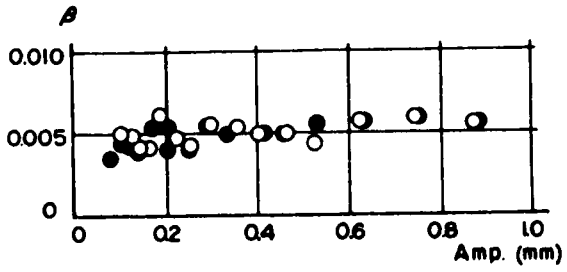

(c) Masutani Bridge

Fig. 3.4.1

CONCLUDING REMARKS

1. Summary of the Results

In PART I of this paper, a method of analysis of the suspension bridge subjected to the ground motions in the direction of the bridge axis was derived employing a physical model having finite degrees of freedom.

Natural frequencies and modes of the considered system were obtained on the ILLIAC, the high speed digital computer of the University of Illinois, and the following remarkable conclusion was derived. That is, the long span suspension bridge has its vibration modes in which the deformations of the towers are predominate in addition to the vibration modes which had been discussed in the ordinary analyses of the suspension bridges. Natural frequencies of the vibration modes thus obtained are within the range of frequencies of earthquake motions, and it was concluded that some resonant actions between them are possible.

Static deformations due to static ground displacements, steady forced vibration, and transient vibrations due to ground motions were discussed by using the modal analysis. Displacement of the anchorage causes large deflections of the suspended structures. This is quite important for the design of the cable anchorage. Allowable dislocation of the anchorage due to an earthquake must be determined from the allowable displacements of the suspended structures. Displacement of the tower base gives almost no effects to the static displacement of the suspended structures.

Steady forced vibration amplitude-frequency relations, resonance curves, were computed and given in the form of amplification factors. Transient response due to ground motions with different periods was investigated employing a simple harmonic ground motion, and response spectra due to differentperiods of ground motions were obtained. Transient vibration due to an actual earthquake was discussed using the earthquake record of 1957 So. California Earthquake. The responses were computed, by summing up the modal responses, on the KDC-I, Kyoto University high speed digital computer. The additional stresses due to 1957 So. California Earthquake are less than 250 kg/cm^2 in the tower, less than 10 kg/cm^2 in the suspended structures, and less than 90 kg/cm^2 in the cables. It was concluded, that the incremental stresses in the towers are much more important than those in the other parts of the suspension bridge.

In PART II of this paper, was discussed the elastic-plastic analysis of the suspension bridge towers. Some of the effects of the cables and suspended structures to the behavior of the towers were taken into the analysis. The analytical method derived is applicable to any tall structures subjected to a large axial force and the ground motions. Some of the assumptions on the elastic-plastic properties were made and earthquake responses were obtained on the KDC-I. 1957 So. California Earthquake multiplied some load factors were used as external ground motion and the relations between the maximum amplitudes and the load factors were obtained. The large energy dissipation due to plastic deformation decreases the maximum dynamic response, and it is quite advantageous to the design of the tower and the substructures. Dynamic instability of the tower due to the axial force and plastic limit of the tower did not occur even multiplying the 1957 So. California Earthquake by the load factor 40. Extremely large earthquakes such as load factor 300 or 600 produced an instability of the tower due to the axial force and yield moments. It is clear that the earthquakes of such magnitude may not occur.

In PART III, some of the experimental studies on vibration of suspension bridges were described. Although the experiments were limited to free and steady forced vibrations, some of the basic dynamic properties of the suspension bridges were made clear. In the experiment of the tower model, some of the resonance curves were given and the importance of the higher mode vibrations were emphasized. Some of the considerations on structural damping were also given in the same part.

2. Problems of Further Investigations

In this paper, the effects of the ground motions in the direction of the bridge axis were investigated. For the practical design of the bridge the following investigations are, moreover, necessary.

(1) Responses due to the ground motions of random direction, including the transverse direction, must be studied.

(2) Earthquake action from the superstructures to the rigid structures, such as the anchorages, the piers, etc. can be primarily computed from the analysis given in this paper. The behaviors of massive structures under such action, including direct action from the ground, must be made clear.

(3) The effects of vertical ground motions may be not small since the towers are supported at the top by the cables in the vertical direction. These effects can be analysed by the same kinds of analytical methods described in this paper and must be investigated.

(4) The earthquake ground motion used in this paper, 1957 So. California Earthquake, has only two predominate disturbances, and the effects of repeated cycles, resonant action, cannot be investigated by the ground motion used. Other strong motion displacement records must be applied to the same structure, and responses due to these ground motions have to be obtained.

(5) In the analyses of this paper, the towers were assumed to be fixed at their bases. The properties of the substructures, including the effects of the properties of ground and water, must be investigated.

(6) One of the difficulities of the analysis on earthquake response is a lack of strong motion records in Japan. In the analysis of the earthquake response of suspension bridges, displacement records are more important than acceleration records. The displacement recorder program, like the program at USCGS, must be included to the Japanese Strong Motion Acceleration Committee.

3. Considerations on Aseismic Design of the Long Span Suspension Bridges

As mentioned in the INTRODUCTION, an earthquake has different effects on the different types of structures depending upon their rigidities.

It is clear from theoretical investigations given in PART I and PART II that the maximum ground accelerations or the maximum ground displacements are not the proper designation in the design of the structures having various rigidities as the suspension bridges.

In the recent building code [401] for the earthquake resistant design the effects of the following properties are taken into considerations.

(a) The effects of rigidities of the structures are taken into account by decreasing a seismic coefficient in accordance with the following formula.

$$C = \frac{0.05}{\sqrt[3]{T}} < 0.1$$

A flexible structure requires less coefficient than a rigid structure.

(b) For tall buildings the lateral force is distributed variably over the height of the buildings. This method of distribution may be a consideration to the higher mode vibrations.

(c) The effects of plastic deformations are taken into the design multiplying a horizontal force factor "K" in accordance with types of the structres. The value of K is varied from 0.67 to 1.50.

In the design of long span suspension bridges, the situation is quite different from that of the ordinary buildings. As already shown in the analysis of this paper, the combination of structural parts of the various rigidities in suspension bridges results in unusual problems in the analysis of earthquake response. The seismic forces applied to the various parts of the structures must be correlated each other, and no individual considerations are allowable in the structure considered. The methods of design codes of the ordinary structures, however, are not necessarily applied to the design of the long span suspension bridges, since the number of long span suspension bridges in existance or under the planning is quite limited.

The design method proposed by the author is as follows.

(1) First, desin the suspension bridge without much consideration on aseismisity of the structures.

(2) Compute the additional stresses and deformations due to earthquakes. High speed computers can effectively be used for the computation of the responses.

(3) If necessary, correct the dimensions of the structure and repeat the designs (1) through (3).

(4) If the modifications of the structure were done in the preceding step of the design, ascertain the stresses and deformations of the structure whether these are within the allowable limits or not under the action of the ordinary live loads.

(5) It is preferable to compute the behaviors of the structures, including plastic deformations, under the action of the extremely large external load, and obtain the limit capacity of the structure.

ACKNOWLEDGEMENTS

The author would like to express his appreciations to the Professors of the Department of Civil Engineering, Kyoto University, and especially to Professor Ichiro Konishi whom he owes so much for the complition of this paper. He also expresses his thanks to the kind assistance of the staffs of the Bridge Engineering Laboratory of the Department of Civil Engineering.

Some of the computations were done on the KDC-I, Kyoto University High Speed Digital Computer. He also wants to express his appreciation to the Computing Center of Kyoto University.

BIBLIOGRAPHY

(1) Earthquake Resistant Design, Engineering News Record, Aug. 17, 1939, pp. 228-229

(2) Moisseiff, L. S., Provision for Seismic Forces in Design of Golden Gate Bridge, Civil Engineering, Vol. 10, No. 1, pp. 33-35 Jan. 1940

(3) Raab, N. C. and H. C. Wood, Earthquake Stresses in the San Francisco-Oakland Bay Bridge, Transaction ASCE, Vol. 106, pp. 1363-1390, 1941

(4) Konishi, I. and Y. Yamada, Earthquake Responses of a Long Span Suspension Bridge, Proc. of the II WCEE, Vol. II, pp. 863-878, Japan 1960

(5) Kubo, K., Aseismicity of Suspension Bridges Forced to Vibrate Londitudinally, Proc. of the II WCEE, Vol. II, pp.913-020, Japan 1960

(6) Hirai, A., T. Okumura, M. Ito, and N. Narita, Lateral Stability of a Suspension Bridge Subjected to Foundation Motion, Proc. of the II WCEE, Vol. II, pp.931-945, Japan, 1960

(7) Cloud, W. K. and D. S. Carder, The Strong Motion Program of the Coast and Geodetic Survey, Proc. of the (First) WCEE, pp. 2.1-2.10 1956

(8) Bycroft, G. N., Analogue Computer Techniques in Aseismic Design, Proc. of the II WCEE, Vol. II, pp. 669-679, Japan, 1960

(9) Bycroft, G. N., White Noise Representation of Earthquake, Proc. of ASCE, EM-2, April, 1960

(10) United States Earthquake 1957, U. S. Department of Commerce, Coast and Geodetic Survey, Washington

(101) Hawranek and Steinhardt, Theorie und Berechnung der Stahlbrücken, S. 318-320, Springer, 1957

(102) Bleich, Fr. and Others, The Mathematical Theory of Vibration in Suspension Bridges, pp. 18 -29, Department of Commerce, Bureau of Public Roads, U. S. Govt. Printing Office, 1950

(103) ILLIAC . Active Program Library, M-19, Solution of the Matrix Equation $Ax = \lambda Bx$ Where A + B are Symmetric and B is Positive Definite, The University of Illinois Computing Center

(104) (102) : pp. 282 - 329

(105) Newmark, N. M., Computation of Dynamic Structural Response in the Range Approaching Failure, Proc. of the Symposium on Earthquake and Blast Effects on Structures, 1952

(106) Newmark, N. M., A Method of Computation for Structural Dynamics, Proc. ASCE, Vol. 85, EM-3, p.199, July, 1959

(201) Veletsos, A. S. and Newmark, N. M., Effect of Inelastic Behavior on the Response of Simple Systems to Earthquake Motion, Proc. of the II WCEE, 1960

(202) Berg, G. V. and S. S. Thomoides, Energy Consumption by Structures in Strong Motion Earthquakes, Proc of the II WCEE, 1960

(203) Penzien, J., Elasto-Plastic Response of Idealized Multi Story Structure Subjected to A Strong Earthquake, Proc. of the II WCEE 1960

(204) Norris, C. H., and Others, Structural Design for Dynamic Loads, p.8, McGraw-Hill, 1959

(205) (204) : p. 15

(206) Hodge, P. G., Plastic Analysis of Structures, p. 170, McGraw-Hill, 1959

(207) KDC-I Library, KDC-I Manual Vol. 3, p. 75, Kyoto University Computing Center, 1961

(208) Yamada, Y. and H. Terada, Dynamic Studies on Elastic-Plastic Beams by Physical Analogy, Proc. of the 9th Japan National Congress for Appl. Mech., 1959, pp.339-402, 1960

(209) Baron, M. L., H. H. Bleich, and P. Weidlinger, Dynamic Elastic-Plastic Analysis of Structures, Proc. of ASCE, Vol. 87, EM-1. Feb. 1961

(301) Vincent, G. S., Logarithmic Decrement Field Damping, Prototype Prediction, Part 5 of the Report of Washington Univ. Aerodynamic Stabilities of Suspension Bridges, 1954

(302) A. Selberg, Damping Effect in Suspension Bridges, Publication of IABSE, Vol. 10, pp. 183-198, 1950

(303) Structural Damping, pp. 16 - 32, Pergamon Press, 1960

(304) (303) : pp. 35 - 48

(305) Pian, T. H. H. and F. C. Hallowell, Structural Damping in a Simple Built up Beam, Proc. of First U. S. Nat'l. Cong. of Appl. Mech. June 1951, p. 97.

(306) Pian, T. H. H., Structural Damping, Random Vibration (Crandall) pp. 91 - 108, Joint Publ. by MIT and Wiley, 1959

(401) Earthquake Resistant Regulations of the World, pp. 137 - 144, Organizing Committee of the II WCEE, 1960

APPENDIX

SOLUTION OF n-SIMULTANIOUS SECOND ORDER DIFFERENTIAL EQUATIONS WITH INITIAL CONDITIONS SPECIFIED (Newmark's β Method) (β = 1/6)

Yoshikazu Yamada

Description

This routine will integrate n second order differential equations of the type:

$$y_i'' = f_i(y_0, y_1, y_2, \ldots, y_{n-1}, y_0', y_1', y_2', \ldots, y_{n-1}') \qquad (1)$$

The numerical procedure is given by Eqs. (2), (3), and (4).

$$y'_{i,j,k} = y'_{i,j-1} + (h/2)f_{i,j-1} + (h/2)f_{i,j,k} \qquad (2)$$

$$y_{i,j,k} = y_{i,j-1} + hy'_{i,j-1} + (h^2/3)f_{i,j-1} + (h^2/6)f_{i,j,k} \qquad (3)$$

$$\begin{aligned} y_{i,j} &= y_{i,j,k} \\ y'_{i,j} &= y'_{i,j,k} \\ f_{i,j} &= f_{i,j,k} \end{aligned} \qquad (4)$$

If for all i, the relation

$h^2 | f_{i,j,k} - f_{i,j,k-1} | < \delta$ is satisfied.

i indicate the variable of integration,
j indicate the step of integration, and
k indicate the number of interations.

Linkage

M-1	STX	30	M+6
M	JSX	30	INTG
M+1	(AD)	AUX	location of the first word of auxiliary routine I
M+2	(AD)	Y_0	Storage positions $Y_i = Y_0 + i$ contain dependent variables y_i (i = 0, 1, 2, ..., n-1) Storage positions $n + Y_0 + i$ contain $h^2 y_i''$.

Storage positions $2n+Y_0+i$ contain values of h^2y_i'' founded by the Auxiliary routine I.
Storage positions $3n+Y_0+i$ contain hy_i'.
Storage positions $4n+Y_0+i$ contain the values $y_{i,j-1}+hy'_{i,j-1}+(h^2/3)f_{i,j-1}$.
Storage positions $5n+Y_0+i$ contain the values $hy'_{i,j-1}+(h^2/2)f_{i,j-1}$.

M+3	(AD)	n	n is the number of differential equations.
M+4	(FL)	δ	
M+5	(AD)	PRINT	location of the first word of Auxiliary routine II.
M+6	SEX	30 ( )	

Auxiliary routine I

The purpose of the auxiliary routine I is to take the quantities y_i and hy_i' and compute the quantities h^2y_i'', then place them to the location $2n+Y_0+i$. This routine preferably is stored in Q-band. (between Location 4037-4199)

```
AUX   ----------
      ----------
      JMP   30  1
```

Auxiliary routine II (Output routine)

The purpose of the output routine (Aux. Routine II) is to print or punch the quantities obtained at the end of each step and to read in the necessary quantities in the next step of the calculation.

```
PRINT ----------
      ----------
      JMP   30  1
```

Note

A part of the subroutine (the part of iteration) is stored in the Q-band (Location 4000-4036) without any particular input preparations.

```
0  INTG LDA/ 30  3          323 300 ω3"
        STA      LOOP       306 040 ω32"
        STA      LOOP1      306 000 ω4002"
        STA      NO01       306 000 ω4016"
        STA      NO02       306 000 ω4029"
5       ADA  30  3          102 300 ω3"
        STA      LOOP2      306 000 ω4015"
        STA      LOOP3      306 000 ω4028"
        ADA  30  3          102 300 ω3"
        STA      NNN1       306 040 ω28"
10      STA      NNN2       306 000 ω4005"
        ADA  30  3          102 300 ω3"
        STA      N401       306 040 ω29"
        STA      N402       306 000 ω4007"
        ADA 30   3          102 300 ω3"
15      STA      N501       306 040 ω23"
        STA      N502       306 000 ω4004"
        LDA/  30 2          323 300 ω2"
        ADA   30 3          102 300 ω3"
        LWA      1          134 000 ω1"
20      STA      COUNT      306 000 ω4036"
        LDA/  30 1          323 300 ω1"
        STA      JTAU       306 000 ω4011"
        LDA/  30 5          323 300 ω5"
        STA      JTPR       306 040 ω5"
25      JSX   24 1          856 240 ω1"
        RAX   20 3          832 200 ω3"
        STX   20 ATE2       822 200 ω4033"
   STEP STX   30 SAVE1      822 340 ω2"
   JTPR JSX   30 (    )     856 300 ω"
30 SAVE1 SEX  30 (    )     830 300 ω"
        LXA   10 COUNT      820 100 ω4036"
        LXA   23 2          820 230 ω2"
   LOOP LDM   20 ( n )      320 200 ω"
        FMP/     RSIX       221 040 ω10"
35      STO      TEMP       300 040 ω11"
        FMP/     HALF       221 040 ω9"
   NNN1 FAD   20 ( 3n )     200 200 ω"
   N501 STO   20 ( 5n )     300 200 ω"
        FSB      TEMP       204 040 ω7"
```

```
   40        FAD    20 0                 200 200ω"
        N401 STO    20 ( 4n )            300 200 ω"
             .JXU   20 LOOP              854 240 ω9991"
             JMP       ITRA              714 000 ω4000"
        RSIX (FL)      1/6               +166666667+0"
   45   HALF (FL)      1/2               +5+0"
        TEMP                             0000"
                                         08
                                         830 100 ω4000"
                                         714 000 ω4"

4000    ITRA LXA    10 COUNT             820 100 ω4036"
             LXA    23 2                 820 230 ω2"
        LOOP1 LDM   20 ( n )             320 200 ω"
             FMP/      HALF              221 000 ω4034"
        N502 FAD    20 ( 5n )            200 200 ω"
4005    NNN2 STO    20 ( 3n )            300 200 ω"
             FMP/      RSIX              221 000 ω4035"
        N402 FAD    20 ( 4n )            200 200 ω"
             STO    20                   300 200 ω"
             JXU    20 LOOP1             854 200 ω4002"
4010         STX    30 SAVE2             822 300 ω4012"
        JTAU JSX    30 (    )            856 300 ω"
        SAVE2 SEX   30 (    )            830 300 ω"
             LXA    10 COUNT             820 100 ω4036"
             LXA    23 2                 820 230 ω2"
4015    LOOP2 FAD/  20 ( 2n )            201 200 ω"
        NO01 FSB    20 ( n )             204 200 ω"
             SSP                         510 000 ω"
             FSB    30 4                 204 300 ω4"
             JMI       NEXT              750 000 ω4023"
4020         LDA       ATE1              322 000 ω4032"
             STA       ATE3              306 000 ω4031"
             JMP       CHAG              714 000 ω4026"
        NEXT JXU    20 LOOP2             854 200 ω4015"
             LDA       ATE2              322 000 ω4033"
4025         STA       ATE3              306 000 ω4031"
        CHAG LXA    10 COUNT             820 100 ω4036"
             LXA    23 2                 820 230 ω2"
        LOOP3 FAD/  20 ( 2n )            201 200 ω"
```

```
     NOC2    STO   20 ( n )          300 200 ω"
4030         JXU   20 LOOP3          854 200 ω4028"
     ATE3    JMP      (    )        714 000 ω"
     ATE1    NOP      ITRA          514 000 ω4000"
     ATE2             (    )        0000"
     HALF    (FL)      1/2          +5+0"
4035 RSIX    (FL)      1/6          +166666667+0"
     COUNT                           0000"
```

FLOW CHART

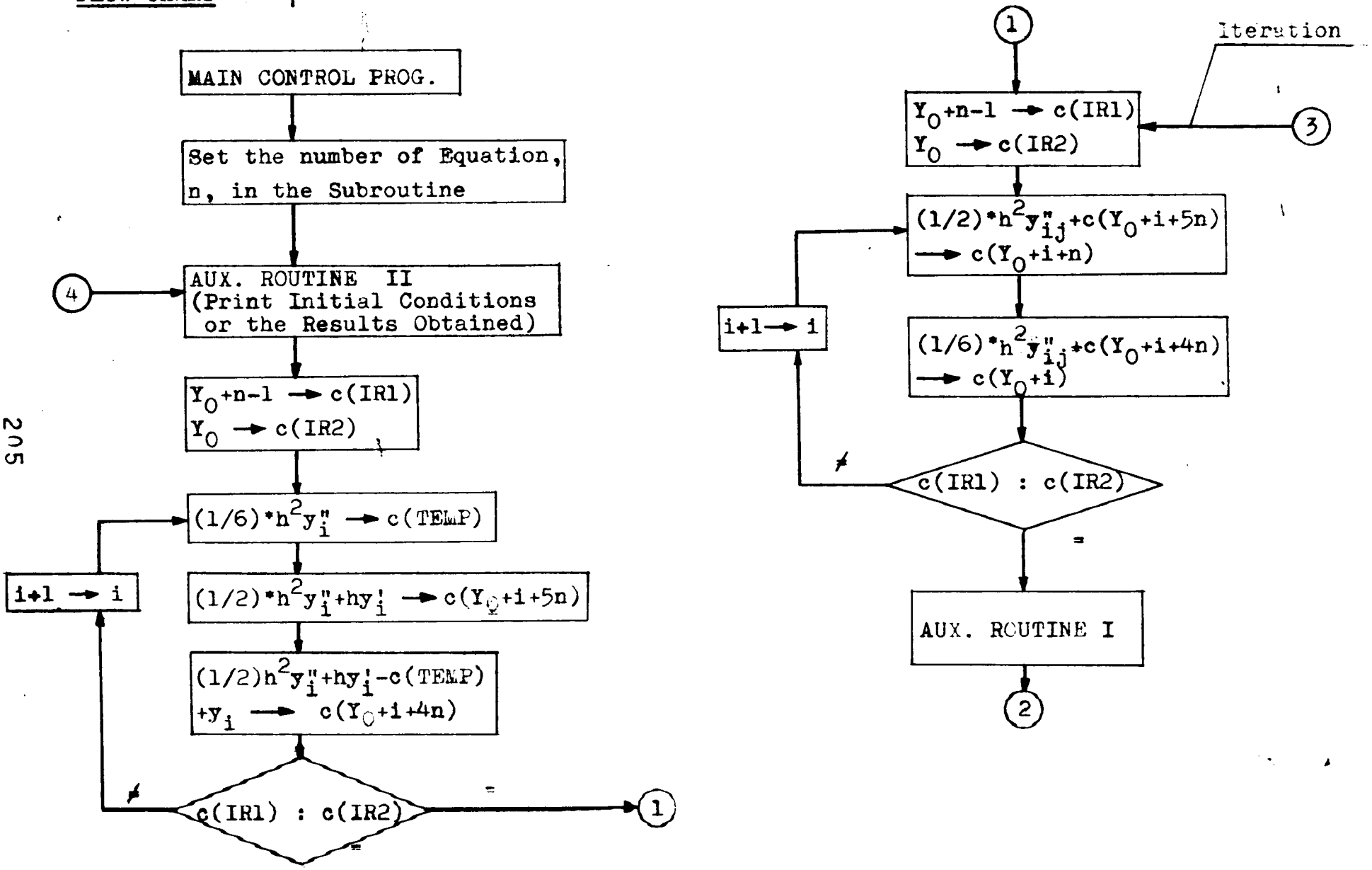
MAIN CONTROL PROG.
Set the number of Equation, n, in the Subroutine
4
AUX. ROUTINE II (Print Initial Conditions or the Results Obtained)
$Y_0+n-1 \rightarrow c(IR1)$
$Y_0 \rightarrow c(IR2)$
$(1/6)*h^2y''_i \rightarrow c(TEMP)$
$(1/2)*h^2y''_i+hy'_i \rightarrow c(Y_0+i+5n)$
$(1/2)h^2y''_i+hy'_i-c(TEMP)+y_i \rightarrow c(Y_0+i+4n)$
i+1 → i
≠
c(IR1) : c(IR2)
=
1
1
Iteration
3
$Y_0+n-1 \rightarrow c(IR1)$
$Y_0 \rightarrow c(IR2)$
$(1/2)*h^2y''_{ij}+c(Y_0+i+5n) \rightarrow c(Y_0+i+n)$
$(1/6)*h^2y''_{ij}+c(Y_0+i+4n) \rightarrow c(Y_0+i)$
i+1 → i
≠
c(IR1) : c(IR2)
=
AUX. ROUTINE I
2

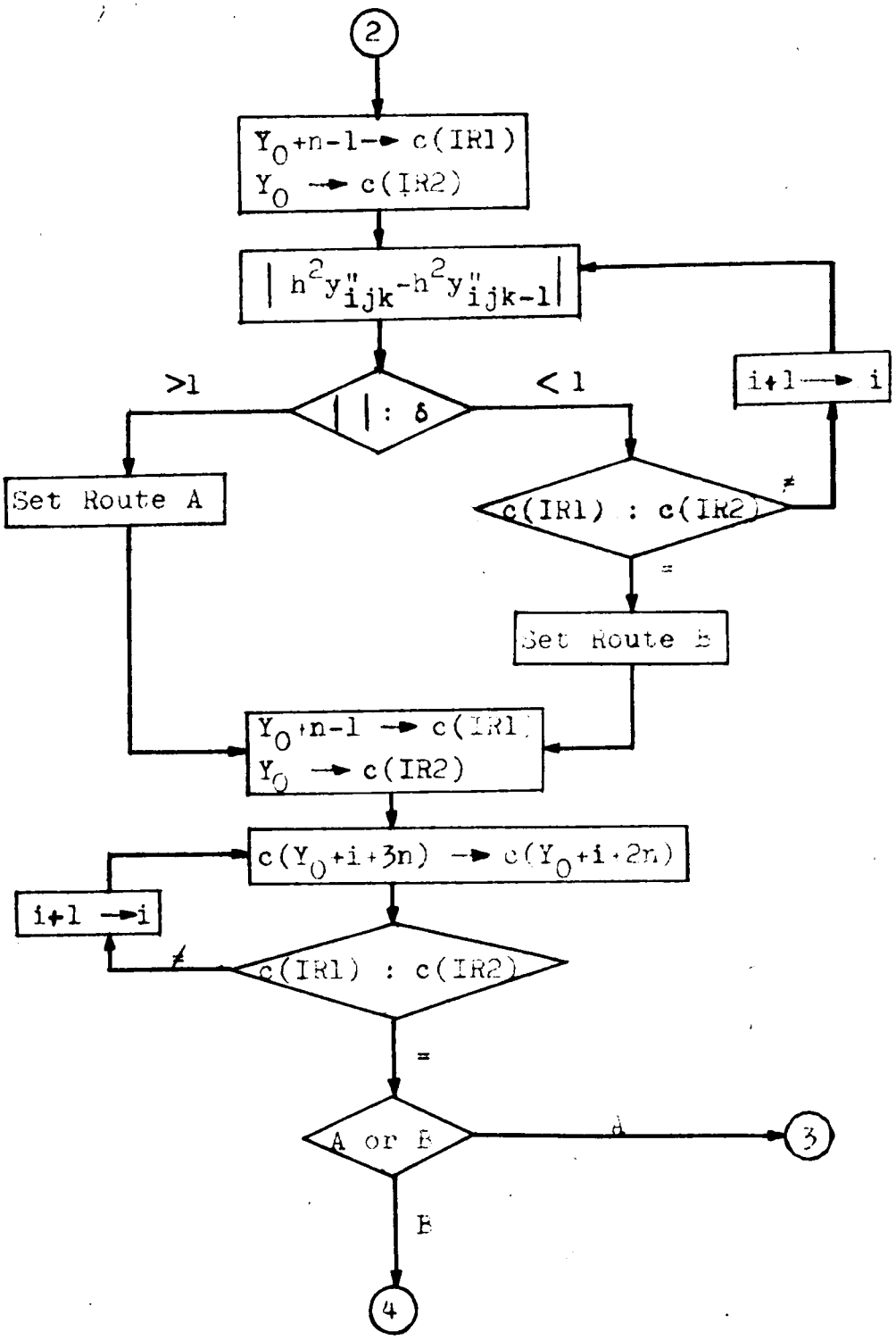
2
Y_0+n-1 → c(IR1)
Y_0 → c(IR2)
$|h^2y''_{ijk}-h^2y''_{ijk-1}|$
>1
| | : δ
< 1
i+1 → i
Set Route A
c(IR1) : c(IR2)
≠
=
Set Route B
Y_0+n-1 → c(IR1)
Y_0 → c(IR2)
c(Y_0+i+3n) → c(Y_0+i+2n)
i+1 → i
≠
c(IR1) : c(IR2)
=
A or B
A
3
B
4